CRANFIELD UNIVERSITY

Laura Gendre

A STUDY OF EMISSION OF NANOPARTICLES DURING PHYSICAL PROCESSING OF AGED POLYMER-MATRIX NANOCOMPOSITES

School of Aerospace, Transport and Manufacturing
PhD in Transport Systems

PhD
Academic Year: 2012 - 2016

Supervisors: Dr Hrushikesh Abhyankar & Dr James Brighton
November 2016

CRANFIELD UNIVERSITY

School of Aerospace, Transport and Manufacturing
PhD in Transport Systems

PhD

Academic Year 2012 - 2016

Laura Gendre

A Study of Emission of Nanoparticles during Physical Processing of Aged Polymer-Matrix Nanocomposites

Supervisors: Dr Hrushikesh Abhyankar & Dr James Brighton
November 2016

ABSTRACT

Nanotechnology research and its commercial applications have experienced an exponential rise in the recent decades. Although there are a lot of studies with regards to toxicity of nanoparticles, the exposure to nanoparticles, both in terms of quality and quantity, during the life cycle of nanocomposites is very much an unknown quantity and an active area of research. Unsurprisingly, the regulations governing the use and disposal of nanomaterials during its life cycle are behind the curve.

This work aims to assess the quantity of nanoparticles released along the life cycle of nanocomposites. Machining operations such as milling and drilling were chosen to simulate the manufacturing of nanocomposites parts, and impact testing to recreate the end-of-life of the materials. Several studies have tried to simulate different release scenarios, however these experiments had many variables and in general were not done in controlled environments. In this study, a reliable method was developed to assess the release of nanoparticles during machining and low velocity impact of nanocomposites. The development and validation of a new prototype used for measurement and monitoring of nanoparticles in a controlled environment is presented, as along with release experiments on different nanocomposites.

Every sample tested was found to release nanoparticles irrespective of the mechanical process used or the type of material tested. Even neat polymers released nanoparticles when subjected to mechanical forces. The type of matrix was identified to play a major role on the quantity of nanoparticles release during different process. Thermoset polymers (and especially polyester) were found to release a higher number concentration of particles, mainly due to their brittle properties. A polyester sample was found to release up to 48 times more particles than a polypropylene one during drilling. The nanofiller type and percentage used to reinforce the polymer is also a key point. For example, the addition of 2 wt.% of nano-alumina into polyester increases the number concentration of particles by 106 % following an impact. The nanofiller chosen and its quantity affect the mechanical properties and machinability of the composites and therefore its

nanoparticles release potential. The mechanical process and the process parameters chosen were also found to be crucial with regards to the nanoparticles released with different trends observed during drilling and impact of similar materials. Finally, thermal ageing of nanocomposites increases the number concentration of nanoparticles released (by 8 to 17 times after 6 weeks).

Keywords:

Nanosafety, Nanocomposites Machining, Low Velocity Impact, Life Cycle Analysis, Standardization

CONTRIBUTIONS TO THE THESIS

During the completion of the PhD thesis, the following dissemination works were conducted:

- Publications:
    - Gendre, L., Marchante, V., Abhyankar, H., Blackburn, K., Temple, C. and Brighton, J.: Development of CNC Prototype for the Characterization of the Nanoparticle Release during Physical Manipulation of Nanocomposites, *Journal of Environmental Science and Health, Part A: Toxic/Hazardous Substances and Environmental Engineering,* **51 (6),** 495-501, 2016. DOI: 10.1080/10934529.2015.1128720.
    - Gendre, L., Blackburn, K., Brighton, J., Marchante, V. and Abhyankar, H.: Nanomaterials Life Cycle Analysis: Health and Safety Practices, Standards and Regulations – Past, Present and Future Perspectives. *International Research Journal of Pure & Applied Chemistry,* **5 (3),** 208-228, 2015. DOI: 10.9734/IRJAC/11122233304.
    - Njuguna, J., Gendre, L., and Sachse. S.: Nanoparticles Released into Water Systems from Nanoproducts and Structural Nanocomposites Applications, *Applications of Nanotechnology in Water Research,* p21-36, Wiley-Scrivener, Scrivener Publishing LLC, 2014.
    - Gendre, L., Njuguna, J., Abhyankar, H. and Ermini, V.: Mechanical and Impact Performance of Three-Phase Polyamide-6 Nanocomposites, *Materials & Design*, Volume 66, Part B, p486-491, Feb 2014. DOI: 10.1016/j.matdes.2014.08.005.
- Conference Papers Published:
    - Gendre, L., Marchante, V., Abhyankar, H., Blackburn, K. and Brighton, J.: Measurement of Nanoparticles Release during Drilling of Polymer Nanocomposites. *Journal of Physics: Conference Series* **617** (2015) 012027 (presented at the 4th International Conference on Safe Production and Use of Nanomaterials, Nanosafe2014, Grenoble, France, November 2014).

- Gendre, L., Njuguna, J., Abhyankar, H. and Ermini, V.: Mechanical Properties of Three-Phase Polyamide-6 Nanocomposites, *Advances in Manufacturing Technology XXVII, Proceedings of the 11th International Conference on Manufacturing Research,* p375-380, ISBN 978-1-907413-23-0 (presented at ICRM2013, Cranfield, UK, September 2013).
- Sachse, S., Gendre, L., Silva, F., Zhu, H., Leszczynska, A., Pielichowski, K., Ermini, V. and Njuguna, J.: On Nanoparticles Release from Polymer Nanocomposites for Applications in Lightweight Automotive Components, *J. Phys.: Conf. Ser.* **429** 012046 (presented at *NanoSafe*, Grenoble, France, November 2012).

- Conference Presentation:
  - Gendre, L., Sachse, S., Silva, F. and Njuguna, J.: Effect of nano-fillers percentage on mechanical properties and energy absorption of three-phase polymer nanocomposites. ICCS17, Porto, Portugal, June 2013.
- Poster Presentations:
  - Blazquez, M., Unzueta, I., Marchante, V., Gendre, L., Blackburn, K., Brighton, J. and Abhyankar, H.: Emission Scenarios for Engineered Nanomaterials as Plastic Additives. A Case Study of the SIRENA-Life. ECHA – Topical Scientific Workshop – Regulatory Challenges in Risk Assessment of Nanomaterials, Helsinki, Sweden, October 2014.
  - Gendre, L., Blackburn, K., Marchante, V. and Abhyankar, H.: Measurement of Nanoparticles Release during Drilling of Polymer Nanocomposites, NANOTOX 2014, Antalya, Turkey, April 2014. Abstract published.
  - Gendre, L., Njuguna, J. and Sachse, S.: Effect of Nano-Fillers Rate on Mechanical Properties and Energy Absorption of Three-Phase Polymer-Nanocomposites. ICCM19, Montreal, Canada, July 2013. Abstract published.
  - Gendre, L., Njuguna, J. and Sachse, S.: Polymer-Matrix Nanocomposites for Automotive Applications. NanoStruc2012, Cranfield, UK, July 2012. 3rd award for best poster.

ACKNOWLEDGEMENTS

First, I want to thank Dr. Hrushikesh Abhyankar, and Dr. James Brighton, my supervisors for their guidance and help in my work. I'm also grateful to Dr. Veronica Marchante Rodriguez who was always a great support, it was a pleasure to work with her.

I would like to acknowledge Dr. Kim Blackburn and Simon Stranks for all the time, help and advice they gave me to set-up my experiments.

Also, I can't forget to thanks all my PhD colleagues and interns from the CAT department with whom I shared my time since I arrived in Cranfield. Especially I want to thank Ian Butterworth who always helped me and supported me even when I was not that easy to deal with, and Sophia Sachse who made my start at Cranfield simpler and funnier.

I am grateful to Dr. James Njuguna who gave me the opportunity to join the Centre for Automotive Technology, first as an intern, and then as a PhD student.

I wish to thank the European Commission for funding this study, as well as representatives of Tecnalia and Inkoa, partners of SIRENA project (LIFE11 ENV/ES/596), for their availabilities and guidance.

A big thanks to all my friends who helped me to relax during the bad moments and for all the parties and good time we enjoyed together. Especially, thanks to Anuszku and Katuszku for being such good friends and housemates and Julien for all the time shared in the car. Also, a special thanks to all the players from the handball team for the fun on the court, the trips, parties and great memories!

I am grateful to my family for their support and acceptance of my decisions.

To finish, I would like to thank Albain for always believing in me. I know that without him I would have probably never finished. Also, thanks to the cutest little boy ever, Ezra for his smiles, laughs and amazing progress who make me think that anything is possible.

TABLE OF CONTENTS

LIST OF FIGURES

LIST OF TABLES

LIST OF EQUATIONS

LIST OF ABBREVIATIONS

ABS	Acrylonitrile Butadiene Styrene
Ag	Silver
Al_2O_3	Aluminium oxide
APS	Aerodynamic Particle Sizer
ASTM	American Society for Testing and Materials
BAS	Button Aerosol Sampler
BSI	British Standards Institute
C	number concentration of particles
$CaCO_3$	Calcium carbonate
CEN	European Committee for Standardization
CeO_2	Cerium oxide
CLTE	Coefficient of linear thermal expansion
cm^3	cubic centimetres
CNC	Computer Numerical Control
CNFs	Carbon NanoFibers
CNTs	Carbon NanoTubes
Co	Cobalt
COSHH	Control of Substances Hazardous to Health
CPC	Condensation Particle Counter
Cu	Copper
CVD	Chemical Vapour Deposition
d	particles diameter
DMA	Differential Mobility Analyser
D-LS	Dynamic Light Scattering
e	Exponential
E	Epoxy
EC	European Commission
ECHA	European Chemicals Agency
EDX	Energy-dispersive X-ray spectroscopy
EINECS	European Inventory of Existing Commercial Substances
ELPI	Electrical Low-Pressure Impactor
ENMs	Engineered NanoMaterials

ENP	Engineered NanoParticle
EPA	Environmental Protection Agency
EPDM	Ethylene Propylene Diene Terpolymer
ESC	Environmental Stress Cracking
ESP	Electrostatic precipitator
EU	European Union
Fe	Iron
Fe_2O_3	Iron(III) oxide
Fe(OH)	Iron hydroxide
FMPS	Fast scanning Mobility Particle Sizer
FPSS	Fast Particle Size Spectromer
FTIR	Fourier Transforms Infrared Spectroscopy
g	grams
GF	Glass Fibres
GPa	GigaPascal
h	hour
HDPE	High-density polyethylene
HDT	Heat Deflection Temperature
HEPA	High Efficiency Particulate Air
HRR	Heat release rate
HSS	High-Speed Steel
ICP-MS	Inductively coupled plasma mass spectrometry
ISO	International Organization for Standardization
J	Joules
k	Removal rate
kg	kilograms
kJ	kilojoules
kN	kiloNewton
kV	kilovolt
l	litre
LCA	Life Cycle Assessment
ln	Natural logarithm
LPI	Low Pressure Impactor

LVGG	Low Velocity Gas Gun
m	metre
$m_{drilled}$	Mass drilled
MEAD	Modified Electrical Aerosol Detector
MeO	Methoxy
mg	milligrams
min	minutes
ml	millilitre
mm	millimetres
mm^3	Cubic millimetres
MMT	Montmorillonite
Mn	Manganese
MOUDI	Multi-Orifice Uniform Deposit Impactor
MPa	MegaPascal
MWCNT	Multi-Walled Carbon NanoTube
Na	Sodium
NaCl	Sodium chloride
NAS	Nanomater Aerosol Sampler
NCAP	New Car Assessment Programme
nm	nanometres
NSAM	Nanoparticle Surface Area Monitor
OELs	Occupational Exposure Limits
OMMT	Organically Modified Montmorillonite
OPC	Optical Particle Counter
O_2	Oxygen
P	Emission rate
P	Polyester
PA	Polyamide
PAS	Publicly Available Specification
PA6	Polyamide-6
PA66	Polyamide-66
PECVD	Plasma-Enhanced Chemical Vapour Deposition
PEN	Project on Emerging Nanotechnologies

PHRR	Peak of heat release
POM	Polyoxymethylene
PP	Polypropylene
PS	Polystyrene
PU	Polyurethane
PVD	Physical Vapour Deposition
rpm	Rotation per minute
s	seconds
S	Siemens
SEM	Scanning Electron Microscopy
SiO_2	Silicon dioxide
SMPS	Scanning Mobility Particle Sizer
SMPS+C	Scanning Mobility Particle Sizer plus Particle Counter
SNUR	Significant New Use Rule
$SrCO_3$	Strontium carbonate
SWCNT	Single-Walled Carbon NanoTube
t	time
TALC	Talcum
TEM	Transmission Electron Microscopy
TEOM	Tapered Element Oscillating Microbalance
T_g	Glass transition temperature
TGA	Thermal gravimetric analysis
THR	Total heat released
TiO_2	Titanium dioxide
TTI	Time to ignition
UNPA	Universal NanoParticle Analyzer
UV	Ultraviolet
V	Volume
vol	volume
WO	Wollastonite
WO_3	Tungsten trioxide
wt	weight
XRD	X-Ray Diffraction

ZnO	Zinc oxide
#	number
%	percentage
˚C	Degree Celsius
µm	micrometres

1 INTRODUCTION

Nanocomposites are one of the most promising technologies of this century. They are defined as materials composed of several phases one of which is a nano-object i.e. has at least one external dimension of less than 100 nanometers [1]. Usually, a nanocomposite consists of a matrix (like ceramic, metal or polymer) with an addition of nanofillers of varying shapes, like spheres, fibres, platelets, particles, or tubes, and of different chemical compositions.

Nowadays, industrial sectors, such as automotive or aerospace industry, include more and more nanocomposites materials in their products. In fact polymer-matrix nanocomposites seem to be a good alternative to replace metallic parts. They allow a considerable weight and cost reduction, and the use of nanofillers presents some advantages compared to traditional macro or microfillers: good mechanical properties, high energy absorption capability, recyclability, resistance to corrosion and chemical attack, high heat-distortion temperature, etc. Compared to the traditional reinforcement, the addition of nanofillers in polymer implies a minor increase in the cost but reduces the weight. Actually, it is known that an addition of only 5 wt.% of inorganic nanoparticles in polymers is enough for a considerable improvement of the material's behaviour and properties compare to 20 wt.% for a micro filler [2], [3]. These improvements can be explained by the fact that fillers in nanosize allow a high surface area to volume ratio of the nanoparticles, and so an increase of the contact surface between matrix and fibre [4]. It also allows a low inter-particles distance compare to micro-size fillers and reduces stress concentrations around the fillers.

The annual consumption of nanocomposites was estimated at 118,768 metric tons, which correspond to over $800 million, for 2010 [5]. Clay nanocomposites represent more than 50 % of this annual consumption, and carbon nanotubes composites 21 % [5]. The Project on Emerging Nanotechnologies (PEN) inventory currently lists more than 1800 consumer products based on nanotechnology on market from 662 companies in 32 countries [6], [7].

This craze for nanocomposites is not going to slow down. In fact, a significant growth is expected in the annual consumption of nanocomposites in the next few year. The BCC research [8] predicts an increase of 160 % in 5 years for the nanocomposites consumption (from 225,060 metric tons in 2014, to 584,984 metric tons in 2019).

However, the risk involved in the use and disposal of such particles is not well known. The current legislation with regards to chemicals and environment protection doesn't cover nanomaterials. Nevertheless the release of nanosized particles from parts made from nanocomposites can be a risk to human health and environment, and especially the physio-chemical properties of the nanoparticles embedded into the polymeric-matrix are unknown along the whole life cycle of the nanomaterials. Industries need a standard method to evaluate nanoparticles release during products' life cycle in order to improve the knowledge in nanomaterials risk assessment, and to inform customers about the safety of nanomaterials and nano-products. It is safe to say that, given the explosive R&D and commercial uptake of nanomaterials (for example, the number of submissions per year to the Journal of Nanoparticle Research increased every year and reached 2149 in 2013 [9]), unsurprisingly, the regulations governing the use and disposal of nanomaterials during its life cycle is behind the curve. The wide acceptance of nanotechnology by the consumers depends on alleviating the perceived safety related concerns. In this context, many projects, aiming to understand the effects of nanomaterials usage on human health and environment, were and still are funded by the European Commission. The Nanopolytox project studied the "toxicological impact of nanomaterials derived from processing, weathering and recycling from polymer nanocomposites used in various industrial applications" [10]. MARINA and NanoValid are two other projects funded by the European Commission in this aim.

Project NEPHH (Nanomaterials related Environmental Pollution and Health Hazards throughout their life cycle, [11]) was focused on the identification and quantification of nanoparticles released in the life cycle of silicon-based polymer

nanocomposites. Drilling and crashing experiments were conducted. The results highlighted several issues with regards to measurement of airborne particles during drilling tests: particle loss during the measurement, low volume flows of the equipment leading to particle loss and long sample time, background noises due to uncontrolled ambient environment affecting the results and the importance of controlled drilling parameters (feed rate, spindle speed, etc).

Following these conclusions, project SIRENA (SImulation of the RElease of NAnomaterials from consumer products for environmental exposure assessment) aimed to demonstrate and validate a methodology to simulate the unintended release of nanomaterials from consumer products by replicating different life cycle scenarios to be adopted by a wide number of industrial sectors in order to get the necessary information for exposure assessment [12]. In order to replicate different stages of products' life cycle, two types of experiments will be conducted: impact (to simulate accidental or intended fractures), and drilling (which is a common procedure in different stages of product's usage phase). During these experiments, nanoparticles released have to be collected, sampled and characterised (chemical composition, shape, size, quantity, size distribution), in order to assess the risk to human health and environment. The main motivations of this work are:

- Provide different industrial sectors with a standard method to evaluate the release of nanoparticles from nano-products during their life cycle, and so link to the potential risk to human health and environment.

- Increase and improve actual knowledge in nanomaterials risk assessment, in order to implement EU legislation in relation to chemicals and environmental protection.

- Inform consumers and general public about the safety of nanomaterials and nano-products, and thus increase their market penetration.

This study was inspired by the objectives of project SIRENA. The aim of this study (PhD) is to assess the release of nanoparticles from nanocomposites along their life cycle. To reach this goal, the following objectives have to be completed:

- Setting up a system to simulate the unintentionally and intentionally release of nanoparticles. The inside environment of the system has to be controlled to avoid contamination. And also, the system has to be as much automatized as possible to ensure reproducibility;
- Quantify and characterise the dust generated during different release scenarios (drilling, milling and impact);
- Evaluate the effect of ageing on the release of nanoparticles from nanocomposites samples.

Focus was given to polymer nanocomposites upon ceramic or metal-matrices nanocomposites as they are already widely implemented in different sectors such as automotive, aerospace and construction. Also, the use of polymer and polymer composites for lightweight applications to replace metal, for example in the automotive industry is the most researched currently and polymer nanocomposites present several advantages to improve the lightweighting possibilities. Therefore, a choice was made to compare the release of neat polymers or polymer composites with their potential nanocomposites replacement.

In the following section, a comprehensive literature review is presented covering the state-of-the-art about the advantages of nanocomposites, the release of nanoparticles form nanocomposites during their life cycle and the methods to assess it, as well as the current state of regulations and standards with regards to nanomaterials. Also, future challenges and necessary work to ensure the success of nanotechnologies are reviewed. This section helps to establish the gap in literature as well as basis for improvements to be made in current established practices in the area of nanomaterials health and safety assessment.

2 LITERATURE REVIEW

2.1 What is a Nanocomposite?

Nanocomposites are materials composed of several phases one of which is a nano-object i.e. has at least one external dimension of less than 100 nanometers [1]. Usually, a nanocomposite consists of a matrix (like ceramic, metal or polymer) with an addition of nanofillers of varying shapes, like spheres, fibres, platelets, particles, or tubes, and of different chemical compositions. Nanofillers can be classified in three different types according to their shape:

- *Nanoparticles:* the three external dimensions are in the nanoscale [1], for example SiO_2 nanoparticles with a spherical shape and a diameter around 10nm. Figure 1 [13] is a SEM image of modified silica nanoparticles.

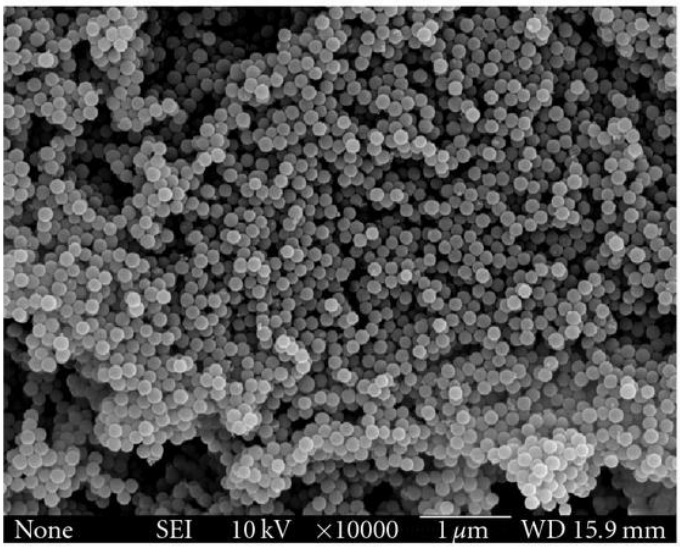

Figure 1: Example of nanoparticles: SEM image of polyethyleneimine modified silica nano-particles [13]

- *Nanofibres:* with a diameter less than 100nm and a length/diameter ratio superior to 3 [1]. The most known filler of this type are carbon-nanotubes. Figure 2 [14] is a TEM image of carbon nanofibres.

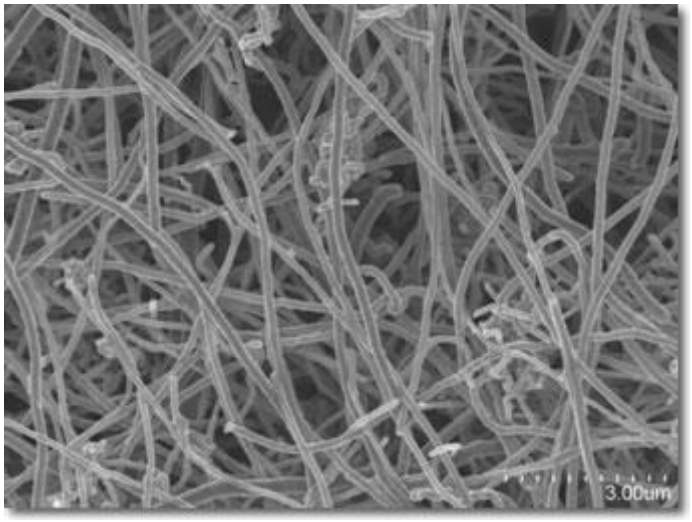

Figure 2: Example of nanofibres (carbon nanofiber, Pyrograf III from Applied Sciences, Inc [14])

- *Nanoplates:* in this shape, it is the thickness which has a nanosize [1]. Clay, like Montmorillonite, are the most studied due to their natural presence and ease to extract. Figure 3 [15] represents Fe_3O_4 nanoplates.

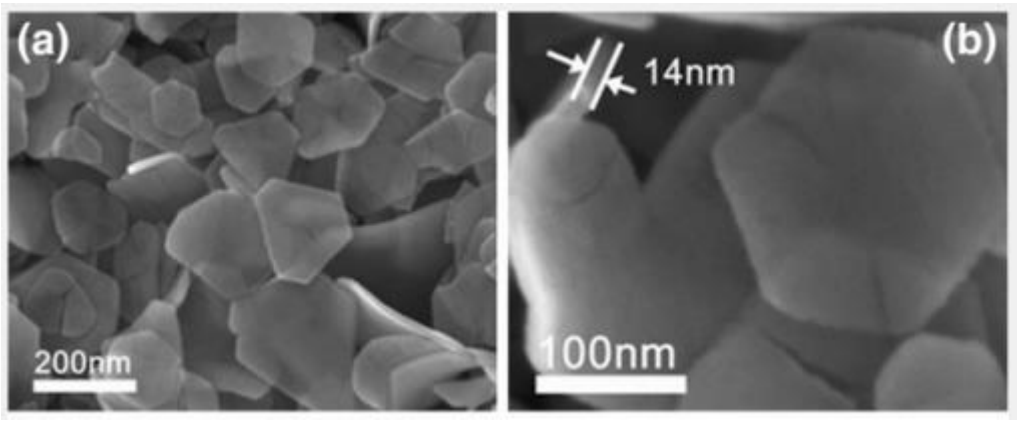

Figure 3: Example of nanoplates: Low- (a) and high-magnification (b) SEM images of the as-prepared Fe_3O_4 nanoplates [15]

At present, research and applications are mainly focused on nanocomposites based on polymer-matrices, as the manufacturing processes of polymers are the most suitable, in terms of cost and implementation [16]. Reinforced polymers with micro-fillers are already well known, and the use of polyamide reinforced by glass fibre became widely used in automotive applications for example. Fillers in nanosize allow an increase of the contact surface between matrix and fibre and a low inter-particles distance compare to micro-size fillers, resulting in enhanced mechanical properties. Also, it is known that an addition of only 5 wt.% of inorganic nanoparticles in polymers is enough for a considerable improvement of the material's behaviour and properties [2], [3], [17]. Compare to the traditional reinforcement, the addition of nanofillers into polymer matrices results in a minor increase in the cost and the weight.

2.2 What are the Advantages of Nanoscale Fillers in Polymeric Nanocomposites?

The nanosize of fillers allows some improvements in the polymer behaviour and properties compared to micro-size reinforcements. The advantages of nanocomposites are mainly the result of high surface area to volume ratio of the nanoparticles [4], and an increase in area of contact between matrix and filler. The main improvements reported in literature are as follows:

- *Higher heat-distortion temperature (HDT)*: Toyota researchers found that the addition of 4.7 wt.% of clay (Montmorillonite) in polyamide-6 improved the heat distortion temperature by 87 °C compare to neat polyamide-6 [18], [19]. Similarly, the use of 7 wt.% of organically modified Montmorillonite into PLA enhanced the HDT by 18 °C [20]. Also, an addition of clay (between 1 and 9 wt.%) into a polyurethane matrix improved the thermal stability compared to neat polyurethane [21].
- *Scratch resistance and tribological properties*: the smaller size of the fillers generates less stress concentration around the particles, which reduces the risk of damage and crack propagation and in case particles are displaced, holes in the matrix are smaller [2]. Sanes et al. [22]

showed that the addition of ZnO nanoparticles into epoxy resin reduces the final surface damage, i.e. the residual depth of scratch, after viscoelastic recovery. This result was explained by the improvement in stiffness of the material. In another study, the tribological behaviour of silica microparticles was compared to zirconia/silica nanoparticles as reinforcement for Filtek Supreme Standard, a resin matrix for dental polymer composites [23]. It was found that nanoparticle filled composites, on the opposite of micro-reinforced composites, present a uniform fillers distribution in the matrix and a homogenous hardness. Also, nanocomposites show better tribo-mechanical performances, with regards to elastic modulus, hardness, wear resistance and friction behaviour than micro-reinforced composites. It can be explained by the high specific surface area of nanoparticles which lead to a strong fillers/matrix interfacial bonding [23], [24].

- *Dimensional and thermal stability*: the coefficient of linear thermal expansion (CLTE) decreases with the addition of nanofiller, which is an essential parameter for dimensional stability and allows to manufacture bigger parts [2]. The thermal stability is generally assessed by thermo gravimetric analysis (TGA) and concerns the degradation (in term of mass loss) of a polymeric materials at high temperature [25]. Vyazovkin et al. [26] found that the decomposition temperature under nitrogen or air was increased by 30-40 °C for PS nanocomposites compared to neat one. This improvement can be explained by the role of clay as a mass transport barrier for the volatile products and the formation of char which prevents the decomposition and diffusion of volatile products [27]–[29]. This last phenomenon allows to improve the water permeability and thermal permeability of polymeric materials [27]. For example, the water permeability decreased by 40 % for polyamide-6/clay nanocomposites compared to neat polyamide-6 [18].
- *Corrosion resistance* [16], [30]: polyaniline is a polymeric material often used as a coating on C45 steel in order to protect it from corrosion. Kalaivasan et al. [31] reported that the addition of Na-MMT (sodium

Montmorillonite) intercalated with the organic aniline monomer improved the corrosion protection of the C45 steel into 3.5 % aqueous NaCl. Ramezanzadeh et al. [32] found similar results with an epoxy-polyamide coating with ZnO nanoparticles (between 2 and 6.5 wt.%) in order to protect St-47 steel.

- *Electrical conductivity*: The addition of nanoparticles into a polymeric matrix can enhance the dielectric properties. Yang et al. showed that the increase of TiO_2 nanoparticles content with crosslinker into a copolymer matrix increases the relative permittivity and decreases the dielectric loss tangent, resulting in an improvement in the dielectric properties [33]. In another study [34] low-density polyethylene was loaded with TiO_2 nanoparticles: untreated or polar-treated on the surface. The surface modification was done by a polar silane coupling agent. In both cases, the electrical properties were improved, and the nanocomposites with polar-treated nanoparticles exhibited the best electrical properties. Indeed, some nanoparticles are especially used for their electrical behaviour, for example graphite nanoplatelets allows an electrical insulator like polystyrene to become an electrical semiconductor [16].
- *Flame retardancy*: the flame retardancy of a material is characterised by various properties such as heat release rate (HRR), peak of heat release (PHRR), time to ignition (TTI) and total heat released (THR) [25]. Usually, it was found that the nanocomposites presented a better PHRR than neat polymers, but a lower TTI and equivalent THR [35]–[37]. Also, it was reported that the clay should be well dispersed, but not necessarily delaminated to obtain good results [28], [38].

Further, integration of nanofillers in polymers was shown to improve stiffness, strength and modulus, and energy absorption. These properties will be studied in more details in the following sections.

2.2.1 Mechanical Properties

The effect of nanofillers on the mechanical properties of polymeric materials is detailed in the following section:

Hartmut Fischer (TNO, Netherlands), found an improvement of 40 % for the tensile strength, and of 70 % for the modulus, at ambient temperature, by loading polyamide with 5 % of Montmorillonite clay [39]. Kojima et al. reported that nylon 6-clay hybrid (NCH: 4.7 wt.% montmorillonite) had superior strength and modulus compared to nylon 6, a flexural strength two times higher and a flexural modulus four times higher than for nylon 6 [19]. The addition of clay can enhanced the performance of polyurethane. It has been found that 9 wt.% of MO-MMT into a PU matrix allows an improvement of 300 % of the storage modulus and 667 % of the loss modulus compared to a neat PU at -45 ºC [21]. This great improvement is mainly due to the interaction between the matrix and the fillers. If this interaction is poor, the load is principally supported by the matrix, which is weakened by the presence of the fillers and it causes a decrease in properties. However, enhanced interaction between the matrix and the nanofillers involves a more efficient repartition of the load, so it increases modulus and strength [40].

In order to control these properties, it is important to understand which parameters have influence on strength, modulus and stiffness. The Kerner equation, valid for composite materials with spherical particles in a matrix, and which can be extended to nanocomposites, reported a dependence of volume fraction for the modulus [41].

2.2.1.1 Effect of the Filler Size

The size of filler influences directly two mains factors related to the performances of nanocomposites: the surface area to volume ratio of the fillers and the excluded volume interactions [42]. For example, in the same volume element, nanofibres with a diameter of 10 nm will have a specific area 1000 times bigger than fibres with a diameter of 10 µm [43]. Larger fillers create more stress concentrations around the fillers, so it lowers ductility. Ng et al., in 1999, studied the effect of size of TiO_2-particles loading epoxy resin. The addition of micro-size (0.24 µm)

particles presents an increase in modulus but also a decrease in strain at break, whereas the nanosize (32 nm) TiO_2-particles enhanced both properties [44].

2.2.1.2 Effect of the Filler Shape

The three main filler shapes were presented in the earlier section 2.1. An increased surface area to volume ratio involves a better adhesion of the filler to the matrix [2] hence the enhanced mechanical properties. A nanofiber, for example, has a surface area to volume ratio up to 10^3 times higher than a conventional microfiber [43]. The shape of the filler directly changes this ratio.

For spherical particles with a radius r, the surface area to volume ratio is:

$$\frac{A_S}{V_S} = \frac{4\pi r^2}{\left(\frac{4}{3}\right)\pi r^3} = 3/r \qquad \textbf{(2-1)}$$

For a cylindrical filler of radius *r* and length *L* (fibrous materials: *r*<*L*; layered materials: *r*>*L*), the surface area to volume ratio is:

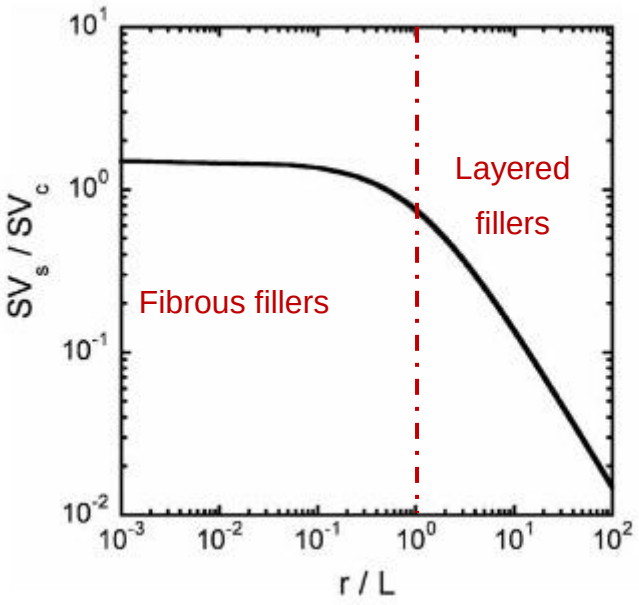

Figure 4: Surface Area to Volume Ratio for Spherical Particles (SV_S) Compared to Surface Area to Volume Ratio for Cylindrical Particles (SV_C) as a Function of Particle Radius (*r*) and Length (*L*) [42]

$$\frac{A_C}{V_C} = \frac{2\pi r^2 + 2\pi rL}{\pi r^2 L} = \frac{2}{r} + \frac{2}{L} \quad \textbf{(2-2)}$$

The comparison between spherical and cylindrical fillers at equal volume fractions gives us the following equation:

$$\frac{SV_s}{SV_c} = \frac{3}{2\left(1 + \frac{r}{L}\right)} \quad \textbf{(2-3)}$$

In both cases, plates ($r>L$) or short rods ($L<2r$), the surface area to volume ratio is higher for the cylindrical fillers, and it is even better with layered nanofillers ($r<L$) as shown Figure 4 [42].

However, it is difficult to clearly measure the influence of this parameter on the mechanical properties on its own as most of the time, a type of nanofiller is used in a preferred shape.

2.2.1.3 Effect of the Volume Fraction of Fillers

Yang et al. [45] reported a significant influence of the percentage of modified silica-fillers in polyamide-6 matrix (Figure 5). It shows that the modulus was significantly increasing when the volume fraction of filler was greater. With regards to the strength and elongation at break, they had an optimum around 5 wt.% in nano-SiO_2. Above this content, these properties decreased again. A possible explanation is the presence of particles 'agglomeration, which had more chance to occur with filler loading. The agglomerations create stress concentration in the matrix, and result in material failure.

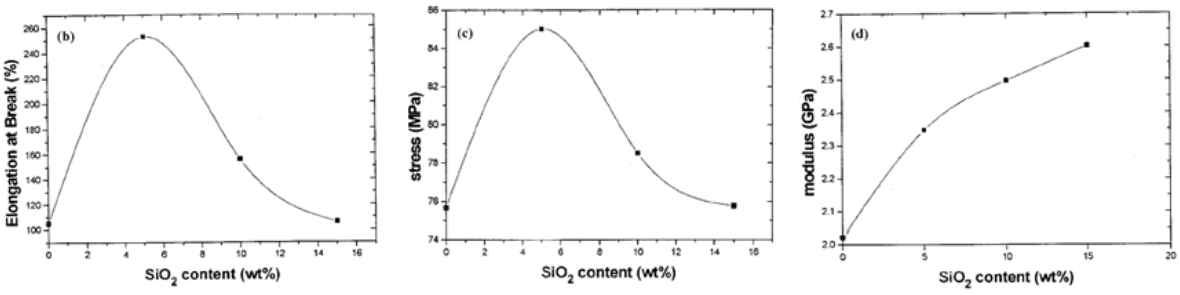

Figure 5: Elongation at Break, Stress and Modulus in Function of Nano-SiO_2 Content for a Modified Silica Polyamide 6 Nanocomposites [45]

The addition of clay resulted in performance enhancement of polyurethane. It was shown that the moduli were improved with addition of clay (between 1 and 9 wt.%). Mishra et al. [46] studied the influence of organically modified Montmorillonite (OMMT) on polyamide-66 nanocomposites. They loaded the polymeric matrix with different percentages of nanofillers (between 0 and 4 wt.%). It has been found that the increase in OMMT content increases the Young's modulus, elongation at break and tensile strength, respectively by 68 %, 46 % and 35 % compared to the neat polymer.

Zhou et al. [47] investigated the mechanical properties of polypropylene nanocomposites. The results showed that the addition of un-treated nanosilica is effective at a low filler fraction. At a filler loading higher than approximately 0.5 vol.%, both tensile strength and notched Charpy impact strength decrease. The addition of reactive monomers and cross-linking agents during the melt compounding permits to increase both strength and toughness of the polypropylene nanocomposites thanks to a better filler/matrix interaction.

Different percentages of nanofiller can be found as optimum, they are dependant of the matrix, nanofiller type and also of the property which is studied. For example, Wetzel et al. [48] noticed that the addition of TiO_2-nanoparticles and Al_2O_3-nanoparticles into an epoxy matrix can improve flexural modulus, flexural toughness and fracture toughness and at the same time, keep good thermal properties. These enhancement were found to be better with the increase in filler content, up to 10 vol.%.

2.2.2 Energy Absorption and Impact properties

The energy absorption and impact properties are important criteria for materials' selection for structural parts in car industry. Indeed, the materials need to absorb impacts and do not transmit them inside the vehicle as the aim is to protect the passengers.

To characterise the crash behaviour, two criteria can be used:

- *The energy absorbed (kJ)*, defined by the area under the curve load vs displacement. To maximize the value of energy absorbed, it's

necessary to find a compromise between a material which is able to deform considerably, and a material which is able to support higher loads.

- *The specific energy absorption (kJ/kg)*, which is defined as the energy absorbed per unit mass: $E_S = W/m_c$, where *W* is the total absorbed energy in kJ, and m_c, the crash mass in kg.

These criteria, and impact behaviour, are dependent on many parameters such as filler type, filler shape, specimen geometry, processing condition, filler volume fraction or testing speed [49]. The influence of fillers properties are described in the following sections.

2.2.2.1 Effect of the Filler Stiffness

The influence of particles stiffness on impact properties was studied by Bartczak et al. [50] with notched Izod impact testing. These experiments allow to highlight the improvement in impact properties thanks to the addition of elastic rubber and rigid calcium carbonate particles in a polyethylene matrix. The insertion of 22 vol.% of elastic rubber enhanced notch toughness by 16 times compared to neat polyethylene which can be due to the crack bridging effect of the rubber particles. Subramaniyan et al. [51] reported that core shell rubber nanoparticles were better at an equivalent weight fraction than MMT nanoclay particles in order to enhance fracture toughness of an epoxy vinyl ester resin. Core shell rubber nanoparticles had a soft rubber core and a glassy shell, and so were less stiff than the MMT particles.

2.2.2.2 Effect of the Filler Geometry

As for the mechanical properties, it is difficult to analyse the effect of this parameter alone as usually a type of filler is used in a preferred shape. However, the surface area to volume ratio changes according to the filler shape, so it has an influence on the matrix-filler interaction.

Addition of Montmorillonite, layered nanofillers, was found to decrease the impact toughness of polymers [52], while the addition of fibrous nanofillers such as Al_2O_3 nanowhiskers and wollastonite into similar polymeric matrix enhance the fracture

toughness compared to neat polymer [53]. With regards to spherical nanofillers, silica nanoparticles reinforcing polymer could also lead to improvement in the impact toughness of polymeric-composites, but it is important that the nanoparticles are well dispersed in the matrix, and agglomerations have to be avoided [54].

2.2.2.3 Effect of the Filler Fraction

Zhang et al. [55] studied the effect of montmorillonite (MMT) content in polypropylene matrix (Table 1). It can be seen that the filler fraction was a significant parameter for the impact properties. There was a significant improvement in the notched Izod impact strength at 5 °C, for less than 1 wt.% of MMT. However, above 5 wt.%, it was lower compared to neat polypropylene which can be explained by the higher possibility of agglomerations with an increase percentage of nanofiller.

Table 1: Influence of MMT Content on Notched Izod Impact Strength for PP-MMT Nanocomposites [55]

C-18-MMT content (wt%)	*Tensile strength (MPa)*	*Notched Izod impact strength (KJ m^{-2}) (5°C)*
0.0	28.6	9.4
0.1	30.2	25.9
0.3	30.5	19.8
0.5	31.4	19.1
1.0	31.2	13.0
2.0	30.6	15.2
3.0	31.1	12.8
5.0	31.3	9.3
7.0	31.3	5.9

The effect of volume percentage of Al_2O_3 nanoparticles loading epoxy matrix was reported by Wetzel et al. [48]. It was shown that nanofillers addition improved Charpy impact energy compared to virgin epoxy. An optimum was found at filler content of around 1 and 2 vol.%.

Considering different syntactic foams (hollow particles filled composites) reinforced by nanoclay, it was shown that the increase in surface modified nanoclay content improved the energy absorption capabilities under a quasi-

static compressive solicitation [56]. The improvement compared to neat foams was between 80 to 200 % considering the area under the stress-strain curves.

2.2.2.4 Effect of the Filler Size

The properties of polyurethane foams reinforced by micro or nanosilica fillers were investigated by Javni et al. [57]. The rebound resilience was decreased for the nanosilica filled polyurethane foams, but the hardness and compression strength were higher, which indicates that nanosilica reinforced foams have higher energy dissipation. A comparison between syntactic foams filled with 40 µm or 75 µm size rubber particles at a content of 2 vol.% was conducted by Maharsia et al. [58]. The results showed an increase of energy absorption capabilities for the foams filled with the smaller particles.

Chen et al. studied the size effect of particles on the damage dissipation in nanocomposites [59]. Figure 6 shows that the energy dissipation increased for filler size up to around 200 nm and above this value, the energy dissipation decreased. This could be on account of the stress concentration produced by the size of the fillers. The crack propagates easily and less energy was absorbed when the particles were bigger. However, when the particles were small, they could not reinforce the structure.

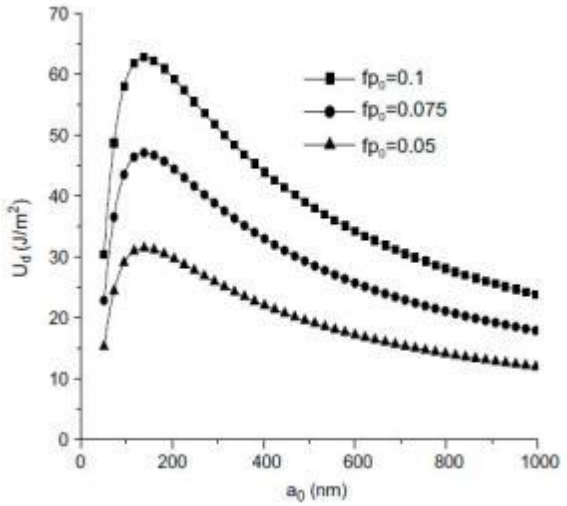

Figure 6: Energy Dissipation against Particle Size [59]

2.2.3 Three-Phase Composites

In the previous sections, it was discussed that the addition of nanofillers instead of micro-fibres significantly improves the mechanical and impact properties, and thus decreases the possible weight of a component. However, another option exists: reinforced polymeric materials with both nano and micro sized fillers.

Wu et al. studied the behaviour of polyamide-6 reinforced by glass fibre and nanoclay [60]. He concluded that a polyamide-6/clay with 30 wt.% of glass fibre had an enhanced tensile strength of 11 %, and a tensile modulus enhancement of 42 % compared to polyamide-6 with 30 wt.% of glass fibre. The flexural strength and flexural modulus were similar, but a significant improvement was observed in heat distortion temperature, which was 80 °C higher with both nano and micro sized fillers. Polyamide-6 reinforced by glass fibre and layered nanosilicate was studied by Vlasveld et al. [61]. The nanofillers, as nanoplatelets, had a negative effect on the fibre/matrix adhesion which lead to decrease in mechanical properties.

Another study showed that the addition of secondary filler in a polypropylene matrix had only negative effect on mechanical properties due to a poor dispersion of the nanofiller in the matrix and a weak filler/matrix interaction [62]. However, it enhanced mechanical properties for polyamide matrix. An addition of 2 wt.% of Montmorillonite, in the 30 wt.% glass fibre/polyamide-6 increased modulus by 10 % and elongation at break by 2 %. As little as 2 % of SiO_2 nanoparticles also enhanced the modulus by 4.7 % and elongation at break by 32 %. This was mainly due to the failure mode: a high matrix/fibre interaction which led to matrix and fibre cracking instead of fibre pull-out. The energy absorption capabilities were also improved with the addition of nano-SiO_2 which changed the mode of failure of the structure [62].

Helal et al. [63] went one step further and combined the high conductivity of single wall carbon nanotubes, good dielectric properties of titanium dioxide nanospheres, and the lightweight structure of polyvinylidene fluoride matrix. The permittivity and crystallinity was also improved compared to neat polymer.

2.3 Ageing of Polymeric Matrix Nanocomposites

Most of the studies referred to in the earlier sections were based on properties of nanocomposite materials but the ageing of the material isn't considered. However, in order to have a complete analysis, it is important to study the behaviour of the nanoproducts along the whole life cycle of the product, from the manufacturing to the end of use. Ageing of materials is a phenomenon which has a significant influence on the different properties of the products.

In most of the cases, during ageing of polymer composites, the polymer matrix has been identified as the constituent which lead the changes, in term of mechanical properties (stiffness, strength and fatigue) and the degradation of polymer-based composites [64].

So, the same method and standard as for plastics can be used in order to assess the effect of ageing on polymeric-matrix nanocomposites. These standards will be listed later in this section.

Ageing or degradation of polymers encompasses different phenomenon such as biodegradation, pyrolysis, oxidation, mechanical, photo and catalytic degradation, or chemical and physical ageing. Three main types of ageing can be highlighted:

- *Chemical Ageing:* The chemical ageing such as thermo-oxidative, thermal, or hydrolytic ageing, usually causes degradation of the mechanical properties and increase of the glass transition temperature (T_g: temperature at which a polymer become soft and rubbery). This is the result of the increase of cross-linking density in the polymer chain [64];
- *Physical Ageing:* Physical ageing corresponds to changes in the materials' properties only by the action of time (constant temperature, no stress or any influence form other external conditions) [65]. It corresponds to the relaxation process in which molecular mobility occurs in order for the material to reach an equilibrium. The physical ageing of polymers and polymer composites causes modification of the

thermodynamic properties (free volume, enthalpy, entropy) of the polymers, which affect the mechanical properties [64];

- *Mechanical degradation:* The last type of ageing mechanism cited by Gates et al. [64] is the mechanical degradation. This mechanism is irreversible, can be observed on a macroscopic scale, and results in change in mechanical properties, such as stiffness and strength. Mechanical degradation can be in the form of matrix cracking, delamination, interface degradation, fibre breaks, etc.

2.3.1 Protocols and Standards for Ageing of Plastics

In order to obtain representative and acceptable results, the ageing protocol needs to replicate the changes that occur in service life [64]. Gates et al. [64] suggested a general procedure with regards to the ageing of polymers and polymer composites. First, identify the class of the material selected (thermoplastic or thermoset), and the mechanism to evaluate, like thermal stability or matrix cracking. Then, choose the environmental conditions (heat, moisture, mechanical load etc.) for ageing. Conduct ageing experiment following established methods, and finally test the aged samples and compare the results to the un-aged specimens. Several protocols have been described in the literature in order to study the ageing of polymeric materials according to different criterion. Two mains scenarios are historically used in order to accelerate ageing of polymer composites: increase of mechanical stress, and increase of temperature [66]. However, these two mechanisms have their weaknesses. Increase in the temperature can cause degradation that does not happen during use at normal temperature, or produce a degradation rate not representative of the reality [64]. The consequences of increased mechanical stress due to physical ageing are not well understood [64].

International standards were defined in order to assess the effect of different types of ageing conditions on plastics. Some of them are as follows:

- For thermal ageing:
    - ISO 188/ASTM D573/ASTM D3045: heat ageing;

    - BS EN 60216-1/ISO 2578/UL 746B: determination of thermal endurance;
    - ISO 11346: Estimation of lifetime and maximum service temperature of use.
- For the resistance to fluids and effect of chemical:
    - ISO 1817/ASTM D471: Determination of the effect of liquids;
    - BS EN ISO 175: Plastics – Methods of test for determination of the effects of immersion in liquid chemicals.
- To assess long-term mechanical behaviour:
    - BS EN 899-1 & BS EN 899-2: Plastics – Determination of creep behaviour, Tensile Creep & Flexural Creep by three-point loading;
    - BS EN ISO 22088-1: Plastics – Determination of resistance to environmental stress cracking (ESC).
- For the effect of weathering:
    - BS ISO 29664: Plastics – Artificial weathering including acidic deposition;
    - BS 2782-5/Method 552A/ISO 4582: Methods of testing plastics – Optical and colour properties, weathering – Determination of changes in colour and variations in properties after exposure to daylight under glass, natural weathering or laboratory light sources;
    - ASTM D 2565: Standard practice for Xenon-Arc Exposure of Plastics Intended for Outdoor Applications.

2.3.2 Ageing of Nanocomposites

Some results in the area of ageing of nanocomposites have already been published in the literature. The major conclusions regarding polymeric materials reinforced by nanoclay are as follow.

Kiliaris et al. used ageing in an air circulating oven in order to compare lifetime of clay-reinforced polyamide-6 to neat polyamide-6. They found that the integration of a nanofiller prevented the material from the degradation during processing,

and improved its durability but also decreased the crystallinity with ageing [67]. However, the use of Montmorillonite for filling different polymers, such as polypropylene, polyethylene or EPDM was found to accelerate the degradation by photo-oxidation compared to the neat polymers [68]–[71]. This was due to the iron impurities present in nanoclay and the bad alkyl-ammonium cation exchanges [68].

Some other studies report that the phenomenon of volatilization began at an higher temperature for nanocomposites than for micro-composites [72]. It can be explained by the fact that the nanoclay acts as a heat barrier and insulator and avoids the volatile products generated during the materials decomposition to be transported [72]. It was shown that the addition of nanoclay into a polymeric matrix tends to improve the thermal stability of the materials under inert and oxygen atmosphere [72]. However, nanocomposites show higher degradation under UV light than neat polymers [72] as it increases the risk of chain scission [68]. The presence of clay inside the matrix will interfere with oxygen, so O_2 will stay longer in contact with the matrix and the degradation will be faster [38]. For example, polyethylene samples and polyethylene nanocomposites (filled with organically modified Montmorillonite) were exposed to UV light under oxygen atmosphere. After 200 hours of irradiation, the nanocomposites were significantly more degraded [36].

With regards to polyamide-6, it was found that the addition of nanofillers accelerated the degradation of the materials. With the presence of clay, the nanocomposites started to degrade at 240 °C, while the virgin polyamide-6 did not [73]. And, in general, polyamide-6 nanocomposites were found to degrade easily compared to neat polyamide-6 [74]–[77]. The degradation of polyamide-6/nanoclay was reported to be due to unsaturation, hydrolysis and the onium nature of the surfactant [75].

Overall, it can be concluded that the ageing of polymeric-matrix nanocomposites led to significant changes in the behaviour of the materials, and often had a detrimental effect. So, the study of ageing is indispensable in order to have an overview of the life cycle of any product containing nanofillers. Also, even if the

degradability of nanocomposites has been well studied, especially for the polyamide-6 nanocomposites [38], from a health & safety point of view some gaps still exist. For example, the changes of physio-chemical properties of nanoparticles and their ability to be released during post ageing solicitations had not been studied.

2.4 Release and Control of Nanosized Particles from Nanocomposites

Despite all the good qualities of nanoparticles, the risks of using nanocomposites to human health and environment are not well known [78]–[85]. But, it is known that during their life cycle, nanotechnology-based products will suffer from different mechanical stress situations and physical or chemical ageing [80]. These different situations can lead to a release of nanosized particles and changes of nanoparticle characteristics [86], [87]. So, it is essential to take into account the whole life cycle of a product in order to assess the performance of nanoproducts related to environmental sustainability [88], [89].

2.4.1 Nanoparticles Toxicity

The risk to human health and environment due to the use of nanocomposites is not well known [78]–[85]. However, some studies done on animals have raised concerns about the potential risk associated with the use of nanocomposites [90], [91]. Also, studies about human exposure have already proved that nanoparticles can be hazardous to human health [92], [93]. For example, inhalation of Carbon NanoTubes (CNTs) can have harmful effects on health: they facilitate blood coagulation, granuloma formation or lungs' inflammation [94], and nanosilver easily accumulates in kidneys or other tissues, especially on female subjects [95]. Engineered nanoparticles were also found to be harmful for the environment. ZnO nanoparticles are toxic for both aquatic and terrestrial species even at low quantity (1 mg/l is enough) [96] and TiO_2 nanoparticles are considered as a risk for the aquatic environment [97].

2.4.1.1 Parameters defining Nano-Objects Toxicity

To evaluate the risk of nanomaterial use, two areas need to be determined and combined: the exposure and their hazard potential (i.e. toxicological properties) [98].

For bulk or micro materials, toxicological properties are defined in term of mass, i.e. the limits are defined by the quantity, in grams, that you are exposed to during a given time. On the contrary, for nanomaterials, toxicity is directly linked to their physio-chemical properties. It has been established that the following characteristics influence the toxicity levels of the nanomaterials [99], [100]:

- **Size:** as seen before, the reduction in particle size increases the surface area to volume ratio, and so enhances toxicity per mass unit, and therefore are more likely than bigger particles to penetrate deeper into lungs, internal organs or blood-brain barrier [91], and to cause inflammation and epithelial damage [101]. For example, TiO_2 nanoparticles were found to be much more harmful in terms of pulmonary-inflammatory neutrophil response than fine TiO_2 [91];
- **Shape**: the shape, just as the size, influences the surface area to volume ratio, and so toxicity per mass unit. Also, the shape influences the possibility of nanofiller to adhere to human tissues, cellules…;
- **Chemical composition**: chemical properties of nanomaterials are of importance to determine their toxicology [87]. For example, it was proved that carbon black was more harmful in terms of inflammation and epithelial damage than TiO_2 nanoparticles [101];
- **Surface modification and charge**: an enhanced surface area was described as a possible cause of tissue inflammation [99]. Surface modifications such as by functionalization of single-walled carbon nanotubes [102] or coating of iron oxide nanoparticles (SPION) [103] were used in order to reduce cytotoxicity of nanomaterials;
- **Solubility and persistence**: a low solubility or degradability of nanomaterials allow them to persist in biological systems for longer time, and so increase the exposure time of toxic substances [99].

Exposure to nanoparticles may happen in the following three ways: inhalation, ingestion or dermal penetration [104], [105]. The most likely to occur is through inhalation [105], but data related to monitoring exposure of nanomaterials during the life cycle of nanomaterials is not available for most of the scenarios. Indeed, the number of scenarios to study is extremely wide. The different mechanical or chemical stress situations, such as drilling, cutting, ageing, or abrasion, to analyse crossed with the number of engineered nanomaterials/matrix combination existing lead to a considerable amount of work. Also, the behaviour of nanomaterials with respect to living systems is not fully understood [106].

2.4.2 Importance of the Life Cycle Analysis

The ISO 14040:2006 standard defines the Life Cycle Assessment (LCA) as the compilation and evaluation of the inputs, outputs and the potential environmental impacts of a product system throughout its life cycle [107]. In other words, it is the analysis of the impacts of a product on its environment during the different stages of its life (from the acquisition or production of the raw materials, to its disposal as a waste or recycling).

Currently, studies evaluating the potential risk to human health and environment only consider pristine engineered nanoparticles, but it is known that during their life cycle, nanotechnology-based products will undergo different mechanical stress situations and physical or chemical ageing. These different situations can lead to a release of nanosized particles but also to changes of nanoparticle characteristics [86], [87]. So, the nanoparticles released during the LCA can be very different, in terms of shape, chemical composition, or surface modification compared to the pristine engineered nanoparticles (ENP) integrated in the matrix as shown in Figure 7 [79] and it is essential to take into account the whole life cycle of a product in order to assess the relative performance of nano-products regarding environmental sustainability [88], [89].

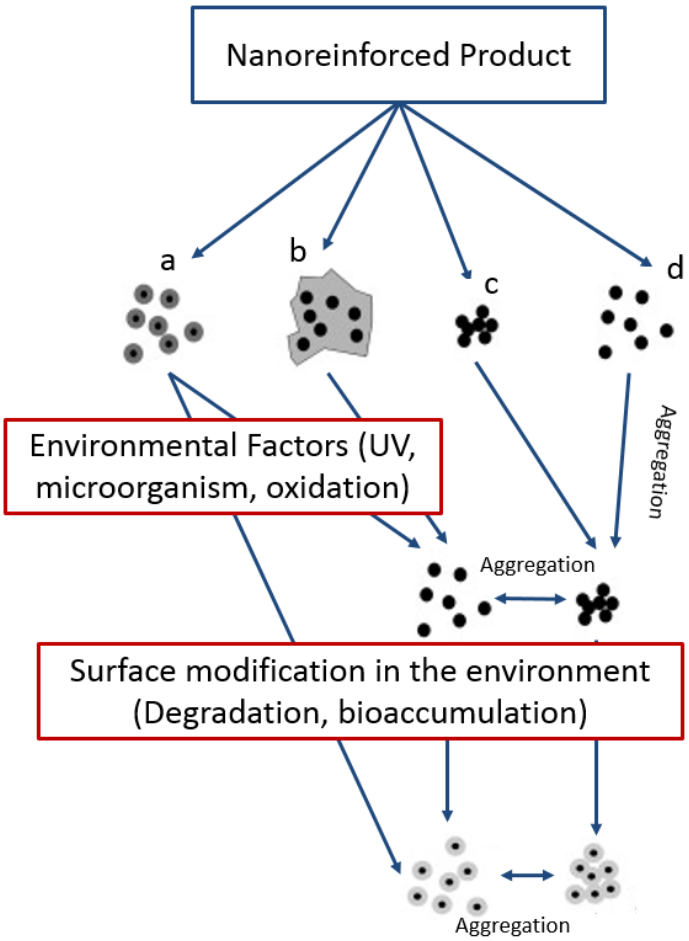

Figure 7: Release of Nanoparticles from Products and (Intended or Unintended) Applications: (a) Release of Functionalized Nanoparticles, (b) Release of Nanoparticles Embedded in a Matrix, (c) Release of Aggregates of Nanoparticles and (d) Release of Free Nanoparticles. Environmental Factors (e.g. Light, Microorganisms) results in Formation of Free Nanoparticles that can Undergo Aggregation Reactions, Moreover, Surface Modifications (e.g. Coating with Natural Compounds) can affect the Aggregation Behaviour of the Nanoparticles [79]

Also, exposure is a key factor to assess the risk associated with nanomaterials [87]. Engineered NanoMaterials (ENMs) have various applications, and so interact in different ways with the environment. Koehler et al. [108] estimated that the amount of nanoparticles released from a nano-product depends of the content of nanofillers in the product, the product's lifetime, the manufacturing process of the product and the use of it. So, for a good assessment of the exposure scenarios and health & safety risks, it is the life cycle of the nanoproducts

containing nanomaterials which need to be studied [88]. The life cycle of nanoproducts can be described in 3 main stages: production of nano-objects and nanomaterials, manufacturing and use of nanocomposites and the end-of-life (recycling or waste).

2.4.2.1 Manufacturing of Nano-Objects and Nanomaterials

Exposure measurement is necessary in order to assess acceptable exposure levels and so to implement correct Health & Safety regulations. Exposure studies and measurement of nanoparticles was carried out at companies or laboratories producing engineered nanomaterials [109]–[113]. An overview of the different studies found in the literature is presented Table 2. They can be classified in two different types: real exposure measurements carried out in industry and laboratory experiments, aiming to reproduce an industrial process but with a considerable reduction of the background noise. The results of these studies indicated that workers were most likely to be exposed to free ENMs during the production and the handling of dry powders.

Table 2: Release Scenarios with regards to Manufacturing and Handling of Nano-Objects/Nanomaterials found in the Literature

Nano-objects	Activities	Used Equipment[1]	Ref.
Carbon Black	Reactor & Pelletizing	SMPS, APS & TEOM	[114]
Carbon Black, MWCNT, Fullerenes	Probe sonication & weighting	CPC	[115]
SWCNT	Handling	CPC & OPC	[116]
Fumed silica	Bag emptying	SMPS or ELPI & CPC	[117]

[1] *SMPS: Scanning Mobility Particle Sizer; APS: Aerodynamic Particle Sizer; TEOM: Tapered Element Oscillating Microbalance; CPC: Condensation Particle Counter; OPC: Optical Particle Counter; ELPI: Electrical Low-Pressure Impactor; MEAD: Modified Electrical Aerosol Detector; NSAM: Nanoparticle Surface Area Monitor; FMPS: Fast Mobility Particle Sizer; FPSS: Fast Particle Size Spectromer; UNPA: Universal NanoParticle Analyzer*

Carbon Black	Packaging, Warehouse & Pelletizing	MEAD, NSAM & SMPS	[118]
Silver	Liquid phase process & Handling	SMPS	[119]
CNT, CNF, Fullerenes	Production (arc reaction, sweeping & vacuuming)	SMPS & CPC	[113]
Fullerenes	Production (bagging & agitation)	SMPS & OPC	[110]
MWCNT	Production (synthesis by Chemical Vapour Deposition)	FMPS & APS	[120]
CNF	Production, Mixing, Drying & Thermal treatment	CPC, ELPI & FPSS	[121]
Silicon nanoparticles	Production (generation in reactor, collection, bagging, packaging & cleaning)	UNPA, FMPS, NSAM, CPC & SMPS	[122]
CNTs	Mixing with polymer, Extrusion, Water cooling & Pelletizing	UNPA	[122]
CNTs	Production (by CVD) & Handling	FMPS & CPC	[109]
MeO	Production, Handling, Packaging & Cleaning	CPC & SMPS	[123]
CNFs	Handling & Mixing of CNFs	CPC & ELPI	[112]
TiO_2, SiO_2, WO_3, CU/ZnO, Cu/SiO_2	Production (Flame Spray Pyrolysis)	SMPS, CPC, DustTrakTM & SidePakTM	[124]
ZnO	Production (Mixing into water, handling & spraying)	SMPS & CPC	[125]
Lithium titanate metal oxide	Wet milling & Spray drying	CPC & OPC	[126]
Nanofillers	Vapour Deposition Process (PECVD & PVD) & Polymers extrusion	SMPS	[127]
Al_2O_3	Twin screw extrusion	FMPS	[128]
CNFs	Production of composite material, chemical treatment, packaging	CPC & OPC	[129]
MWCNT, Carbon nanopearls	Chemical Vapour Deposition		
Fullerenes, MWCNT	Weighing, Mixing & Sonicating		
TiO_2	Weighing & Transferring		
Mn, Ag, Co and Fe oxides	Gas phase condensation reaction		

TiO_2 & Ag	Production (Chemical synthesis & ICPA)	SMPS	[130]
TiO_2 & SiO_2	Handling (Free fall)	ELPI	[131]
TiO_2, SiO_2, Fe(OH), Al_2O_3	Handling	FMPS & APS	[132]
OMMT	Handling	FMPS & APS	[133]
SWCNT, MWCNT, Fullerenes, ZnO, TiO_2	Handling	OPC, APS, CPC & SMPS	[134]
MWCNTs	Aerosolization by atomizing and shaking	SMPS & APS	[135]
CeO_2, TiO_2, TiZrAlO, $SrCO_3$	Simulation of pipe leak	SMPS	[136]
Al_2O_3	Twin screw extrusion	FMPS	[137]

Also, release and exposure to nanoparticles is related to the mechanical or chemical process undergone by the material and the type of materials. Depending on the type of nanofillers, the production consists of milling and grinding of bulk material or starts from nucleation with particle growth by condensation and/or coagulation [98]. In the second option, the release of nanosized particles is influenced by two parameters:

- production via the gas [122] or liquid phase [119];
- production in an open [123] or closed process [114].

In general, compared to other processes, production of nanomaterials via liquid phase process was the safer option as it was less likely that the nanomaterials would be inhaled during the processing. However, more work needs to be done to establish the relative ‘safety’ of the processes as Park et al. [119] found that nanoparticles and agglomerates were released in the air from the reactor during production of silver nanoparticles by liquid phase. Also, the number concentration of nanoparticles was higher than for nanoparticles release during handling of a dry powder of silver nanoparticles.

Production in an open process results in high concentration of airborne nanoparticles which are breathable by workers [123]. On the other hand, in the case of a closed process, several studies found that enclosures are efficient and particle concentrations are negligible outside it [109], [114], [118], [122]. For

example, it was shown [114] that the release of nanoparticles was negligible during production of Carbon Black in a reactor. The same study points to the fact that preventive maintenance is necessary in order to keep normal operating conditions. Indeed, after a leak in the pelletizing area, the number concentration of nanoparticles was found to be around 106 particles/cm^3. Similar conclusions were drawn by Wang et al. [118] who studied nanoparticle exposure in a Carbon Black manufacturing industry.

Also, several studies point the fact that ventilation and good enclosure are key factors in order to reduce the workers' exposure to nanoparticles released during production [111], [116], [120]. For example, Han et al. [111] found that an enclosure and exhaust ventilation could reduce the nanoparticles concentration from around 180 CNT/cm^3 to 0.05 CNT/cm^3 during blending of MWCNTs. Usage of a fume hood during synthesis of SWCNTs in a furnace by chemical vapour deposition was also demonstrated to efficiently remove the released nanoparticles. Indeed, the amount of nanoparticles was negligible (2000 particles/cm^3) outside the fume hood, at the breathing zone, compared to a concentration of 10^7 particles/cm^3 measured inside the fume hood, next to the source [120].

Production of engineered nanomaterials also generates waste. Characterisation of this waste is not available [88] and so the safe disposal process is also not defined. Breggin and Pendergrass [138] reported that the distinction between normal waste, hazardous waste, waste for incineration or for landfilling, in order to define these waste was not clear. However, some countries have made significant progress in the last few years. The British Standard Institution, for example, published in 2012 a guide for "Disposal of manufacturing process waste containing nano-objects" [139]. This guide defines how to treat nano-objects containing waste according to their phases (solid or liquid) and their characterization (hazardous or not, water soluble/insoluble). Also, behaviour regarding contaminated wipes, clothing and filters is defined. In United States, disposal and waste management of nanomaterials is regulated by a law named Resource Conservation and Recovery Act, subtitle C, which covers hazardous

waste in general and ensure their correct handling, storage, transportation and disposal [140].

2.4.2.2 Machining of Nanomaterials Parts and Usage Phase

Recent studies have shown that nanoparticles get released from polymer-matrix nanocomposites during the functional life cycle of polymer products [141]–[148]. Not much information is available on this subject. In 2014, Froggett et al. made an inventory of 54 studies about the release of nanomaterials from solid nanocomposites [149] with only half of them being controlled experiments, and 23 on machining scenarios.

However, the number of studies in this field is increasing quickly. In the recent past, researchers have investigated the release of nanoparticles in different mechanical stress situations such as shredding, drilling, sanding, and abrasion of nanocomposites [147], [148], [150]. These situations are supposed to represent different common machining operations of nanoproducts. Table 3 presents the different release scenarios (for machining and usage phase of nanocomposites and nanocoated materials) that can be found in the literature.

Table 3: Release Scenarios found in the Literature for Machining and Usage Phase of Nanomaterials Parts

Investigated Nanomaterial	**Activities**	**Used equipment**[2]	**Ref.**
Composites:			
Polymer/CNT	Dry/wet drilling	FMPS, APS	[141]
Polymer/CNT	Dry/wet cutting	FMPS, CPC	[142]
POM/CNT, PA/SiO_2 & cement/CNT	Sanding, Weathering & Abrasion	SMPS	[143], [144]
Epoxy/CNT	Abrasion	SMPS	[145]
Polymer/CNT	Burning	ELPI	[146]

[2] *FMPS: Fast Mobility Particle Sizer; APS: Aerodynamic Particle Sizer; CPC: Condensation Particle Counter; SMPS: Scanning Mobility Particle Sizer; ELPI: Electrical Low Pressure Impactor; MOUDI: Multi-Orifice Uniform Deposit Impactor.*

Epoxy/CNT	Sanding	CPC	[147]
PP/OMMT	Shredding	DustTrak and FMPS	[148]
Polymer/CNF	Wet sawing	CPC & ELPI	[112]
Epoxy/CNF	Wet sawing & Grinding	CPC & ELPI	[151]
PP/SWCNT	Microgrinding	-	[152]
PA/OMMT & PA/SiO_2	Drilling	SMPS+C	[153], [154]
Epoxy/CNT	Grinding	SMPS+C	[155]
Epoxy/CNT	Sanding	CPC & OPC	[156]
Coatings:			
ZnO	Abrasion	CPC & SMPS	[150]
OMMT	Abrasion	CPC & SMPS	[157]
Fe_2O_3 & ZnO	Sanding	FMPS	[158]
TiO_2	Abrasion	ELPI	[159]
TiO_2	UV light	SMPS	[160]
CNT	Shaving	FMPS	[109]
TiO_2 & Carbon Black	Sanding	FMPS & APS	[161]
SiO_2 & $CaCO_3$	Sanding	APS & FMPS	[162]
CNT	Abrasion	CPC & SMPS	[163]
Powders:			
ZnO & TiO_2	Rotating drum	SMPS, APS & MOUDI	[164]

Sachse et al. studied the release of nanosize particles during the drilling of different polyamide-6 nanocomposites [154] They found that the integration of nanofillers into a polymeric matrix influences the material behaviour, the quantity of particles released during drilling experiments and the physical properties of the nanosized particles emitted. Addition of nanosilica fillers increased the nanoparticles emission by 56 times; however, the nanoclay reduced it by 0.7 times compared to pure matrix.

Wohlleben et al. studied the effect of manual sanding on thermoplastic nanocomposites: PA with 4 wt.% of nano-SiO_2 and POM with 5 wt.% of CNT [143]. It showed that the addition of nanofillers into the matrix does not affect significantly the particle size distribution and the surface chemistry of the released particles. Furthermore, non-free nanofillers (i.e. nanofillers embedded in matrix) were found in the dust generated. Similar results were observed by Vorbau et al. [150] as significant quantity of nanoparticles were not released from ZnO coatings

by abrasion. Also, the engineered nanomaterials were still embedded in larger matrix particles.

The addition of CNTs into polymeric matrix also did not significantly modify the concentration of the released nanoparticle, their size distribution and surface area during dry or wet abrasion of nanocomposites [142]. However, differences were found according to samples characteristics such as composite thickness and polymeric matrix type. Also, experimental set-ups are a crucial point in the release of nanoparticles. Cutting of nanocomposites produced high amount of nanosized and fine particles in dry conditions. Using water and guard around the rotary wheel allowed significant reduction of exposures to nanoparticles.

The release of nanoparticles during the usage phase of nanomaterials has not been researched sufficiently. Only few studies about the use of current nano-products exist as most of the work is focused on laboratory simulation. For example, Kaegi et al. [165] evaluated the emission of TiO_2 nanoparticles used in the exterior paints. The chemical composition of the samples was investigated by EDX, and bulk chemical analysis was carried out in the runoff samples with the ICP-MS method. They found that a significant quantity of nano-TiO_2 particles can be released into the aquatic environment. This study also showed that the amount of nanoparticles released is lower in a two-year old facade than for a freshly painted one.

Few studies are assessing the release of nanoparticles in a controlled environment [155], [157]. A closed chamber with HEPA filters were used in these papers. However, the process itself was a source of nanoparticles emission (for example, particles generated by metallic brush motors of a drill) and no control was implemented to reduce this. The particles generated by the process can interact with the particles generated by the materials (agglomerations for example) and influence the results. These methods are not optimal.

2.4.2.3 Recycling and Waste of Nanomaterials

The risk of engineered nanomaterials' release during disposal and recycling of nano-products was evaluated by the Royal Society and Royal Academy of

Engineering [166] and a guide was published by the BSI group: PAS 138:2012 – Disposal of manufacturing process waste containing manufactured nano-objects [139]. Waste incineration and landfill are the most frequent and simplest end-of-life of waste, and represent 98 % of composites disposal [167]. Unfortunately, nowadays not much information is available about the behaviour of engineered nanomaterial during this process: how many particles stay in the slag or become airborne, do they degrade due to high temperature, and others important questions remain unanswered [88].

CNTs have a decomposition temperature higher than polymer materials and can be stable to temperature up to 600 °C [168] and then in case of incineration they can potentially be released into the environment. Several studies [169], [170] with regards to flame retardancy properties of polymer reinforced with CNTs showed the presence of free CNTs or CNT network in the remaining char, which then could be released into environment in the case of an accidental fire or waste incineration. One study also revealed the presence of significant quantities of free CNTs and agglomerates of CNTs in the air following the combustion of CNT/ABS composite [171]. Uddin et al. [172] also found CNFs in the remaining char after combustion experiments.

2.4.2.4 Challenges in Exposure Assessment

The work, and studies cited previously reveal the potential of exposure to nanoparticles but are not able to provide a quantitative assessment of exposure to nanoparticles [117]. Some challenges still lie ahead.

A complete analysis of the possible exposure scenarios is necessary. However, the number of cases according to the nanofillers, the matrix used and the process studied to release nanoparticles (cutting, abrasion, handling, etc.) makes this task difficult. It is important to define what parameters influence the release of nanoparticles. For example, as it is shown by Schneider et al. [132] with a same process (rotating drum), the size distribution and the total number of particles released depended on the nanopowder type tested. Processing fumed silica with a rotating drum released around 14.3×10^{-7} particles with a mean diameter of

219 nm while the same process for ultrafine TiO_2 resulted in a release of $344.8x10^{-7}$ particles with a mean diameter of 200 nm.

Also, there is no standard method of measurement and characterization of nanoparticles released during mechanical stress situations. The devices used varied in every study as along with the chamber or point of measurement which made it impossible to compare the results obtained by two different studies.

2.5 Methods of Measurement and Collection of Airborne Nanoparticles

2.5.1 Methods of Measurement of Airborne Nanoparticles

The air monitoring instruments typically used to measure airborne particles are: Condensation Particle Counter (CPC), Scanning Mobility Particle Sizer (SMPS), Fast scanning Mobility Particle Sizer (FMPS), Electrical Low Pressure Impactor (ELPI) and Tapered Element Oscillating Microbalance (TEOM). The choice of the equipment mainly depends of the size range and release scenario. Lack of standard set ups and standardised sampling protocols at present make the comparison between different studies' results difficult. A summary table of the different equipment available for airborne measurement established by Sachse [173] was reproduced in Table 4.

Table 4: Summary Table for Equipment Used to Measure Airborne Nanoparticles [173]

Equipment	Measurement Parameters	Size range [µm]	Response time [s]	Sample flow [1/min]
CPC	Number concentration	0.003-0.025	4	0.3-3
SMPS	Size distribution, number concentration	0.0025-1	30-600	0.2-4
FMPS	Size distribution, number concentration	0.0056-0.56	1	10
ELPI	Size distribution, number concentration	0.03-10	<5	10 or 30
TEOM	Mass concentration	2.5-10	0.5	0.5-5

The advantages and disadvantages of all the instruments for aerosol measurement also established by Sachse [173] can be found Table 5.

Table 5: Advantages and Disadvantages of the Main Equipment for Airborne Measurement [173]

Instrument	Advantages	Disadvantages
CPC	Portable CPC available (small dimensions) Some models compatible for use with SMPS	Only number concentration measured For some models external vacuum source needed
SMPS	Highest-resolution (up to 64 channels/decade)	Retarded respond time
FMPS	Use unipolar charger (eliminate the need for a radioactive neutralizer) Real-time particle size distribution and total concentration	Only for monitoring particle size up to 0.56 µm Particle concentration vary by size
ELPI	Possibility for chemical characterisation of size classified samples Real-time particle size distribution and total concentration	High acquisition cost High sample flow rate & heavy (35 kg)
TEOM	Real-time mass concentration averages Only instrument that measures mass concentration	Weight Unstable behaviour when operating with particle free air

Scanning Mobility Particle Sizers (SMPSs) was noted to be the instrument with the highest accuracy in the determination of particle size distribution [174]. The disadvantage of this equipment is the lag in response time, which make the results less meaningful if the size distributions change quickly [174]. Combined a SMPS, with a CPC can increase the accuracy. Indeed, CPCs are some of the most accurate instruments for measurement of particle number concentration [174].

For the SIRENA project, drilling and impact of different polymer-matrix nanocomposites was tested using protocol established in NEPHH project. In reference to previous projects: Project NEPPH [11], Project Nanopolytox [10] and some studies conducted by Wohlleben et al. [143], Sachse et al. [175] and Njuguna et al. [176], the methodology chosen to evaluate the exposure to

nanoparticles generated throughout the life cycle of nanotechnology based products used a SMPS combined to a CPC.

2.5.2 Methods of Collection and Sampling of Airborne Nanoparticles

An issue with all the devices mentioned before is that they do not distinguish manufactured ENPs (Engineered NanoParticles) and ultrafine particles from background air. In order to know the chemical and physical properties of the dust released during different mechanical stress situations several techniques exist, such as Scanning Electron Microscopy (SEM), Transmission Electron Microscopy (TEM), or Dynamic Light Scattering (D-LS). Filtration is one of the solutions but due to the nanosize of the samples, and to the ease of contamination, other solutions which directly sample the aerosol on TEM/SEM grid are preferred. The characteristics of different sampling equipment summarised by Sachse [173] are available Table 6.

When SMPS+C is used for measurement of airborne particles an Electrostatic Precipitator from GRIMM is the most suitable sampling instrument.

Table 6: Sampling Instruments for Nano-Sized Particles [173]

Instrument	Model / Manufacturer	Size range [nm]	Sample flow rate [l/min]	Sampling substrate	Additional instruments
ESP (Electrostatic Precipitator)	5.561/Grimm Aerosols	0.8-1100	0.3 to 5	SEM/TEM Ni-grids	DMA
NAS (Nanometer Aeorosol Sampler)	3089/TSI	2-100	0.2 to 2.5	SEM/TEM Ni-grids	DMA
LPI (Low Pressure Impactor)	DLPI/Dekati	30-10µm	10 or 30	Collection plates	N/A
BAS (Button Aerosol Sampler)	Different Filter sizes/SKC	<100µm	4	Filter	N/A

2.5.3 Conclusion

The equipment used in order to estimate the quantity of nanoparticles released in the air is also the source of error for an accurate measurement. The method applied to estimate the size of the particles makes the assumption that the particles 'shape is spherical which is usually not the case. Different types of particle counters do not allow the classification of nanoparticles according to their composition. This means that the quantity of nanoparticles measured can include free engineered nanoparticles, nanoparticles embedded into matrix, agglomerates but also other nanosized particles present in the environment such as nanoparticles produced by the process or some naturally present in the atmosphere. It was for example shown that particles under 50 nm released during sanding process were mainly due to the sander itself [161]. For now, it is necessary to combine 'activity-based monitoring' method with a second method in order to clarify the nature of particles measured [126], [128]. Collection, sampling, filtration and analysis of samples allow characterisation of the physico-chemical properties of airborne particles with microscope techniques such as SEM (Scanning Electron Microscopy), TEM (Transmission Electron Microscopy) and XRD (X-ray Diffraction). However, these techniques are time consuming, expensive and difficult to apply to real industrial cases. Once again, standardisation of the method is needed.

As mentioned by Yeganeh et al. [113] background noises, due to type of other activities carried out in the plant/lab, number of people present, ventilation, workers techniques, outdoor particle concentrations [113], carbon brushes from different types of machine's motors [110] were often reported as a source of variability in the results. Again, the actual solution is the characterisation of the particles released in order to differentiate the one produced by the materials, and the external ones. But this solution does not provide a quantitative result. The other solution is to work in a perfectly clean room or chamber where only the particles induced by the process can be measured but again a standard method does not exist yet.

Five main issues can be identified for the measurement or sampling of airborne particles:

- Particle losses: small particles, especially the ones smaller than 10 nm, have a larger diffusion coefficient, which can lead to a particle loss in the sampling tubes [177];
- Particle shapes: for the measurement of size distribution with an equipment based on an electrical mobility principle or optical properties, it is assumed that particles are spherical which is not always the case [98];
- Background noises: As the particles counted are nano-size, the entire environment can affect the results, e.g. the humidity or the movement in the room, etc. Especially, some studies report that the machine itself (in this case, a sander) can be the source of nanoparticles [133], [161];
- Low volume flows: first, this can be a cause of particle losses [177], secondly it involves a longer sampling time;
- Contamination of sampled particles: filtration can cause a lot of contamination, especially due to evaporation. Also, the electrostatic precipitators can create ozone and oxidant ions due to the high-voltage electric field, which can react with the particles.

2.6 Health and Safety Practices, Standards and Regulations

The introduction of a novel technology on the market results in the creation of new gaps in regulations. The Commission of the European Communities evaluated in 2008 [178] that health, safety and environmental risks caused by nanomaterials are currently covered by the legislation under REACH. However, this point of view is not shared by everybody. The European Parliament resolution on regulatory aspects of nanomaterials judged that the current legislation is insufficient and too limited to include the health and safety aspects of nanomaterials [179].

The following part aims to review the practices, standards and regulations in relation to nanomaterials in order to evaluate the current situation and gap to focus on in the future.

2.6.1 Actual Industrial Practices

More than 1800 consumer products based on nanotechnology were on the market in 2015 according to the Project on Emerging Nanotechnologies (PEN) inventory [6], [7]. However, the laws and regulations that govern these products and their use were not appropriate from a Health & Safety point of view. New regulations need to be created and adopted, and this process will take several years. Helland et al. [99] investigated the actual practices of industries regarding nanomaterials and their risks. A survey was conducted on 40 companies. It was reported that less than 10 % investigated the potential risk for environment or human health over a part of life cycle of nanoproducts, only 32.5 % performed risk assessments where nano-particulate materials were involved, and 25 % conducted toxicity studies. In general, it was shown that industries were not totally aware of risks related to nano-particulate materials, no standard procedures existed and such measures were not of high priority for them. Gerritzen et al. [180] reported, following an international survey, that most of the companies dealing with nanomaterials applied safety practices based on conventional practices for chemicals and not specifically for nanomaterials. Furthermore, this survey showed that companies were expecting industrial and governmental guidance on risk assessment and Health & Safety practices about nanomaterials from the authorities.

The importance of the principle of precaution and of safer practices for production and use of nanomaterials was highlighted during several conferences, clusters or workshops about nanomaterials (Nanosafe 2014 [181], Workshop on the Second Regulatory Review on Nanomaterials [182]). Jamier et al. [100] advised a strategy for production and use of nanomaterials in industry based on two principles of precautionary approach. The first principle was the safety-by-design which consists of the evaluation of risk of nanomaterials at an early stage of product design, and so an adequate choice for materials, design and process of nanoproduct safe for the consumer. However, this will only be possible when data regarding toxicity and risk of nanomaterials will be available. This is a difficult task. There is limited amount of data available on the release scenarios during nanomaterials life cycle. Only a few papers discuss the ways to control the

release of nanosized particles from nano-products [183]. Reijnders [183] lists the different options to reduce hazards from release of nanoparticles. These include, but were not limited to, adherence of nanoparticles in nanocomposites, including persistent suppression of oxidative damage to polymer by nanoparticles, changes of nanoparticle surface, structure or composition, and design changes leading to the release of relatively large particles. The second principle recommended by Jamier et al. [100] is called the ALARA (As Low As Reasonably Achievable) principle and consist of preventive and protective measures to protect workers during nano-objects and nanomaterials production based on the ones used to reduce and control workers exposure to hazardous aerosols.

2.6.2 Standard Related to Nanomaterials

A guide [184] produced by BSI (British Standard Institute), suggested exposure limits values for different types of nanomaterials, defined by mass:

- Fibrous materials: 0.01 fibre/ml, value realized by scanning electron microscopy;
- Nanomaterials based on carcinogenic, mutagenic or reproduction toxic substances: exposure limits 10 times inferior for the nanometric substances than for the substances;
- Insoluble nanomaterials: 0.066 times the exposure limits for the chemical substances in micro-sized;
- Soluble nanomaterials: 0.5 times the exposure limits for the micro-form.

However, as it was mentioned previously (Section 2.4.1), a definition of toxicity by mass is not suitable for nanomaterials. The important parameters are size, shape, chemical composition, surface modification and charge, and solubility and persistence.

The European Committee for Standardization (CEN) and the International Organization for Standardization (ISO) are two organisations developing standard and have recently started to work specifically on nanomaterials. Four

working groups had been defined by these organisations on this subject in order to split and focus on the most urgent activities [185]:

- “Terminology and nomenclature: define and develop unambiguous and uniform terminology and nomenclature in the field of nanotechnologies to facilitate communication and to promote common understanding;
- Measurement and characterization: the development of standards for measurement, characterization and test methods for nanotechnologies, taking into consideration needs for metrology and reference materials;
- Health, safety and environment: the development of science-based standard in the areas of health, safety and environmental aspects of nanotechnologies;
- Material specifications”.

Nowadays, we can list 43 ISO standards link to ‘nano’ or ‘nanotechnologies’. Around half of these standards were published in the last 4 years, which shows the increase interest in nanotechnologies. They can be classified in different categories: characterisation of nano-objects (16), terminology and nomenclature (14), toxicity of nano-objects (6) or health, safety and environment (4). The 3 standards remaining concern the exposure and so are particularly of interest for this study. They are:

- ISO/TR 27628:2007- Workplace atmospheres. Ultrafine, nanoparticle and nano-structured aerosols. Inhalation exposure characterisation and assessment.
- ISO 10801:2010 – Nanotechnologies. Generation of metal nanoparticles for inhalation toxicity testing using the evaporation/condensation method.
- ISO/TS 12025:2012 – Nanomaterials. Quantification of nano-object release from powders by generation of aerosols.

ISO/TR 27628:2007 is a technical report referencing the equipment which can be used as well as the properties that can be characterise for the aerosols. ISO 10801:2010 aims to measure the airborne nanoparticles emitted during the

process of evaporation/condensation method which is a process to generate nanoparticles. And finally, ISO/TS 12025:2012 is especially interesting as it describes how to choose the measurement device and the sampling procedure to follow. However, the document addresses release of nano-objects from powders and not from actual nano-products as solid parts undergoing mechanical stress situations.

Simulation of the release of nanosized particles during experimental processes in several studies [132], [133], [143], [145], [150], [157], [159] used some existing standardized procedures. These procedures address abrasion and dustiness tests. Moreover, the standards used are the EN-15051 (Workplace atmospheres. Measurement of the dustiness of bulk materials. Requirements and reference test methods) [186] for the dustiness test and the ISO 5470-1:1999 (Rubber- or plastics-coated fabrics. Determination of abrasion resistance. Taber abrader) [187] and the ASTM C1353-07 (Standard Test Method Using the Taber Abraser for Abrasion Resistance of Dimension Stone Subjected to Foot Traffic) [188] for the abrasion tests. These standards only cover the equipment to use and procedure to follow in order to carry out the mechanical tests but do not mention the measurement of nanoparticles released or their collection.

There is currently 25 standards under development concerning ‘nano’ or ‘nanotechnologies’ when searching on the ISO standard website. Again, the majority of them is related to the terminology or the characterisation of nano-objects. Two standards under development are particularly interesting for the exposure assessment:

- ISO/AWI TR 21386 – Nanotechnologies. Considerations for the measurement of nano-objects, and their aggregates and agglomerates (NOAA) in the environment.
- ISO/NP TS 21623 – Workplace exposure. Assessment of dermal exposure to nano-objects and their aggregates and agglomerates (NOAA).

2.6.3 Regulations around the World

2.6.3.1 European Union

In 2007, Chaudhry et al. [189] reported the lack of regulation specific to nanotechnology in the European Union, or globally [190], and the fact that they are covered by regulation on conventional chemical substances was denounced. The European Union regulation REACH (Registration, Evaluation, Authorisation & restriction of CHemicals) does not even explicitly refer to nanomaterials. This kind of materials was supposed to be regulated by the fact that they can be covered by the definition of a chemical substance. However, the EU Scientific and Advisory Committees recommends to perform a case-by-case risk assessment on nanomaterials, according to their properties and specific uses. Indeed, the Control of Substances Hazardous to Health (COSHH) regulation which controls the hazardous substances in the workplace is based on Occupational Exposure Limits (OELs) for individual substances. This limit is calculated with the mass of inhaled particles, which is not relevant for nanomaterials as it is now known that the toxicity of nanoparticles is related to their size and other physico-chemical characteristics [129], [166], [191]. Moreover, nanomaterials are still not classified as new substances under the EINECS (European Inventory of Existing Commercial Substances) but are considered as the same substances as the bulk version. The lack of information about nanomaterials is changing as the European Chemicals Agency (ECHA) published a guidance on information requirements and chemicals safety assessment, including recommendations for nanomaterials in 2012 [192].

In European Union, there are directives that regulate manufacturing and commercialization of any products [193]–[196]. Safety and health of workers at workplaces is defined by the EU directive 89/391/EEC [196] to ensure a high level of protection to workers during their work by implementation of preventive measures. This includes exposure to nanomaterials through hazardous substances. The Council Directive 98/24/EC [193] presents the protection of workers at work against the risks caused by chemical agents and the obligations related to identification and assessment of risk due to use of hazardous chemical

agents. Nanomaterials are not mentioned in this document. Also, every consumer product is subject to the General Product Safety Directive [192] which imposes risk assessment on their environmental impact and contains provisions for health and safety of workers, consumers, patients, and users. Nanomaterials have to follow this regulation. With regards to the disposal and waste, the Directive 2008/98/EC [191] defined which waste is hazardous, and set obligations on Member States to ensure that the waste treatment is safe regarding human health and environment. Again nanomaterials were not clearly specified. Current legislation is supposed to cover the risk to human health and environment along the life cycle of every product. However, as nanomaterials are not referenced, current practices tend to be insufficient in this regard.

Several others reports have been published [197]–[200] with regards to the lack of knowledge and regulations about nanomaterials and their uses and Kuhlbusch et al. [98] reported the urgent need of standardization for test procedures simulating workplace activities and processes. The Second Regulatory Review on Nanomaterials, published by the European Commission, concluded that one of the actual priorities is to establish validated methods and instrumentation for detection, characterisation and analysis in order to complete information on hazards of nanomaterials and develop methods to assess exposure to nanomaterials [178].

2.6.3.2 U.S.A.

Several reports published by organisations from United States stated the importance of nanosafety for the success of nanotechnology [201], [202]. Also, in United States, the Environmental Protection Agency (EPA) works for the implementation of a Significant New Use Rule (SNUR) which intend to increase the available data about nanomaterials risks and safety. Any entities intending to manufacture or process new nano-products has to submit a basic set of information (chemical identification, material characterisation, physical/chemical properties, commercial use, production volume, exposure and fate data, and toxicity data) to the EPA at least 90 days before the beginning of the activity [203]. With regards to wastes and end-of-life, two laws regulate these issues in United

States: RCRA (Resource Conservation and Recovery Act) and CERCLA (Comprehensive Environmental Response, Compensation, and Liability Act). In theory, these laws cover nanomaterials and nanowastes. However, they were judged to be inappropriate [138]. For example products containing nanomaterials can be considered as household waste and so, non-hazardous. The Environmental Protection Agency recommends implementation of these laws [138] to classify specific nanowastes as hazardous wastes, and the need of research in order to determine if the existing practices for disposing and treating bulk forms of solid wastes are appropriate for the nanoforms of similar chemicals.

2.7 Nanosafety: Future Perspectives

2.7.1 Nanosafety related Projects

The European Commission is investing money in nanosafety related research. The Sixth Framework Programme included 13 projects on nanosafety with a budget of €31 million [106] and one of the 7 priority thematic area was 'Nanotechnologies and nanosciences, knowledge-based functional materials, new production processes and devices' [204]. Following FP6, the 7th Framework Programme for Research and Technological Development was conducting from 2007 to 2013 with an overall budget over €50 billion [205]. Again, one of the ten key thematic areas was dedicated to nanoresearch: 'Nanosciences, nanotechnologies, materials and new production' [205]. Through this programme 34 projects related to nanosafety were financed with a budget of €106 million [106].

Project MARINA and NanoValid were two such projects that concluded at the end of 2015. MARINA (MAnaging RIsks of NAnomaterials) goal was to develop and validate a risk management method for nanomaterials by developing tools to assess the state-of-the-art and the risk management strategy around four areas: materials, exposure, hazard and risk [206]. Project NanoValid's objective was to improve risk and life cycle assessment of nanomaterials including methods for the fabrication, physiochemical characterisation, hazard identification, exposure assessment and dispersion control and labelling of engineered nanomaterials [207]. Also, project QNano (FP7 funded) grouped the most important

nanotechnology, medicine and natural sciences facilities in order to improve and develop nanosafety assessment [208].

The members of the NanoSafety Cluster (initiative of the European Commission Directorate-General for Research to maximise synergies between research projects related to nanosafety) concluded that these projects increased the availability of data on the potential hazard of Engineered NanoMaterials [106]. However, they also raised a number of unknown points to work on [106]:

- The need of information related to exposure of Engineered NanoMaterials and safety of nano-products during their life cycle still exists;
- Standardized methods to assess the exposure of NanoParticles and reference materials for toxicity assessment are a priority for the future research;
- Interactions between NanoMaterials and environment and living systems need to be assessed and understood.

Since 1992, the European Commission funded several nano-related projects through LIFE programme. Between 2012 and 2015, 4 projects were launched in the area of nanomaterials and all of them addressed environmental and safety aspects of nanomaterials. Project SIRENA [12] (SImulation of the RElease of NAnomaterials from consumer products for environmental exposure assessment) was part of this programme. SIRENA's aim was to demonstrate and validate a methodology to simulate the unintended release of nanomaterials from consumer products by replicating different life cycle scenarios, to be adopted by a wide number of industrial sectors in order to get the necessary information for exposure assessment.

Also, the EU Framework Programme for Research and Innovation, Horizon 2020 intends to fund several projects related to the assessment of release and fate of nanomaterials with the coordination of several Small and Medium Sized Enterprises through the Nanotechnologies, Advanced Materials, Advanced Manufacturing, and Processing, and Biotechnology area [209].

2.7.2 Key Area for Future Research

The members of the Nanosafety Cluster defined 4 key areas of research for the next 10 years [106]:

- Nanomaterials identification and classification. Classification should either be done by shape, composition/chemistry, complexity/functionality, or biointerface;
- Nanomaterials exposure and transformation. Exposure and behaviour of nanomaterials needs to be assessed along the life cycle, from the production to the end-of-life, and covering handling, use and ageing;
- Hazard mechanisms related to effects on human health and environment. Research has to be focus on understanding toxicity including grouping, translocation and clearance of nanomaterials, and behaviour regarding vulnerable populations and environment. This is a real challenge considering that nanoparticles can interact with living systems at a molecular or cellular levels;
- Tools for predictive risk assessment and management including databases and ontologies. Standardization of risk assessment method of nanomaterials is the key point of a successful progress of research in this field.

In the United States, different research directions were set in order to identify potential hazards associated with nanotechnology and evaluate risks related to the environment and human health and safety. This key theme research was resumed in seven different questions by the United States Environmental Protection Agency [198]:

- “Which nanomaterials have a high potential for release from a life cycle perspective?
- What technologies exist, can be modified, or must be developed to detect and quantify engineered nanomaterials in environmental media and biological samples?

- What are the major processes/properties that govern the environmental fate of engineered nanomaterials, and how are these related to physical and chemical properties of these materials?
- What are the exposures that will result from releases of engineered nanomaterials?
- What are the effects of engineered nanomaterials and their applications on human and ecological receptors and how can these effects be best quantified and predicted?
- Does agency risk assessment approaches need to be amended to incorporate special characteristics of engineered nanomaterials?
- What technologies or practices can be applied to minimize risks of engineered nanomaterials throughout their life cycle, and how can nanotechnologies' beneficial uses be maximized to protect the environment?"

2.8 Conclusions

Nanomaterials have already invaded the market and research and development centres thanks to their many advantages. However, the Health and Safety aspects and potential risks of this new technology still need to be studied in depth to ensure their continued success.

Concluding this literature review, it is safe to say that the risks of nanomaterials are defined according to two factors: toxicity and exposure. Toxicity of nanomaterials was found to be dependant of different parameters: shape, size, chemical composition, surface modification and charge, and solubility and persistence. This is not in line with the classical chemical substances for which the toxicity is defined by mass. However, current legislations and regulations classify toxicity of nanomaterials in proportion of the toxicity of their bulk substances, then in term of mass. Change of regulations specific to nanomaterials is the first step to be taken.

Route of exposure and behaviour of nanomaterials with regards to human health and environment are also a crucial point to understand. ENMs are different from

nanoparticles released during ageing or mechanical stress situations handle by a nano-product. The assessment of toxicity and exposure need to be done throughout the life cycle of products, and a complete analysis of all the possible exposure scenarios is necessary. Also, standard methods need to be developed in order to have comparable results.

Standards and regulations are actually the heart of the problem. Currently, only one standard explains how to choose the measurement device and the sampling procedure to follow, but it is specific to nanopowders. Standards related to different nano-product forms need to be developed. Also, standardized methods and reference tests should be produced in order to create a reference database to compare results from experiments with new materials and applications.

The general conclusion for this literature review is that considerable efforts and work is needed by both research institutions and government agencies in order to ensure a successful future for nanomaterials.

2.8.1 Gap in the Knowledge

The current work published in the area of exposure to nanoparticles is not able to provide a quantitative assessment of exposure to nanoparticles [117]. Some challenges still need to be tackled:

- A complete analysis of all the possible exposure scenarios is necessary;
- No standardised method exists to measure and characterize nanoparticles released during mechanical stress situations;
- The equipment used in order to estimate the quantity of nanoparticles released in the air can be a source of error for an accurate measurement;
- Background noises were often reported as a source of variability. One solution is to work in a perfectly clean room or chamber where only the particles induced by the process can be measured but again the perfect or standard method or equipment does not exist yet.

- The lack of standard methods for the measurement and collection of released nanoparticles makes the comparison between the results of different studies difficult, and the risk assessment of nano-products by the industry impossible. Also, the guides mentioning exposure to nanomaterials define occupational exposure limits in term of mass. This is not relevant as it is known that toxicity is linked to size and surface area of nanoparticles. Thus, it is necessary to undertake a study to define not only the quantity (mass) but also the quality (shape, size, chemistry, etc.) of nanoparticles released.
- The release of nanoparticles and the evolution of nanofillers after ageing of the nanocomposites have not been studied so far, and it is an important factor to simulate the end-of-life implications of a nanotechnology-based product. Also, even though the ageing of polymers has been studied for a long time, the ageing of polymeric-matrix nanocomposites is still not well known.

The gap in the knowledge graph is presented in Figure 8.

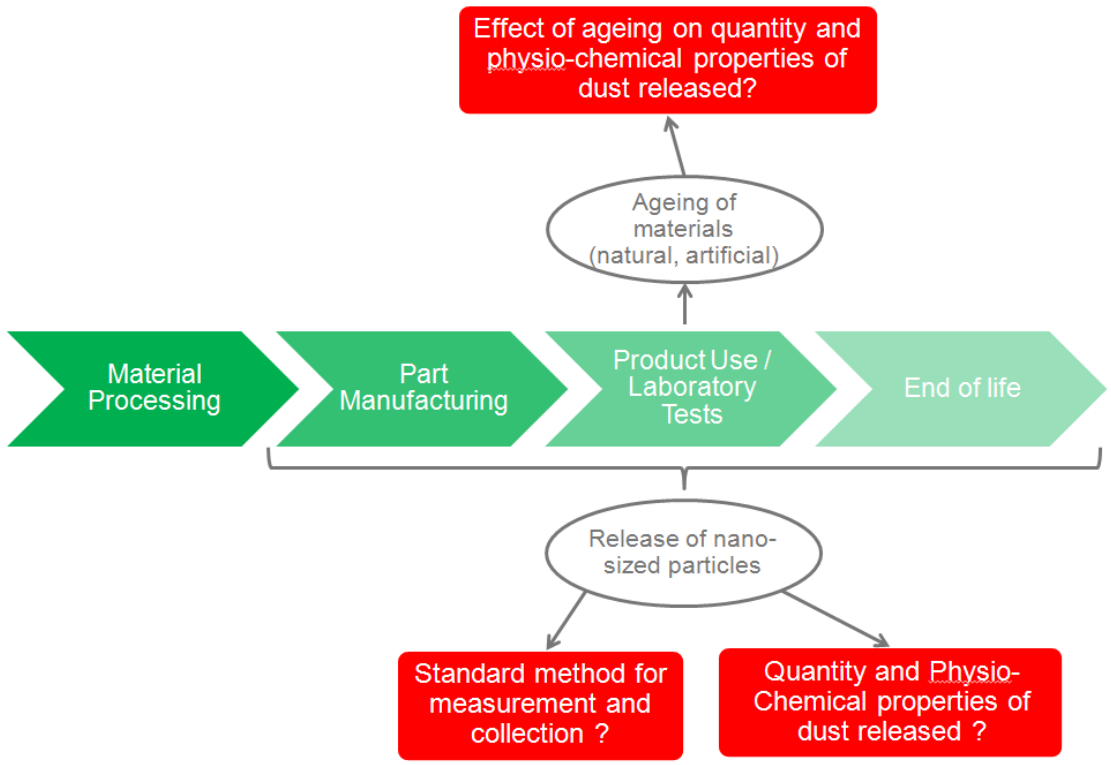

Figure 8: Gap in the Knowledge

2.8.2 Methodology

In order to fill the gap in the knowledge and reach the aim and objectives previously explained, a methodology was defined. The different tasks for the methodology are presented Figure 9.

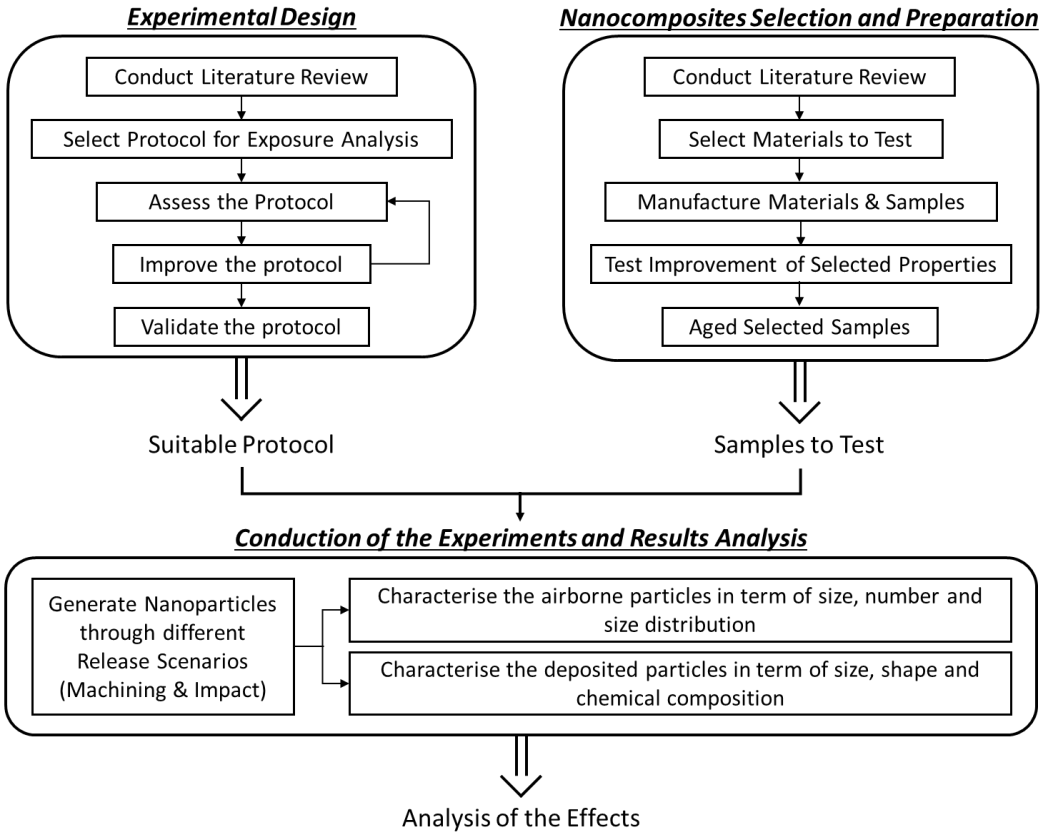

Figure 9: Methodology

A literature review was conducted in order to select the polymer matrices and nanofiller additive combinations to test. The materials and samples selected were manufactured and then tested to assess the improvement in term of mechanical or electrical properties of nanocomposites materials compared to neat polymers. Temperature ageing was also performed on a set of nanocomposites.

In parallel, the literature review helped to select potential exposure scenario to test and existing protocol currently used. Three types of experiments viz. drilling, milling and impact were selected to simulate different potential release scenarios along the life cycle of a nanocomposite component. Drilling and milling are common procedures in different stages of product's usage phase, and impact

recreates accidental or intended fractures. After an assessment of the protocols used in the literature, a new method overcoming the deficiencies observed in the previous ones (high background noise in the measurement, high effect of the process on the measurement…) was set-up, improved and validated.

With a suitable protocol, all types of materials selected were exposed to physical degradation (either drilling, milling or/and impact) in order to generate particles. Deposited and airborne particles collected were characterised taking into account shape, size, chemical composition, number concentration, and size distribution. Following the experimental work, an analysis of the effect was conducted regarding the effect of the materials parameters: matrix type, filler type and percentage, ageing, and the effect of the processes studied.

The following chapters will first present the implementation of a standard method to assess the release of nanoparticles during physical processing of nanocomposites parts (the experimental design). Then, the three next chapters will focus on the three types of experiments conducted: drilling, milling and impact. Each chapter will include the manufacturing process for the materials and samples, as well as their electrical or mechanical properties. This will be followed by characterisation of the particles emitted during physical processing and a discussion about the effect of matrix materials, nanofiller type and percentage, process parameters and ageing on the nanoparticles emitted.

3 IMPLEMENTATION OF A STANDARD METHOD TO ASSESS THE RELEASE OF NANOPARTICLES DURING PHYSICAL PROCESSING OF NANOCOMPOSITE PARTS

In 2014, Froggett et al. made an inventory of 54 studies about the release of nanomaterials from solid nanocomposites [149], of which 23 were dedicated to machining scenarios and only 2 specifically focused on drilling. The common point between the issues related to these studies was mainly the lack of control of the experiments. For example, Koponen et al. [161], [162] studied the release of particles from sanding conventional and nano-based paints coatings. They developed an experiment to replicate the process. However, they themselves raised some deficiencies in their work: the sanding device itself was a source of nanoparticles, and the parameters (pressure applied) were difficult to control.

The aim of this chapter is to develop and validate a method able to measure the dust generated during different physical processing of nanocomposites. For this purpose, an existing method / protocol was replicated (Protocol A). The results and deficiencies observed with this protocol led to the implementation of a new experimental set-up. A characterization and validation of the chamber used for this work was done in order to assess the controllability of the environment and the replicability of the experiments (Protocol B).

3.1 Preliminary Study – Replication of a Previous Protocol (Protocol A)

A preliminary study was carried out in order to assess the protocol and the chamber used during the NEPHH project [11] and presented in two papers [153], [154]. The protocol will be referred to as Protocol A. Only one other study is known to describe the release of nanoparticles during the drilling of nanocomposites, study published by Bello et al. [141]. In this paper, the release of nanoparticles during core drilling of CNT composites was evaluated. Up to $1x10^7$ particles/cm^3 could be generated during these experiments. However, no control over the particles emitted by the process itself was in place.

3.1.1 Protocol A – Materials and Methods

3.1.1.1 Material Description

PA6-NanoSilica and PA6-Nanoclays are already commercialized in automotive applications, especially under-the-hood such as inverter, engine bay or timing belt covers. Three-phase nanocomposites are not yet widely used, however, as mentioned in the literature few studies [60]–[63] report their advantages and can be seen as future potential candidates for such applications. For this reason, three-phase polymer matrix nanocomposites were chosen for this study: Polyamide-6 (Durethan B30) reinforced by 30 wt.% of Glass Fiber (ThermoFlow 672) and different percentage of either nano-SiO_2 (Aerosil R 974) or organically modified Montmorillonite (OMMT, Dellite 43B).

In total, seven materials were manufactured with different content of nanofillers (Table 7 and Table 8).

Table 7: Composition of the OMMT-Nanocomposites Tested

Name	Type of Matrix	wt% of PA6	Type of Glass Fibre	wt% of GF	Type of filler	wt% of filler
PA6-GF-OMMT-5	Durethan B30	65	ThermoFlow 672	30	Dellite 43B	5
PA6-GF-OMMT-7.5	Durethan B30	62.5	ThermoFlow 672	30	Dellite 43B	7.5
PA6-GF-OMMT-10	Durethan B30	60	ThermoFlow 672	30	Dellite 43B	10

Table 8: Composition of the Silica-Nanocomposites Tested

Name	Type of Matrix	wt% of PA6	Type of Glass Fibre	wt% of GF	Type of filler	wt% of filler
PA6-GF-SiO-0.5	Durethan B30	69.5	ThermoFlow 672	30	Aerosil R 974	0.5
PA6-GF-SiO-1	Durethan B30	69	ThermoFlow 672	30	Aerosil R 974	1
PA6-GF-SiO-1.5	Durethan B30	68.5	ThermoFlow 672	30	Aerosil R 974	1.5
PA6-GF-SiO-3	Durethan B31	67	ThermoFlow 673	30	Aerosil R 974	3

3.1.1.2 Materials and Samples Manufacturing

The nanomaterials were prepared by using a twin-screw extruder at Fraunhofer – Institute of Chemical Technology in Germany. In the case of OMMT-nanocomposites, the polyamide granulates and nanoclay particles were premixed in the main hopper and melted in a hot cylindrical barrel, where the twin endless screw homogenized the mix. The process parameters used can be found in Appendix A.

Along the screw, the temperature was increased up to 280 °C. Glass fibres were added using a side feeder. Then, the mixing of the three components was extruded through a die. Finally, the product was cooled in a water bath; cut by the pelting machine in order to obtain granulates and dried over 8 hours at 80 °C. For the silica-based nanocomposites, the nano-SiO_2 particles were mixed with the glass fibres in the side feeder instead of the main hopper in order to have a better dispersion of the nanofillers.

The test specimens (plates, dumb-bell samples and crash cones) were also manufactured at Fraunhofer ICT, Germany. They were produced by injection moulding process. This technique is one of the most used in industry for the manufacturing of polymer products. The injection moulding parameters can be found in Appendix B, Appendix C and Appendix D.

Figure 10 shows a schematic representation of an injection moulding process. The plastic granulates are introduced in a barrel, where their temperature increases to or just above the melting point. An endless screw pushes the melted

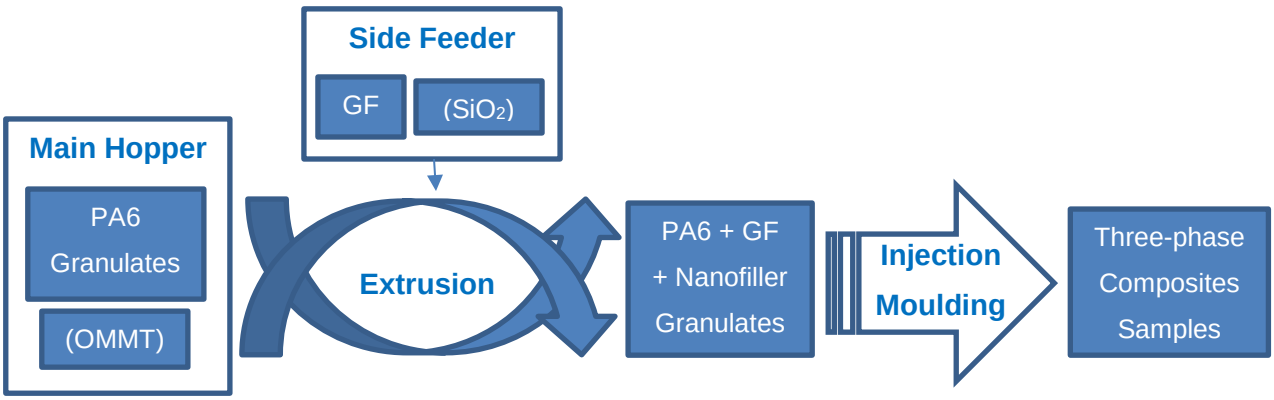

Figure 10: Manufacturing Process for the Three-Phase Composites Samples

plastic to the entrance of the mould. Then, the material is injected in the mould under pressure. The plastic cools, becomes solid, and takes the shape of mould. To finish, the mould is opened, and the part is ejected. This process is very quick, for example a crash cone is injection moulded in less than 2 minutes. A last step is necessary: it consists of trimming the “deadhead” of the core sample in order to obtain the final product.

For the following experimental section, the dimensions of the samples were 160 mm for the external diameter, 100 mm for the internal diameter, and 4 mm for the thickness as seen Figure 11.

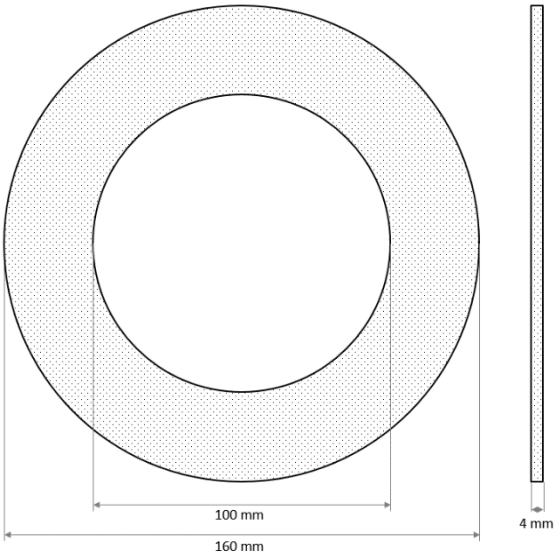

Figure 11: Dimensions of the samples drilled

3.1.1.3 Assessment of Nanoparticles Released during Drilling

The equipment used in this study to measure and quantify the nanoparticles released during machining is a SMPS+C (Scanning Mobility Particle Sizer plus Particle Counter) from Grimm Aerosol. It is composed of a Vienna type DMA (Differential Mobility Analyser) and a CPC (Condensation Particle Counter) model 5.403. The SMPS+C (without the connections) can be seen Figure 12.

Figure 12: SMPS+C used in this study

Explanation of the principle of the SMPS+C is described by Grimm Aerosol [210]. The equipment works as follow: first the particles are sucked into an antistatic hose. Larger particles are removed at the entrance of the DMA by an impactor. Fine and ultrafine particles are classified according to their electrical mobility: a high voltage is applied to the inner electrode of the DMA which makes the particles to be attracted to it. Smaller particles have a higher mobility and so move faster and will reach the inner electrode first. The change of the DMA voltage allows to control which particles size can go through a slot at the bottom of the inner electrode and so to measure the size distribution. A schematic of a DMA produced by TSI Incorporated is reproduced Figure 13 [211].

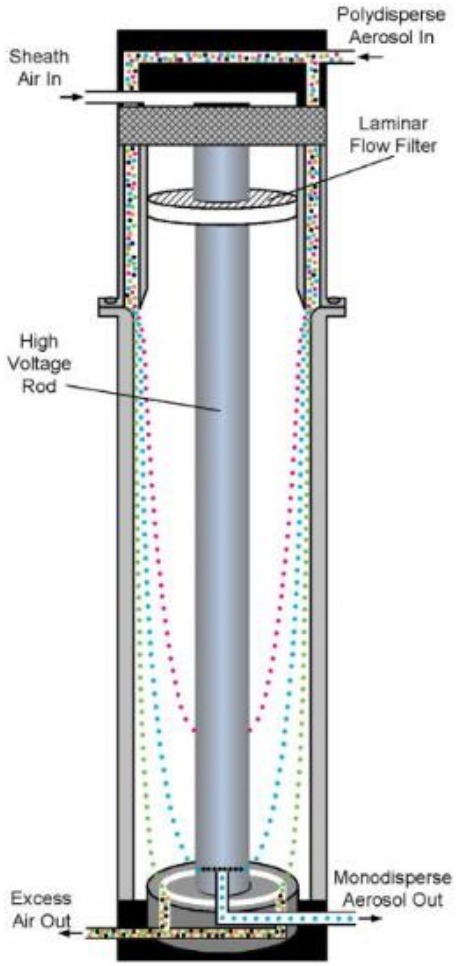

Figure 13: Schematic of a DMA [211]

The particles of a specific size that go through the slot at the bottom of the inner electrode are then conducted to the CPC. Here, they are grown by the condensation onto them of butanol vapour. With this new size, the particles can be optically detected and counted when crossing a laser beam.

For these experiment, the SMPS+C had a size resolution of 44 channels over a size range of 11.1-1083.8 nm. Every channel take just under 10 seconds to be classified and counted. With these parameters, the equipment needs approximatively 7 minutes to build the full size distribution of the aerosol generated. It is then fundamental that the experiment generate a constant flow of particles during 7 minutes.

Drilling of nanocomposites plates was conducted according to the protocol implemented in NEPHH project (Protocol A). The experiments were carried out in a closed chamber, with the following dimensions: width of 690 mm, depth of 330 mm and height of 560 mm. The samples were fixed into the chamber and the angle drill (Makita BDA351Z 18V LXT Angle Drill) was completely enclosed into the chamber for the duration of the measurement cycle. An overview of the installation can be found Figure 14.

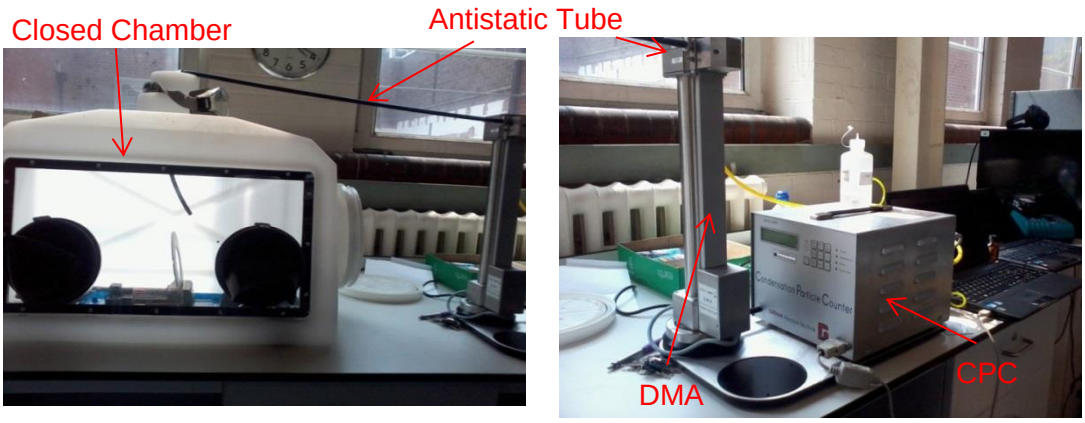

Figure 14: Overview of the Set-Up for the Replication of the Assessed Methodology (Protocol A)

Also, similar measurement cycle was followed (Figure 15). It included 20 minutes with the chamber open in order to purge it with lab air before the measurements. After, the chamber was closed and the measurements started with 30 minutes of

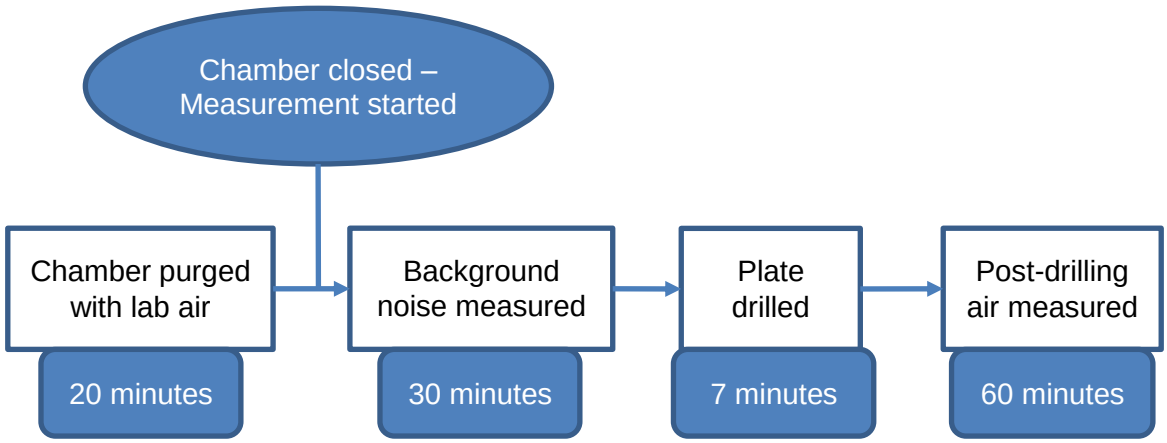

Figure 15: Measurement Cycle for the Drilling Experiments (Protocol A)

record of the background noise, then a plate was drilled during 7 minutes, and the cycle finished with 60 minutes measurement of post-drilling.

Two drill bit sizes were studied (5 mm and 8 mm diameter). The angle drill was used at its maximum spindle speed: 1800 min^{-1}. This speed is controlled by an analogue switch with hand pressure. So, the value of the spindle speed can only been known when it's at its maximum (1800 min^{-1}). In total, 7 holes (through holes) were drilled during 7 minutes for each experiment. The experiment was repeated 3 times for each material composition and drill bit size. In addition, every morning one measurement cycle was conducted in order to record the noise of the drill itself.

The SMPS+C works with the software GRIMM Universal Nano Software which directly calculates the number, surface and mass size distributions according to the standard ISO 15900. The sequential alteration of the total number concentration of particles along the measurement cycle and the size distribution at a given time was calculated for every experiment.

The emission rates were calculated using the same method as previous studies [173], [212], [213]. Three assumptions were made for this model as follows:

- Background concentration is zero;
- Particle concentrations are homogenous within the chamber;
- Emission rate and decay rate of the particles remain constant throughout the entire period of generation [173].

It has to be noted that these three assumptions are far from reality: the background concentration is not null and during drilling the particles concentration will be higher near the drill so not homogeneous in the chamber.

First, the removal rate k_x (min^{-1}) was calculated for every size x of the particles:

$$k_x = \frac{\ln\left(\frac{C_x}{C_{max;x}}\right)}{t_{max} - t} \quad \textbf{(3-1)}$$

With C_x: number concentration of particles of a size x at the time t, (particles/cm^3)

$C_{max;x}$: maximum number concentration of particles of a size x at the time t_{max}, (particles/cm^3)

Then, the emission rates of particles of size x, P_x (min^{-1}) were evaluated, using a chamber of volume V=1,265·10^5 cm^3:

$$P_x = \frac{V C_x k_x}{1 - e^{k_x * t}} \quad \textbf{(3-2)}$$

3.1.2 Protocol A – Results and Conclusions

The main results are presented Table 9 and Table 10, where d_{median} is the median particle diameter during drilling. Also, a general view of the evolution of maximum airborne particle concentration with time can be found in Figure 16 and Figure 17.

Table 9: Main Results for the Experiments on OMMT-nanocomposites using the Protocol A

	C_{max} (#/cm^3)		P_{total} (min^{-1})		d_{median} (nm)	
	5mm Ø	8mm Ø	5mm Ø	8mm Ø	5mm Ø	8mm Ø
PA6-GF-OMMT-5	1.33·10^5	6.09·10^5	1.2·10^{10}	2.8·10^{10}	23.3	36.75
PA6-GF-OMMT-7.5	1,85·10^5	2.71^{1}·10^5	1.7·10^{10}	1.8·10^{10}	25.9	22.7
PA6-GF-OMMT-10	3.05·10^5	1.45·10^5	1.7^{e+10}	8·10^9	26.09	27.01

Table 10: Main Results for the Experiments on Silica-nanocomposites using the Protocol A

	C_{max} (#/cm^3)		P_{total} (min^{-1})		d_{median} (nm)	
	5mm Ø	8mm Ø	5mm Ø	8mm Ø	5mm Ø	8mm Ø
PA6-GF-SiO-0.5	5.32·10^5	1.23·10^6	1.6·10^0	4.3·10^{10}	38.97	24.15
PA6-GF-SiO-1	4.97·10^5	1.13·10^6	1.6·10^0	3.9·10^{10}	35.6	27.31
PA6-GF-SiO-1.5	4.79·10^5	1.05·10^6	1.4·10^0	2.9·10^{10}	26.8	28.17
PA6-GF-SiO-3	2.20·10^5	9.80·10^5	8.6·10^9	2.7·10^{10}	24.93	27.52

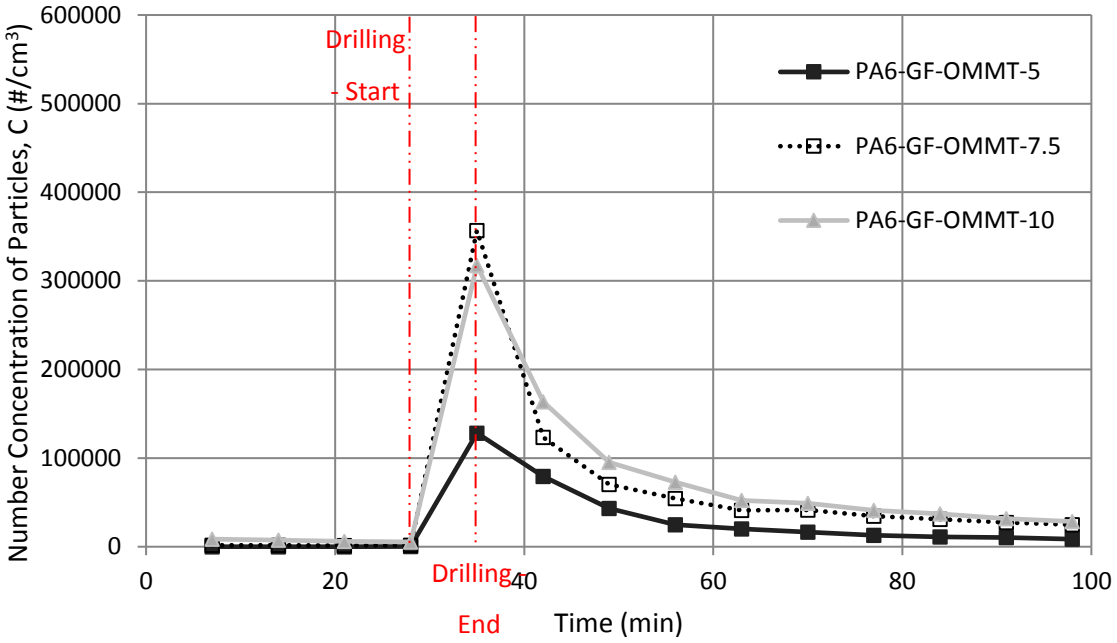

Figure 16: Sequential Alteration of Number Concentration during the Measurement Cycles using a 5 mm Drill Bit for the OMMT-Nanocomposites

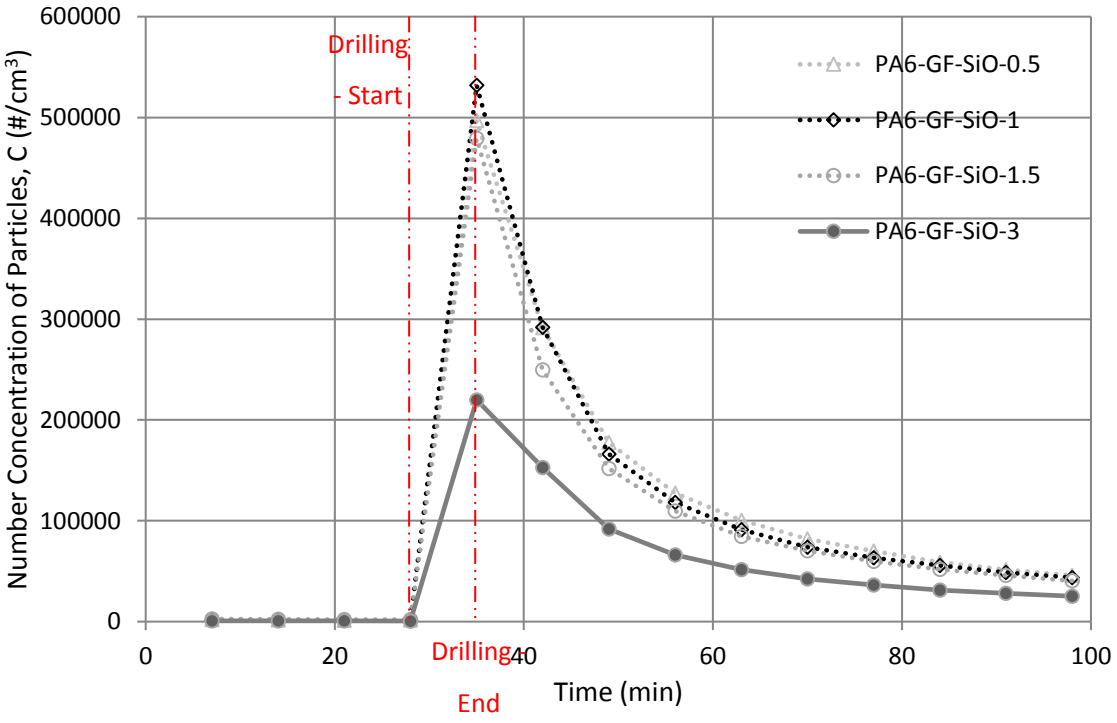

Figure 17: Sequential Alteration of Number Concentration during the Measurement Cycles using a 5 mm Drill Bit for the Silica-Nanocomposites

The background noise in the chamber recorded before drilling was around 10000 particles/cm^3. The concentration of particles was in every case at its maximum at the end of the 7 minutes of active drilling. Maximum number concentration of airborne particles using a 5 mm drill bit were in the range 133000 particles/cm^3 to 532000 particles/cm^3. These experiments and the results helped to point out several deficiencies of this protocol and will be developed in the following paragraphs:

Effect of the feed rate

Figure 18 presents the typical particle size distribution observed for every material during the measurement cycle. One curve was plotted every 7 minutes. It is important to note the fact that the particles are mainly under 100 nm diameter, which means they are within the standard definition of a nanoparticle. It can again be noticed that after the active drilling period, the concentration of the particles in the chamber decreases. The median particle size diameter seems to increase with time. Some phenomena involved in the removal of particles from the chambers are diffusion, gravitational deposition, convection, collision and coagulation [173]. The small particles are mainly influenced by the diffusion process and the bigger particles by gravitation. The increase in the mean diameter can be explained by the fact that the equipment, in order to count the

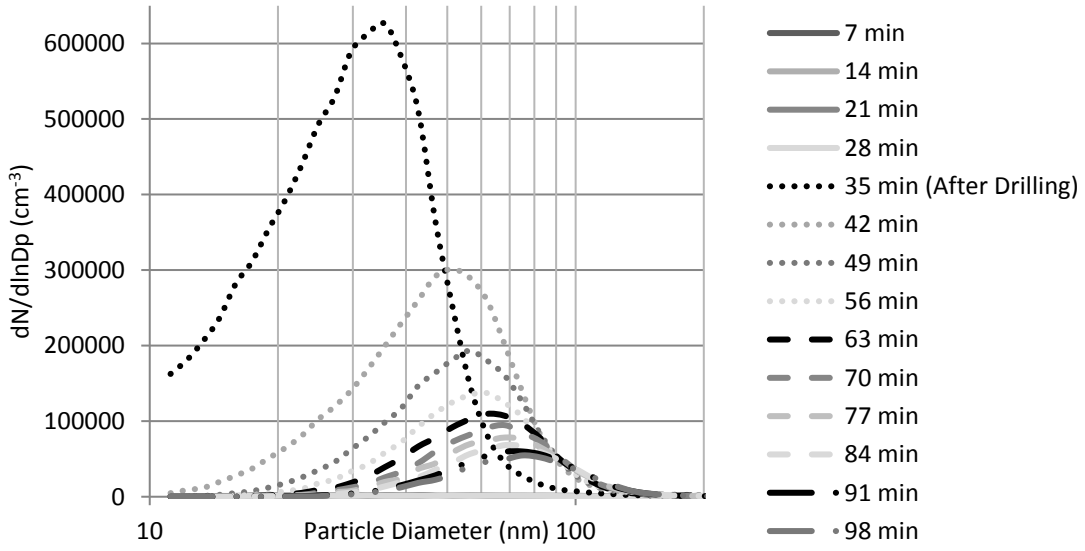

Figure 18: Typical Normalised Particle Size Distribution along the Measurement Cycle

particles, sucks up the air and the small particles, which are lighter are sucked up faster than the bigger ones.

As the angle drill used was manually operated, the feed rate was only controlled by the pressure exercised by the drill on the plate, so by the pressure exerted by hand. This parameter is clearly difficult to control and replicate. Two different feed rates were studied, 4 mm/min and 1.14 mm/min, which correspond respectively to one hole per minute and 2 holes in 7 minutes. Results of the particle size distribution at *t*=35 min (just after drilling) can be seen in Figure 19.

The difference in the size distribution and number concentration of particles released is clear. With a fast feed rate, the number concentration of particles produced is 100 times higher than at slow speed rate when the volume drilled is only 3.5 times greater. Also, the mean diameter of particles is smaller at a high feed rate (around 20 nm) than at slow speed rate (around 70 nm). These results show that the feed rate is an important parameter to control to have repeatable results as it has a significant influence on the size distribution and number concentration of particles released.

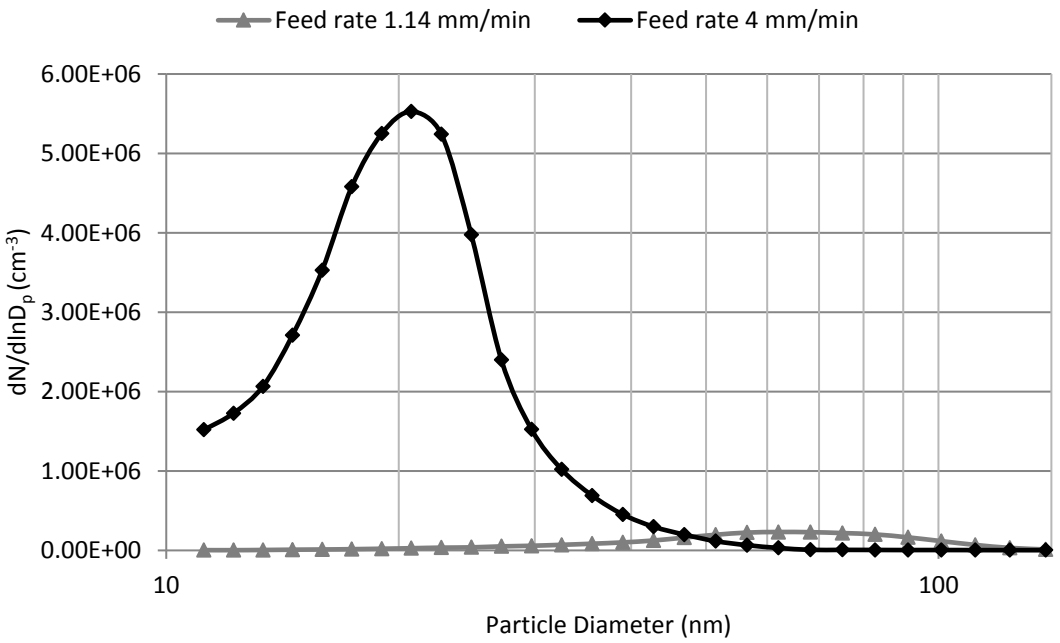

Figure 19: Normalised Particle Size Distribution (d*N*/dln(D_p)) inside the chamber at *t*=35 min

Influence of the background particles

Every day, one cycle measurement was carried out in order to record the background noise of the drill itself (no sample drilled). Different activities had been carried out in the workplace at the same time as the drilling experiments, and so, they could involve changes in the atmosphere and the environment. Some examples are presented in Figure 20. Background concentrations were varying from around 70000 particles/cm^3 to 700000 particles/cm^3. The number concentration of particles without any activity in the chamber i.e. background is around 10000 particles/cm^3. The particles produced by the drill itself were significant. Therefore, all the previous results can be affected by the drill. Some studies [133], [161], [214] regarding machining such as cutting, drilling or sanding had already reported the effect of environment and tools as noise from airborne nanosized particle measurements. They can be classified in two categories: particles released from electrical motors used in the process [161], [162], [215] which can be for example copper particles [215] or particles produced unintentionally from the process as a side product.

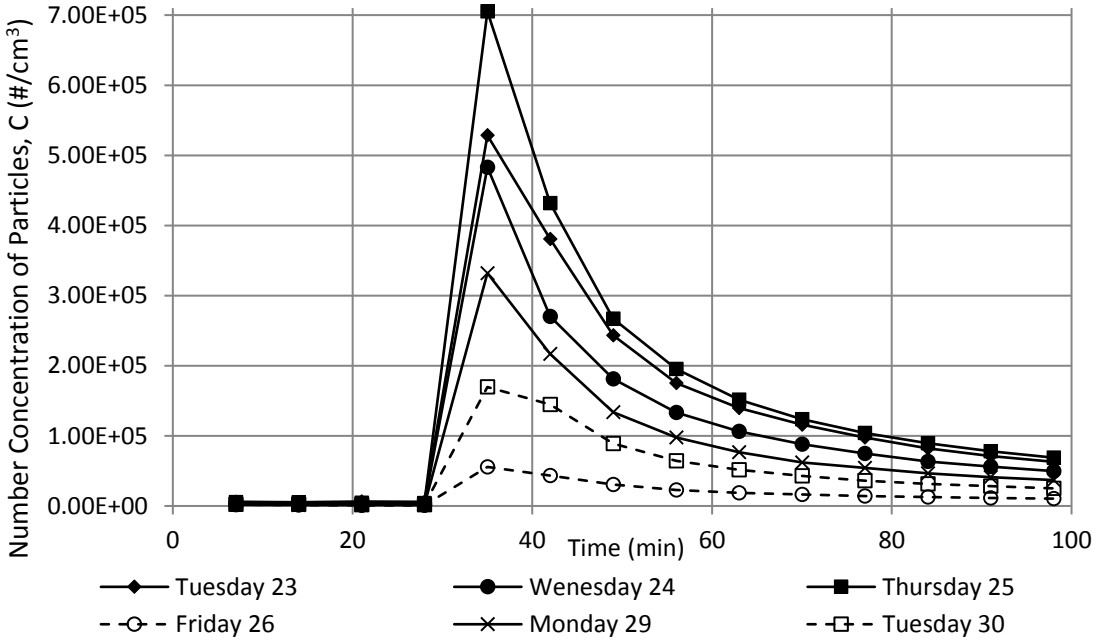

Figure 20: Number Concentration of Particles vs Time during Different Days without any Machining Operations on Samples

3.1.3 Protocol A – Identification of the Deficiencies

As a result of the analysis of the experiments, the deficiencies of the Protocol A were identified. It was concluded that there was a need to develop a new protocol for an accurate evaluation and simulation of the release of nanoparticles from nanocomposites. Several suggestions to improve the existing protocol and to overcome the deficiencies are summarised in Table 11.

Table 11: Deficiencies Observed in the Protocol A and Suggestions to Solve them

Parameter	Deficiencies observed	Suggestions
Spindle speed	The spindle speed was set up at 1800 min^{-1} by keeping maximum pressure (manually) on the button during all the experiments. As the spindle speed was controlled by an analogue switch with manual pressure, the speed could only been known when it was at its maximum.	This method was not satisfactory as the spindle speed was a parameter that needs to be studied in order to know its influence on nanoparticle release, and with manual pressure, the reproducibility of the experiments was compromised. A new prototype for drilling, including a CNC machine, had been designed and built for this purpose.
Feed rate	It was not possible to control the feed rate as a manual angle drill was used. Therefore, this parameter had been identified to be a crucial point influencing the quantity of particles released.	As mentioned above, a new system which allows to control these variables has been set in place instead of the reference protocol.

Background noise	It was noticed that the drill itself produced noise (particles). The noise was variable depending on the prevalent laboratory conditions, and could be up to 50 % of the nanoparticles measured. This was deemed too high.	The engine of the new spindle drill is totally sealed and cooled down with a water system. The noise is controlled as no emission from the engine is possible. In addition, the air with which the chamber is filled is filtered with an HEPA H14 filter to avoid contamination.

3.2 Protocol B – Characterisation of the Machining Chamber

A new protocol (Protocol B) was set-up in order to overcome the deficiencies listed above. The system is capable of assessing the release of nanoparticles during general machining operations such as drilling, cutting or milling in a controlled environment.

3.2.1 Description of the Chamber

The device set-up for the exposure assessment during machining is composed of different features and elements which are:

- *Environmental control*: the system comprised of a sealed chamber with a fan, BenchVent I100-4. In addition, pre-filter and HEPA filter H14 were used to clean the air inside the chamber. An air recirculation system was also implemented in order to reduce the amount of 'dirty' air from the room to enter the chamber. This configuration ensured a good control of the environment inside the chamber, as well as protection for the operator. An overview of the set-up can be seen Figure 21, Figure 22 and Figure 23. In addition gloves were added to the chamber door in order to transform the chamber into a glove box and so avoid the opening of the chamber during the full measurement cycle.

Figure 21: BenchVent Fan

Figure 22: Air Recirculation System

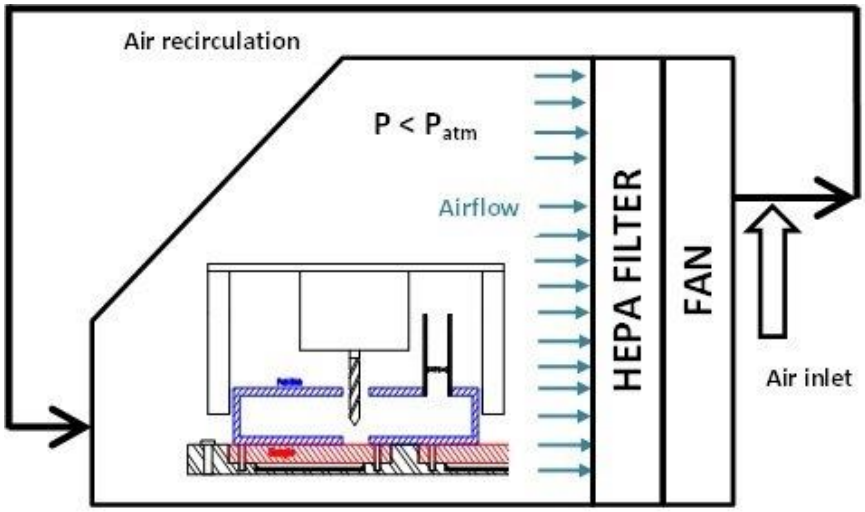

Figure 23: Scheme of the Chamber

- *Automatic system for mechanically processing samples*: a CNC machine (Figure 24) was designed and built at Cranfield University (not off-the-shelf), which allowed to have precise control of machining parameters (feed rate, spindle speed, etc.), and thus to have reproducible and repeatable tests. Additionally, a water cooled spindle drill (Figure 25) was used in order to avoid background noise or particles produced by the motor, as the motor is totally sealed.

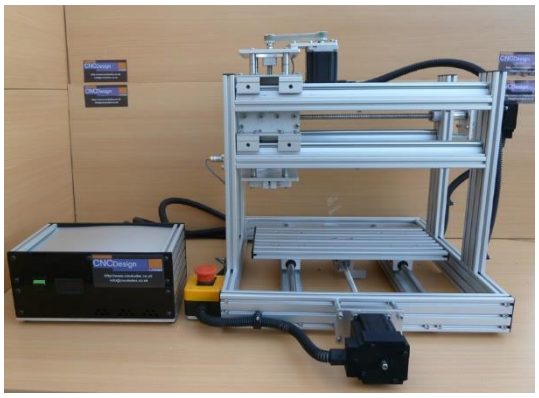

Figure 24: CNC Machine Implemented in the Chamber for Machining Operations

Figure 25: Water-Cool Spindle Drill

- *Dust collection system*: the fixture system comprised of a base plate made of antistatic polymer (Tecafine HDPE), with a pattern to drill the holes in the samples. In addition, a petri dish with lid, adapted for the drilling process was located on the surface of the sample. Therefore, the deposited fraction of particles could be easily collected into the petri dish. After the experiment, the petri dish was sealed and used as a container. This way, the collection and storage of generated dust was reduced to a single step (Figure 26). The collection of the deposited fraction was done after the drilling of a single blind hole.

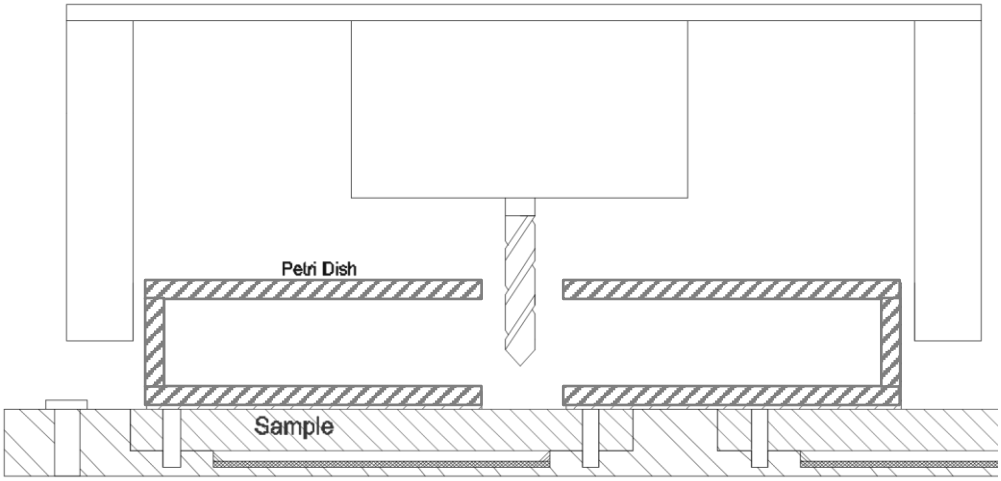

Figure 26: Schematic of the Dust Collection System

- *Instrumentation*: a scanning mobility particle sizer counter (SMPS+C) from Grimm Aerosol with a Condensation Particle Counter (CPC) model 5.403 with a classifier type Vienna, long U-DMA was used for the measurement of the airborne particles. This equipment was connected to the chamber using antistatic tubes. The measurement of the airborne particles released was done in a different step than the collection of the deposited particles. In this phase, the drilling occurred for 7 minutes during which 45 blind holes were drilled. The measurement point of the SMPS+C during this phase can be seen Figure 27.

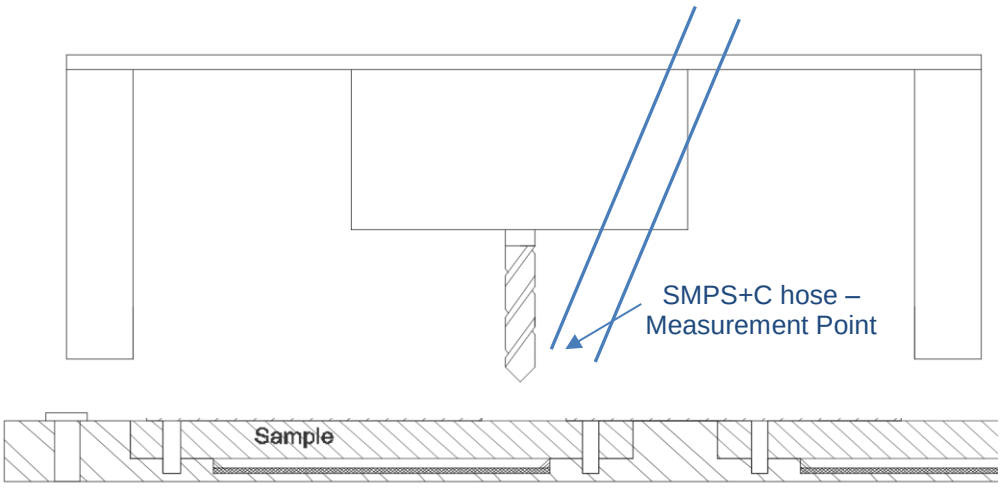

Figure 27: Measurement point of the SMPS+C

3.2.2 Protocol B – Characterisation of the Background Environment

To characterise the background environment, the first stage was to assess the properties of the air in the room where the experiment takes place. Table 12 shows a summary of different measurements of the room air done at different periods. The average number concentration of particles was 6702 particles/cm^3, which was similar to the number concentration of particles in the chamber as a background during the NEPHH experiments. Also, Figure 28 shows the particle size distribution in the lab air. Most of these particles are under 100 nm and especially the highest number concentration of particles were between 10 to 20 nm. Thus, it is important to avoid the measurement of these particles during the experiments.

Table 12: Measurement of the Number Concentration of Particles (*C*, #/cm^3) of the Lab Air

Measurement	Number concentration of particles in room air (C_{room}, #/cm^3)
1	7695
2	8177
3	9508
4	5797
5	4474
6	4563
Average	**6702**
Standard deviation	**2069**

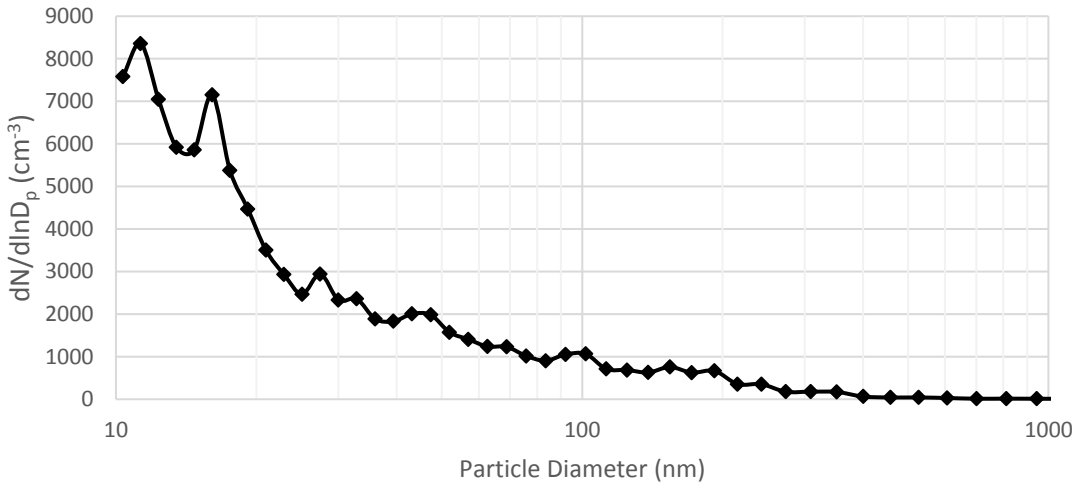

Figure 28: Particle Size Distribution in the Lab Air

Then, a baseline experiment was conducted in order to characterize the air inside the chamber. Figure 29 presents the results. We can see that the air in the lab is usually around 6000 particles/cm^3. Then, when the fan is on, and the air recirculated, it takes around 2 hours to reach an acceptable level of particles (under 1000 particles/cm^3) inside the chamber. The number of particles is decreasing as the air recirculated in the chamber through the HEPA filter. The environment was then stabilized and the average number concentration of particles inside the chamber was 312 particles/cm^3, which was an improvement compared to the chamber used previously. Also, the number concentration of particles was stable when the fan was stopped after the chamber was cleaned with the recirculation system. Finally, a leak test was performed by an external company (Crowthorne Hi-Tec Services Ltd) in order to guaranty that the chamber is air tight (i.e. no particles can enter and exit the chamber).

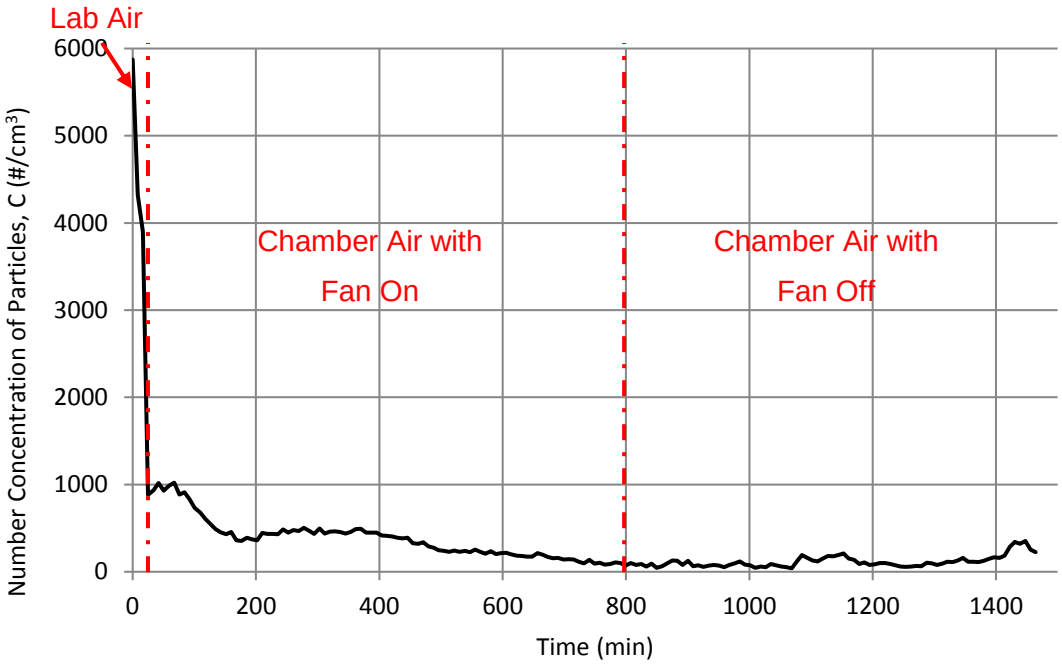

Figure 29: Baseline Test of the Air inside the Chamber Prior to Milling or Drilling Activities

3.2.3 Protocol B – Influence of the Process Itself

One of the main deficiencies from the Protocol A described previously was the influence of the manual angle drill on the particles release. The motor of the drill with metallic brushes emitted metallic nanoparticles resulting in unreliable data. A totally sealed water cooled spindle drill was therefore used. Comparison of the two methods is presented below.

The manual angle drill was enclosed in the chamber and kept on for 7 minutes at a maximum speed (1800 rpm), but no sample was machined to ensure the measurement of the particles produced by the drill. The air inside the chamber was monitored with the fan on to provide a constant clean air prior the use of the manual drill. The air inlet of the SMPS+C was placed near the drill bit. The same experiment was repeated with the spindle drill of the CNC machine. The total number concentration of particles recorded during these experiments are presented Figure 30. For comparison purpose, the air outside the chamber (room air) was monitored prior to the start of the experiment.

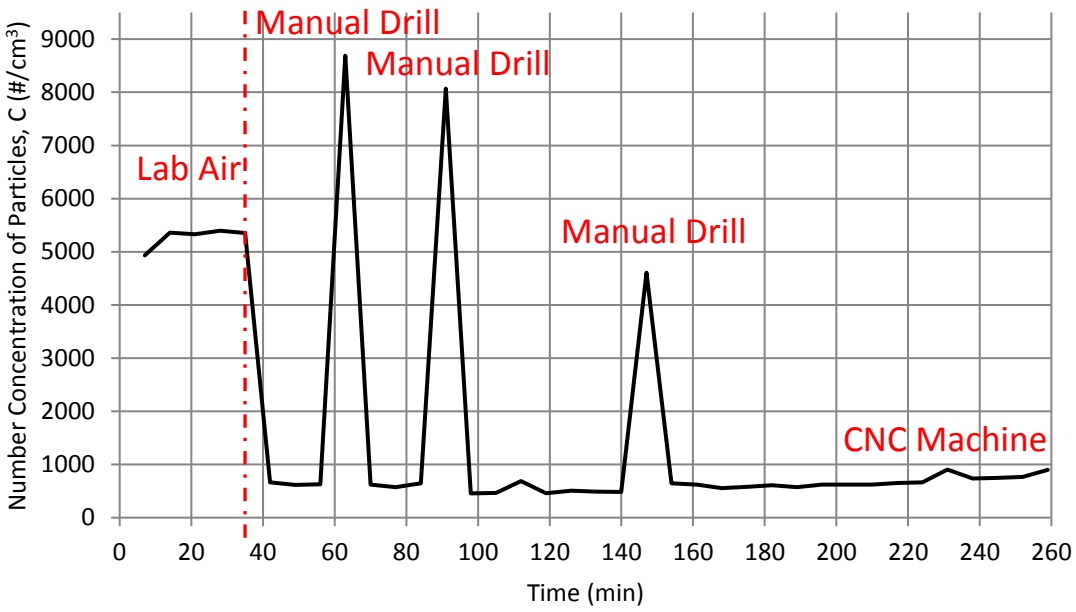

Figure 30: Characterisation of Particles from the Manual Drill and from the CNC Machine

The average of particles in the room air was 5274 ± 173 particles/cm^3 (scans 1 to 5). Inside the chamber, the average number concentration of particles was about 590 ± 75 particles/cm^3. In case of the manual drill, it was switched on for 7 minutes on 3 occasions, but no sample was drilled. These occasions correspond to scans 9, 13 and 21, in which, *C* increased to 8688, 8066 and 4609 particles/cm^3 respectively (the manual drill was running out of battery in the last case, and so the spindle speed was lower). Under similar operating conditions (7 minutes working but drilling no sample), for the CNC machine (scan 32) *C* increased only to 903 particles/cm^3. This experiment proved that, unlike the manual drill from the assessed protocol, the CNC machine is not a significant source of contamination.

In addition, another test was done with the fan off to recreate the conditions under the assessed protocol. In this case, the manual angle drill was reported to release a number concentration of particles higher than 65000 particles/cm^3, which is about 10 times higher than the normal concentration in the room outside the chamber. Figure 31 presents the particle size distribution during this test. It is clear that the particles released by the manual drill were under 100 nm diameter.

These are probably metallic particles produced by the engine of the manual drill which are metal brushes. Therefore, in the Protocol A, a considerable part of the particles measured were a contribution of the manual drill and not from the samples tested. This problem is solved by the use of the sealed spindle drill for the Protocol B.

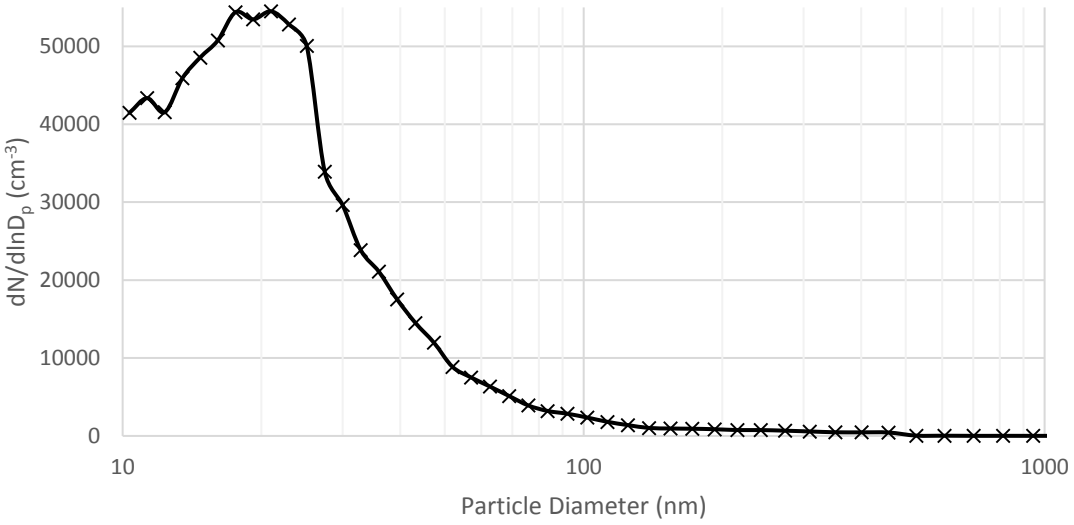

Figure 31: Particle Size Distribution inside the Chamber, without the Air Recirculation System during a Blank Test with the Manual Angle Drill

3.3 Characterisation of the Impact Chamber

The same idea developed for the machining experiments was replicated in order to assess the release of nanoparticles during impact of nanocomposites plates or components. Description of the chamber and validation of the method are presented in the following sections.

3.3.1 Description of the Chamber

The set-up of prototype equipment developed for the impact experiments comprised of:

- Environmental control: a 820*600*650 mm^3 sealed chamber with a fan, HEPA filters and a recirculation system similar to the drilling chamber were used to create a clean environment.

- Dust collection system: Double side tape was placed at the back of the sample, in order to collect the fragments generated by direct impact of the bullet. Also, a bag was placed under the fixture in order to collect the other fragments.
- Instrumentation: the same SMPS+C was used to quantify and measure the airborne particles released during the impact. Also a high speed camera was used to record the impact.

A schematic of the set-up and the chamber used for the impact experiment can be found Figure 32.

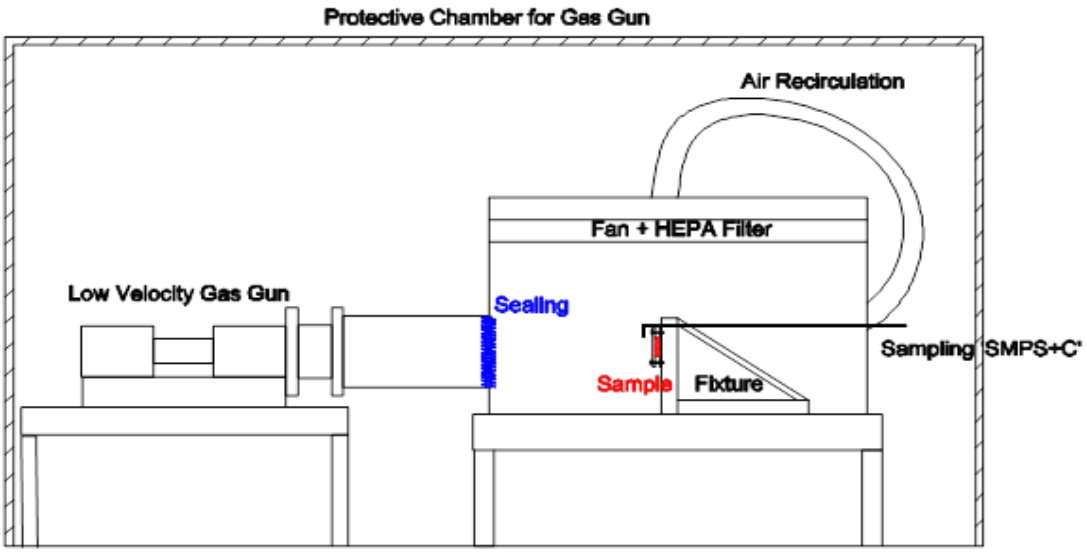

Figure 32: Schematic of the set-up and chamber for the impact experiment

3.3.2 Characterisation of the Background Environment

An overview of the general background particles measured in the chamber can be found in Figure 33. On this graph, the first point (7598 particles/cm^3) corresponds to the number concentration of particles in the lab air. Then, the particles are measured inside the clean chamber, with the fan off. The average number concentration of particles during the period of 84 minutes was 404 ± 58 particles/cm^3. This level is relatively low and stable over a period of time longer than the necessary time for one experiment.

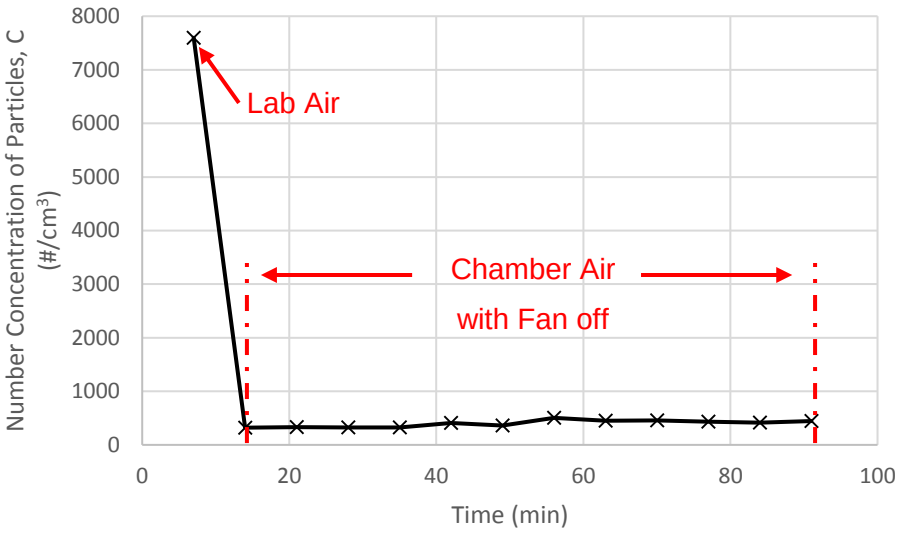

Figure 33: General Background Measured in the Impact Chamber

3.3.3 Influence of the Impact Process

The effect of the gas gun itself was also studied in order to assess the repeatability of the data and to ensure that no particles were emitted by the shot and that the gas gun does not influence the results. For this purpose, the number concentration of particles was measured inside the chamber while the gas gun fired a bullet into few layers of plastic paraffin film instead of the sample in order to prevent the impact on the fixture. The results of this experiment are presented in Figure 34. Similar to the previous graph (Figure 33), the first measurement is from the air lab (5316 particles/cm^3). Three 'blank shot' were taken, respectively at 35, 63 and 91 minutes. The average number concentration of particles generated by these events was 339 ± 80 particles/cm^3. The average number concentration of particles inside the chamber (fan off) was 281 ± 72 particles/cm^3. It can be concluded that the shooting itself does not generate a significant number concentration of particles.

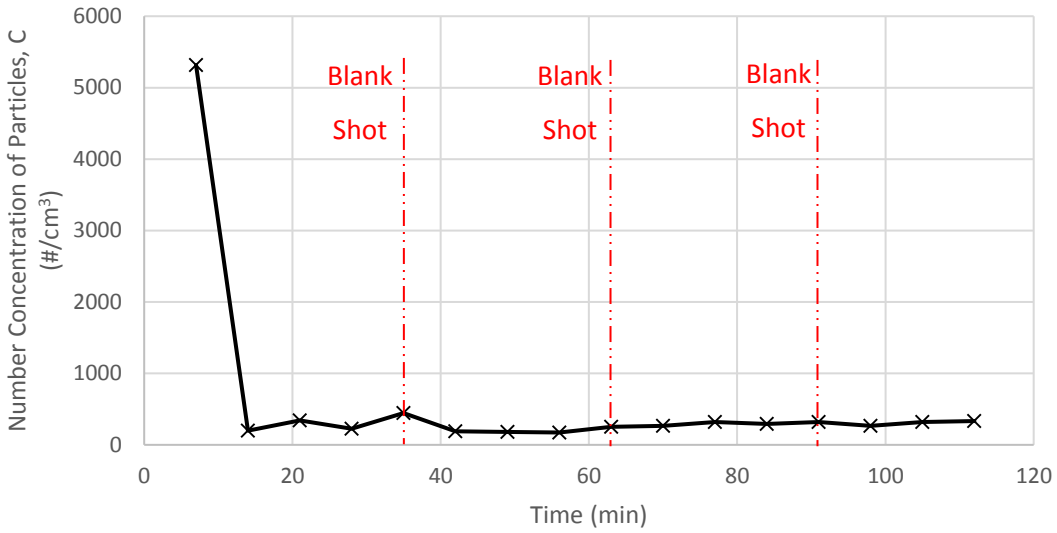

Figure 34: Influence of the Process on the Number Concentration of Particles in the Chamber

3.4 Conclusion

A reliable and repeatable method was developed to assess the exposure to nanoparticles over the life cycle of the product. Preliminary tests were performed in order to assess the important parameters to control during the experiment. The validation of the new prototype used for the measurement and monitoring of nanoparticles in a controlled environment was described. This methodology was compared with the methodology applied in other studies. Also, this method was adapted for different case studies: machining (drilling and milling), as well as impact testing.

The next step was to use this protocol in order to assess the nanoparticle released from potential commercial nanocomposites. The drilling experiments are presented in the following chapter.

4 CHARACTERISATION OF THE PARTICLES RELEASED DURING DRILLING OF POLYMER BASED NANOCOMPOSITES

4.1 Introduction

Drilling is a common machining operation within industry especially related to the assembly process [216]. Its importance is relatively high given that 60 % of the rejected parts are rejected because of defects induced by holes [217]. Therefore, extensive literature can be found on machining of conventional composite materials. However, the study of drilling nanocomposites was not investigated in depth so far and there is a lack of knowledge on this subject [216].

Also, the release of nanoparticles during nanocomposites service life has not been researched in depth. Only few studies focus on the use and/or hazards of existing nano-products, as most of the work is concentrated on laboratory simulation. For example, Sachse et al. studied the release of nanosize particles during the drilling of different polyamide-6 nanocomposites [173]. They found that the integration of nanofillers into a polymeric matrix influences the material behaviour, the quantity of particles released during drilling experiments and the physical properties of the nanosized particles emitted. However, this study had several problems and deficiencies that were analysed in Chapter 3. Therefore, the results from this study do not represent the actual release of nanoparticles from the nanocomposites. As presented in Chapter 3 a new prototype was developed in order to overcome the deficiencies observed in Sachse's studies [173]. The aim of this chapter is to assess the release of nanoparticles from potential commercial nanocomposites. This chapter focuses on the measurement of airborne nanoparticles generated as a result of physical damage or machining operation (drilling) in thermoset and thermoplastic nanocomposites.

4.2 Materials and Methods

4.2.1 Materials' Description and Manufacturing

Three types of nanocomposites were chosen each corresponding to a different sector for industrial applications: Epoxy matrix for the aerospace industry,

Polypropylene-based samples for the automotive sector and Polyester based materials for the construction. The composition of the different grades can be found in Table 13.

Table 13: Composition of the Nanocomposites

Name	Matrix	Additive	Application	Process
E	Epoxy	-	Aerospace	Drilling/Impact
E-CNT	Epoxy	CNT (2 %)	Aerospace	Drilling/Impact
E-CNF	Epoxy	CNF (2 %)	Aerospace	Drilling/Impact
PP	Polypropylene	-	Automotive	Drilling/Impact
PP-TALC	Polypropylene	Talc (20 %)	Automotive	Drilling/Impact
PP-WO	Polypropylene	WO (5 %)	Automotive	Drilling/Impact
PP-MMT	Polypropylene	MMT (5 %)	Automotive	Drilling/Impact
P	Polyester	-	Energy	Drilling/Impact
P-SiO	Polyester	SiO_2 NPs (2 %)	Energy	Drilling/Impact
P-AlO	Polyester	Al_2O_3 NPs (2 %)	Energy	Drilling/Impact

All the samples were manufactured in Tecnalia (San Sebastian, Spain).

Polyester based materials were produced by high speed mixer, and casted into a mould: Polyester resin was introduced into the mixing vessel of a high speed mechanical mixer, a 'Planetary Mixer Dispermat' model CA-60-C with vertical oscillation E05268008; and 2 wt.% of nanoparticles were added to the resin. The Dispermat mixed the materials during 10 minutes at 1500rpm and after that the mixture was degased in a vacuum chamber during 30 minutes. At the end, 3 wt.% of catalyst was added and mixed manually avoiding air entrapment. The final mixture was cast in a mould and cured at room temperature. The mould (dimensions 90x130 mm^2) was made of stainless steel and formed by a flat plate and a 5 mm thick frame fixed with screws. The mould was cleaned and permanent release agent Marbocote GRP-ECO was applied. Unsaturated orthophthalic polyester was supplied by Gazechim Composites (France), and nanofiller, nanosilica type 1 and nanoalumina type 1 by Torrecid Group (Spain).

Epoxy-based nanocomposites plates were prepared by calendering and curing in oven: the epoxy resin was hand mixed with the nanofiller for 3 minutes. The

mixture was poured into a commercially available laboratory scale three-roll mill (EXAKT 80E, EXAKT Technologies Inc.). The rotation speeds of the feed, central and apron rolls were 28, 83 and 250 rpm respectively. A total of 5 passes with different gap configurations were applied. The epoxy/nanofiller dispersion obtained after calendering was mixed with the hardener for 15 minutes by mechanical stirring at 20rpm under vacuum. Then the mixture was cast in a metallic mould, degassed during 20 minutes and oven cured for 75 minutes at 160 ºC plus 2 h at 180 ºC. Epoxy resin MVR444R was provided by Cytec Solvay Group, and the nanofillers, carbon nanotubes multi-walled Graphistrength C100 by Arkena, and carbon nanofibers Pyrograf PR24-XT-LHT by Applied Sciences Inc.

Polypropylene samples were extruded and injected moulded: Pellets of PP with 5wt% MMT or WO and 2 wt.% MAPP coupling agent were obtained using the COPERION ZSK 26 MEGA extruder. Extrusion parameters used for formulation preparation were: 800rpm screw speed, lateral feeding type, and temperature profile from feed to die 0-190-195-200-205-210 ºC. These formulations were injected to produce the sample plates of dimensions 140x100x1.6 mm^3 for testing. MOPLEN HP 648T was used for the polypropylene, and hostacom XM 2416 for the polypropylene reinforced with 20 wt.% of talcum, both from Basell. The Wollastonite Harwoll 7ST5 was supplied by Nordkalk and the Montmorillonite Nanomer I30 by Nanocor. A coupling agent (MAPP) polybond 3200 from Addivant was used for the PP nanocomposites.

The nanocomposites were chosen for their potential improved properties compared to the matrix materials related to the use and industrial field specified. Epoxy nanocomposites, used in aeronautical industry, can improve the electrical conductivity performance of neat epoxy. The volume conductivity increased from $2.6x10^{-14}$ S/cm for neat epoxy to $7x10^{-7}$ S/cm for E-CNT and $9.6x10^{-8}$ S/cm for E-CNF [218].

To improve the mechanical performance of polyester materials used in the energy or construction industry, nanosilica and nanoalumina were used. The characterisation of the composites showed a similar hardness of 75 shore C for

the three materials and enhanced flexural properties for the nanocomposites. The flexural modulus of 3140 MPa for polyester, 3200 MPa for nanosilica doped polyester and 3220 MPa for nanoalumina polyester [218].

PP-Talc and PP-WO exhibit similar tensile properties (respectively a modulus of 2418 MPa and 2409 MPa), however, the density of the PP-WO is 10 % lighter than the PP-Talc [218].

4.2.2 Generation of Nanosized Particles by Drilling

Drilling parameters were selected according to industrial guidance for machining composites and plastics [219] as it is likely that after manufacturing the nanocomposites undergo machining modifications. Feed rate and cutting speed were kept reasonably high to prevent melting of the matrix. Low feed rate and/or cutting speed can result in long processes, increasing the temperature of the sample at the cutting point up to the glass transition point and melting the polymer. The conditions and parameters were:

- Tool: High-Speed Steel (HSS) plain shank short drill bit, 3.5 mm diameter;
- Spindle speed: 8500 rpm;
- Feed rate: 200 mm/min.

The drilling experiment was repeated twice for each sample, in order to measure particles released and to collect dust. The inlet of the hose connected to the SMPS+C was placed next to the drill.

Each test starts with the measurement of the background noise of the chamber. The concentration of particles was stabilized in the chamber to start the drilling. The drilling operations were carried out over 7 minutes in order to allow the SMPS+C to characterise the full size distribution of particles present in the chamber. Then, the air inside the chamber was monitored until it reached a level similar to before the start of the drilling.

A second experiment was carried out on the same sample. A single hole was drilled with the same machining parameters in order to collect the dust generated during the drilling inside a petri dish for further characterization.

In addition, samples and material collected in the petri dish were weighed before and after every experiment for mass balance calculations.

4.2.3 Characterisation methods of the Dust Generated

The airborne particles emitted were characterised in terms of size and number by the SMPS+C.

The deposited particles (i.e. the ones that were not collected by the SMPS+C) generated during the drilling experiments were collected into a petri dish for further analysis. They were examined with FEI XL30 field emission scanning electron microscope (FE-SEM). The operating voltage was in the range of 10-20 kV and the specimens were gold sputtered to minimize charging of the samples.

Fourier transforms infrared spectroscopy (FTIR) was performed on the samples prior to drilling and on the dust collected in the Petri dish. FTIR spectroscopy model Jasco 6200 with accessory ATR IR from Pike - model miracle window - diamond/ZnSe. The scan range was from 4000 to 500 wavenumber.

4.3 Results and Discussion

4.3.1 Airborne Particles Emitted during Drilling

The Scan Mobility Particle Sizer plus Particle Counter ('SMPS+C') provides the number concentration of particles and size distribution during the time that the scan lasts, i.e. 7 minutes.

It must be noted that background concentration varied slightly among experiments, and also the amount of sample drilled. Samples were weighed before and after the experiment. Thus, data from the SMPS+C was normalised by extracting the background concentration (given by the value of C before drilling) for each particle size and for the total concentration, and divided by the mass of sample drilled ($m_{drilled}$, g).

4.3.1.1 Polyester Samples

Table 14 presents the average values calculated for the drilling experiments on Polyester based samples. C_{Peak} represents the number concentration of particles released during the 7 minutes drilling in particles/cm^3. The background noise (number concentration of particles measured in the chamber previous to drilling) was subtracted from this value. $C_{Normalised}$ is similar to C_{Peak} but was divided by the mass of samples drilled for every specimen to obtain a number concentration of particles released by cm^3 and by mass drilled. d_{median} (nm) represents the median particle diameter (half of the particles have a smaller diameter than d_{median} and the other half a higher diameter) and d_{hncp} (nm) the size where the highest number concentration of particles were produced.

Table 14: Average Values for Background Number Concentration of Particles removed (C_{Noise}), Total Number Concentration of Particles (C_{Peak}), Total Normalised Number Concentration of Particles ($C_{Normalised}$), Median Particle Diameter (d_{median}) and Diameter of the Highest Number Concentration of Particles (d_{hncp}) during Impact Drilling of Polyester Based Samples

	C_{Noise} (particles/cm^3)	C_{Peak} (particles/cm^3)	$C_{Normalised}$ (particles/cm^3.g)	d_{median} (nm)	d_{hncp} (nm)
P	526 ± 213	101665 ± 55916	30984 ± 17193	51.66	47.3
P-AlO	686 ± 73	211859 ± 95417	64116 ± 28621	61.52	56.96
P-SiO	498 ± 263	137117 ± 92178	43256 ± 31054	54.11	47.3

The standard deviation is extremely high even though 5 replicates were performed for each grade. A source of error from the protocol used comes from the equipment used. The SMPS+C as explained earlier assumes that every particles is spherical which is obviously not the case. There this can influence on the results.

Even though the standard deviation is high, it is clear that the nanocomposites are releasing more nanoparticles than the neat Polyester samples (an increase of 39 % and 106 % by adding silica and alumina particles respectively). The SMPS+C do not give information about the chemical composition of the

nanoparticles released. Polyester samples can only emit airborne particles composed of the neat polymer materials. However, the particles released by the nanocomposites can be formed of matrix materials, free engineered nanoparticles or nanoparticles embedded in the matrix. The difference in the quantity of submicron particles generated can be due to the change in the properties of the materials, and due to the change of machinability of the nanocomposites.

Figure 35 represents the number concentration of particles generated by the three types of Polyester composites along time. The first scan (0-7 minutes) is null as it was used to assess the background noise. The three grades follow the same trend. During the drilling (7-14 minutes), the number concentration of particles increased drastically, and when the drilling stopped (from minute 14), the number concentration of particles decreased gradually until the particles were back to a level similar to background. Different complex phenomenon can explain the evolution of the particles inside the chamber. Diffusion, sedimentation,

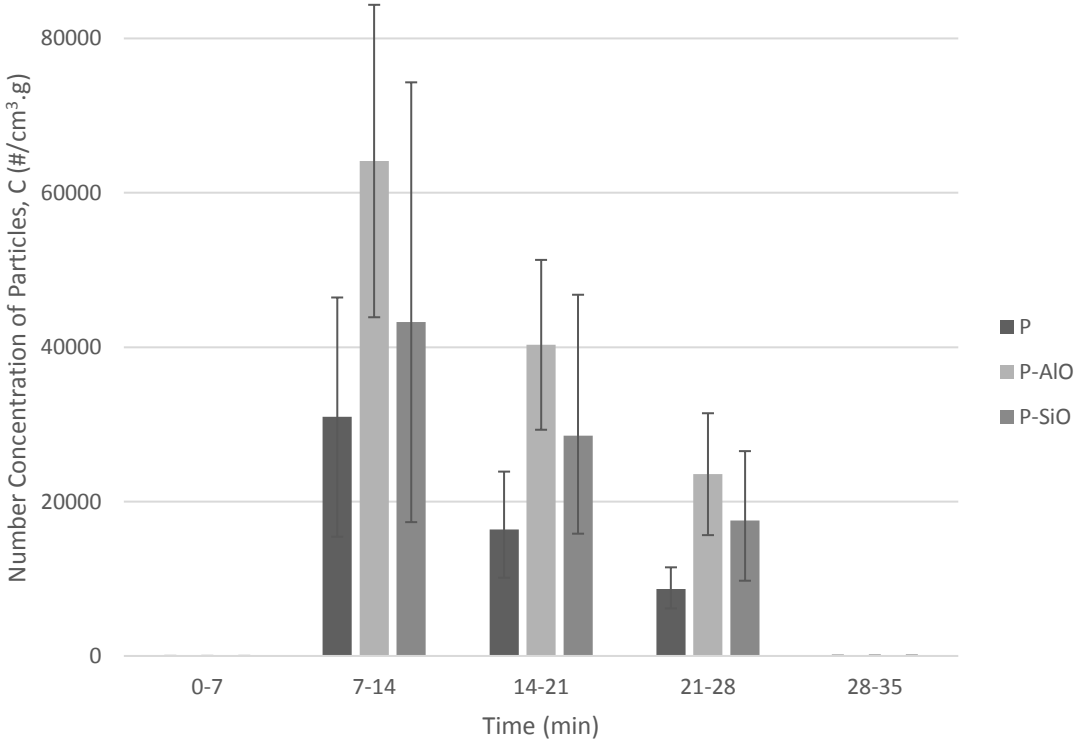

Figure 35: Total Number Concentration of Particles $C_{Normalised}$ for Polyester Samples during Drilling Experiments

convection, or coagulation are some of them [173]. Large particles are mainly removed by sedimentation when smaller ones disappear by diffusion [173]. Also coagulation can be neglected in this case as this phenomenon is linked to the number concentration of particles which was pretty low.

The average particle size distribution for each grade of Polyester-based materials studied during drilling (7-14 minutes) is shown Figure 36. The data was normalised to background noise. The size distribution for every grade has a similar profile: a bell curve of different intensity according to the quantity of particles released. The first comment to make is that around 90 % of the particles measured have a size under 100 nm, so are, according to the standard definition, nanoparticles. Also the peak concentration is between 50 to 60 nm for the different grades: 51.66 nm for the P samples, 61.52 nm for the P-AlO and 54.11 nm for the P-SiO. So, the samples emitting the highest number concentration of particles (P-AlO) are actually producing particles with a slightly bigger diameter.

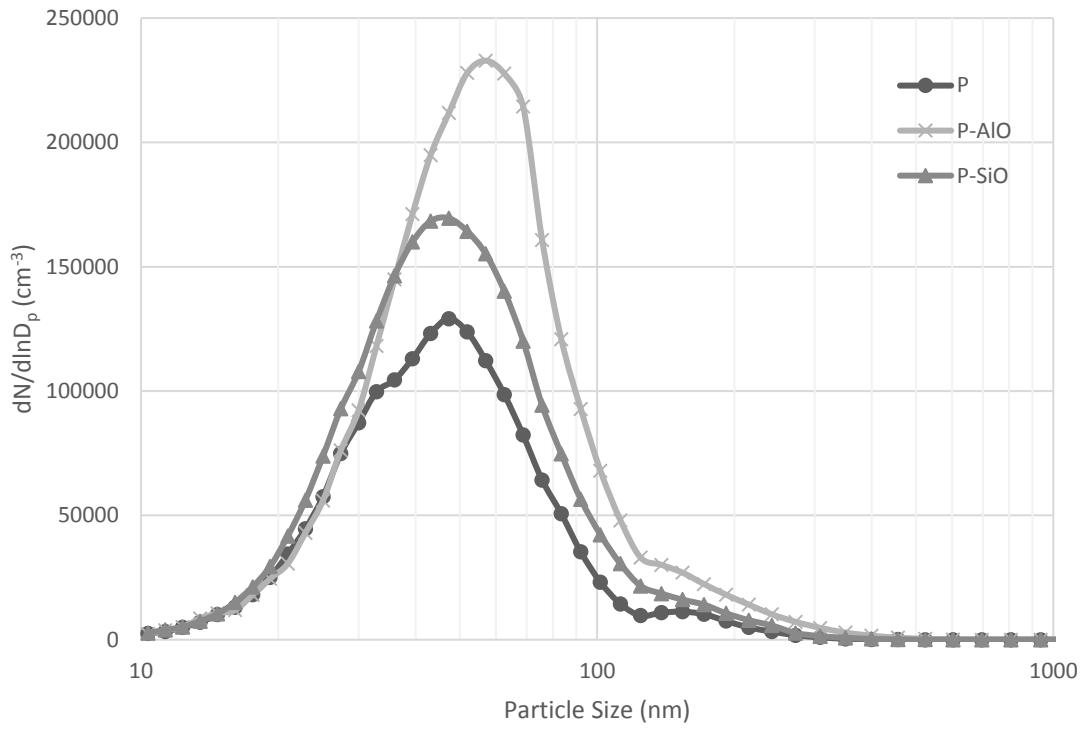

Figure 36: Size Distribution during Drilling of Polyester-based Samples

4.3.1.2 Epoxy Samples

Average values for the total number concentration of particles C and particle diameters *d* are summarized Table 15.

Table 15: Average Values for Background Number Concentration of Particles removed (C_{Noise}), Total Number Concentration of Particles (C_{Peak}), Total Normalised Number Concentration of Particles ($C_{Normalised}$), Median Particle Diameter (d_{median}) and Diameter of the Highest Number Concentration of Particles (d_{hncp}) during Drilling of Epoxy based Samples

	C_{Noise}	C_{Peak}	$C_{Normalised}$	d_{median}	d_{hncp}
	(particles/cm^3)		(particles/cm^3.g)	(nm)	(nm)
E	471 ± 314	7555 ± 6563	5761 ± 3123	97.98	101.66
E-CNT	352 ± 183	4410 ± 1329	6523 ± 2759	121.98	124.59
E-CNF	158 ± 40	4619 ± 1104	10267 ± 3951	92.80	112.45

The results for the number concentration of particles measured (C_{Peak}, particles/cm^3) showed that the neat Epoxy samples were emitting the highest number concentration of particles, and similar quantity was generated by E-CNT and E-CNF samples. However, the normalised data calculated by removing the background noise and the mass balance of materials drilled lead to different conclusions. Indeed, after normalisation of the data, it was found that the neat Epoxy released the lowest number concentration of particles. The number concentration of particles emitted by E-CNT was similar. E-CNF produced the highest number concentration of particles. The data was normalised for background noise and total weight of the material drilled as the samples were irregular and the volume / mass of material drilled was different.

Figure 37 shows the evolution of normalised number concentration of particles over the duration of the experiment. The trend was similar to the polyester grades. The number concentration of particles increased dramatically during the 7 minutes of drilling (7-14 min) to reach a maximum, and then the number concentration of particles decreased gradually to go back to a level close to before the start of the experiment.

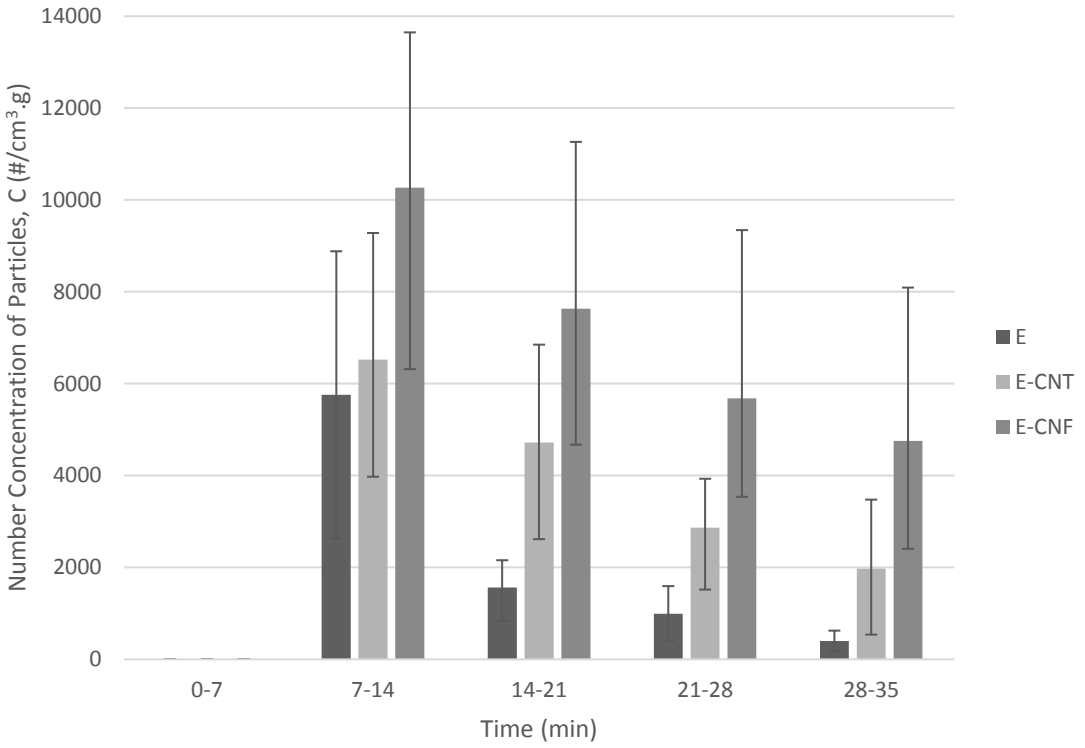

Figure 37: Total Number Concentration of Particles $C_{Normalised}$ for Epoxy Samples during Drilling Experiments

The average size distribution for the different Epoxy grades is presented in Figure 38. As for the Polyester samples, the curves also present a bell shape but at a higher particle size. Epoxy materials had a median peak concentration at 97.98 nm, E-CNT at 121.98 nm and E-CNF at 92.80 nm. It is also important to notice that the E-CNF samples showed a second higher particle concentration in the smaller particle diameter (around 10 to 25 nm). A size distribution with a double or multi-peak curve can illustrate the presence of a mixture of aerosols such as agglomerates and free engineered nanoparticles for example [220]. It would be interesting to repeat this experiment with a short DMA to measure particles of a diameter smaller than 10 nm. Also, unlike the Polyester grades, the number concentration of particles measured of diameter under 100nm was lower: 51 % for the E and E-CNF materials and only 33 % for the E-CNT samples.

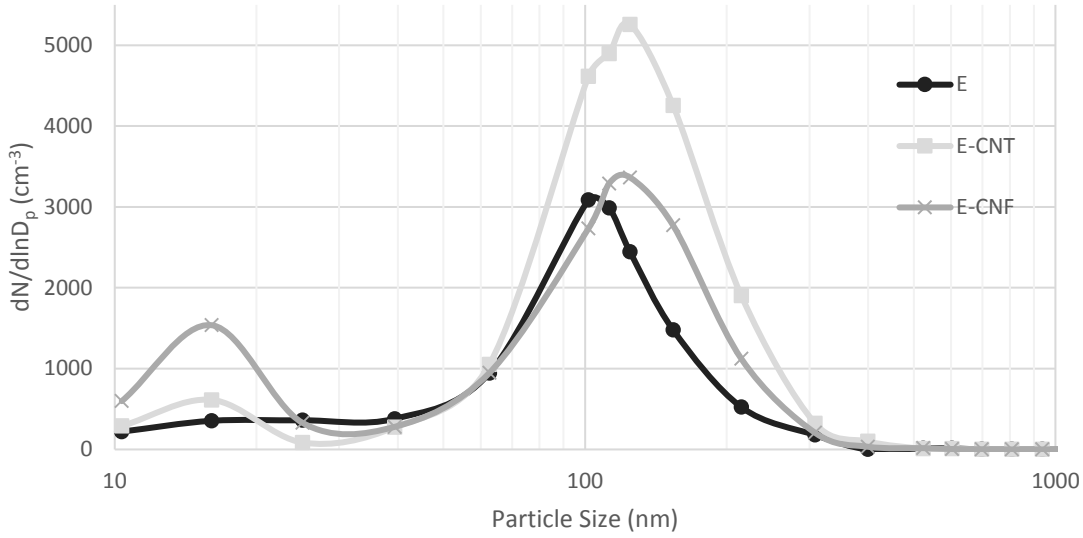

Figure 38: Size Distribution during Drilling of Epoxy-based Samples

4.3.1.3 Polypropylene Samples

In the set of samples with PP, the baseline to compare the PP-MMT and PP-WO nanocomposites with was PP plus 20 % talc. It is a most common material used in automotive applications than neat PP.

Table 16: Average Values for Background Number Concentration of Particles removed (C_{Noise}), Total Number Concentration of Particles (C_{Peak}), Total Normalised Number Concentration of Particles ($C_{Normalised}$), Median Particle Diameter (d_{median}) and Diameter of the Highest Number Concentration of Particles (d_{hncp}) during Drilling of Polypropylene based Samples

	C_{Noise}	C_{Peak}	$C_{Normalised}$	d_{median}	d_{hncp}
	(particles/cm^3)		(particles/cm^3.g)	(nm)	(nm)
PP	602 ± 61	632 ± 191	2683 ± 772	61.57	32.82
PP-TALC	332 ± 104	740 ± 70	1597 ± 134	62.40	25.06
PP-WO	433 ± 22	680 ± 111	3067 ± 1161	68.73	101.66
PP-MMT	395 ± 123	712 ± 158	2453 ± 452	82.05	101.66

Table 16 presents the average results for the drilling experiments of the different PP grades. C_{Peak} (number concentration of particles, particles/cm^3) represents the number concentration of particles released during the drilling with the background noise removed, while $C_{Normalised}$ (particles/cm^3.g) is the number concentration of particles with the background removed and normalised with the

weight of samples removed by the drilling action. The number concentration of particles released for these types of samples was extremely low (under 750 particles/cm^3 after subtraction of the background noise). This level is similar to the number concentration of particles that can be measured in the chamber when no activity occurs. Also, it was significantly lower than the average number concentration of particles in the normal lab air (around 6700 particles/cm^3). In addition, no significant differences could be observed between the neat Polypropylene, the nanoreinforced Polypropylene, and the one filled with talcum. The low level of particles might be explained by the nature of the matrix: polypropylene is a thermoplastic while polyester and epoxy tested previously were thermosets materials. Especially, Polypropylene melts at 130 °C. The heat released during the drilling could then melt the matrix and trap the particles. As for the thermoset materials, the matrix was breaking in small pieces. To avoid the melting of polypropylene, higher spindle speed and feed rate would be recommended. However, the quality of the holes drilled in PP composites with similar parameters than for thermosets (spindle speed of 8500 rpm and feed rate at 200 mm/min) seems reasonable.

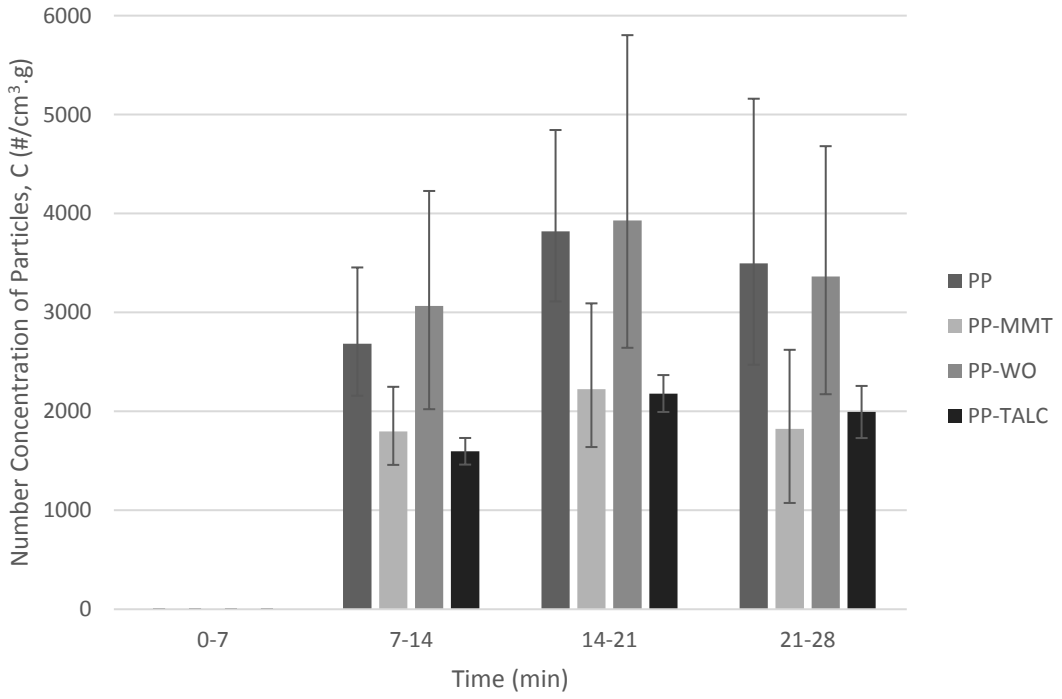

Figure 39: Total Number Concentration of Particles $C_{Normalised}$ for Polypropylene Samples during Drilling Experiments

Figure 39 represents the normalised number concentration of particles over time during the drilling experiments. As for the previous experiments, the first scan (0-7 minutes) measured the background particles in the chamber, and then was reduced to zero for the normalised data. These data points differ to the ones from the thermosets samples. In this case, the concentration of particles increased during the drilling process, but once it was stopped, the concentration of particles kept increasing for the next scan and slowly decreased during the last one. This indicates that the airborne particles released do not sediment, but remain in the environment for a longer period. One possible reason for this is the low density of the polypropylene (≈900 kg/m^3) compared to polyester (≈1400 kg/m^3) and epoxy (≈1250 kg/m^3).

The average size distribution for the particles emitted during drilling (7-14 minutes) of the Polypropylene samples is presented Figure 40. In this case, around 75 % of the measured particles were under 100 nm. The size distribution curves were similar for all the grades with a median peak concentration around 60 to 80 nm. It has to be noted that the number concentration of particles emitted in this case was really low (under 750 particles/cm^3). This level was lower than the common lab air. Also the size distribution was not dissimilar to the one observed earlier in the chamber.

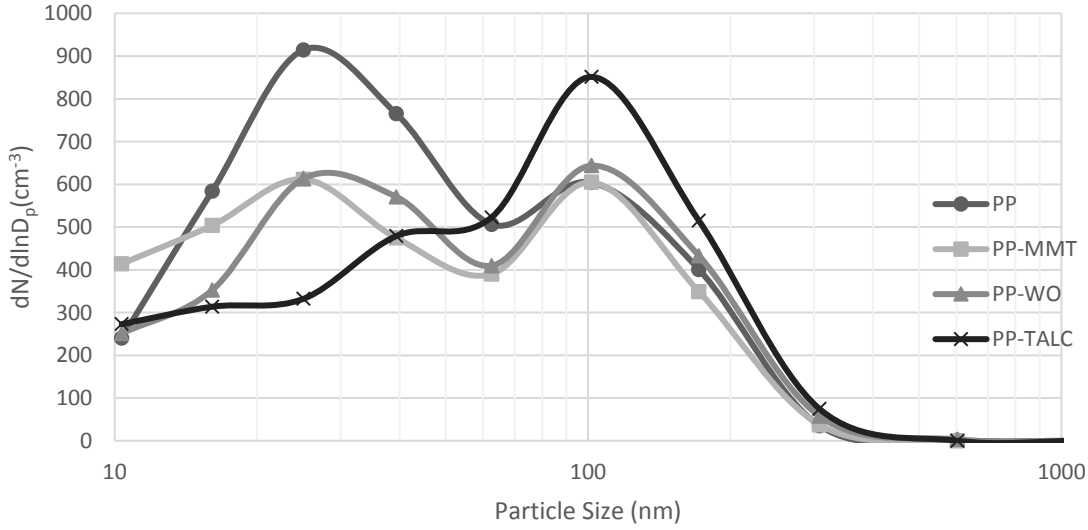

Figure 40: Size Distribution during Drilling of Polypropylene-based Samples

4.3.2 Characterisation of the Deposited Particles

SEM analysis was conducted on the deposited particles collected in a petri dish during the second set of experiments (drilling a single hole). In images at low magnification (Figure 41) the different behaviour of the matrices reacting to the drilling can be noticed. This also helps to understand the difference in the quantity of nanoparticles released by different matrix materials. In the case of the thermosets, Polyester (Figure 41, (a)) and Epoxy (Figure 41, (b)), the turns look like thin slices. The edges of the turns collected are curved and nicely defined and the surfaces full of little strips. On the contrary, the turns collected from the drilling of Polypropylene (Figure 41, (c)), thermoplastic material, appear to be like an agglomeration of materials after melting. This behaviour can explain the low quantity of nanoparticles released from the polypropylene samples, as the nanoparticles could have been retained in the melted materials instead of being released. This also demonstrates that process parameters could lead to thermal

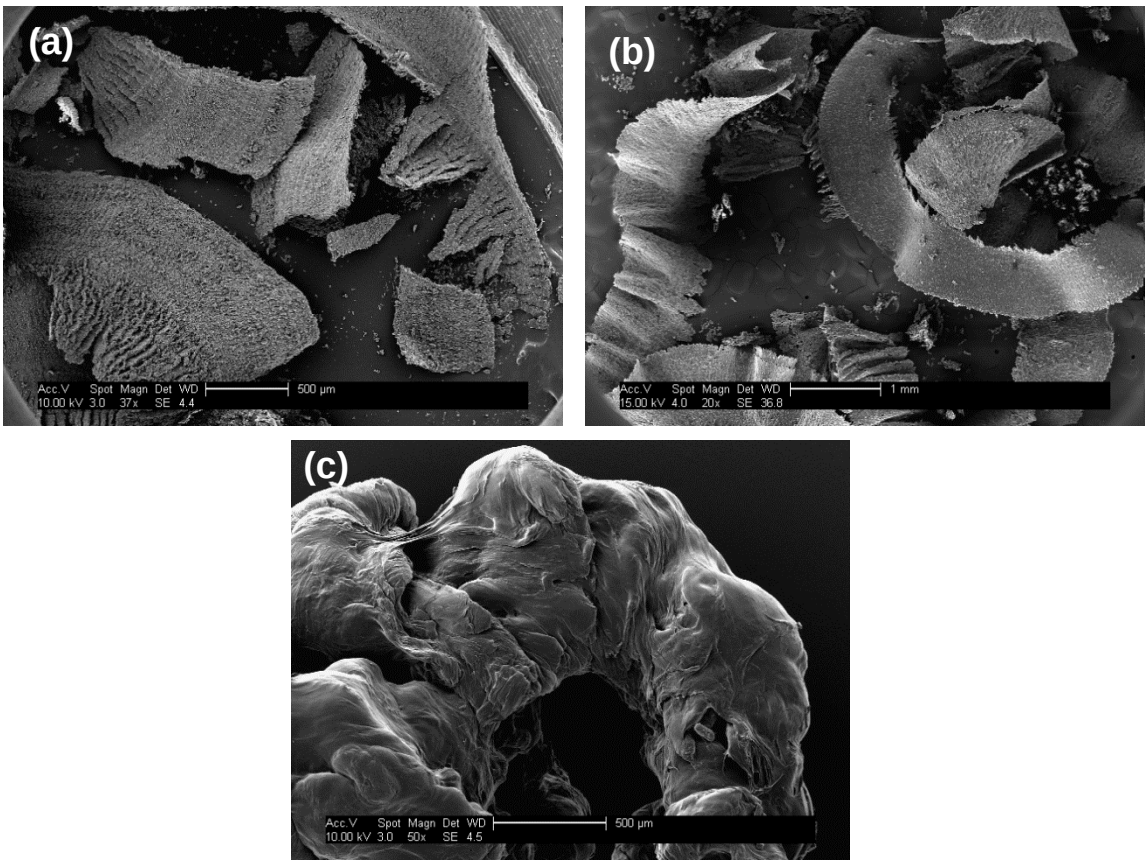

Figure 41: SEM Images of the Turns Collected from a P-AlO (a), a E-CNT (b) and a PP (c) Samples at Low Magnification

degradation on the nanocomposite. This thermal degradation can potentially be a source of nanoparticles (as a result of chemical reactions) different from a mere physical process.

4.3.2.1 Polyester Samples

At a macroscale, no difference could be observed between the turns produced by the drilling of the three grades of polyester. Figure 41, (a) was representative of the Polyester grades observed at low magnification. However, at smaller scale (Figure 42) nanoparticles were observed on the surface of the turns of the different Polyester samples, especially on P-Al_2O_3 (Figure 42, (d)). It is worthy to mention that the sample with no nanofiller (Figure 42, (a)) also presents nanoparticles on its surface which can be particles made of the matrix (neat polymer) materials generated during the drilling. The nanoparticles observed could be attached or adhered to the surface. Presumably, the nanoparticles measured with the 'SMPS+C' come from the physical degradation of the samples

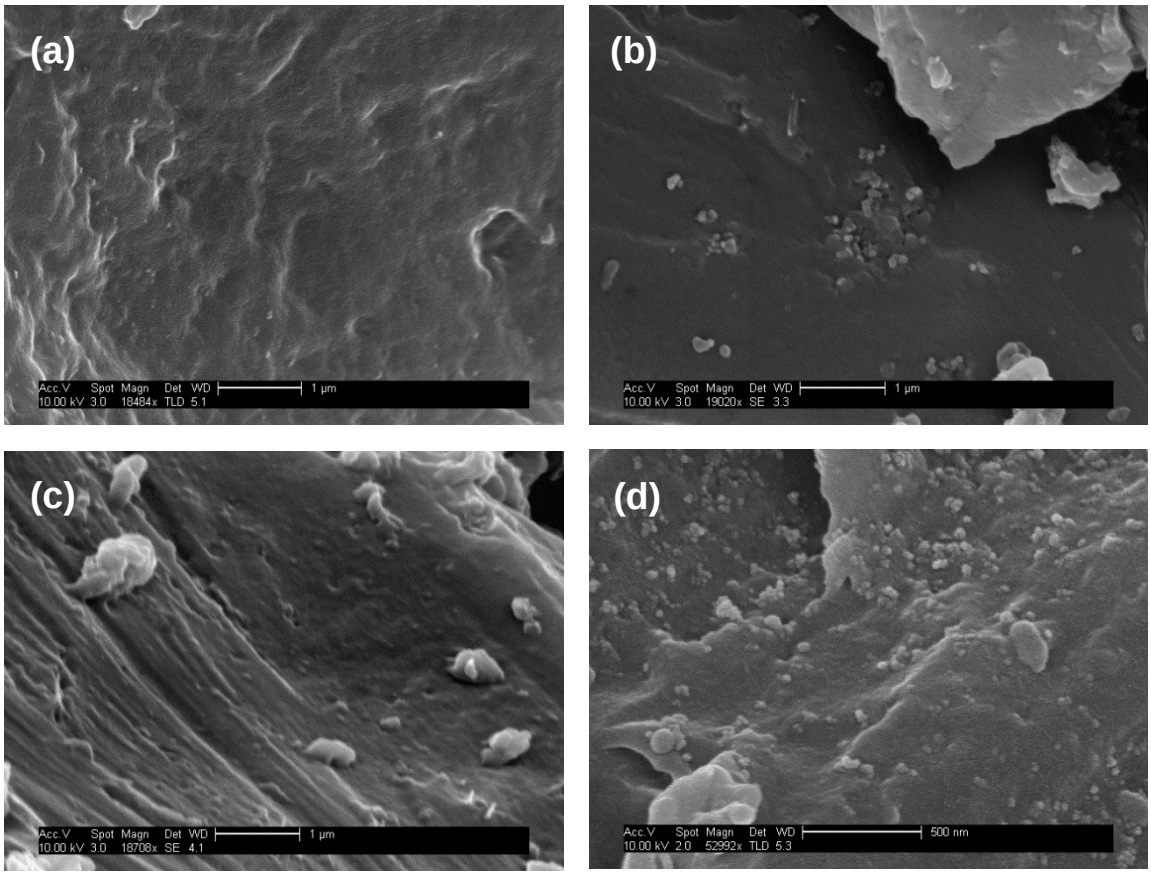

Figure 42: SEM Images of the Surface of a Turn Collected from a P (a), a P-SiO (b) and a P-AlO (c) Sample, and a P-AlO Sample at Higher Magnification (d)

surface. However, it was difficult to distinguish between nanoparticles that completely separated from the surface or adhered to it. One of the main contamination routes was skin contact. Therefore, it is important to determine if the big particles (’chips’) can be a source of contamination. Additionaly, EDX was carried out on the samples. The technique was unsuccessful as no distinction could be done between the particles and the rest of the sample. However, as good care was taken to store the samples to avoid external contamination, it is believed that the particles are the one geenrated by the drilling.

4.3.2.2 Epoxy Samples

At low magnification, the three types of epoxy samples had features similar to those presented in Figure 41, (b). Also, no significant difference could be observed at high magnification (x20000, Figure 43) between the neat epoxy and nanocomposite samples. Nanoparticles and agglomerates can be noticed on the

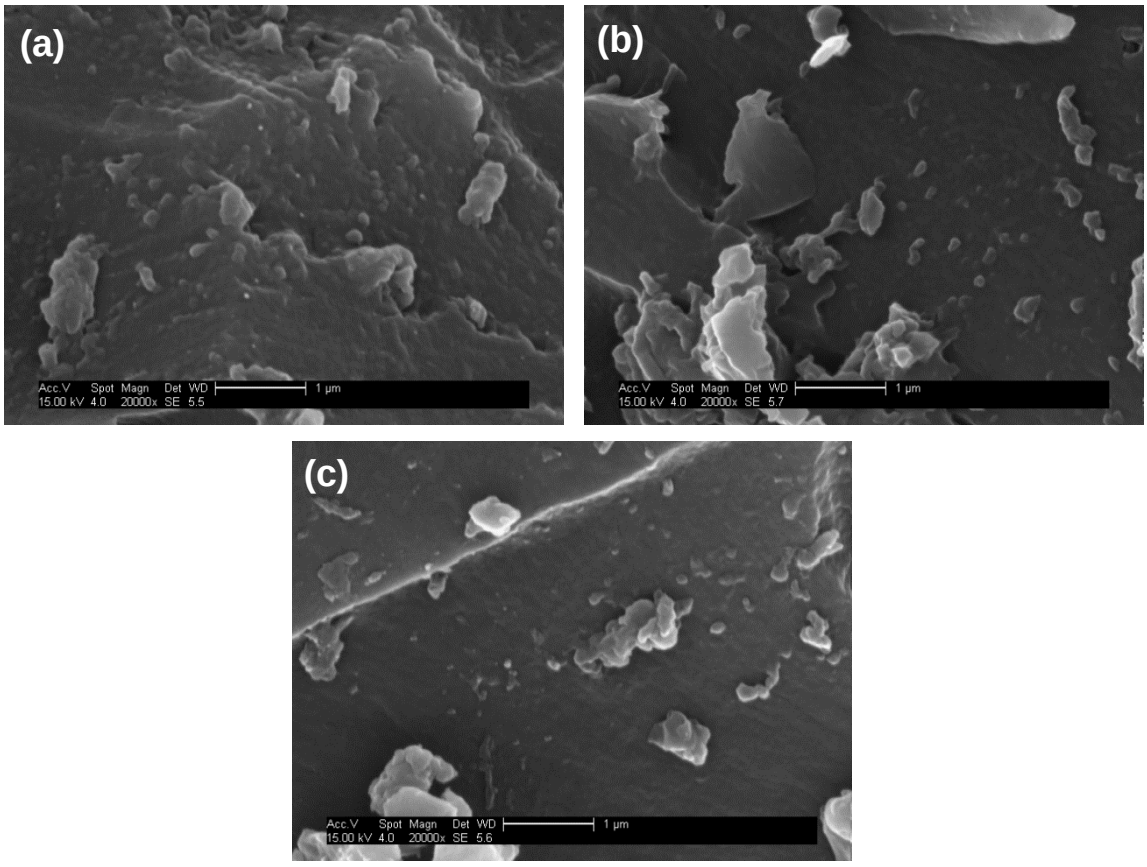

Figure 43: SEM Images of the Turns Collected from an E-CNT (a), an E-CNF (b) and an E (c) sample at high magnification

three images indicating the presence of nanoadditives in the material. The shape and size of the particles was similar, also no free CNT or CNF could be observed with this magnification. The results of the SEM analysis were in line with the data from the airborne particles where the three types of epoxy materials were found to emit a similar amount of particles with similar diameter.

4.3.2.3 Polypropylene Samples

At low magnification, it was noticed that the Polypropylene matrix had melted (Figure 41, (c)). This was the case for every grades of polypropylene material. However, at high magnification (x20000, Figure 44) PP and PP-MMT specimens (Figure 44, (a) and (c)) showed a textured surface and no nanoparticles could be distinguished. The PP-Talc sample (Figure 44, (d)) presented the same textured surface but in addition, several fibril materials were seen with a diameter of around 90 nm. One of them was clearly embedded in the matrix, and the distinction between the matrix and the filler was not detectable. It was hard to

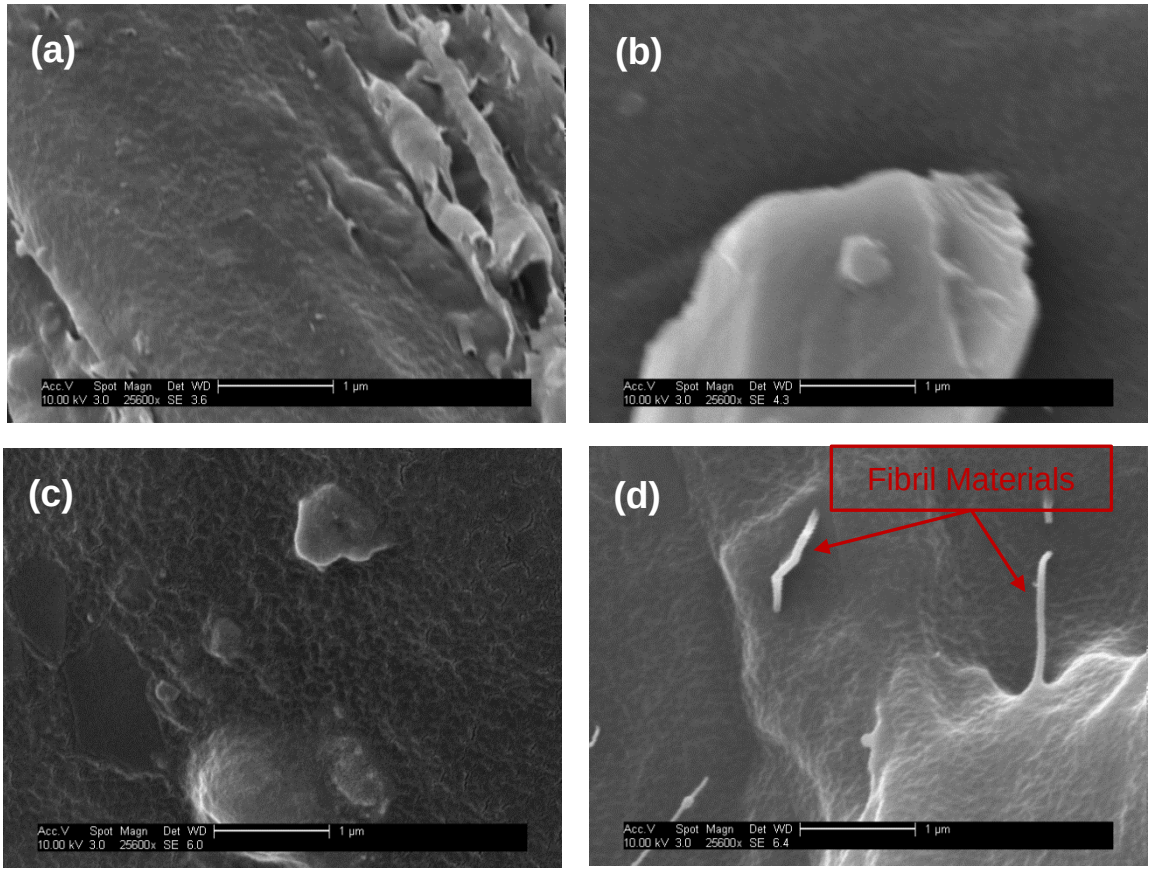

Figure 44: SEM Images of the Surface of a Turn Collected from a PP (a), a PP-WO (b), a PP-MMT (c) and a PP-Talc (d) Sample at High Magnification

define if these fibre shapes were talcum or part of the matrix. EDX was used but the technique didn't succeed in differentiating between the matrix and the filler. The last image (Figure 44, (b)) represents the PP-WO sample. The occurrence of large particles (over 2.5 µm of diameter) was consistent on the surface of the sample. Wollastonite are needle shapes of median size of 8.5 µm. However, their diameter is in the nanorange. Therefore, these large particles cannot be free Wollastonite as they were too big.

4.3.2.4 FTIR Analysis

Fourier Transform Infrared Spectroscopy (FTIR) analyses was performed on the bulk materials prior to drilling as well as on the dust collected in the petri dish after drilling in order to identify possible chemical change in the particle released. The results are presented Figure 45, Figure 46 and Figure 47.

The characteristic peaks of polyester, nanosilica and nanoalumina are reported Table 17 [221]–[224]. The characteristic peaks for polyester were indicated on the FTIR spectrograms for the polyester grades (Figure 45). On this spectrogram, it was not possible to identify clearly the peaks related to nanosilica and nanoalumina. This might be due to the high thickness of the sample characterised for the bulk materials and the low content of nanofiller but can also prove a good exfoliation of the fillers. Also several characteristic peaks for nanosilica or nanoalumina (for example the Si-O asymmetrical stretch in SiO_2, at 959, 938 and 875 cm^{-1}) already appear in the neat polyester sample.

Also, no significant changes appear between the bulk and drilled specimens. The same characteristic peaks can be observed in both cases for the three types of samples. The only difference was in their intensity. However, the bulk material was characterised with a solid plate (5 mm thick) while the drilled material was in dust/powder shape. The difference in intensity was due to the difference in thickness of the samples characterised.

Table 17: Characteristic Peaks in FTIR of Polyester, Nanosilica and Nanoalumina

Material	Band (cm^{-1})	Assignment
Polyester	3448	O-H stretch
	3060 3026 2982	Aliphatic C-H stretch
	1728	C=O stretch
	1599 1580 1493	Aromatic ring stretch
	1453	CH_3 asymmetrical bend
	1380	CH_3 symmetrical bend
	1284	CH_2 twist
	1121	C-O stretch
Nanosilica	3457	O-H stretch in silanol hydroxyls
	1268-1132	Si-O-Si stretch
	966	Si-OH bond
	959 938 875	Si-O asymmetrical stretch in SiO_4
	810	Si-O asymmetrical stretch
	525 511	O-Si-O out-of-plane bending
	450	O-Si-O in-plane bending
Nanoalumina	1200-950	Al-O-M bonds
	3092 2090 1920	-OH groups in alumina

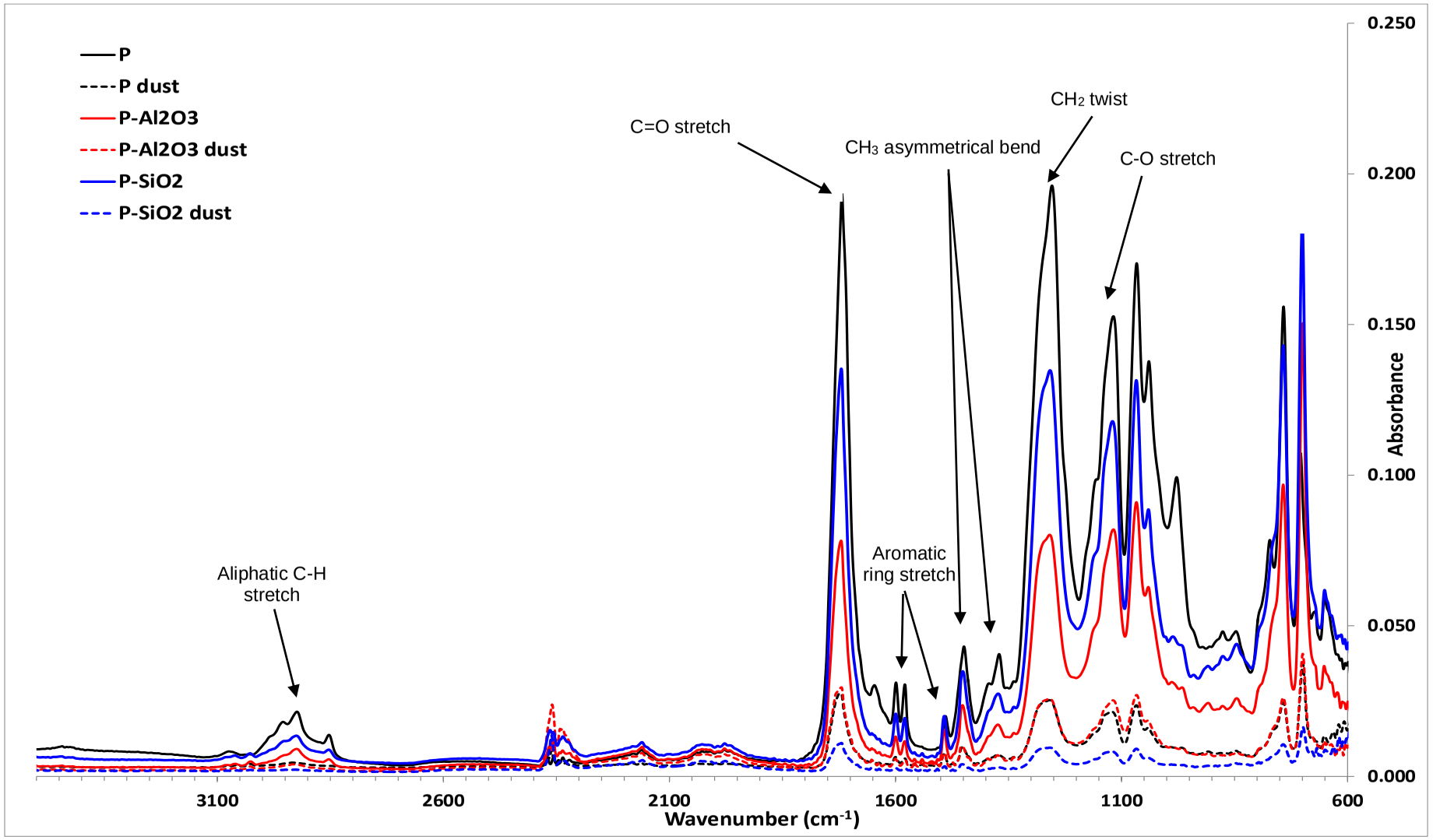

Figure 45: FTIR Spectrograms for Polyester-based Samples

Similar conclusions were drawn for the Epoxy based samples. The characteristic peaks of epoxy, CNTs and CNFs are reported Table 18 [221], [225]–[227]. The characteristic peaks for epoxy were indicated on the FTIR spectrograms for the epoxy grades Figure 46. No clear identification of the peaks related to CNTs and CNFs could be observed. Also, no significant changes appear between the bulk and drilled specimens.

Table 18: Characteristic Peaks in FTIR of Epoxy, CNTs and CNFs

Material	Band (cm^{-1})	Assignment
Epoxy	3364	O-H stretch
	2925	Aliphatic C-H stretch
	2862 1608 1510	Aromatic ring stretch
	1453	CH_3 asymmetrical bend
	1376	CH_3 symmetrical bend
	1296	Epoxy ring mode: C-C, C-O
	1243 1176 1108	Ar-O-R asymmetrical bend
	1036	Ar-O-R symmetrical bend
	828	Aromatic ring bend out of plane
	753	Monosubstituted aromatic ring stretch
CNTs	2962 2928 2856	CH_x groups
	1725	COOH groups
	1584	G band
	1200	D band
CNFs	2870-2931	CH_2 stretch
	2245	C≡N stretch
	1732	C=O stretch
	1684	Amide group
	1450	CH_2 bend

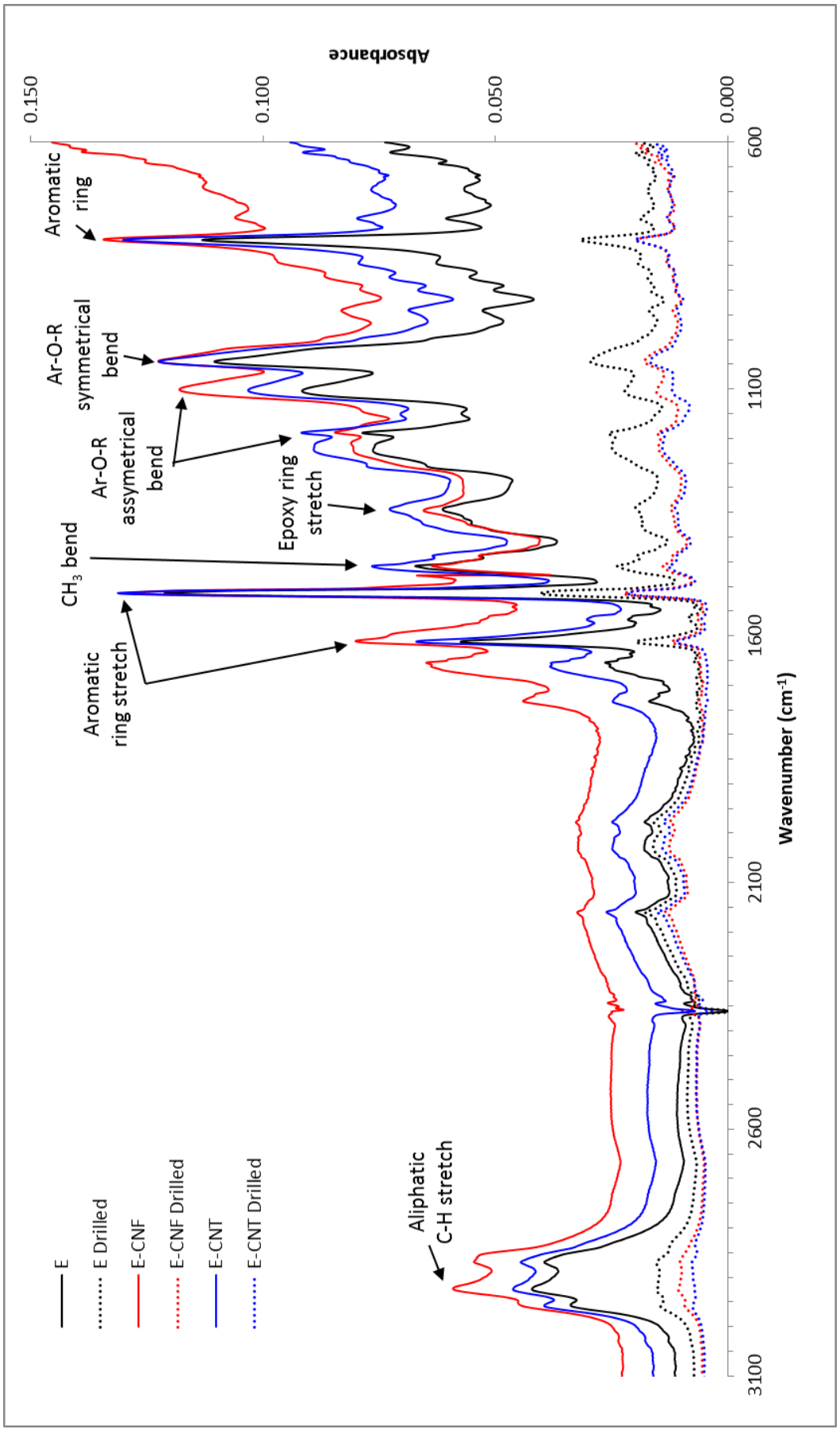

Figure 46: FTIR Spectrograms for Epoxy-based Samples

The characteristic peaks of polypropylene, talcum, MMT and WO are reported Table 19 [228]–[231]. The characteristic peaks for polypropylene and talc were indicated on the FTIR spectrograms for the polypropylene grades (Figure 47). No clear identification of the peaks related to MMT and WO could be observed. However, characteristics peaks related to talc was clearly noticed. This was due to the high percentage of talcum (20 %) present in the polypropylene matrix. Also, no significant changes appear between the bulk and drilled specimens.

Table 19: Characteristic Peaks in FTIR of Polypropylene, Talcum, MMT and WO

Material	Band (cm^{-1})	Assignment
Polypropylene	2970	CH_3 asymmetric stretch
	2910	CH_3 symmetric stretch
	2870	CH_2 asymmetric stretch
	2840	CH_2 symmetric stretch
	1460	CH_3 asymmetric bend
	1370	CH_3 symmetric bend
Talcum	1018-1045	Si-O stretch
	670-690	Si-O bend
MMT	1165	CaO stretch
	1120	
	1049	
	918	Al-Al-OH deformation
	845	Al-Mg-OH deformation
	798	Si-O stretch
	778	
WO	1631	CaO
	875	
	1440-1450	Carbonate
	960	Si-O-Si, Si-O-Ca

In conclusion, no chemical changes were observed between the bulk and drilled materials.

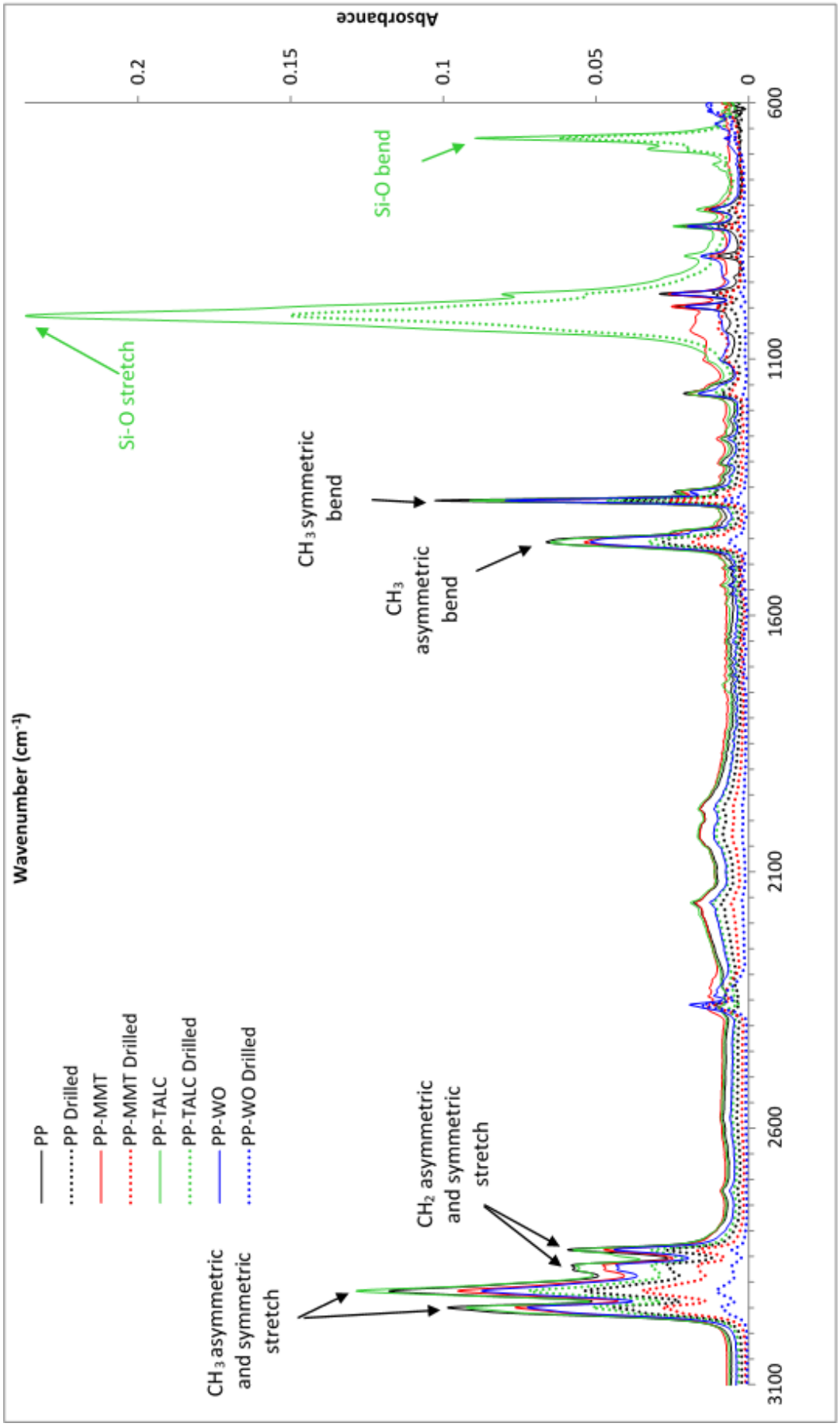

Figure 47: FTIR Spectrograms for Polypropylene-based Samples

4.4 Conclusion

In this work, the release of nanoparticles from commercial nanocomposites was evaluated by applying a validated methodology described in the Chapter 3. This method was applied in order to assess the particles emitted during drilling of nanocomposites. Summary of the results for the drilling experiments can be found Table 20. It was identified that the type of matrix plays a major role on the number concentration of nanoparticles released during drilling of nanocomposites. Thermosets polymers (Polyester and Epoxy) release a higher number concentration of particles than Polypropylene samples (respectively 19 times and 3 times higher for the normalised values). Thermoplastics are typically drilled at higher spindle speed and feed rate. For comparison the same spindle speed and feed rate was implemented for all the samples. Surface analysis revealed that the thermoplastic matrix melted during the drilling operation and as a result less amount of particles were generated. This was also corroborated with SEM images. SEM analysis revealed the presence of nanoparticles on the surface of thermoset samples (P and E), but hardly any nanoparticles or nanoagglomerates were found on the surface of thermoplastics (PP samples).

Table 20: Average Values of C during Drilling by Type of Nanocomposites

	Nanoadditives	$C_{drilling}$ (particles/cm^3)	Normalised $C_{drilling}$ (particles/cm^3.g)	d_{median} (nm)
P samples	SiO_2; Al_2O_3; -	150200 ± 45900	46100 ± 13700	50-60
E samples	CNT; CNF; -	5500 ± 1400	7500 ± 1900	90-120
PP samples	WO; MMT; TALC; -	690 ± 40	2450 ± 540	60-80

Also, the nanoadditives seem to impact the release of particles during drilling for thermosets materials. The differences between the neat matrix and the nanocomposites were significant. The addition of Silica or Alumina into Polyester increased the number concentration of particles by 39 and 106 % respectively (for the normalised values). For the Epoxy samples, the addition of CNT was found to slightly increase the number concentration of particles released by

13 %, and the CNF addition to increase it by 78 % (again for the normalised values).

To conclude, it was shown that thermoplastics based nanocomposites are less likely than thermoset ones to release nano-sized particles during machining of nanocomposite parts. However, every materials tested was found to emit nano-sized particles and this even for neat polymers. As drilling is a common practice in a wide range of industries, it is important to consider these results regarding to the health and safety of workers dealing with such activities. Also, the present study informs on the quantity, size and shape of the nanoparticles release i.e. the potential exposure, these results should be combine with toxicity analysis in order to assess the potential hazard of this activity and then quantify its risk.

5 EMISSION OF NANOSIZED PARTICLES BY IMPACT ON POLYMER BASED NANOCOMPOSITES

5.1 Introduction

Sachse et al. [232] studied the behaviour of crash cones to simulate an automotive part in a collision context. The cones were made of Polypropylene reinforced with glass fibres and either nanosilica, nanoclay or microsilica. This work had some deficiencies as the environment was not controlled allowing activities taking place in the area to influence the results. To the best of the author's knowledge, this is the only study on release of nanoparticles during impact simulating the end-of-life by destruction of a part.

In this chapter, release of nanoparticles from nanocomposites following an impact was studied. Nano-objects can be emitted from the surface of the matrix under lower velocity impact. But in order to release pristine nanofillers from a matrix, considerable accelerations are necessary to generate forces able to compete with van der Waals forces, for example through instantaneous shocks [232], [233].

5.2 Materials and Methods

5.2.1 Materials' Descriptions and Manufacturing

The materials tested by low velocity impact were described previously in 4.2.1 and are similar to the ones testing by drilling (Chapter 4).

5.2.2 Measurement of Nanoparticles Released during Low Velocity Impact

The impact experiments aim to simulate the release of particles during the destruction (by impact) of a nanocomposite. Given that these nanocomposites were designed to be used in the automotive sector, it was decided to follow the test conditions of the Euro NCAP regulation for 'Impact testing' [234]. The experiments were carried out using a Low Velocity Gas Gun (LVGG, manufactured by SABRE Ballistics) and the following parameters were used:

- Impact speed: 15,6 m/s;
- Projectile: m=22g, shape: hemi-spherical head made of steel with cylindrical PA6 body, 25 mm diameter.

One of the main advantages of using the LVGG is the control over the test conditions. Using this equipment it is possible to apply the same energy to all the samples, as it depends on the mass and speed of the projectile (bullet). The speed of the bullet is controlled by the pressure applied in the barrel. In addition, the software records every time the speed of the bullet.

The chamber, described previously in Section 3.3, designed for the impact experiment with the gas gun was used in order to ensure a constant clean environment for the measurement of particles and reproducible data for the experiments. The sample was placed in the chamber using a fixture and the measurement point for the SMPS+C was on top of the sample, as close as possible of the impact point. An overview of the set-up can be seen Figure 48 and Figure 49.

Each measurement cycle (scan) lasted approximately 7 minutes. These measurements give the number concentration of particles (*C*, particles/cm^3) and particle size distribution.

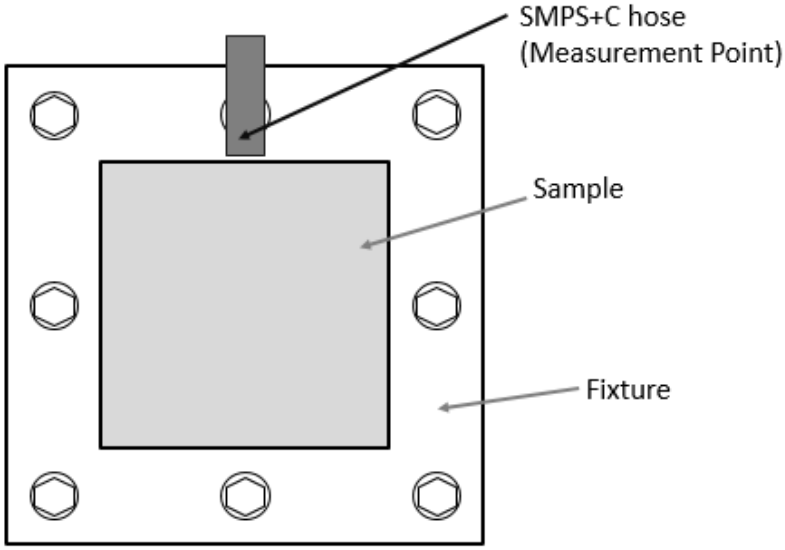

Figure 48: Measurement Point for the Impact Experiments

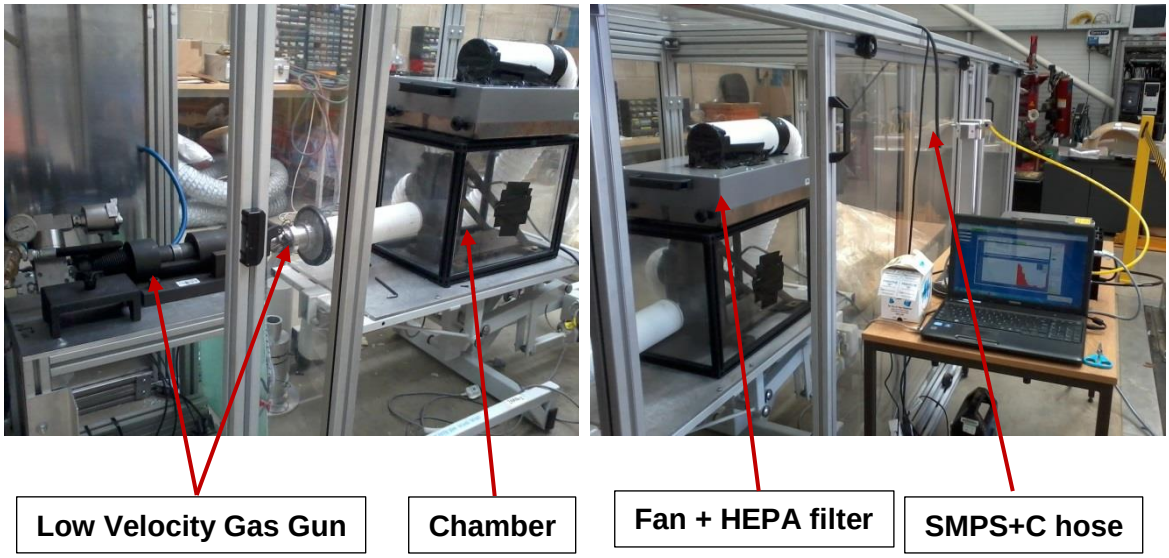

Figure 49: Experimental Set-Up (Low Velocity Gas Gun, Chamber and SMPS+C)

The measurement cycle used for every experiment was as follows: one measurement of the air in the lab followed by one measurement of the air inside the chamber with the fan on in order to clean the chamber. Then, two measurements of 7 minutes each with the 'SMPS+C' were done of the air inside the chamber with the fan off in order to ensure a constant number concentration of particles and assess the background level of particles. The projectile was fired during the next cycle (fan off), such that the SMPS+C was able to measure the smaller particles (<100 nm) in order to catch the nanoparticles released during the impact straight away. Then the measurement continued until the level of particles was back to the original background.

A high speed camera (FASTCAM SA4 Model 500K M1) was used to record the impact of the tested plates.

5.2.3 Characterisation of Fragments Generated during Impact

The pieces collected after impact of the test plaques were analysed with a FEI XL30 field emission scanning electron microscope (SEM). The operating voltage was in the range of 10-20 kV and the specimens were gold sputtered to minimize charging of the sample.

5.3 Results and Discussion

5.3.1 Impact Performance of Nanocomposites

All the specimens were impacted with the same level of energy (corresponding to a velocity of 15 m/s). Pictures of the fragments collected after impact can be seen in Figure 50 and Figure 51. Double sided tape was placed behind the samples on the fixture, which allowed to collect most of the pieces affected directly by the impact. The broken pieces can give an indication on the failure mode of the samples. No differences were seen between the different grades of Polyester. An example of the failure pattern is shown Figure 50, (a). Similarly, Figure 50, (b) represents a typical failure pattern for an Epoxy grade. Both failed in a brittle manner. The broken pieces collected were relatively small.

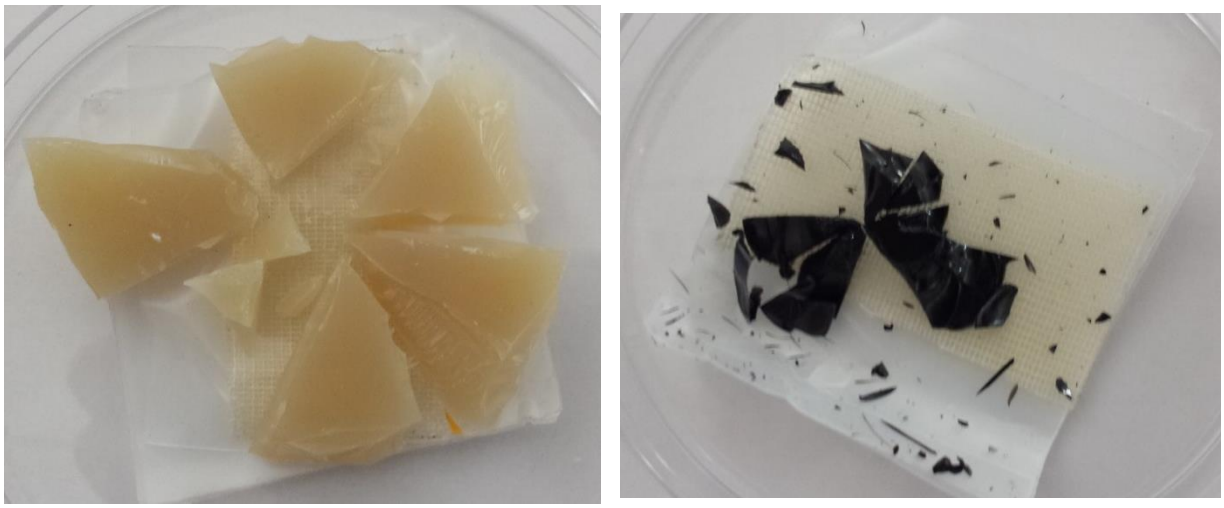

Figure 50: Broken Fragments from a (a) P-SiO Plate, and from a (b) E-CNT Plate after Impact

Figure 51 represents the failure pattern for PP based samples. However, the PP samples reinforced with talc did not fracture. No cracks were visible on the surface of the impacted plate. This material performed better than the nanoreinforced one. The other PP samples (PP, PP-MMT and PP-WO) fracture according to the pattern seen Figure 51. For these samples, only 4 or 5 big pieces were formed after impact. The cracks were long and neat. This might be due to the lower strength and less brittle nature of PP compared to the thermosets tested. It however had a better energy absorption capability and was able to deform elastically.

Figure 51: Broken Fragments from a PP-MMT Sample After Impact

5.3.2 Particles Generated during Impact

The Scan Mobility Particle Sizer plus Particle Counter ('SMPS+C') provides the number concentration of particles and size distribution during the time that the scan lasts, i.e. 7 minutes. However, background concentration varied slightly among experiments. So, data from the SMPS+C was normalised by extracting the background concentration (given by the value of C before the experiments starts) for each particle size and for the total concentration.

In this section the average values for each grade (total number concentration of particles emitted and particle size distribution after impact) are presented. In addition, results are analysed and discussed.

5.3.2.1 Polyester Samples

Main results for the impact experiments of the Polyester based nanocomposites are presented Table 21.

Table 21: Average Values for Background Number Concentration of Particles removed (C_{Noise}), Total Number Concentration of Particles (C_{Peak}), Median Particle Diameter (d_{median}) and Diameter of the Highest Number Concentration of Particles (d_{hncp}) during Impact of Polyester based Samples

	C_{Noise} (particles/cm^3)	C_{Peak} (particles/cm^3)	d_{median} (nm)	d_{hncp} (nm)
P	582 ± 176	13399 ± 5936	24.72	14.97
P-AlO	642 ± 285	29375 ± 15091	24.33	21.33
P-SiO	734 ± 193	19571 ± 9579	22.24	12.55

The average values of *C* versus time for each grade (P, P-Al_2O_3 and P-SiO_2) are presented in Figure 52 (normalised data). In all the cases, it can be observed that

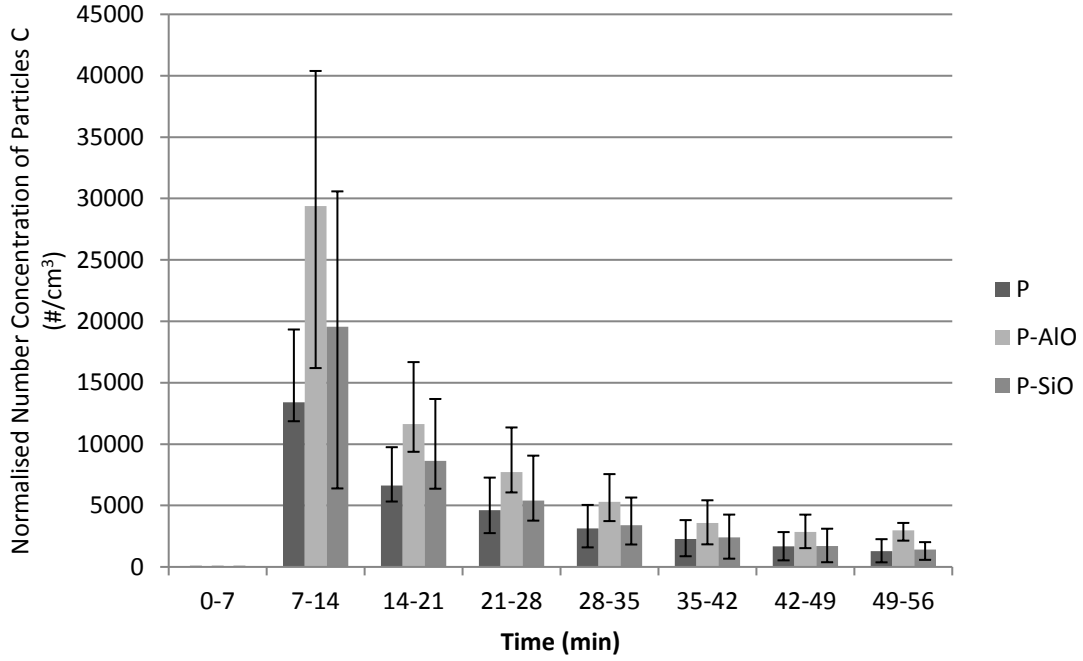

Figure 52: Total Number Concentration of Particles versus Time for Polyester Grades during Impact Experiments

there is a peak in *C* when the impact is happening, i.e. for between 7 and 14 minutes. After that, the total concentration of particles decreases gradually, which is in contradiction to the findings of Sachse et al. [173], as they found that the total number concentration of particles increased dramatically after the impact of nanocomposites cones, but coming back to a normal level for the following measurements. According to the average values, the grade P-Al_2O_3 released higher concentration of particles, which was already the case for the drilling experiments presented previously. However, a very high standard deviation was also observed. Standard deviation varies from 45 to 50 % just after the impact. The polyester nanocomposites released a number concentration of particles in the range of 7500 to 45000 particles/cm^3, when they are impacted.

The average particle size distributions for polyester based samples are presented in Figure 53. The three types of samples mainly produced particles size under 100 nm, though they are classified as nanoparticles according to the ISO 27687. The great majority of the particles released fall in the size range of 10 to 80 nm. It must however be noted that the SMPS+C considers that the particles are spherical which is not representative of the reality and can create errors in the interpretation of the results. The particles are detected by optical light scattering.

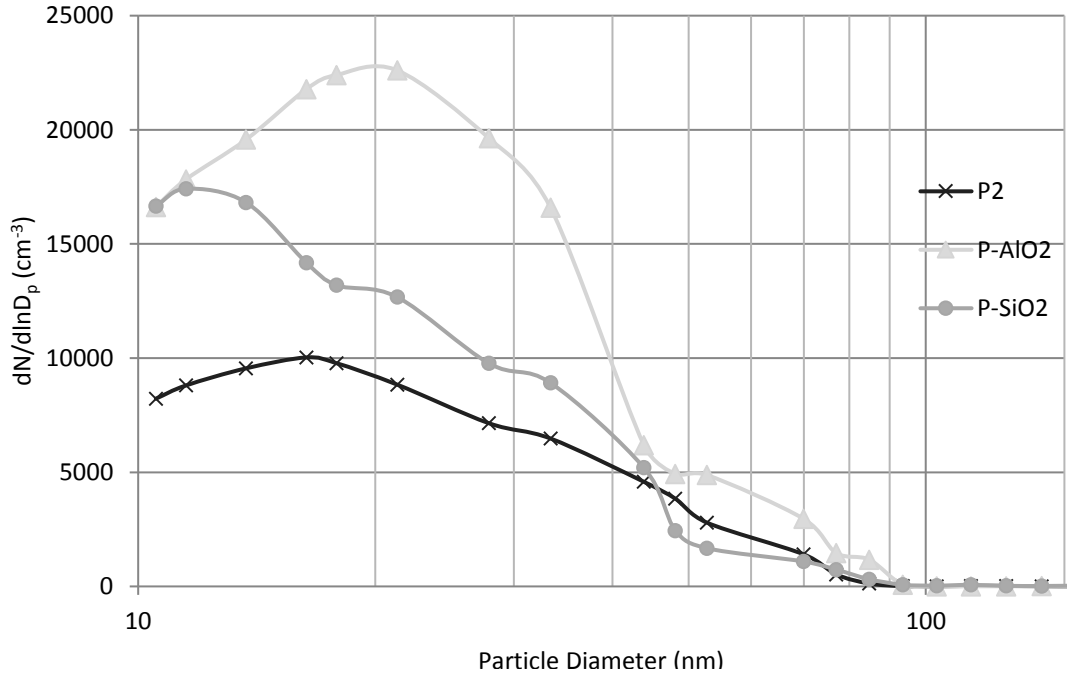

Figure 53: Size Distribution after Impact of Polyester-based Samples

5.3.2.2 Epoxy Samples

Table 22 presents the main results of the impact experiments for the epoxy samples.

Table 22: Average Values for Background Number Concentration of Particles removed (C_{Noise}), Total Number Concentration of Particles (C_{Peak}), Median Particle Diameter (d_{median}) and Diameter of the Highest Number Concentration of Particles (d_{hncp}) during Impact of Epoxy based Samples

	C_{Noise} (particles/cm^3)	C_{Peak} (particles/cm^3)	d_{median} (nm)	d_{hncp} (nm)
E	535 ± 195	15727 ± 11917	20.99	19.39
E-CNT	453 ± 339	20990 ± 1582	19.67	13.62
E-CNF	371 ± 208	14039 ± 11811	20.02	13.62

The total number concentration of particles (with the background noise subtracted) along the time of the experiment is presented Figure 54. The trend is similar to the P samples: Average value for total number concentration of particles (C) reached a maximum after the impact of the sample and then decreased

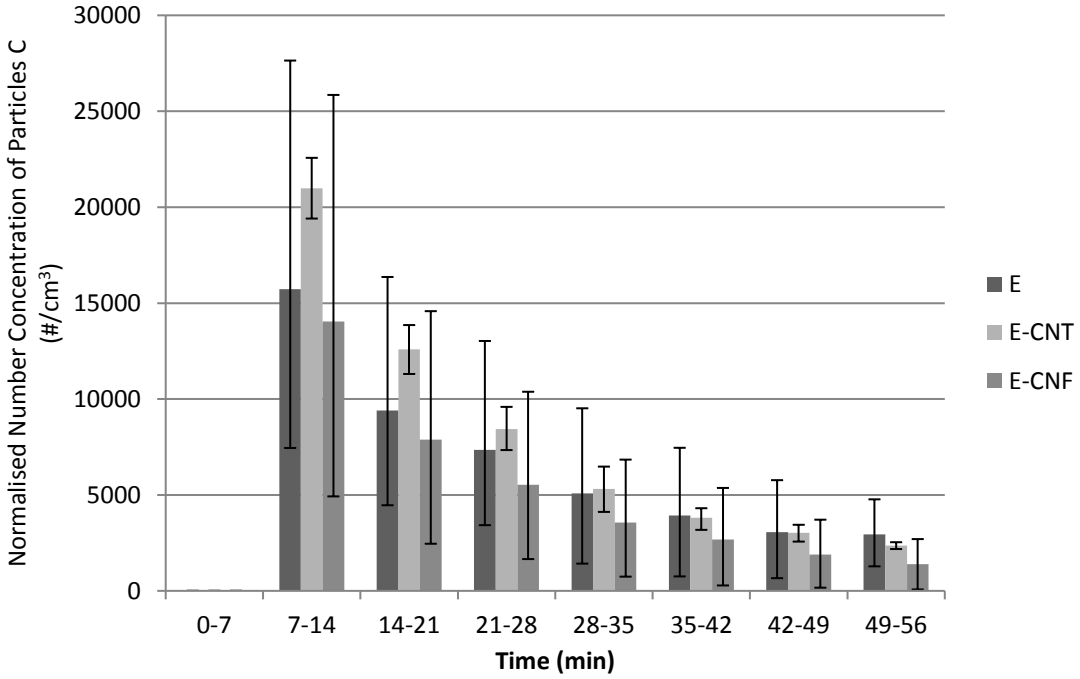

Figure 54: Total Number Concentration of Particles versus Time for Epoxy Grades during Impact Experiments

progressively. For this set of samples, the range for the level of particles after the impact was 5000 - 27000 particles/cm^3. The average level of particles was similar for both E and E-CNF samples (around 15000 particles/cm^3). However, for these two grades the standard deviation was high (around 80 %). The E-CNT samples released more particles (on average) than the other one (an average of 21000 particles/cm^3). It must be noted that in the case of E-CNT samples, the standard deviation was low (only 7 %), this was the only grade which presented reproducible results. Due to the really high standard deviation on the E and E-CNF samples it is hard to conclude on the influence of nanofiller on the number concentration of particles they release.

The particle size distribution after the impact of the samples (Figure 55) showed that in the case of the three types of samples, the concentration of particles was mainly under 40 nm of diameter. E samples present a peak around 19 nm, but E-CNF and E-CNT samples around 13 nm. However, for all grades the median diameter of the particles released was around 20 nm. The introduction of nanofiller into an epoxy matrix does not have a significant effect on the physical properties of the nanoparticles emitted during impact.

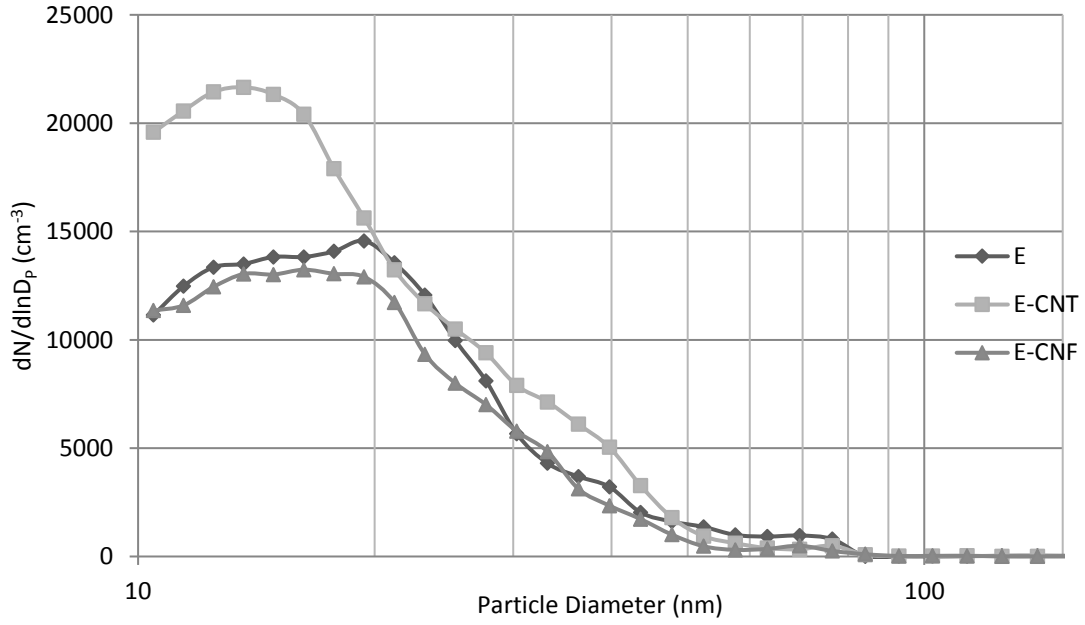

Figure 55: Size Distribution after Impact of Epoxy-based Samples

5.3.2.3 Polypropylene Samples

In the set of samples with PP, the baseline to compare the nanocomposites with was PP plus 20 % talc and neat PP. It must be noted that the Polypropylene samples are only 1.6 mm thick compared to 5 mm for the epoxy and polyester samples but the energy incident on the sample was not modified (2.68 J).

Table 23 presents the data of normalised total concentration of airborne particles for the PP samples. The total concentration of airborne particles released from the PP samples was much lower than the Polyester or Epoxy samples. In general, all the grades released low amount of particles. The value of *C* during the impact process was in the range of 300 to 800 particles/cm^3. The low amount of particles released following the impact can be explained by the thickness of the sample (1.6 mm compared to 5 mm for Epoxy and Polyester samples), but also by the fact that the matrix is a thermoplastic and not a thermoset (Polyester and Epoxy) which changes the failure mechanism of the samples.

Table 23: Average Values for Background Number Concentration of Particles removed (C_{Noise}), Total Number Concentration of Particles (C_{Peak}), Median Particle Diameter (d_{median}) and Diameter of the Highest Number Concentration of Particles (d_{hncp}) during Impact of Polypropylene based Samples

	C_{Noise} (particles/cm^3)	C_{Peak} (particles/cm^3)	d_{median} (nm)	d_{hncp} (nm)
PP	541 ± 178	710 ± 52	18.43	10.52
PP-TALC	383 ± 55	135 ± 8	29.26	16.34
PP-WO	334 ± 133	354 ± 183	25.71	10.52
PP-MMT	522 ± 218	535 ± 96	23.00	12.54

Also, it must be noted that the PP-TALC samples didn't break with an impact of the projectile at 15 m/s. The level of particles was similar to the level of particles in the chamber before the impact (between 100 to 300 particles).

Figure 56 presents the normalised concentration *C* (particles/cm^3) along the whole experiment. The first measurement corresponds to the background concentration and then it is normalised to zero and the impact occurs during the second cycle. The rest of measurements were taken after the impact, still with the fan off. The behaviour of the PP samples was similar to that observed for the P and E samples. The concentration of particles increased (only slightly this time) just after the impact of the sample and decreased slowly in the following scans.

Looking at Figure 56, it can be noticed that PP samples were the grade that produced the higher level of particles after impact. The PP-MMT grade was second, and the PP-WO grade was the one emitting less nanoparticles.

Also, from a mechanical strength point of view the PP-TALC grade still was better than the nanoreinforced samples as the PP-TALC samples didn't break after an impact of the energy selected (2.68 J).

The level of particles produced after the impact for any of the PP grades was really low (up to 800 particles/cm^3) and lower than the usual level of particles that

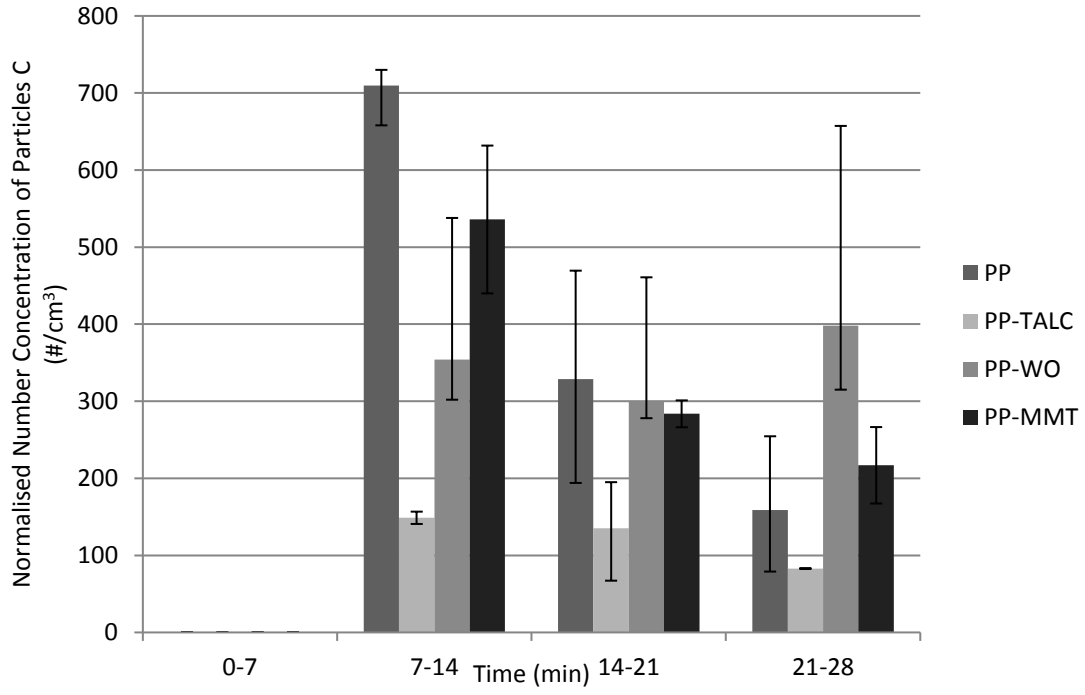

Figure 56: Total Number Concentration of Particles versus Time for Polypropylene Grads during Impact Experiments

can be measured in the lab area (outside the chamber) which is a minimum of 5000 particles/cm^3. However, as we can see on the size distribution graph (Figure 57) the particles emitted during the impact of polypropylene nanocomposites are of a size inferior to 100 nm (as the definition of a nanoparticle).

In general, the total concentration of particles released after impact of PP samples was lower than after impact of polyester or epoxy samples. This could be due to the nature of the matrix. PP is a thermoplastic polymer. It is less brittle and can undergo more plastic deformation before failing. Looking at the pieces collected after impact, it is visible that the fracture mechanism of the polyester samples resulted in the propagation of small cracks involving the destruction of the sample in many small pieces. In case of Polypropylene, the sample broke along long lines resulting in a smaller area of fracture that is able to generate nanoparticles. This indicates that the total concentration of airborne particles depends on the type of matrix more than on the type of nanoadditive used, which was already observed during the drilling process.

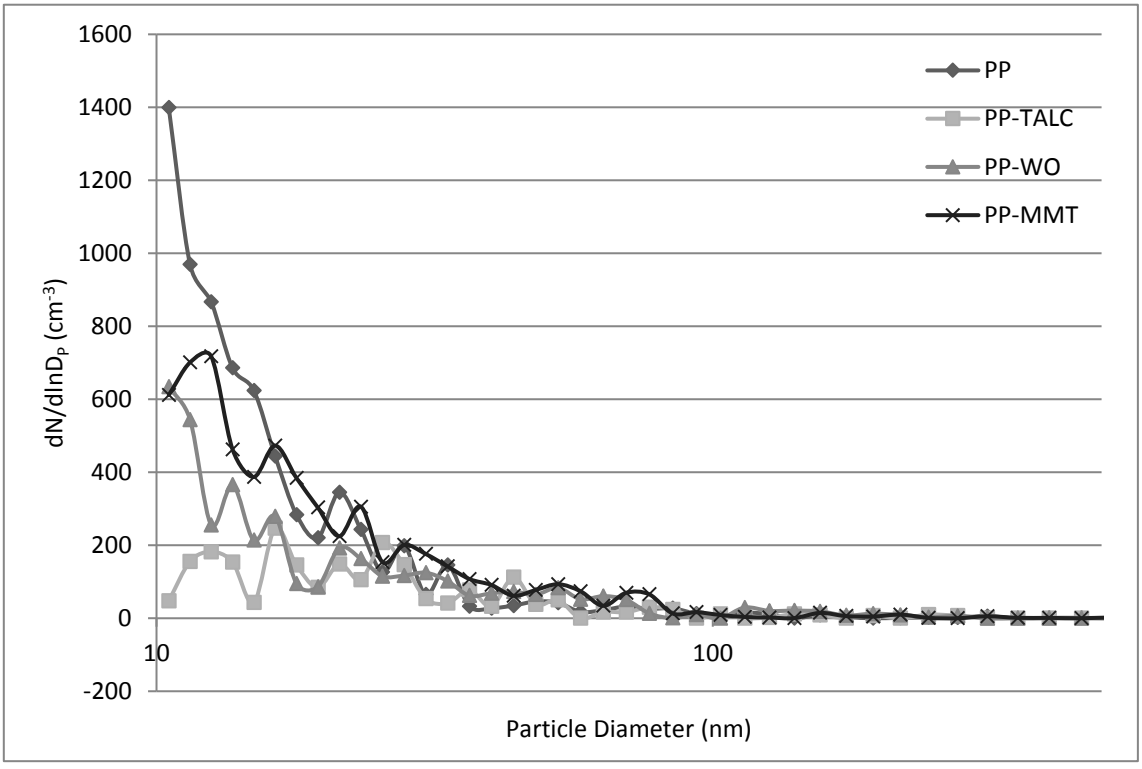

Figure 57: Size Distribution After Impact of Polypropylene-based Samples

5.3.3 Characterisation of Fragments Generated during Impact

The debris of the samples collected on the double face tape placed behind the sample was analysed with a SEM in order to understand the failure mechanism and study the aspect of the surface and the presence of nanoparticles.

5.3.3.1 Polyester Samples

At low magnification (x350, Figure 58), the three types of polyester samples all show a similar fracture surface. The matrix appears rough and presents plastic deformation which is typical of a ductile behaviour. However, polyester resin is known to be a brittle material [235], [236]. The analysis of the broken pieces after impact (Figure 50) confirmed this hypothesis. The sharp edges, different fracture orientations and slivers appearing on the matrix can be the cause of the small pieces and dust ejected during the impact and might have induced the release of nanoparticles.

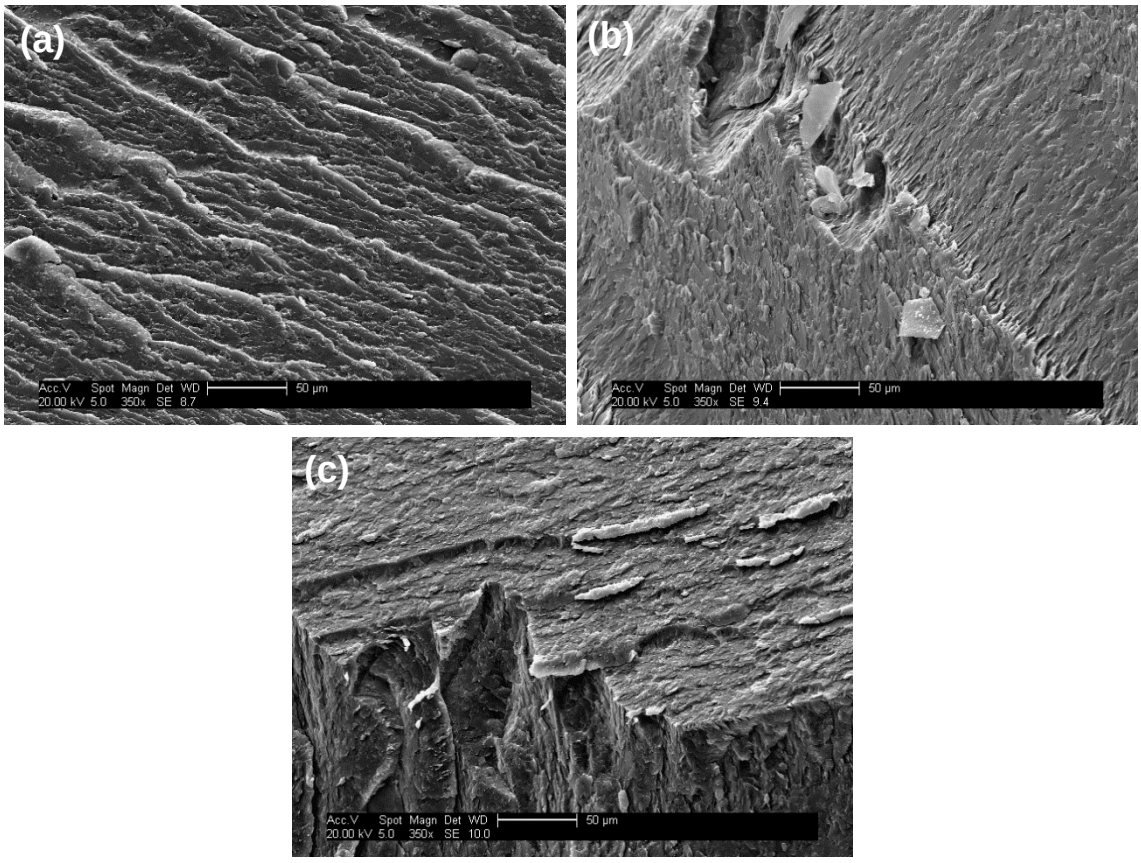

Figure 58: SEM Images of the Pieces Collected after Impact from a P-AlO (a), a P (b) and a P-SiO (c) Samples at x350 magnification

At high magnification (x8000, Figure 59) the surfaces show the presence of plastic deformation resembling a ductile fracture. Nano-objects can only be observed on the P-AlO samples (Figure 59, (a)) which are the samples found to release the highest number concentration of particles during impact. The presence of nanoparticles can be a hazard as it is likely to be in contact with skin. However, it was not possible to determine the type of nanoparticles with the SEM analysis and EDX was unsuccessful.

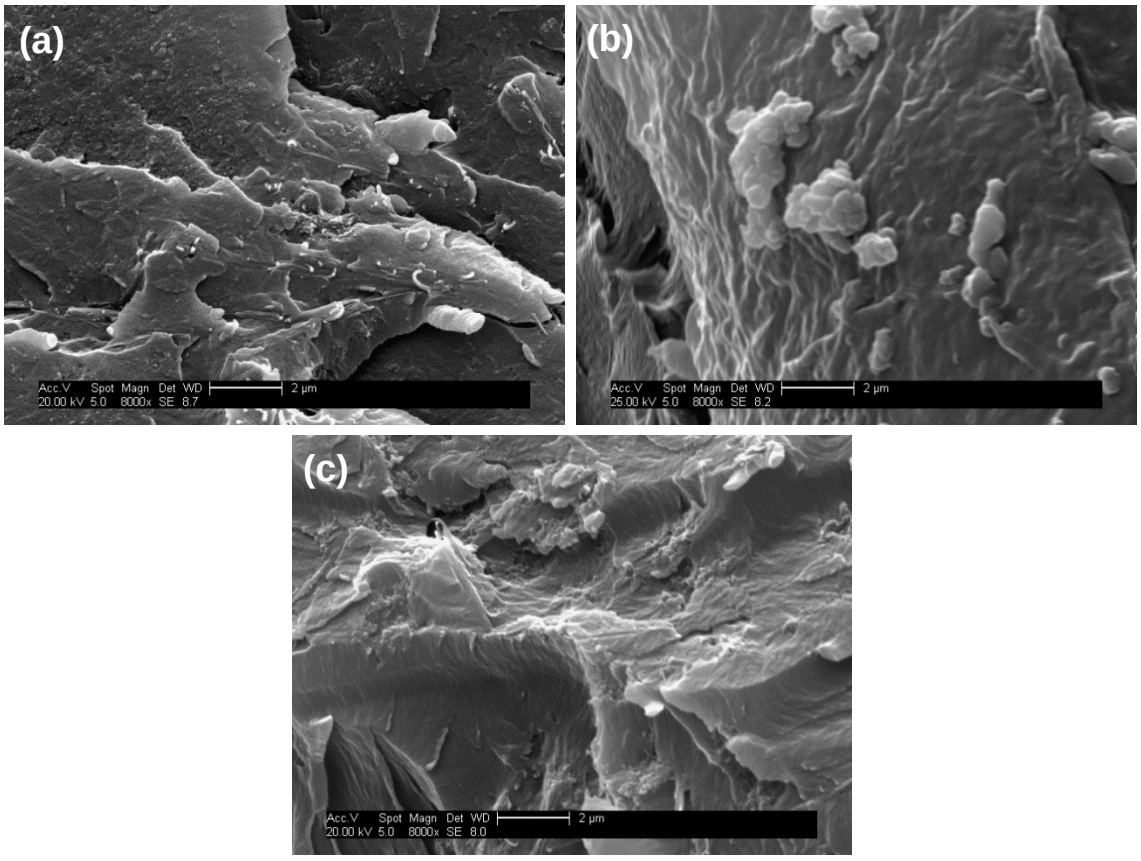

Figure 59: SEM Images of the Pieces Collected after Impact from a P-AlO (a), a P (b) and a P-SiO (c) Sample at x8000 Magnification

5.3.3.2 Epoxy Samples

At low magnification (x200, Figure 60), all the Epoxy samples appeared to have similar fracture surfaces. The surfaces are smooth, typical of a brittle fracture with the presence of fibrils like shapes. It must be noted that the neat Epoxy sample also presents, in addition to the filaments, broken spherical parts of the matrix (Figure 60, (a)).

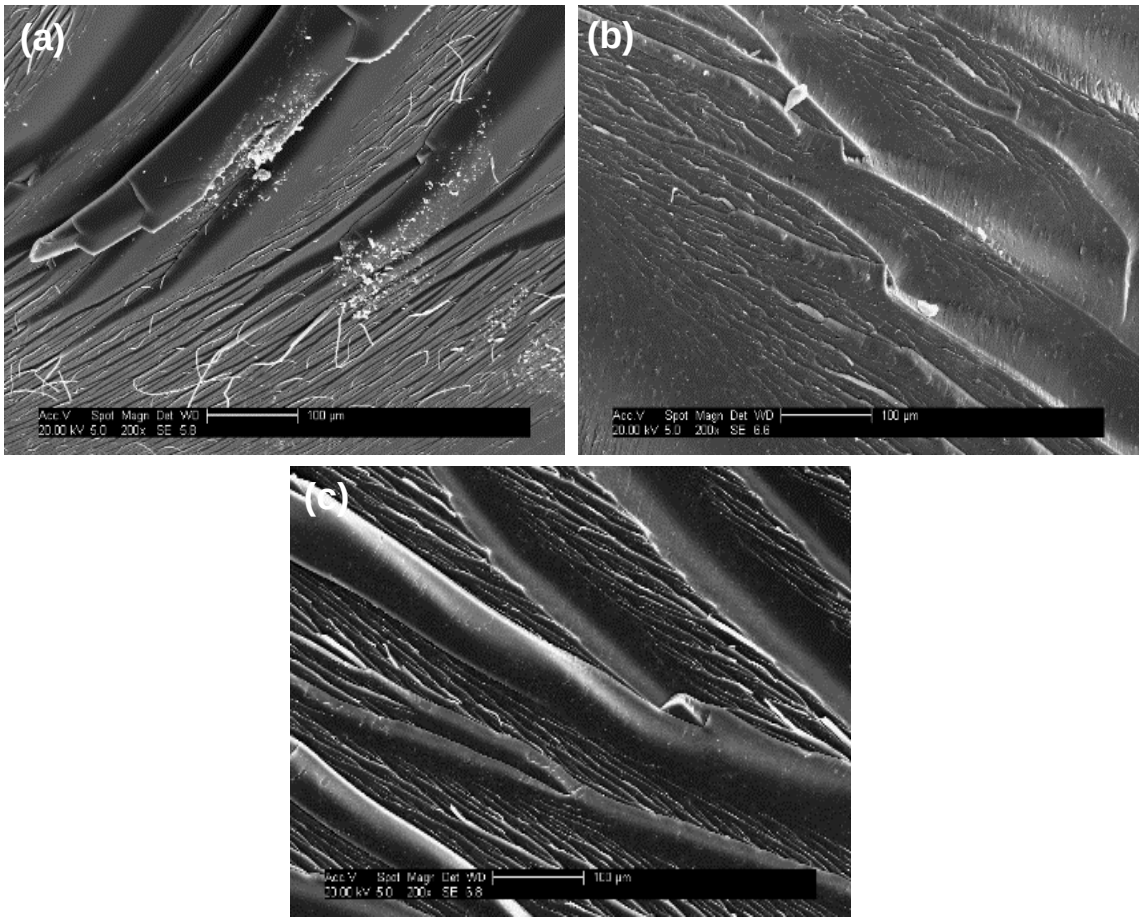

Figure 60: SEM Images of the Pieces Collected after Impact from an E (a), an E-CNF (b) and a E-CNT (c) Sample at x200 Magnification

At higher magnification (x8000, Figure 61), the neat Epoxy sample was analysed at two different places, where the filaments of matrix appear (Figure 61, (a)) and where the matrix was broken into spherical pieces (Figure 61, (b)). Figure 61, (a) shows a brittle failure as the surface is still smooth and the filaments are the sign of very little plastic deformation, relief in the matrix. However the presence of particles of matrix of size around 500 nm can be noticed in Figure 61, (b).

Figure 61, (c) and (d) show the fracture surfaces of E-CNF and E-CNT samples, respectively. Both surfaces still present a typical brittle fracture with a smooth surface. Small inclusions which were measured to be around 60 to 90 nm are also visible for both samples. However only one particle can be seen on the E-CNF sample (Figure 61, (d)), but the E-CNT surface is covered by

nanoparticles (Figure 61, (c)). E-CNT samples were found to be the Epoxy samples which released the highest number concentration of particles. As skin contact can be one of the main sources of exposure, the presence of submicron particles on the surface of the fragments collected can be considered as a hazard. However, further characterisation to determine the chemical composition of these particles would be necessary.

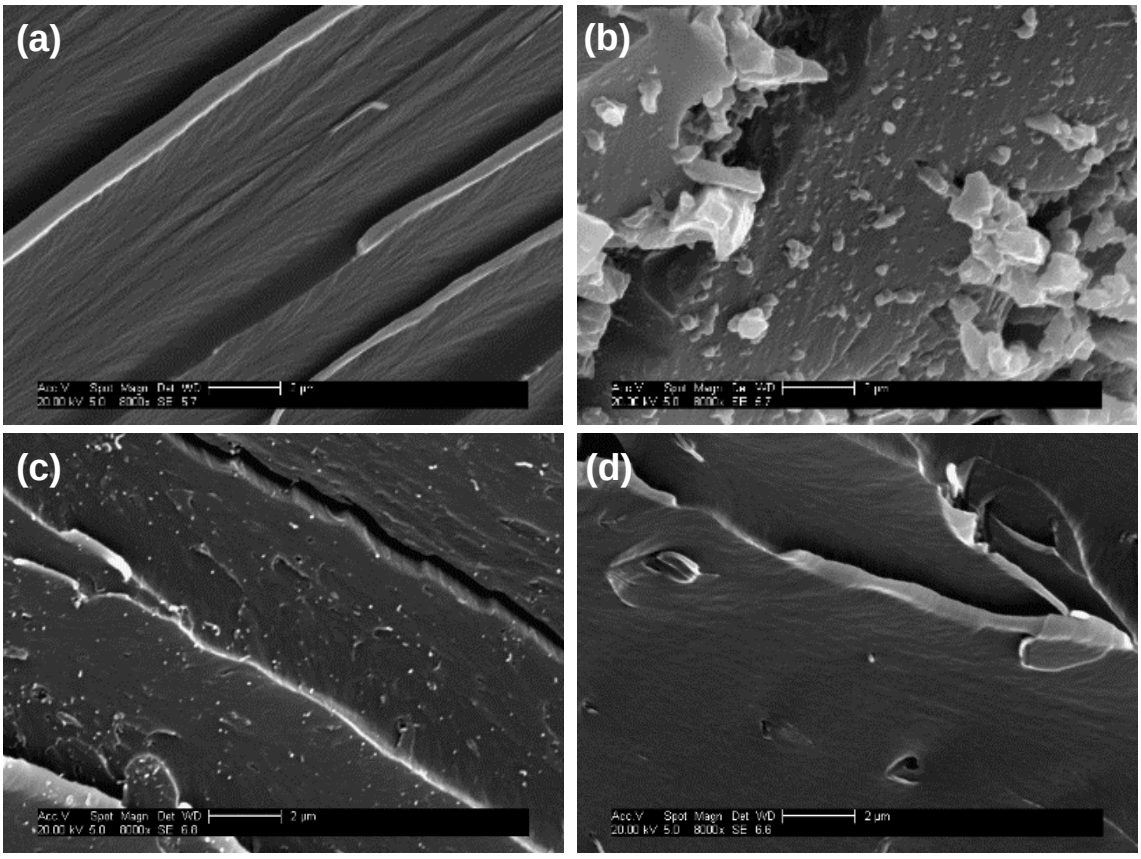

Figure 61: SEM Images of the Pieces Collected after Impact from an E (a), an E (b), an E-CNT (c) and an E-CNF (d) Sample at x8000 Magnification

5.3.3.3 Polypropylene Samples

PP-TALC samples are not analysed as the samples didn't break for the impact energy chosen.

At low magnification (x200, Figure 62) Polypropylene samples show a ductile fracture with the presence of plastic deformation and a rough surface (Figure 62). The presence of stratum is visible for every grade of polypropylene. This indicates that the materials broke in different similar step and reinforces the assumption of

ductile properties of the thermoplastics studied with the observation of a large number concentration of different sizes cracks. The ductile behaviour of the polypropylene samples led to plastic deformation. When a material is brittle, it is not able to deform and has to fracture. Crack formation is easier and results in many large or small broken pieces (as seen Figure 51). In the case of ductile material, the initiation of a crack requires more energy as the material will deform first. The low amount of particles released during the impact of the thermoplastic grades can be due to the matrix deformation that keep the particles embedded into it while in a brittle fracture, the matrix break and can release the particles in an easier manner.

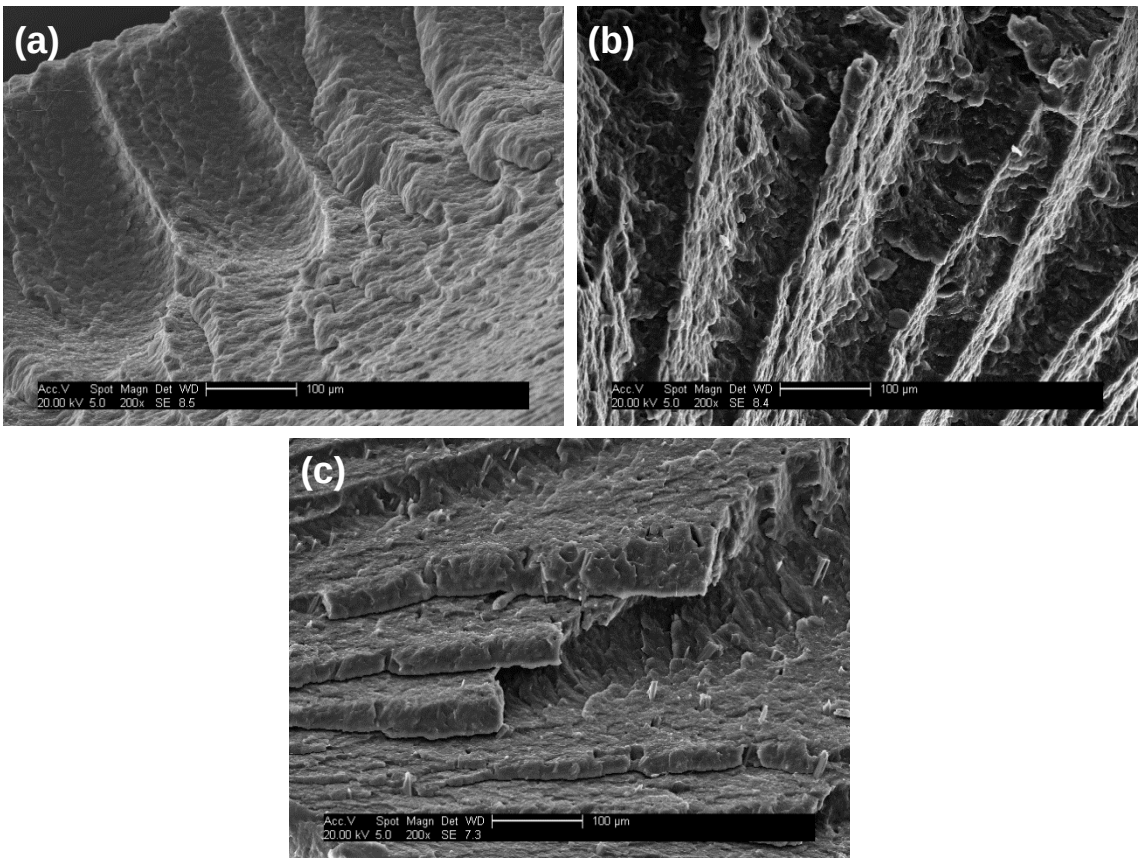

Figure 62: SEM Images of the Pieces Collected after Impact from a PP (a), a PP-MMT (b) and a PP-WO (c) Sample at x200 Magnification

At high magnification (x8000, Figure 63), the matrix still shows a typical ductile fracture with plastic deformation, especially for the PP-WO sample (Figure 63,

(c)). Nanosized elements can only be observed on the surface of a PP-MMT sample (Figure 63, (b)). However, once again it is hard to determine if these elements are part of the matrix, free nanoparticles, or nanoparticles embedded in the matrix and then it cannot be assessed if they present a significant hazard.

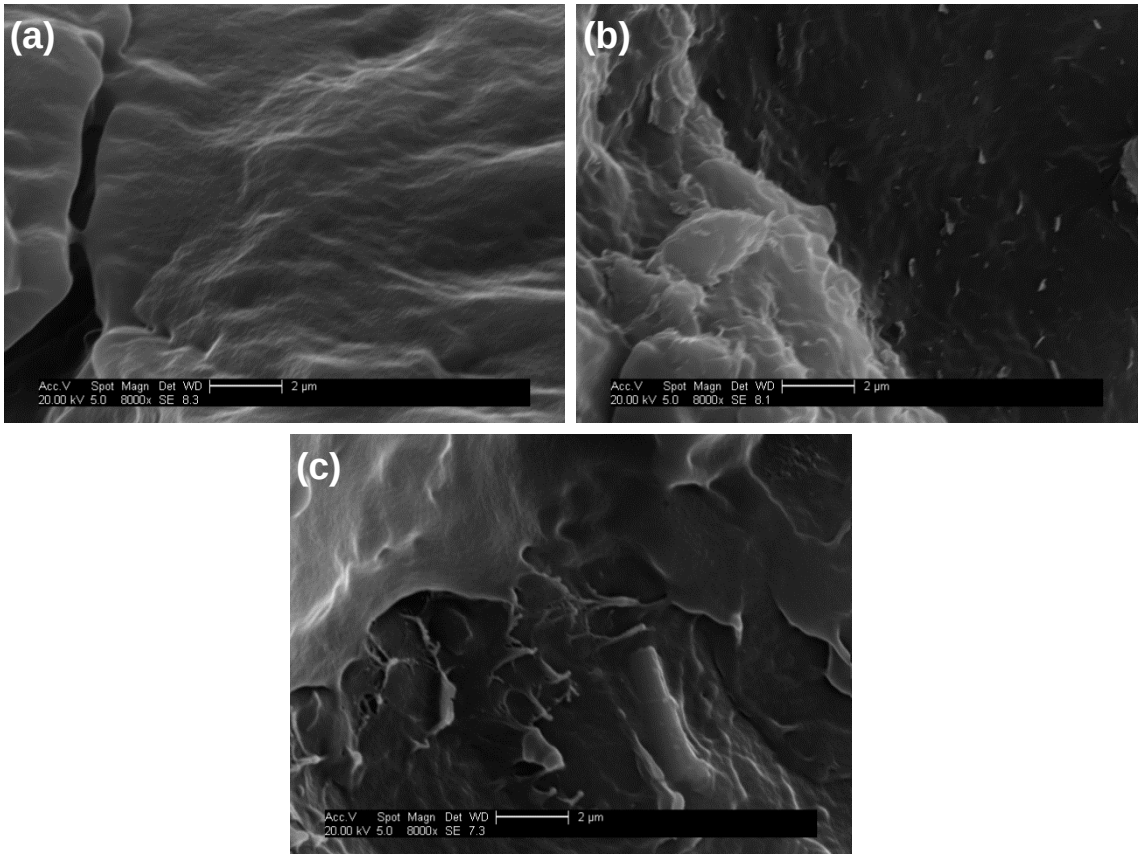

Figure 63: SEM Images of the Pieces Collected after Impact from a PP (a), a PP-MMT (b) and a PP-WO (c) Sample at x8000 Magnification

5.4 Conclusion

Three different types of nanocomposites have been studied: polyester (P), polypropylene (PP) and epoxy (E) nanocomposites. The selection of matrix and nanoadditives was done according to the potential application and sector for these nanocomposites: aerospace, transport and energy. The release of nanoparticles from these materials was investigated this time during impact tests using a low velocity gas gun. The aim of the impact experiments was to simulate the release of particles during the destruction of a nanocomposite. Table 24 summarized the results for these experiments.

Table 24: Summary of the Results of Nanoparticles Released during Impact Experiments

	Additives	Normalised C_{Peak} (particles/cm^3)	d_{median} (nm)	d_{hncp} (nm)
P	-; Al_2O_3; SiO_2	20782 ± 10202	23.76 ± 1.09	16.29 ± 3.70
E	-; CNT, CNF	16919 ± 8437	20.23 ± 0.56	15.54 ± 2.72
PP	-, Talcum, WO, MMT	434 ± 85	24.1 ± 3.96	12.48 ± 2.38

The first conclusion was that the total concentration of airborne particles (C_{Peak}) after impacting a sample was dependant of the type of material tested. A similar trend was observed during the drilling experiments (Chapter 3). Polyester and Epoxy based samples (thermosets) were found to produce a significantly higher number concentration of particles (respectively 48 times and 39 times higher) than PP samples (thermoplastics). The failure mechanism of the sample, which is different for thermoplastics and thermoset materials can explain this phenomenon. Thermoplastics are less brittle, have higher strength and can undergo more elastic deformation, then they also have higher energy absorption capabilities than brittle thermosets materials. Sachse et al. [232] already noticed that brittle materials are less able to absorb energy and also produce a higher number concentration of particles during impact.

Also, the type of nanoadditive was found to influence the nanoparticles release during impact. The addition of alumina and silica nanoparticles into a Polyester matrix increases the number concentration of particles released (respectively 119 % and 46 %). Epoxy-based samples were producing 33 % more particles with the addition of CNT and 11 % less with CNF. In the case of PP samples, the difference was insignificant as the level of particles generated during impact was similar to the background noise measured in the chamber, and at least 10 times lower than the air in the lab. The addition of nanofiller into a matrix changes the behaviour of the material, its failure mechanism and can influence the nanoparticles released.

6 INFLUENCE OF AGEING ON THE NANOSIZED PARTICLES EMITTED DURING THE MACHINING OF POLYAMIDE-6 NANOCOMPOSITES

6.1 Introduction

Glass fibres are a common filler to reinforce plastics for structural parts. However, the use of glass fibre increases the density of the material. Nanofillers can be used as an alternative to glass fibres. In fact only 5 wt.% of nanofiller as against up to 30 wt.% of glass fibres are required to produce any sizeable improvement in the properties of neat polymers [2]. Some parts, like step assist (PP-Nanoclays), or timing belt cover (PA6-Nanoclays) already exist in automotive industry.

A third type of polymer-matrix composite exists: the three-phase composites, which are polymeric materials, reinforced by both micro and nanosized fillers. Some studies show that the combination of these fillers can significantly improve mechanical and impact properties. Wu et al. found that a polyamide-6/clay with 30 wt.% of glass fibre enhanced tensile strength by 11 % and tensile modulus by 42 % compared to polyamide-6/glass fibre [60]. Another work [62] reported that an addition of 2 wt.% of SiO_2 nanoparticles in 30 wt.% glass fibre/polyamide-6, improved the elongation at break by 32 %. And it also changed the mode of failure of the structure, which involved better energy absorption capability.

In this chapter, the mechanical properties of three-phase nanocomposites were investigated. The influence of nanofiller type (OMMT, nano-SiO_2) and percentage on the materials performance are discussed. Also, the effect of thermal ageing on the release of nanoparticles during machining of nanocomposites is studied.

6.2 Materials and Methods

6.2.1 Materials

Two types of nanocomposites were produced for ageing experiments: polyamide-6 (Durethan B30) reinforced by 30 % of glass fibre (ThermoFlow672) and particles of SiO_2 (Aerosil R 974), and polyamide-6 reinforced by 30 % of glass

fibre and Montmorillonite (Dellite 43B). Descriptions of the materials' composition, manufacturing and samples manufacturing were previously reported in section 3.1.1.

6.2.2 Ageing Method

Plates of PA6 based nanocomposites were aged in an oven at 150 °C. Samples were taken out every 7 days during 42 days. Then, they were sealed in a desiccator for 24 hours prior to milling [67].

6.2.3 Mechanical Characterisation

Mechanical characterisation of the different nanocomposites was carried out in order to assess the behaviour and improvement of nanocomposites compared to glass fibre-Polyamide-6 composites.

Figure 64: A Tensile Bar during a Test

Tensile tests, according to the ISO527 standard (Plastics – Determination of tensile properties), were performed in the Instron 5500R electro-mechanical tensile-compression machine at ambient temperature (23 °C). Five specimens, flat dumb-bell type A, were tested at a speed of 1 mm/min. The load was measured with a 100 kN load cell and the longitudinal displacement with a mechanical extensometer. The set-up is shown Figure 64. The dimensions of the samples, which were flat dumb-bell type 1A and injection moulded are presented Figure 65. The thickness of the specimens was 4 mm. The injection moulding parameters can be found Appendix C.

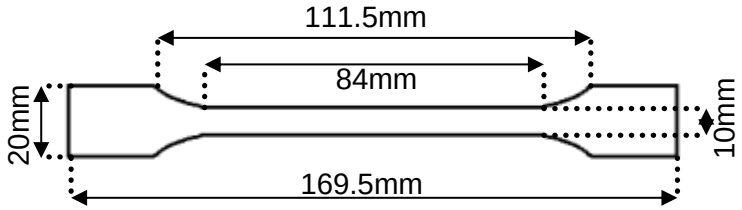

Figure 65: Dimensions of the Tensile Specimens

The fracture surface of the tensile bars was then analysed with a scanning electron microscope (FEI XL 30) in order to understand the failure mechanism and the relation between the matrix and the filler. The samples were gold sputtered to minimize charging of the specimens.

6.2.4 Release of Nanoparticles by Milling of Nanocomposites

The same chamber used for the drilling experiments and presented and validated in Chapter 3 was used for the milling experiments.

Milling parameters were selected according to industrial guidance for machining composites and plastics [219]:

- Tool: Solid Carbide Endmills, 3 Flutes, 2 mm diameter
- Spindle speed:15000 rpm
- Feed rate: 330 mm/min

The samples were milled during 7 minutes continuously on 130 mm long lines. The depth of the milled area was 3 mm, and a 0.5 mm increment was used for every pass. Every pass consisted in 3 lines milled. The total volume removed by the milling operation was around 2184 mm^3. The samples milled were 4 mm thick plaques of dimensions 170 x 170 mm^2. The injection moulding parameters of the samples can be found Appendix D.

Each sample testing started by measuring the air inside the chamber (with the fan off), to obtain the background value for each experiment. Once the concentration of the particles in the chamber was stabilized, samples were milled during 7 minutes (1 scan cycle). After milling, the air inside the chamber was measured until it reached a similar concentration to the initial one (background).

6.3 Results and Discussion

6.3.1 Mechanical Properties

It is of importance to study relevant nanocomposites i.e. materials with potential or current application in the industry instead of research only materials. For this, the nanomaterials selected were tested in order to ensure enhancement of their

mechanical properties compared to reference material (PA6/GF) for a possible use as an automotive component.

6.3.1.1 Tensile Results

Figure 66 and Figure 67 represents respectively the tensile stress vs tensile strain curves for the OMMT-based nanocomposites and for the silica-nanocomposites.

For both filler types, the materials showed a behaviour corresponding to a brittle material without yield point. However, it can clearly be seen that the choice of the filler integrated to the polyamide-6/glass fibre composite, was an important factor. The polyamide-6/glass fibre/OMMT deformed less, the stress vs strain curves report a brittle behaviour with only elastic deformation. Whereas, the SiO_2-nanocomposites were less brittle, the curves show the beginning of plastic deformation before breaking. It is also important to note that OMMT-based composites are stiffer than the nanosilica based ones. However, the SiO_2-nanocomposites present an ultimate strength and strain at break significantly higher than the OMMT-nanocomposites.

The nature of the fillers can explain these results. Indeed, OMMT are nanoplates. These fillers create a high stress concentration in the matrix, so the material is less able to deform and ease the propagation of the fissures. SiO_2 are

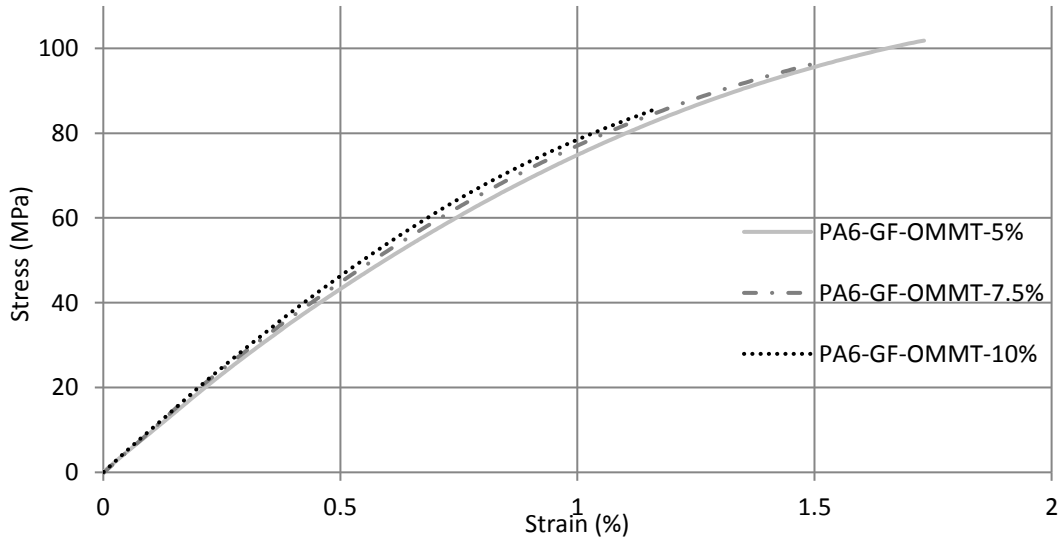

Figure 66: Tensile Stress vs Strain Curves for PA6-GF-OMMT at different OMMT contents

nanoparticles and are smaller, which reduces the stress concentration and allows to block the cracks.

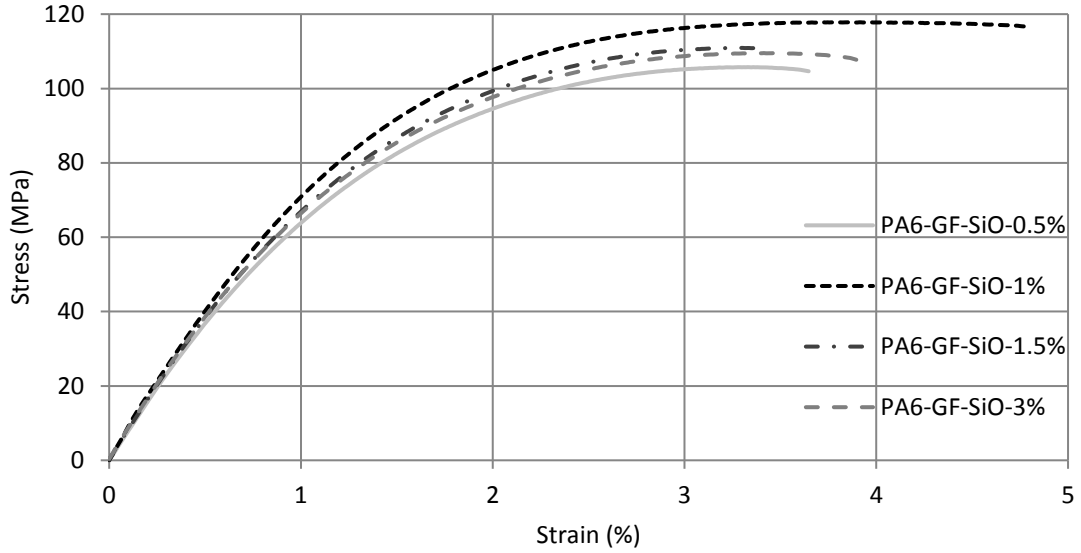

Figure 67: Tensile Stress vs Strain Curves for PA6-GF-SiO at different SiO_2 contents

The average values of the tensile tests results are summarised in Table 25 and Table 26. For comparison, the results of a polyamide-6 reinforced by 30 % of glass fibre and 2 wt.% of OMMT, or 2 wt.% of nano-SiO_2, or without any nanofillers, tested in the same conditions at Cranfield University were added. It was noticed that the addition of a secondary filler of any type significantly improved the Young's Modulus. However, it generally made the material more brittle, and decreased the tensile strength and strain at break.

Table 25: Properties Characterised for the OMMT Filled Nanocomposites

	Percentage of Nanofillers	Young's Modulus (GPa)	Tensile Strength (MPa)	Tensile Strain at break (%)	Ref.
		RT	RT	RT	
PA6 - GF - OMMT	0%	6.92	116.2	5.2	[62]
	2%	7.61	109.7	5.1	[62]
	5%	9.15	101.8	1.73	
	7.5%	9.69	96.9	1.52	
	10%	9.76	85.4	1.16	

The main results of the tensile tests for OMMT-nanocomposites are listed in Table 25. It can be observed that the Young's Modulus was improved with increasing OMMT concentration at the expense of its ability to resist high loading and consequently led to deformation failure at lower stress and strain values as the material became more brittle. These results can be explained by the high content of nanofillers. Akkapeddi [237] found that above 7 wt.% of nanoclay, polyamide-6 nanocomposites tend to present more fillers agglomerates, and he suggested to use a nanofillers content lower than 5 wt.% in order to avoid these agglomerates. Different results were found by Mishra et al. [46] as they reported enhanced modulus, elongation at break and tensile strength with the addition of OMMT into a polyaimde-66 matrix. However, the contents studied were between 0 and 4 wt.%, so it is possible that an optimum for the best tensile properties exists around 4-5 wt.% of OMMT. Also, this work was done on PA66-nanocomposites without glass fibre reinforcement. In the present case, the percentage of OMMT studied are relatively high (5 to 10 wt.%) and the formation of agglomerates of nanofillers is likely. The presence of agglomerates reduces the benefit of the 'nano' size of the fillers by having a lower surface are to volume ratio, increasing stress concentration around the fillers and facilitating the crack propagation.

Table 26: Main Results of the Tensile Tests for the SiO_2-Nanocomposites

	Percentage of Nanofillers	Young's Modulus (GPa)	Tensile Strength (MPa)	Tensile Strain at break (%)	Ref.
		RT	RT	RT	
PA - GF - SiO	0%	6.92	116.2	5.2	[62]
	0.5%	7.78	105.7	3.65	
	1%	8.40	117.8	4.79	
	1.5%	7.95	110.9	3.43	
	3%	7.94	109.5	3.91	

The silica-nanocomposites were prepared at low content of nanofillers (between 0.5 and 3 wt.%). Results of the tensile tests for SiO_2-nanocomposites are presented in Table 26. At room temperature, it can be observed that the material which has the best properties was the polymer filled with glass fibre and 1 wt.% of nano-SiO_2. It was the only nanocomposite which showed an improvement in

both the tensile strength and the modulus compared to glass fibre/polyamide-6, and it had the higher tensile strain at break. These results are in line with the findings of Zhou et al. [47], for nanosilica/polypropylene composites. They reported an optimum between 0.4 and 0.8 vol.% of nano-SiO_2, according to the treatment undergone by the filler.

6.3.1.2 SEM Results

In order to understand the failure mechanism of each nanocomposites, and the relation between the matrix and the filler, the fracture surface of the tensile bars was analysed using a Scanning Electron Microscope (SEM). The samples were previously coated with gold to make them conductive.

The nanoparticles could not be seen with the SEM, however the glass fibre could be observed clearly. Figure 68 shows the fracture of a glass fibre. The black zone on the top of the glass fibre was the part where the crack was initiated. The crack then slowly propagated in the grey part, until the fibre broke and the final fracture can be seen (white part).

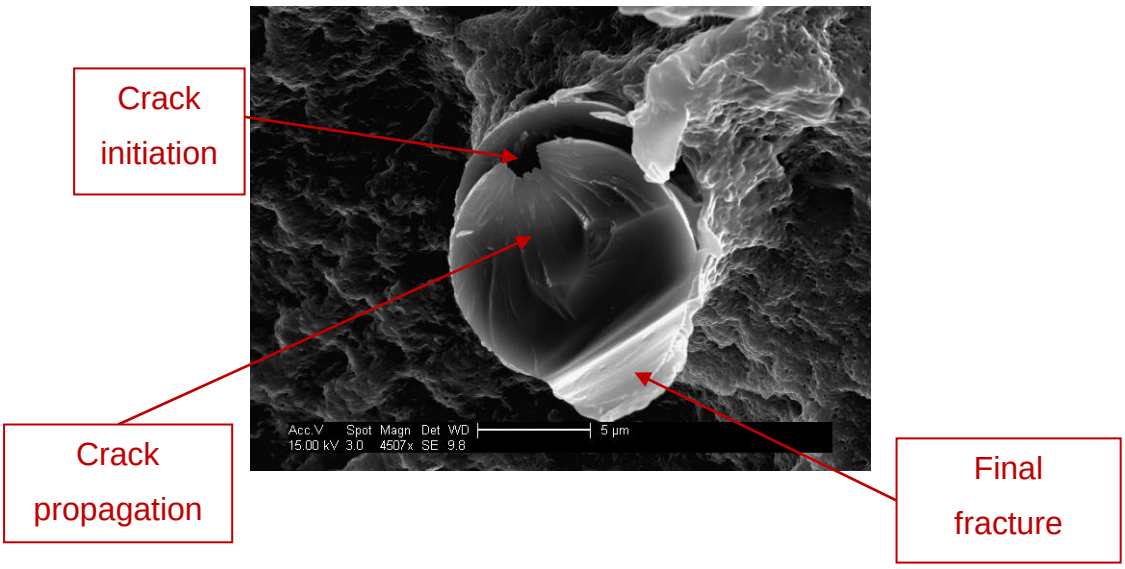

Figure 68: Glass Fibre Fracture

With regards to the surface fracture of the matrix, it could be noticed a different behaviour according to the type of filler used. In the case of polyamide-6 loaded with glass fibre and OMMT, it could be seen a lot of pull-out of the fibre (Figure 69, (a)). The matrix underwent only elastic deformation hence the interaction between the glass fibre and the matrix was considerably weak. The surface is typical from a brittle fracture. The opposite behaviour was found for the materials with glass fibre and nano-SiO_2, as the matrix was plastically deformed and interaction of fibres and matrix was good, the matrix seems to be stuck to the fibres (Figure 70, (a) and Figure 70, (b)). Matrix/fibre relation was very strong and the glass fibres had to break, instead of just pulling-out of the matrix. This explains the higher strength of nanosilica reinforced polyamide-6. The stronger interaction can be the consequence of a higher specific surface area of the nano-SiO_2 particles (150-190 m^2/g [238]) compare to OMMT fillers (6.4-6.9 m^2/g [239]).

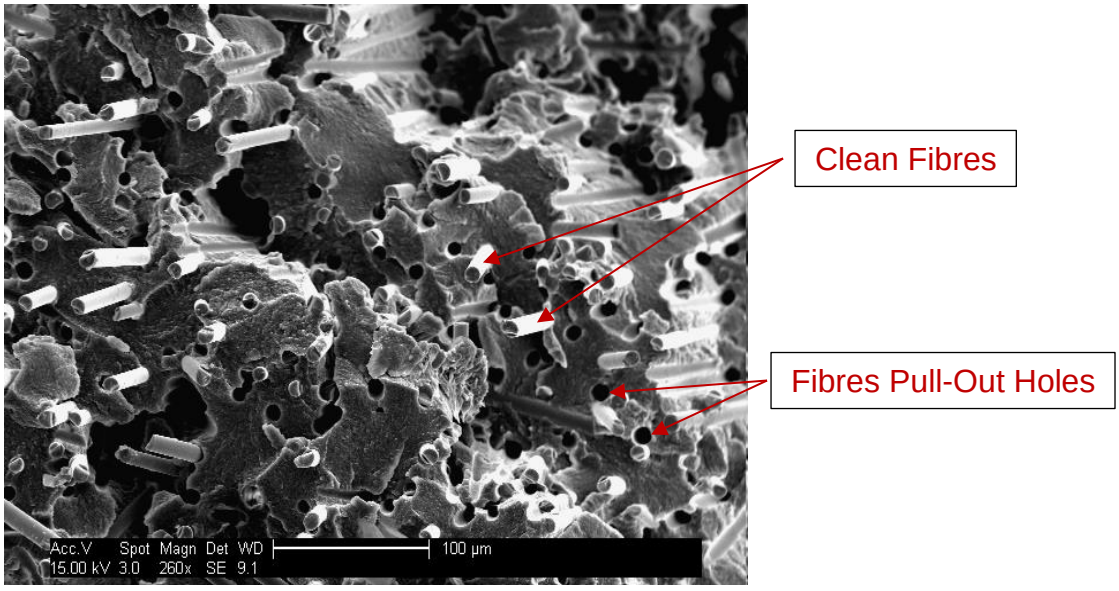

Figure 69: SEM Picture of the Tensile Fracture Surface of a OMMT-Nanocomposite at Room Temperature

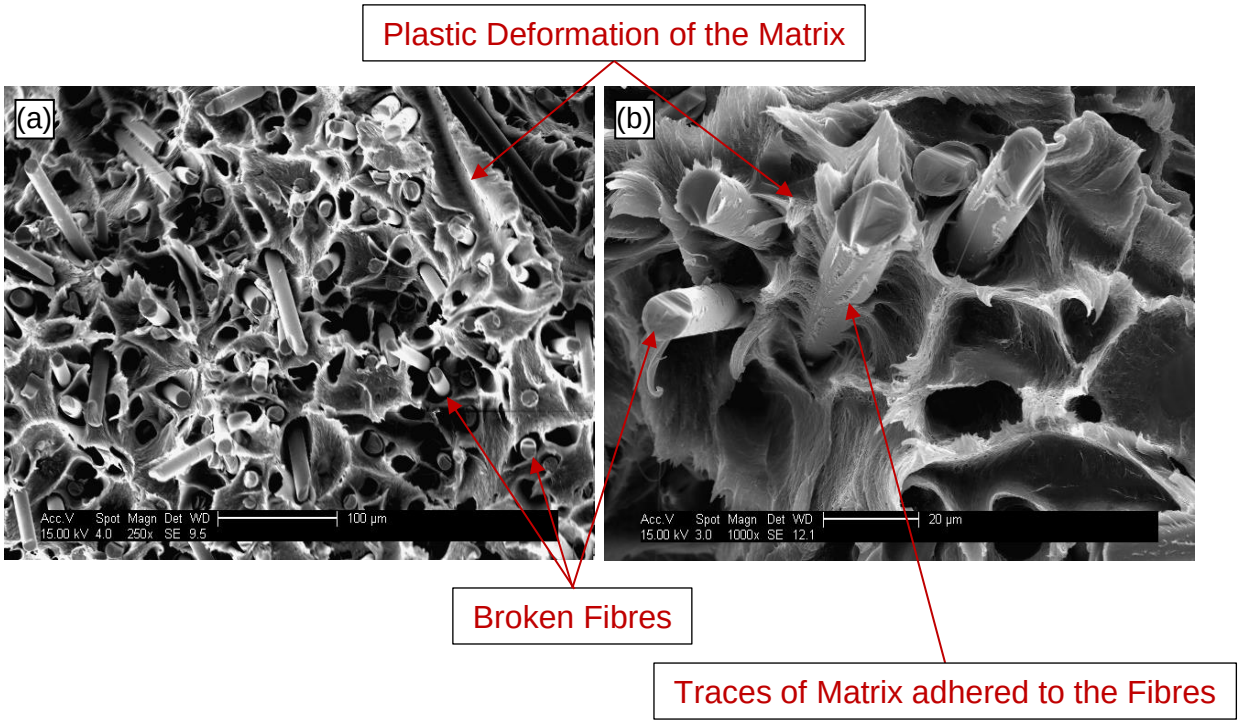

Figure 70: SEM Pictures of the Tensile Fracture Surface of a Silica-Nanocomposite at Room Temperature at low (a) and high (b) magnification

6.3.1.3 Conclusion on Mechanical Properties

It was shown that the increase of OMMT percentage in polyamide-6/Glass Fibre composite made the material more brittle and had a negative effect on the tensile properties. It could be explained by the weak interaction between the matrix and the fibres. The high content can create aggregates of the nanofiller and hence a brittle material behaviour. For the addition in polyamide-6/glass fibre/nanosilica composites, the nanocomposites with 1 wt.% of SiO_2 presented the best tensile properties. In general, it can be said that integration of secondary nanofillers is a good way to enhance the mechanical properties of PA6 composites; however the percentage and type of filler play a crucial point. The addition of a secondary filler changes the interaction between the matrix and the glass fibres. A weak interaction, as seen with the addition of OMMT, can involve debonding of the fibres with the matrix.

6.3.2 Airborne Particles Generated by Milling

Airborne particles between 11.1 to 1083.8 nm were measured during the milling of three phase nanocomposites plates at different stages of ageing. A typical evolution of the number concentration of particles during the time of the experiment is presented Figure 71. The data was obtained from milling unaged 5 wt.% OMMT composites. During the first cycle (minutes 0 to 7), the particles measured were used to establish background noise. Then, the milling of the plate lasted for 7 minutes (second cycle: 7-14 min) and the measurement continued until the number concentration of particles went back to the background noise previous milling. The results were similar to the drilling of polypropylene based composites which might be due to both being thermoplastics. The number concentration of particles increased after the milling for one cycle, and then gradually decreased. The maximum number concentration of particles (C_{Peak}, #/cm^3) measured during the third cycle (14-21 min) for every material tested is reported in Table 27.

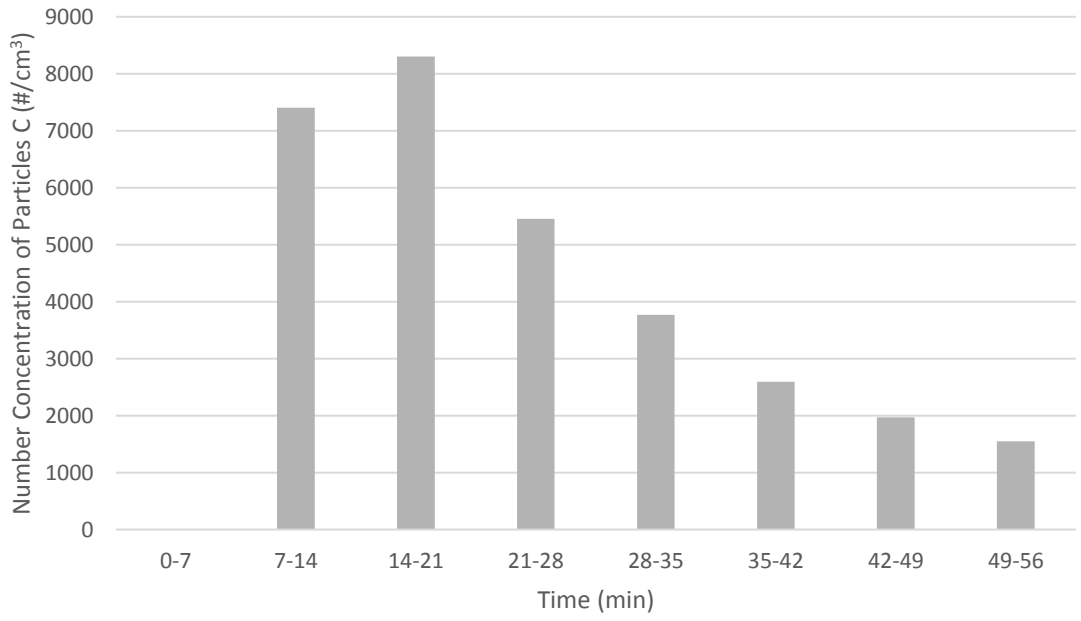

Figure 71: Typical Evolution of the Number Concentration of Particles during the Milling Experiment

Table 27: Number Concentration of Particle (C_{Peak}, #/cm^3) Released during Milling of Aged Nanocomposites

C_{Peak} (particles/cm^3)	Week 0	Week 1	Week 2	Week 3	Week 4	Week 5	Week 6
PA6-GF-OMMT-5%	8828 ± 1347	11911 ± 1779	11153 ± 34	35393 ± 15431	37407 ± 7193	57567 ± 26525	84661 ± 28225
PA6-GF-OMMT-7.5%	7409 ± 791	9727 ± 608	20390 ± 4161	27619 ± 9058	29139 ± 4405	50689 ± 13279	69500 ± 15192
PA6-GF-OMMT-10%	7670 ± 765	10006 ± 896	16662 ± 3785	43541 ± 3184	49227 ± 356	60655 ± 16055	88978 ± 9018
PA6-GF-SiO2-0.5%	9005 ± 464	14456 ± 903	35999 ± 9798	52270 ± 7542	55840 ± 6334	68642 ± 9835	121716 ± 25327
PA6-GF-SiO2-1.5%	6867 ± 1079	22273 ± 7879	29567 ± 4809	51504 ± 12455	63248 ± 10551	72889 ± 16967	118350 ± 35198
PA6-GF-SiO2-3%	9938 ± 506	19198 ± 2811	34849 ± 10858	56323 ± 10705	66462 ± 24639	75655 ± 31709	85797 ± 28013

The number concentration of particles emitted during milling increased with the number of weeks the material was aged. This is the case for every material regardless of the type of filler and the percentage of filler used in the PA6 matrix. Especially, a significant increase (between 100 to 200 %) in the number concentration of particles could be noticed either after the second or third week of ageing. In similar ageing conditions, Kiliaris et al. [67] found that after 3 weeks of ageing PA6 filled with 5 % of montmorillonite the crystallinity of the materials started to decrease considerably. Additionally, thermooxidation is one phenomenon which affects a material, and especially its surface, when subjected to elevated temperature. The bulk properties of the materials can then be affected as well by this condition according to the oxygen diffusion kinetics in the material [168]. The change of physical properties of the materials when aged can explain the increase of number concentration of particles released. Indeed, ageing of polymer-based composites often results in degradation of the polymer and chain scission inducing a reduction of the molecular weight of the material and so a loss of mechanical properties especially in mechanical strength. Also, a decrease of the crystallinity involves a reduction of mechanical strength and modulus but also of the hardness of the material. The hardness of the material is an important property to take into account to choose the right process parameters in order to obtain a machining of good quality. Especially, the harder the material is, the

slower the feed rate and spindle speed should be. This mean that the machining conditions chosen for the unaged material might not be adequate for the artificially aged materials.

Figure 72 presents the maximum number concentration of particles emitted by OMMT-nanocomposites during milling for every week of ageing. Again, it is noticeable that the number concentration of particles increased with ageing. A significant increase was noticed starting from 3 weeks of ageing. Although the number concentration of particles released increased with ageing, there was no specific trend observed between number concentration of particles released and percentage of nanofiller used. Upon ageing, the nanocomposites filled with 7.5 wt.% of OMMT released lower number concentration of particles. The unaged and one week aged samples of nanocomposites filled with 5 wt.% of nanofiller generated the highest number concentration of particles. But from the second week onward, the PA6-GF with 10 wt.% of OMMT emitted a higher number concentration of particles.

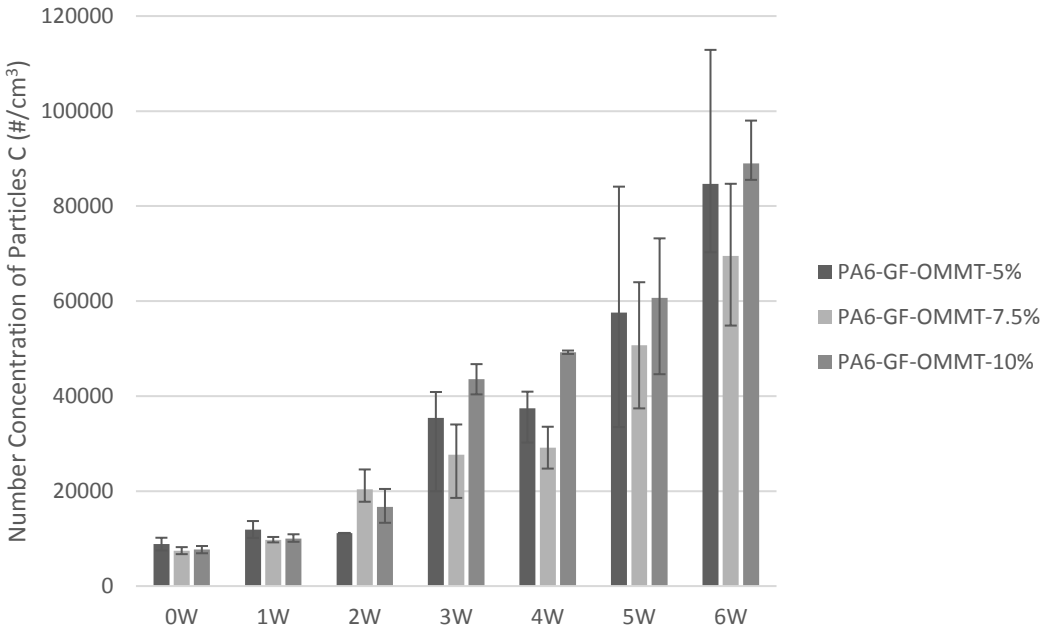

Figure 72: Maximum Number Concentration of Particles Released by Machining of Aged OMMT-Nanocomposites

Figure 73 presents the maximum number concentration of particles released during the milling of the aged nanosilica based composites. As for the OMMT based nanocomposites, the number concentration of particles released increased with the ageing. And again, the trend related to the percentage of filler used was not clear. The lowest number concentration of particles were released from the 1.5 wt.% nanosilica composites for the unaged and up to three weeks of ageing. Then, from four weeks of ageing, the 0.5 wt.% nanosilica composites produced the lowest amount of particles until the last test (6 weeks of ageing) where the 3wt.% nanosilica composites generated only 85797 ± 28013 particles/cm^3. Actually, the 3 wt.% nanosilica composites generated the highest number concentration of particles for the unaged tests and until after 5 weeks of ageing, but an extremely high increase of the number concentration of particles emitted by the 0.5 wt.% and 1.5 wt.% nanosilica composites (respectively by 77 and 62 %) changed the trend. The standard deviation for all of these results was in average of 20 % which is an improvement compared to the results in the previous chapter (4).

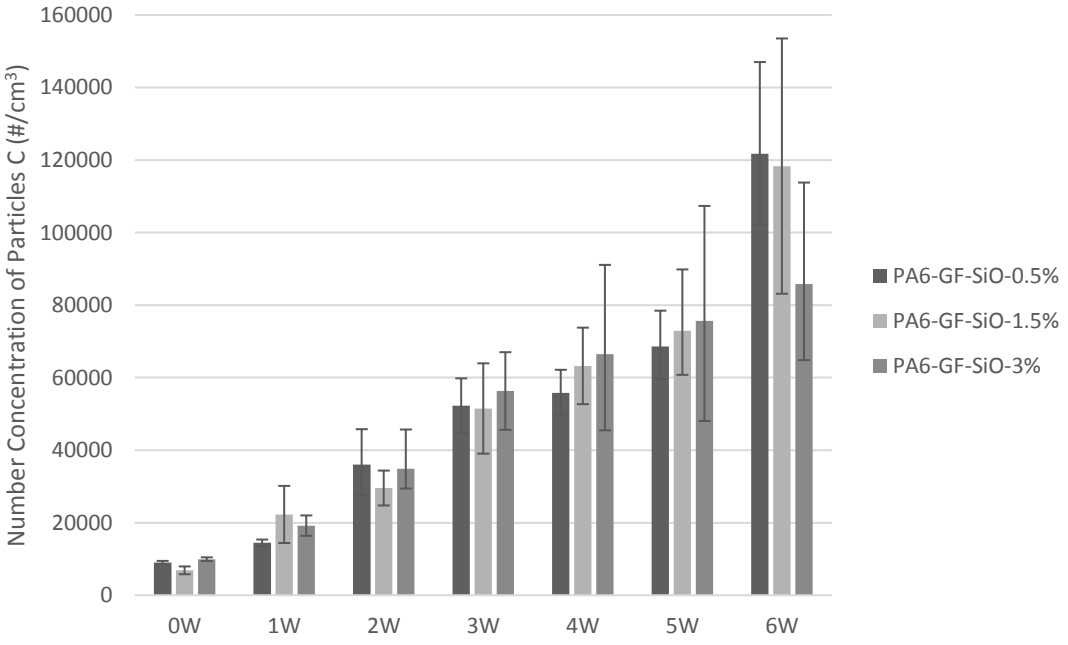

Figure 73: Maximum Number Concentration of Particles Released by Machining of Aged Silica-Nanocomposites

Also, it was noticed that the nanosilica reinforced composites were generally generating more nanoparticles than the OMMT ones even though the percentage of nanosilica was relatively low (less than 3 wt.%) compared to the percentage of OMMT (between 5 to 10 wt.%).

In the previous section (6.3.1), the nanofiller type (OMMT or nano-SiO_2) was found to change the mechanical properties of the polyamide-6 filled with glass fibers. The interaction of the matrix and the glass fibers was considerably improved with nano-SiO_2 compared to OMMT as shown by the SEM analysis. The brittleness of the material was reduced with silica nanofiller, while the OMMT nanoplates increased its ductility. A possible explanation can be the shape of the nanofiller: OMMT are nanoplates, and SiO_2 are spherical. The plate shape creates a higher stress concentration in the matrix so the material is less able to deform and ease the propagation of the fissures, while smaller particles reduce stress concentration and allows to block the cracks. A change of the bulk properties of the material is generally modifying its processability, and the release of nanoparticles can be affected as well.

The median diameter of the particles measured during the milling experiments are reported in Table 28 for every nanocomposites tested at different stages of ageing. We can see that the median particle diameter increased after few weeks of ageing but then following the second week of thermal ageing the median particle diameter reduced and reached a size even lower than that of unaged materials tested. This was the case for all the type of nanocomposites tested.

Table 28: Median Diameter (*d*, nm) of the Particles Released during Milling of Aged Nanocomposites

d (nm)	Week 0	Week 1	Week 2	Week 3	Week 4	Week 5	Week 6
PA6-GF-OMMT-5%	86.9	119.5	108.3	98.38	93.83	93.63	64.75
PA6-GF-OMMT-7.5%	89.98	119.5	114.2	100.6	94.37	94.12	66.17
PA6-GF-OMMT-10%	92.93	129.3	126.8	100.7	94.62	95.17	78.73
PA6-GF-SiO2-0.5%	88.79	132.7	124.6	93.82	87.50	81.12	79.41
PA6-GF-SiO2-1.5%	88.21	125.9	109.9	91.74	82.43	76.96	76.00
PA6-GF-SiO2-3%	86.45	119.9	107.8	85.22	79.18	75.65	71.32

Figure 74 presents the particle size distribution for the 3 wt.% nanosilica composites, unaged and after 6 weeks of thermal ageing. It can be noticed that the number concentration of particles generated by milling increased following 6 weeks of thermal ageing which is believed to be due to the weakest bond of the molecular chain of the polymer matrix following degradation during heat ageing. Also, the median diameter of particles emitted shifted to the smaller size and presents two peaks instead of a simple bell curve. A size distribution with a double or multi-peak curve can illustrate the presence of a mixture of aerosols such as agglomerates and free engineered nanoparticles for example [220]. In this case, the two peaks are almost overlapping with one at 63.53 nm and the second one at 93.36 nm. This could be due to the degradation of the matrix during the ageing and so to the different properties of the matrix at the surface of the sample. An average of 64 % of the particles emitted by unaged samples (all types considered) were smaller than 100 nm, while an average of 78 % of the particles measured were found to be in the nanoscale for the samples aged 6 weeks at 150 °C.

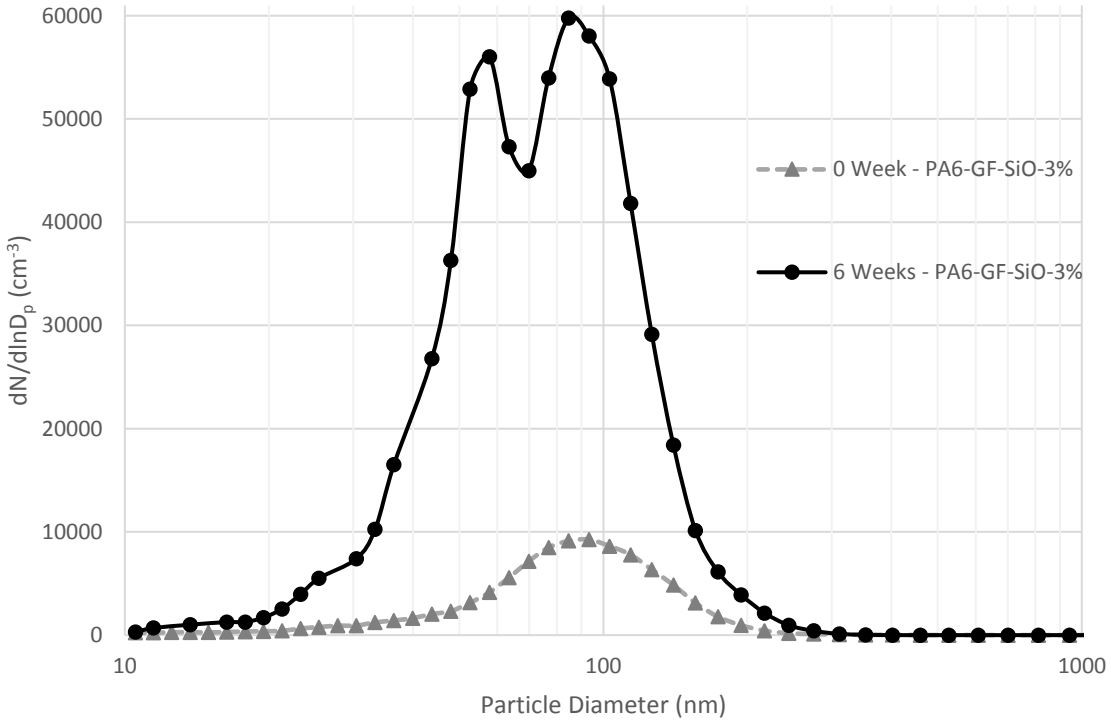

Figure 74: Particle Size Distribution for Nano-Aged and After 6 Weeks of Ageing for the 3 wt.% Nanosilica Composites

6.4 Conclusion

Three-phase nanocomposites using multiscale reinforcements were studied to evaluate the effect of ageing on the emission of nanoparticles during machining. In particular, 30 wt.% glass fibre-filled polyamide-6 (PA6) composites with various weight fractions of nanoclay (montmorillonite, OMMT) and nanosilica (SiO_2) were manufactured and then aged in an oven at 150 °C for up to 6 weeks. Every week, samples were machined in a specified chamber in order to investigate the emission of nanoparticles during milling of nanocomposites.

The results showed that the release of particles increases with the age of the samples. The increase was especially significant after the third and the fifth week of ageing.

The type of nanoadditive used to reinforce the polymer has a significant influence on the number concentration of nanoparticles released during milling of nanocomposites. Nanosilica filled nanocomposites on average generated 50 % more particles compared to the OMMT. This was especially noticeable when the samples were aged. Also, this difference was very significant as nanosilica was used in lower percentages (0.5; 1.5 and 3 wt.%) than OMMT (5; 7.5 and 10 wt.%).

The percentage of nanofiller also played a non-negligible role in the number concentration of particles emitted. For the nanosilica filled composites, the samples made with 3 wt.% of nanofiller (higher percentage for the nanosilica), generated higher number concentration of nanoparticles. However, this trend was reversed for the samples aged 6 weeks.

The OMMT samples with the lowest percentage of OMMT (5 wt.%) produced more particles up to the second week of ageing. Then, the 10 wt.%-OMMT samples showed the highest release rates.

To conclude, the results highlighted an increase in the number concentration of particles released during milling after heat ageing. This can be linked to the likely change of the materials properties which occurred during the heat ageing such as a decrease in hardness. This means that the process parameters need to be adapted according to the age and properties of the materials machined. Also, this

implies that health and safety protections regarding the exposure of workers/consumer should be more restrictive for materials that are subjected to heat ageing.

The importance of considering the life cycle analysis of nanocomposite components is demonstrated here as well: heat ageing has a non-negligible effect on the release of nano-sized particles. It is then of a significant importance to examine the real service conditions of a product in order to predict the possible emission of nanoparticles that could occur during the end-of-life of a nanoproduct. Further work could include the testing of aged nanocomposites for end-of-life scenarios (such as impact or incineration for example).

7 OVERALL DISCUSSION

This chapter aims to analyse and explain the results observed in the thesis. The different parameters influencing the release of nanomaterials are as follows: type of matrix, type and percentage of filler, environmental conditions, process selected and parameters defined within the process (spindle speed, feed rate, impact velocity etc.). The actual effect of these parameters and the possible causes will be investigated and discuss in this chapter.

7.1 Effect of the Process on Nanoparticles Release

In this study, three different mechanical processes and their potential influence on the nanoparticles released from nanocomposites were investigated. Two machining operations: drilling and milling, as well as low velocity impact were selected to represent different stages of the life cycle of a nanocomposite.

The process used to generate particles was found to influence the airborne particles released. For example, epoxy reinforced with CNFs emitted more nanosized particles than epoxy reinforced with CNTs during the drilling experiments. The opposite conclusion was made for the impact experiments. Also, polyester samples generated around 27 times more particles than epoxy samples during drilling of nanocomposites (only 6 times higher when the results are normalised by the mass drilled), while similar level of particles were measured for polyester and epoxy after an impact.

The mechanisms involved in the nanoparticles release are different according to the process. The low velocity impact experiment creates shock waves in the matrix. The force generated by the impact might be sufficient to break the matrix into pieces of various sizes (including nanosize) but also to allow to the Engineered NanoParticles (ENPs) to detach from the matrix. On the other side, machining (drilling, milling, cutting) can emit nanosized particles by different means: friction and deformation of the chips, workpiece and tool, and shearing of the chips [240].

Also, the machining action performed influences the nanoparticles release. The tool used for drilling (a drill bit) has a different shape than a tool used for milling (an end mill), and so interact differently with the material. The movement of the tool in relation to the workpiece is also different which leads to a different mechanism of chips formation in both cases. This conclusion is confirmed by some work found in the literature. Bello et al. [141], [142] investigated cutting and drilling of two different types of hybrid CNT composites. The results highlighted the presence of CNTs agglomerates in the particles released from the drilling experiment, which did not appear during the cutting. Also, the drilling of nanocomposites produced a higher number concentration of particles and in a broader range than during the cutting of nanocomposites.

In addition, looking at the results, further study on the influence of the process parameters would be an interesting topic to investigate. In the preliminary study (Chapter 3), it was seen that the feed rate had an influence on the particle size distribution and number concentration of particles released during drilling of nanocomposites. Also, a study [214] on machining of alloys and steel, focused on the different process parameters which can influence the dust generation during turning. It was shown that the chip formation, the tool lead angle and the cutting speed are important parameters which can be chosen in order to determine the best conditions required for minimal dust emission. Another work [241] showed that the drilling parameters have an influence on the damage of the holes caused by drilling on fibres reinforced plastics. The feed rate was found to affect the damage, surface finish and degradation qualities of the holes the most and the damage increased with a higher spindle speed. Also, the change in parameters can influence the airborne particles release.

With regards to the impact, Sachse et al. [232] found that the impact energy significantly changed the airborne particles release during the impact of nanocomposites cones structures. Other parameters, such as impactor geometry, may affect the particle release.

7.2 Effect of the Matrix Type on Nanoparticles Release

Different types of matrix were assessed related to their potential of releasing nanoparticles in this work. Especially, four different polymer matrices were investigated during machining and low velocity impact: two thermosets (polyester, epoxy), and two thermoplastics (polypropylene and polyamide-6). The results showed that the number concentration of particles emitted was dependant of the type of matrix tested.

The different sets of samples tested can be classified by matrix type. The different grades were found to release a number concentration of particles in the same range regarding the nanofiller used. As we can see Table 29, during the drilling experiments, Polyester grades emitted an average of 150214 particles/cm^3, while Epoxy grades emitted an average of 5528 particles/cm^3, and polypropylene grades an average of 691 particles/cm^3. Polyamide-6 grades released an average of 8286 particles/cm^3 during milling experiments of unaged samples. For the impact experiments, similar observations can be made as the polyester samples released an average of particles around 20782 particles/cm^3, the epoxy an average of 16919 particles/cm^3, and the polypropylene an average of 434 particles/cm^3.

Table 29: Summary of the Release Results

	Number Concentration of Particles, *C* (particles/cm^3)		
Matrix	**Drilling**	**Milling**	**Impact**
Polyester	150 214	-	20 782
Epoxy	5528	-	16 919
Polypropylene	691	-	434
Polyamide-6	-	8286	-

In fact, thermosets (polyester and epoxy) release a higher number concentration of particles than thermoplastics (polypropylene) samples. During the drilling experiments, polyester and epoxy emitted respectively 19 times and 3 times the number concentration of particles emitted by polypropylene. During the impact

experiments, it is 48 and 39 times more particles which were emitted by polyester and epoxy compared to polypropylene.

The nature of polyester and epoxy which fracture in a brittle manner compared to the ductile properties of most thermoplastics materials can have an influence on these results. Especially, in the case of the impact experiments as the failure mode plays an important role in the potential of particles being emitted from the nanocomposites structure. The failure mode and energy absorption capabilities of the materials was also linked to the nanoparticles release in another study [232]. Low velocity impact of crash cones were performed on polyamide-6 and Polypropylene based composites. The polypropylene structures which failed in a progressive manner generated 4 to 8 times less airborne particles than polyamide-6 based structures which were more brittle and less able to absorb energy during impact [232]. It was observed that a brittle material is more likely to generate particles than a ductile materials which have higher strength and can undergo more plastic deformation during an impact/crash test. However, the size of the airborne particles generated was similar for thermoplastics or thermosets.

With regards to the machining of polymer-based nanocomposites, thermosets were also found to release a higher number concentration of particles than thermoplastic materials. However, this finding cannot be linked to the mechanical property of the materials. The reinforcement of PA6-GF with OMMT made the material more brittle, while the reinforcement with nanosilica made it more ductile, which means that the OMMT-nanocomposites was not able to deform plastically before breaking. However, the results on the airborne particles released during the milling operations of unaged nanocomposites showed a slightly higher release for the nanosilica reinforced nanocomposites. This is also corroborated by Khettabi et al. [214] who reported that the formation of brittle chips generated less airborne particles than the formation of ductile chips during the cutting of different aluminium alloys and steels.

Then, in the case of machining, the release of airborne particles seems to be more related to the machinability and thermal properties of the polymer matrix than to its mechanical properties.

Thermoplastics need higher spindle speed and feed rate to be drilled. With lower spindle speed and feed rate, the temperature of the material being machined will increase and in some cases can melt. For comparison purpose the same spindle speed and feed rate were used for all the samples. Surface analysis revealed that the thermoplastic matrix melted during the drilling operation and as a result less amount of particles were generated. This was also corroborated with SEM images. SEM analysis revealed that nanoparticles were present on the surface of thermoset samples (P and E), but hardly any nanoparticles or nanoagglomerates were found on the surface of thermoplastics (PP samples).

The matrix of the nanocomposites tested influenced the release of airborne nanoparticles during mechanical processing of nanocomposites. In fact, even neat polymers were found to release airborne particles in the nanorange, which is confirmed in other studies [141].

7.3 Effect of the Nanoadditive Type on the Nanoparticles Release

As stated previously, the matrix is the main material parameter influencing the release of airborne particles during mechanical processing of nanocomposites. The type of nanofiller was also found to have an influence on the airborne particles released. However, it is only considered as a secondary material parameter as its influence is not significant compared to the matrix type. Indeed, the difference in airborne particles release during drilling between a polyester matrix and an epoxy matrix represents around 25000 particles/cm^3 (corresponding to an increase of 437 % for the polyester compare to the epoxy). When the difference between for example a neat epoxy and an epoxy reinforced by CNTs only represents 1000 particles/cm^3 (only 13 % of the particles generated by a neat epoxy).

During the drilling experiments, the addition of nanofiller into a polymer matrix was found to slightly increase the number concentration of particle released. The addition of alumina and silica nanoparticles into polyester respectively increased the number concentration of particles release by 106 and 39 %. For the Epoxy samples, the addition of CNT increased the number concentration of particles

released by 13 %, and the CNF addition by 78 % (for the normalised values). With regards to the PP samples, the difference was not significant especially as the number concentration of particles released was extremely low. The difference of airborne particles released for the machining operations cannot be explained by the mechanical properties of the samples.

Several studies showed that the glass transition temperature of the polymer is affected by the addition of nanofillers [224], [242]–[244]. In particular, the T_g of polyester decreased by approximately 5 °C with the addition of 2.5 % of Al_2O_3 [242] and also with the addition of 1.5 wt.% of SiO_2 [224]. On the other hand, the T_g of epoxy resin increased by 3 °C by adding 1 wt.% of CNTs [243] and by 22 °C by adding 2 wt.% of CNFs [244]. Looking at the results, the number concentration of particles released before the normalisation, were actually higher for the neat epoxy compared to the nanocomposites. The thermal properties of the nanocomposites might influence the different release mechanism involved during machining and processability.

It was shown by Ponnuvel et al. [245] that the integration of MWCNTs into Epoxy/Glass Fabric polymeric composites improved the quality of the drilled hole at the entrance and exit for every feed rate and cutting speed tested. Alloy matrix composites also present better machining characteristics with MWCNT reinforcement [246]. Especially 0.5 % of MWCNT was found optimal for hardness and young's modulus, and a higher hardness was linked to better stability during the machining operations.

The type of nanoadditive used to reinforce the polymer also had a significant influence on the number concentration of nanoparticles released during milling of nanocomposite the nanocomposites with nanosilica generated in average 50 % more particles compared to the OMMT ones. This was especially noticeable after the ageing of the samples started. Also, this difference was very significant according to the fact that nanosilica was used in low percentage (0.5; 1.5 and 3 wt.%) and the OMMT at high percentage (5; 7.5 and 10 wt.%).

A possible explanation can be the shape of the nanofiller: OMMT are nanoplates, and SiO_2 are spherical. The plate shape creates a higher stress concentration in

the matrix so the material is less able to deform and ease the propagation of the fissures, while spherical particles reduce stress concentration and allows to block the cracks. A change of the bulk properties of the material modifies its processability, and the release of nanoparticles can be affected as well.

With regards to the impact experiments, the addition of alumina and silica nanoparticles into a Polyester matrix increased the number concentration of particles released (respectively 119 % and 46 %). Epoxy-based samples were producing 33 % more particles with the addition of CNT and 11 % less with CNF. In the case of PP samples, the difference was insignificant as the level of particles generated during impact was similar to the background noise measured in the chamber, and at least 10 times lower than the air in the lab. The introduction of a nanofiller into a polymeric matrix changes its mechanical properties and then the failure mode is different. The likelihood of airborne particles to be released is dependant of the failure mode of the nanocomposites (brittle or ductile).

7.4 Effect of the Nanoparticles Percentage on the Nanoparticles Release

Different percentage of OMMT and nanosilica were used to reinforce PA6-GF polymer composites. The six grades were then mechanically characterised and the airborne particles released was measured during the milling of these nanocomposites plates. 5, 7.5 and 10 wt.% of OMMT and 0.5, 1.5 and 3 wt.% of nanosilica were used as reinforcement.

The percentage of nanofiller plays a significant role in the number concentration of particles emitted. For the nanosilica filled composites, the samples made with 3% of nanofiller (higher percentage for the nanosilica ones), generated the highest number concentration of nanoparticles. However, this tendency was reversed for the samples aged 6 weeks in the oven.

The OMMT samples have another trend as samples with the lowest percentage of OMMT produced the highest number concentration of particles up to the second week of ageing. Then, the 10 wt.%-OMMT samples showed the highest release rates.

In addition, the particle mean diameter during the milling of nanocomposites was higher for the samples made with 10 wt.% of OMMT. A higher percentage of filler risked aggregations of the nanofiller. It was seen that the mechanical properties decreased with the increase of OMMT content due to the nanofiller aggregation. At low percentage of nanofiller the possibility of aggregation is lower. The nanosilica-based composites were filled with a maximum of 3 wt.% of nanofiller and showed an optimum at 1.5 wt.% of nanosilica regarding the tensile properties.

Once again, the literature showed a change in the thermal properties of a polymer with the addition of nanofiller [45], [247]. For example, the Heat Deflection Temperature (HDT) was found to increase with percentage of OMMT added to a polyamide-6 matrix [247].

The thermal properties and the machinability of polymer composites were affected by the percentage of nanofiller. This can be linked to the airborne particle release but should however be research with more depth.

7.5 Effect of the Ageing on the Nanoparticles Release

The effect of thermal ageing on airborne particles release was assessed on PA6-GF based nanocomposites. Different percentages of either OMMT or nanosilica were used as nanofillers. Samples were aged in an oven at 150 °C during 6 weeks. Every week the airborne particle release was measured during the milling of the different nanocomposite plates. It was found that for every grade of nanocomposites tested the release of airborne particles increased after thermal ageing of the samples. There was a significant increase after the third week of thermal ageing. For example, a PA6-GF composite filled with 5 wt.% of OMMT released 217 % more particles after third week of ageing compared to the second week. The wear of the tool used for the milling was disregarded as the unaged samples were tested after the aged for 6 weeks (so with an older tool) and still produced a lower number concentration of particles.

Thermal ageing of polymers involves different degradation mechanisms such as oxidation or chain scission which are accelerated with elevated temperatures. In

the case of polymeric nanocomposites, the presence of nanofiller can also accelerate this phenomenon. Iron impurities present in nanoclay used as filler for different polymers were found to accelerate the degradation by photo-oxidation compared to neat polymers [68]–[71]. Especially, polyamide-6 nanocomposites were found to degrade easily compared to neat polyamide-6 [74]–[77].

Also, Kiliaris et al. [67] studied the ageing of polyamide-6 filled with 5 wt.% of OMMT with the same ageing method followed in this work. They found that the crystallinity of PA6 nanocomposites started to dramatically decrease after 3 weeks of oven ageing at 150 °C. This could correspond to the significant increase of number concentration of particles released by aged nanocomposites during milling.

8 CONCLUSIONS AND FURTHER WORK

The main objectives of the PhD was to assess the release of nanoparticles from nanocomposites along their life cycle. For this purpose, a comprehensive literature review on the study of nanoparticles release was conducted, helping to plan a suitable methodology focused on the assessment of nanoparticles released from polymer-matrix nanocomposites during their life cycle. A protocol from the literature was replicated and assessed. Following the identifications of its deficiencies, a new method was developed in order to overcome these deficiencies and propose a standard protocol to get the necessary information for exposure assessment of nanocomposites based consumer products. Different materials grades (4 matrices, and 2 nanofiller types for each matrix) were selected to represent the current of future industrial use of nanocomposites. A selection of scenarios aiming to replicate different stages of products' life cycle was done: machining (drilling and milling) is a common procedure during the product's usage phase, and impact, which simulate accidental or intended fractures at the end-of-life. The new protocol was then applied to quantify and characterise the emission of nanoparticles from the selected nanocomposites during the different scenarios chosen. Several conclusions can be drawn from this study:

- The method implemented in this work to assess the release of nanoparticles from nanocomposites showed several improvements over the methods used in other studies. The new prototype provided reproducibility and reliability, overcoming issues in the previous protocol like contamination from the process, precise control of process parameters and reduction of the contamination from background.
- Every sample tested was found to release nanoparticles regardless of the mechanical process used or the type of material tested. This means that even neat polymer were releasing nanoparticles when subject to mechanical forces.
- The type of matrix was identified to play a major role on the quantity of nanoparticles released during different process. Thermoset polymers

(and especially polyester) were found to release a higher number concentration of particles, mainly due to their brittle properties.

- The nanofiller type and percentage used to reinforce the polymer is also a key point. The nanofiller chosen and its quantity affects/changes the mechanical properties and machinability of the composites. For example, PA6-Glass Fibres composites released 50 % more particles following a milling activity when filled with nanosilica compared to OMMT even though the nanosilica was used in low percentage (0.5; 1.5 and 3 wt.%) and the OMMT at high percentage (5, 7.5 and 10 wt.%).
- The mechanical process used has an influence on the nanoparticles released. An epoxy plate reinforced with CNTs released more particles than an epoxy reinforced with CNFs after impact. The opposite observation was found for the release during drilling.
- The process parameters chosen were also found to be crucial with regards to the nanoparticles released. For example, the feed rate was found to influence not only the quantity of particles released but also their size distribution. However, extensive study on different parameters such as spindle speed for the machining, or impact energy is still necessary.
- Thermal ageing of nanocomposites affects negatively the release of nanoparticles. Six weeks of ageing at 150 ºC increased the number concentration of particles released by 8 to 17 times compared to unaged nanocomposites. Also, the median diameter of particles released decreased, and a higher proportion of the measured particles was in the nanorange after the ageing.

This work is a step towards the standardisation of the evaluation of exposure to nanoparticles in work environment and commercial applications. The results and methodology were used to produce a ‘best practice manual’ directed to industry, research centres and universities dealing with nanomaterials or nanocomposites [248]. This guide presents several steps necessary for the investigation of nanomaterials release from nanocomposites which include the adaptation of

existing standards or methods whenever available, the correlation between the nanorelease processes simulated and the actual life cycle of the nanocomposites evaluated, the importance of monitoring (and isolating) the background particles as well as the ones produced by external elements (such as particles from metallic brushes motor), or the control over the processing conditions for reproducible and reliable results. All these steps are part of the conclusions of the work presented here.

Following these conclusions, further work still remains to be done.

Machining conditions affect the release of nanoparticles, especially in relation to the matrix properties. In this work same machining parameters were applied to all the samples irrespectively of the type of matrix. Future work will involve studying which parameters affect the most the release of nanoparticles, in term of quantity and particle size distribution, considering the increase of temperature in the sample.

The number of possible combinations of matrix and nanofiller type and percentage to create a composite is already huge. Adding to this the different mechanical processes involving the emission of nanoparticles make the task of a complete evaluation of the possible scenarios almost impossible. However, the creation of a database with comparable results of the most likely scenarios related to specific matrix/nanofiller couples would be useful. Different ageing scenarios can also be considered regarding to the industrial application of the composite.

Toxicological characterisations for human health and environment have to be carried out and the chemical characterisation of the particles need to be investigated in depth, especially for the airborne particles.

Correlation studies with different measurement equipment is also necessary. Especially, the SMPS+C used here only measured particles from 10 nm and it would be interesting to assess the release of particles smaller than that.

REFERENCES

[1] ISO Standards, 'ISO/TS 27687:2009 - Nanotechnologies - Terminology and Definitions for Nano-Objects - Nanoparticle, Nanofibre and Nanoplate'.

[2] J. M. Garces, D. J. Moll, J. Bicerano, R. Fibiger, and D. G. McLeod, 'Polymeric Nanocomposites for Automotive Applications', *Adv. Mater.*, vol. no. 23, pp. 1835–1839, Dec. 2000.

[3] D. M. Marquis, E. Guillaume, and C. Chivas-Joly, 'Properties of Nano Fillers in Polymer', *Nanocomposites and Polymers with Analytical Methods*, InTech, pp. 261–284, 2011.

[4] J.-J. Luo and I. M. Daniel, 'Characterization and Modeling of Mechanical Behavior of Polymer/Clay Nanocomposites', *Compos. Sci. Technol.*, vol. 63, no. 11, pp. 1607–1616, 2003.

[5] BCCResearch, 'Nanotechnology - Nanocomposites, Nanoparticles, Nanoclays, and Nanotubes', BCC Research, NAN021D, 2010.

[6] PEN, 'CPI Home'. [Online]. Available: http://www.nanotechproject.org/cpi/. [Accessed: 17-Jun-2014].

[7] M. E. Vance, T. Kuiken, E.P. Vejerano, S. P. McGinnis, M. F. Jr. Hochella, D. Rejeski, and M. S. Hull, 'Nanotechnology in the Real World: Redeveloping the Nanomaterial Consumer Products Inventory', *Belstein J Nanotechnol*, vol. 6, pp. 1769–1780, 2015.

[8] BCC Research, 'Global Markets for Nanocomposites, Nanoparticles, Nanoclays, and Nanotubes - NAN021F', May-2014. [Online]. Available: http://www.bccresearch.com/market-research/nanotechnology/nanocomposites-market-nan021f.html. [Accessed: 14-Jun-2016].

[9] ‘Journal of Nanoparticle Research (JNR)’, *springer.com*. [Online]. Available:http://www.springer.com/materials/nanotechnology/journal/11051. [Accessed: 06-May-2014].

[10] ‘Nanopolytox “Toxicological impact of nanomaterials”’. [Online]. Available: http://www.nanopolytox.eu/. [Accessed: 29-Jan-2013].

[11] ‘Nephh: Home’. [Online]. Available: http://www.nephh-fp7.eu/. [Accessed: 29-Jan-2013].

[12] ‘SIRENA’. [Online]. Available: http://www.life-sirena.com/index.php/en/. [Accessed: 01-Jun-2014].

[13] L. Bergman, J. Rosenholm, A-B. Ost, A. Duchanoy, P. Kankaanpaa, J. Heino, and M. Linden, ‘On the Complexity of Electrostatic Suspension Stabilization of Functionalized Silica Nanoparticles for Biotargeting and Imaging Applications’, *J. Nanomater.*, vol. 2008, pp. 1–9, 2008.

[14] ‘Pyrograf III, Carbon Nanofiber, Carbon Nanotubes | Applied Sciences Incorporated’.

[15] M. Ma, Y. Zhang, Z. Guo, and N. Gu, ‘Facile synthesis of ultrathin magnetic iron oxide nanoplates by Schikorr reaction’, *Nanoscale Res. Lett.*, vol. 8, no. 1, p. 16, 2013.

[16] F. Hussain, M. Hojjati, M. Okamoto, and R. E. Gorga, ‘Review Article: Polymer-Matrix Nanocomposites, Processing, Manufacturing, and Application: An Overview’, *J. Compos. Mater.*, vol. 40, no. 17, pp. 1511–1575, 2006.

[17] M. Rafiee, F. Yavari, J. Rafiee, and N. Koratkar, ‘Fullereneepoxy Nanocomposites-Enhanced Mechanical Properties at Low Nanofiller Loading’, *J. Nanoparticle Res.*, vol. 13, no. 2, pp. 733–737, 2011.

[18] J. Njuguna, I. Pena, H. Zhu, S. A. Rocks, M. Blázquez, and S. A. Desai, ‘Opportunities and Environmental Health Challenges Facing Integration of Polymer NanoComposites Technologies for Automotive

Applications', *Int. J. Polym. Technol.*, vol. 1, no. 1–3, pp. 113–122, 2009.

[19] Y. Kojima, A. Usuki, M. Kawasumi, A. Okada, Y. Fukushima, T. Kurauchi, and O. Kamigaito, 'Mechanical Properties of Nylon 6-Clay Hybrid', *J. Mater. Res.*, vol. 8, no. 05, pp. 1185–1189, 1993.

[20] Y. Kojima, A. Usuki, M. Kawasumi, A. Okada, T. Kurauchi, and O. Kamigaito, 'Synthesis of Nylon 6–Clay Hybrid by Montmorillonite Intercalated with ϵ-caprolactam', *J. Polym. Sci. Part Polym. Chem.*, vol. 31, no. 4, pp. 983–986, 1993.

[21] J. Xiong, Z. Zheng, H. Jiang, S. Ye, and X. Wang, 'Reinforcement of Polyurethane Composites with an Organically Modified Montmorillonite', *Compos. Part Appl. Sci. Manuf.*, vol. 38, no. 1, pp. 132–137, Jan. 2007.

[22] J. Sanes, F. J. Carrión, and M. D. Bermúdez, 'Effect of the Addition of Room Temperature Ionic Liquid and ZnO Nanoparticles on the Wear and Scratch Resistance of Epoxy Resin', *Wear*, vol. 268, no. 11–12, pp. 1295–1302, May 2010.

[23] D. Devaprakasam, P. V. Hatton, G. Möbus, and B. J. Inkson, 'Effect of Microstructure of Nano- and Micro-Particle Filled Polymer Composites on their Tribo-Mechanical Performance', *J. Phys. Conf. Ser.*, vol. 126, p. 012057, Aug. 2008.

[24] A. Dasari, Z.-Z. Yu, and Y.-W. Mai, 'Fundamental Aspects and Recent Progress on Wear/Scratch Damage in Polymer Nanocomposites', *Mater. Sci. Eng. R Rep.*, vol. 63, no. 2, pp. 31–80, Jan. 2009.

[25] S. Pavlidou and C. D. Papaspyrides, 'A Review on Polymer-Layered Silicate Nanocomposites', *Prog. Polym. Sci.*, vol. 33, no. 12, pp. 1119–1198, 2008.

[26] S. Vyazovkin, I. Dranca, X. Fan, and R. Advincula, ‘Kinetics of the Thermal and Thermo-Oxidative Degradation of a Polystyrene–Clay Nanocomposite’, *Macromol. Rapid Commun.,* vol. 25, no. 3, pp. 498–503, 2004.

[27] A. Leszczyńska, J. Njuguna, K. Pielichowski, and J. R. Banerjee, ‘Polymer/Montmorillonite Nanocomposites with Improved Thermal Properties: Part I. Factors Influencing Thermal Stability and Mechanisms of Thermal Stability Improvement’, *Thermochim. Acta*, vol. 453, no. 2, pp. 75–96, Feb. 2007.

[28] S. S. Ray and M. Okamoto, ‘Polymer/Layered Silicate Nanocomposites: a Review from Preparation to Processing’, *Prog. Polym. Sci.*, vol. 28, no. 11, pp. 1539–1641, 2003.

[29] O. Becker, R. J. Varley, and G. P. Simon, ‘Thermal Stability and Water Uptake of High Performance Epoxy Layered Silicate Nanocomposites’, *Eur. Polym. J.*, vol. 40, no. 1, pp. 187–195, Jan. 2004.

[30] S. Mohammadi, H. Shariatpanahi, F. A. Taromi, and J. Neshati, ‘Electrochemical and anticorrosion behaviors of hybrid functionalized graphite nano-platelets/tripolyphosphate in epoxy-coated carbon steel’, *Mater. Res. Bull.*, vol. 80, pp. 7–22, Aug. 2016.

[31] N. Kalaivasan and S. Syed Shafi, ‘Enhancement of Corrosion Protection Effect in Mechanochemically Synthesized Polyaniline/MMT Clay Nanocomposites’, *Arab. J. Chem.*, Aug. 2012.

[32] B. Ramezanzadeh, M. M. Attar, and M. Farzam, ‘A Study on the Anticorrosion Performance of the Epoxy–Polyamide Nanocomposites Containing ZnO Nanoparticles’, *Prog. Org. Coat.*, vol. 72, no. 3, pp. 410–422, Nov. 2011.

[33] T.-I. Yang and P. Kofinas, ‘Dielectric Properties of Polymer Nanoparticle Composites’, *Polymer*, vol. 48, no. 3, pp. 791–798, Jan. 2007.

[34] D. Ma, T. A. Hugener, R. W. Siegel, A. Christerson, E. Martensson, C. Onneby, and L. S. Schadler, ‘Influence of Nanoparticle Surface Modification on the Electrical Behaviour of Polyethylene Nanocomposites’, *Nanotechnology*, vol. 16, no. 6, p. 724, Jun. 2005.

[35] M. Berta, C. Lindsay, G. Pans, and G. Camino, ‘Effect of Chemical Structure on Combustion and Thermal Behaviour of Polyurethane Elastomer Layered Silicate Nanocomposites’, *Polym. Degrad. Stab.*, vol. 91, no. 5, pp. 1179–1191, May 2006.

[36] C. Zhao, H. Qin, F. Gong, M. Feng, S. Zhang, and M. Yang, ‘Mechanical, Thermal and Flammability Properties of Polyethylene/Clay Nanocomposites’, *Polym. Degrad. Stab.*, vol. 87, no. 1, pp. 183–189, Jan. 2005.

[37] M. Costache, D. Jiang, and C. Wilkie, ‘Thermal Degradation of Ethylene-Vinyl Acetate Copolymer Nanocomposites’, *Polymer*, Jan. 2005.

[38] J. K. Pandey, K. Raghunatha Reddy, A. Pratheep Kumar, and R. P. Singh, ‘An Overview on the Degradability of Polymer Nanocomposites’, *Polym. Degrad. Stab.*, vol. 88, no. 2, pp. 234–250, May 2005.

[39] G. Dorairaju, *Additive Synergy in Flexible PVC Nanocomposites for Wire and Cable Applications*. ProQuest, 2008.

[40] J. Njuguna, F. Silva, and S. Sachse, ‘Nanocomposites for Vehicle Structural Applications’, in *Nanofibers - Production, Properties and Functional Applications*, Tong Lin Ed., 2011.

[41] S.-Y. Fu, X.-Q. Feng, B. Lauke, and Y.-W. Mai, ‘Effects of Particle Size, Particle/Matrix Interface Adhesion and Particle Loading on Mechanical Properties of Particulate-Polymer Composites’, *Compos. Part B Eng.*, vol. 39, no. 6, pp. 933–961, 2008.

[42] A. J. Crosby and J. Lee, ‘Polymer Nanocomposites: The “Nano” Effect on Mechanical Properties’, *Polym. Rev.*, vol. 47, no. 2, pp. 217–229, 2007.

[43] M. J. Ellenbecker and C. S.-J. Tsai, ‘Why are we Concerned? The Unique Properties of Nanoparticles’, in *Exposure Assessment and Safety Considerations for Working with Engineered Nanoparticles*, John Wiley & Sons, Inc, 2015, pp. 28–38.

[44] C. B. Ng, L. S. Schadler, and R. W. Siegel, ‘Synthesis and Mechanical Properties of TiO2-Epoxy Nanocomposites’, *Nanostructured Mater.*, vol. 12, no. 1–4, pp. 507–510, 1999.

[45] F. Yang, Y. Ou, and Z. Yu, ‘Polyamide 6/Silica Nanocomposites prepared by In Situ Polymerization’, *J. Appl. Polym. Sci.*, vol. 69, no. 2, pp. 355–361, Jul. 1998.

[46] S. Mishra, S. S. Sonawane, and N. G. Shimpi, ‘Influence of Organo-Montomorillonite on Mechanical and Rheological Properties of Polyamide Nanocomposites’, *Appl. Clay Sci.*, vol. 46, no. 2, pp. 222–225, Oct. 2009.

[47] T. H. Zhou, W. H. Ruan, Y. L. Mai, M. Z. Rong, and M. Q. Zhang, ‘Performance Improvement of Nano-Silica/Polypropylene Composites through In-Situ Cross-Linking Approach’, *Compos. Sci. Technol.*, vol. 68, no. 14, pp. 2858–2863, Nov. 2008.

[48] B. Wetzel, P. Rosso, F. Haupert, and K. Friedrich, ‘Epoxy Nanocomposites – Fracture and Toughening Mechanisms’, *Eng. Fract. Mech.*, vol. 73, no. 16, pp. 2375–2398, Nov. 2006.

[49] G. C. Jacob, J. F. Fellers, S. Simunovic, and J. M. Starbuck, ‘Energy Absorption in Polymer Composites for Automotive Crashworthiness’, *J. Compos. Mater.*, vol. 36, no. 7, pp. 813–850, 2002.

[50] Z. Bartczak, A. S. Argon, R. E. Cohen, and M. Weinberg, ‘Toughness Mechanism in Semi-Crystalline Polymer Blends: I. High-Density Polyethylene Toughened with Rubbers’, *Polymer*, vol. 40, no. 9, pp. 2331–2346, Apr. 1999.

[51] A. K. Subramaniyan and C. T. Sun, ‘Interlaminar Fracture Behavior of Nanoclay Reinforced Glass Fiber Composites’, *J. Compos. Mater.*, vol. 42, no. 20, pp. 2111–2122, Jan. 2008.

[52] J. C. Viana, ‘Polymeric Materials for Impact and Energy Dissipation’, *Plast. Rubber Compos.*, vol. 35, no. 6–7, pp. 260–267, 2006.

[53] C. Yilmaz and T. Korkmaz, ‘The Reinforcement Effect of Nano and Microfillers on Fracture Toughness of Two Provisional Resin Materials’, *Mater. Des.*, vol. 28, no. 7, pp. 2063–2070, 2007.

[54] K. Friedrich, S. Fakirov, and Z. Zhang, *Polymer Composites: From Nano- to Macro-Scale*. Springer, 2005.

[55] Q. Zhang, Q. Fu, L. Jiang, and Y. Lei, ‘Preparation and Properties of Polypropylene/Montmorillonite Layered Nanocomposites’, *Polym. Int.*, vol. 49, no. 12, pp. 1561–1564, Dec. 2000.

[56] N. Gupta and R. Maharsia, ‘Enhancement of Energy Absorption in Syntactic Foams by Nanoclay Incorporation for Sandwich Core Applications’, *Appl. Compos. Mater.*, vol. 12, no. 3, pp. 247–261, 2005.

[57] I. Javni, W. Zhang, V. Karajkov, Z. S. Petrovic, and V. Divjakovic, ‘Effect of Nano-and Micro-Silica Fillers on Polyurethane Foam Properties’, *J. Cell. Plast.*, vol. 38, no. 3, pp. 229–239, Jan. 2002.

[58] R. Maharsia, N. Gupta, and H. D. Jerro, ‘Investigation of Flexural Strength Properties of Rubber and Nanoclay Reinforced Hybrid

Syntactic Foams', *Mater. Sci. Eng. A*, vol. 417, no. 1–2, pp. 249–258, Feb. 2006.

[59] J. Chen, Z. Huang, and J. Zhu, 'Size Effect of Particles on the Damage Dissipation in Nanocomposites', *Compos. Sci. Technol.*, vol. 67, no. 14, pp. 2993–2996, Nov. 2007.

[60] S.-H. Wu, F-Y. Wang, C-C. M. Ma, W-C. Chang, C-T. Kuo, H-C. Kuan, and W-J. Chen, 'Mechanical, Thermal and Morphological Properties of Glass Fiber and Carbon Fiber Reinforced Polyamide-6 and Polyamide-6/Clay Nanocomposites', *Mater. Lett.*, vol. 49, no. 6, pp. 327–333, Jul. 2001.

[61] D. P. N. Vlasveld, P. P. Parlevliet, H. E. N. Bersee, and S. J. Picken, 'Fibre–Matrix Adhesion in Glass-Fibre Reinforced Polyamide-6 Silicate Nanocomposites', *Compos. Part Appl. Sci. Manuf.*, vol. 36, no. 1, pp. 1–11, Jan. 2005.

[62] F. Silva, S. Sachse, and J. Njuguna, 'Mechanical Properties and Impact-Energy Absorption of Injection Moulded Nanocomposites Structures', presented at the ECCM15-15th European Conference on Composite Materials, Venice, Italy, 2012.

[63] E. Helal, Z. Ounaies, and A. B. Meddeb, 'Processing and Characterisation of Two– and Three–Phase Polymer–based Nanocomposites for Energy Storage Applications', *Int. J. Microstruct. Mater. Prop.*, vol. 7, no. 5, pp. 417–427, Jan. 2012.

[64] T. S. Gates and M. A. Grayson, 'On the Use of Accelerated Aging Methods for Screening High Temperature Polymeric Composite Materials', in *40th AIAA Structures, Dynamics and Materials Conference*, 1999, pp. 99–1296.

[65] J. M. Hutchinson, 'Physical Aging of Polymers', *Prog. Polym. Sci.*, vol. 20, no. 4, pp. 703–760, 1995.

[66] A. Hulme and J. Cooper, ‘Life Prediction of Polymers for Industry’, *Seal. Technol.*, vol. 2012, no. 9, pp. 8–12, Sep. 2012.

[67] P. Kiliaris, C. D. Papaspyrides, and R. Pfaendner, ‘Influence of Accelerated Aging on Clay-Reinforced Polyamide 6’, *Polym. Degrad. Stab.*, vol. 94, no. 3, pp. 389–396, Mar. 2009.

[68] A. P. Kumar, D. Depan, N. Singh Tomer, and R. P. Singh, ‘Nanoscale Particles for Polymer Degradation and Stabilization — Trends and Future Perspectives’, *Prog. Polym. Sci.*, vol. 34, no. 6, pp. 479–515, Jun. 2009.

[69] B. Mailhot, S. Morlat, J.-L. Gardette, S. Boucard, J. Duchet, and J.-F. Gérard, ‘Photodegradation of Polypropylene Nanocomposites’, *Polym. Degrad. Stab.*, vol. 82, no. 2, pp. 163–167, 2003.

[70] H. Qin, C. Zhao, S. Zhang, G. Chen, and M. Yang, ‘Photo-Oxidative Degradation of Polyethylene/Montmorillonite Nanocomposite’, *Polym. Degrad. Stab.*, vol. 81, no. 3, pp. 497–500, 2003.

[71] S. Morlat-Therias, B. Mailhot, J.-L. Gardette, C. Da Silva, B. Haidar, and A. Vidal, ‘Photooxidation of Ethylene-Propylene-diene/Montmorillonite Nanocomposites’, *Polym. Degrad. Stab.*, vol. 90, no. 1, pp. 78–85, Oct. 2005.

[72] J. Njuguna and K. Pielichowski, ‘Ageing and Performance Predictions of Polymer Nanocomposites for Exterior Defence and Aerospace Applications’, presented at the Polymers in Defense & Aerospace Applications, Hamburg, Germany, 2010.

[73] D. L. VanderHart, A. Asano, and J. W. Gilman, ‘NMR Measurements Related to Clay-Dispersion Quality and Organic-Modifier Stability in Nylon-6/Clay Nanocomposites’, *Macromolecules*, vol. 34, no. 12, pp. 3819–3822, Jun. 2001.

[74] R. D. Davis, J. W. Gilman, and D. L. VanderHart, ‘Processing Degradation of Polyamide 6/Montmorillonite Clay Nanocomposites and Clay Organic Modifier’, *Polym. Degrad. Stab.*, vol. 79, no. 1, pp. 111–121, 2003.

[75] T. D. Fornes, P. J. Yoon, and D. R. Paul, ‘Polymer Matrix Degradation and Color Formation in Melt Processed Nylon 6/Clay Nanocomposites’, *Polymer*, vol. 44, no. 24, pp. 7545–7556, Nov. 2003.

[76] K. P. Pramoda, T. Liu, Z. Liu, C. He, and H.-J. Sue, ‘Thermal Degradation Behavior of Polyamide 6/Clay Nanocomposites’, *Polym. Degrad. Stab.*, vol. 81, no. 1, pp. 47–56, Jan. 2003.

[77] J. W. Gilman, ‘Flammability and Thermal Stability Studies of Polymer Layered-Silicate (Clay) Nanocomposites’, *Appl. Clay Sci.*, vol. 15, pp. 31–49, 1999.

[78] A. D. Maynard and R. J. Aitken, ‘Assessing Exposure to Airborne Nanomaterials: Current Abilities and Future Requirements’, *Nanotoxicology*, vol. 1, pp. 26–41, 2007.

[79] B. Nowack and T. D. Bucheli, ‘Occurrence, Behavior and Effects of Nanoparticles in the Environment’, *Environ. Pollut.*, vol. 150, no. 1, pp. 5–22, 2007.

[80] B. Nowack, J. F. Ranville, S. Diamond, J. A. Gallego-Urrea, C. Metcalfe, J. Rose, N. Horne, A. A. Koelmans, and S. J. Klaine, ‘Potential Scenarios for Nanomaterial Release and Subsequent Alteration in the Environment’, *Environ. Toxicol. Chem.*, vol. 31, no. 1, pp. 50–59, 2012.

[81] P. J. Borm, D. Robbins, S. Haubold, T. Kuhlbusch, H. Fissan, K. Donaldson, R. Schins, V. Stone, W. Kreyling, J. Lademann, J. Krutmann, D. Warheit, and E. Oberdorster, ‘The Potential Risk of

Nanomaterials: a Review carried out for ECETOC', *Part. Fibre Toxicol.*, 2006.

[82] R. D. Handy, F. von der Kammer, J. R. Lead, M. Hassellöv, R. Owen, and M. Crane, 'The Ecotoxicology and Chemistry of Manufactured Nanoparticles', *Ecotoxicol. Lond. Engl.*, vol. 17, no. 4, pp. 287–314, May 2008

[83] S. J. Klaine, P. J. J. Alvarez, G. E. Batley, T. F. Fernandes, R. D. Handy, D. Y. Lyon, S. Mahendra, M. J. McLaughlin, and J. R. Lead, 'Nanomaterials in the Environment: Behavior, Fate, Bioavailability, and Effects', *Environ. Toxicol. Chem. SETAC*, vol. 27, no. 9, pp. 1825–1851, Sep. 2008.

[84] A. D. Maynard, R. J. Aitken, T. Butz, V. Colin, K. Donaldson, G. Oberdorster, M. A. Philbert, J. Ryan, A. Seaton, V. Stone, S. S. Tinkle, L. Tran, N. J. Walker, and D. B. Warheit, 'Safe Handling of Nanotechnology', *Nature*, vol. 444, no. 7117, pp. 267–269, 2006.

[85] G. Oberdörster, V. Stone, and K. Donaldson, 'Toxicology of Nanoparticles: A Historical Perspective', *Nanotoxicology*, vol. 1, no. 1, pp. 2–25, Jan. 2007.

[86] J. Hock, 'Proceedings of the Workshop on Research Projects on the Safety of Nanomaterials: Reviewing the Knowledge Gaps', Brussels, Apr. 2008.

[87] SCENIHR, 'Scientific Committee on Emerging and Newly-Identified Health Risks : The Appropriateness of the Risk Assessment Methodology in Accordance with the Technical Guidance Documents for New and Existing Substances for Assessing the Risks of Nanomaterials', 2007.

[88] C. Som, M. Berges, Q. Chaudhry, M. Dusinska, T. F. Fernandes, S. I. Olsen, and B. Nowack, 'The Importance of Life Cycle Concepts for the

Development of Safe Nanoproducts', *Toxicology*, vol. 269, pp. 160–9, 2010.

[89] K. Ostertag and B. Hüsing, 'Identification of Starting Points for Exposure Assessment in the Post-Use Phase of Nanomaterial-Containing Products', *J. Clean. Prod.*, vol. 16, no. 8–9, pp. 938–948, May 2008.

[90] A. A. Shvedova, E. R. Kisin, R. Mercer, A. R. Murray, V. J. Johnson, A. I. Potapovich, Y. Y. Tyurina, O. Gorelik, S. Arepalli, D. Schwegler-Berry, A. F. Hubbs, J. Antonini, D. E. Evans, B. K. Ku, D. Ramsey, A. Maynard, V. E. Kagan, V. Castranova, and P. Baron, 'Unusual Inflammatory and Fibrogenic Pulmonary Responses to Single-Walled Carbon Nanotubes in Mice', *Am. J. Physiol. Lung Cell. Mol. Physiol.*, vol. 289, no. 5, pp. 698-708, Nov. 2005.

[91] G. Oberdörster, E. Oberdörster, and J. Oberdörster, 'Nanotoxicology: an Emerging Discipline Evolving from Studies of Ultrafine Particles', *Environ. Health Perspect.*, vol. 113, no. 7, pp. 823–839, Jul. 2005.

[92] L. Reijnders, 'Cleaner Nanotechnology and Hazard Reduction of Manufactured Nanoparticles', *J. Clean. Prod.*, vol. 14, no. 2, pp. 124–133, 2006.

[93] K. Savolainen, L. Pylkkanen, H. Norppa, G. Falck, H. Lindberg, T. Tuomi, M. Vippola, H. Alenius, K. Hameri, J. Koivisto, D. Brouwer, D. Mark, D. Bard, M. Berges, and E. Jankowska, 'Nanotechnologies, Engineered Nanomaterials and Occupational Health and Safety – A Review', *Saf. Sci.*, vol. 48, no. 8, pp. 957–963, Oct. 2010.

[94] P. J. A. Borm and D. Berube, 'A Tale of Opportunities, Uncertainties, and Risks', *Nano Today*, vol. 3, no. 1–2, pp. 56–59, Feb. 2008.

[95] W.-Y. Kim, J. Kim, J. D. Park, H. Y. Ryu, and I. J. Yu, 'Histological Study of Gender Differences in Accumulation of Silver Nanoparticles

in Kidneys of Fischer 344 Rats', *J. Toxicol. Environ. Health A*, vol. 72, no. 21–22, pp. 1279–1284, 2009.

[96] H. Ma, P. L. Williams, and S. A. Diamond, 'Ecotoxicity of Manufactured ZnO Nanoparticles – A Review', *Environ. Pollut.*, vol. 172, pp. 76–85, Jan. 2013.

[97] X. Zhu, J. Zhou, and Z. Cai, 'The Toxicity and Oxidative Stress of TiO2 Nanoparticles in Marine Abalone (Haliotis Diversicolor Supertexta)', *Mar. Pollut. Bull.*, vol. 63, no. 5–12, pp. 334–338, 2011.

[98] T. A. J. Kuhlbusch and C. Asbach, 'Nanoparticle Exposure at Nanotechnology Workplaces: a Review.', *Part. Fibre Toxicol.*, vol. 8, p. 22, 2011.

[99] A. Helland, M. Scheringer, M. Siegrist, H. G. Kastenholz, A. Wiek, and R. W. Scholz, 'Risk Assessment of Engineered Nanomaterials: A Survey of Industrial Approaches', *Environ. Sci. Technol.*, vol. 42, no. 2, pp. 640–646, Jan. 2008.

[100] V. Jamier, I. Gispert, and V. Puntes, 'The Social Context of Nanotechnology and Regulating its Uncertainty: A Nanotechnologist Approach', *J. Phys. Conf. Ser.*, vol. 429, no. 1, p. 012059, Apr. 2013.

[101] L. Renwick, D. Brown, A. Clouter, and K. Donaldson, 'Increased Inflammation and Altered Macrophage Chemotactic Responses caused by Two Ultrafine Particle Types', *Occup. Environ. Med.*, vol. 61, no. 5, pp. 442–447, May 2004.

[102] C. M. Sayes, F. Liang, J. L. Hudson, J. Mendez, W. Guo, J. M. Beach, V. C. Moore, C. D. Doyle, J. L. West, and W. E. Billups, 'Functionalization Density Dependence of Single-Walled Carbon Nanotubes Cytotoxicity In Vitro', *Toxicol. Lett.*, vol. 161, no. 2, pp. 135–142, Feb. 2006.

[103] A. K. Gupta and M. Gupta, ‘Cytotoxicity Suppression and Cellular Uptake Enhancement of Surface Modified Magnetic Nanoparticles’, *Biomaterials*, vol. 26, no. 13, pp. 1565–1573, May 2005.

[104] S. S. Tinkle, J. M. Antonini, B. A. Rich, J. R. Roberts, R. Salmen, K. DePree, and E. J. Adkins, ‘Skin as a Route of Exposure and Sensitization in Chronic Beryllium Disease’, *Environ. Health Perspect.*, vol. 111, no. 9, pp. 1202–1208, Jul. 2003.

[105] M. J. Ellenbecker and C. S.-J. Tsai, ‘Routes of Exposure for Engineered Nanoparticles’, in *Exposure Assessment and Safety Considerations for Working with Engineered Nanoparticles*, John Wiley & Sons, Inc, 2015, pp. 39–50.

[106] K. Savolainen, U. Backman, D. Brouwer, B. Fadeel, T. Fernandes, T. Kuhlbusch, R. Landsiedel, I. Lynch, and L. Pylkkanen, *Nanosafety in Europe 2015-2025: Towards Safe and Sustainable Nanomaterials and Nanotechnology Innovations*, 2013.

[107] BSI Standards, ‘BS EN ISO 14040:2006; Environmental Managment - Life Cycle Assessment - Principles and Framework’. 31-Jul-2006.

[108] A. R. Köhler, C. Som, A. Helland, and F. Gottschalk, ‘Studying the Potential Release of Carbon Nanotubes throughout the Application Life Cycle’, *J. Clean. Prod.*, vol. 16, no. 8–9, pp. 927–937, May 2008.

[109] D. Bello, A. J. Hart, K. Ahn, M. Hallock, N. Yamamoto, E. J. Garcia, M. J. Ellebecker, and B. L. Wardle, ‘Particle Exposure Levels during CVD Growth and Subsequent Handling of Vertically-Aligned Carbon Nanotube Films’, *Carbon*, vol. 46, no. 6, pp. 974–977, May 2008.

[110] Y. Fujitani, T. Kobayashi, K. Arashidani, N. Kunugita, and K. Suemura, ‘Measurement of the Physical Properties of Aerosols in a Fullerene Factory for Inhalation Exposure Assessment’, *J. Occup. Environ. Hyg.*, vol. 5, no. 6, pp. 380–389, Jun. 2008.

[111] J. H. Han, E. J. Lee, J. H. Lee, K. P. So, Y. H. Lee, G. N. Bae, S. B. Lee, J. H. Ji, M. H. Cho, and I. J. Yu, 'Monitoring Multiwalled Carbon Nanotube Exposure in Carbon Nanotube Research Facility', *Inhal. Toxicol.*, vol. 20, no. 8, pp. 741–749, Jun. 2008.

[112] M. M. Methner, M. E. Birch, D. E. Evans, B.-K. Ku, K. Crouch, and M. D. Hoover, 'Identification and Characterization of Potential Sources of Worker Exposure to Carbon Nanofibers during Polymer Composite Laboratory Operations', *J. Occup. Environ. Hyg.*, vol. 4, no. 12, pp. D125-130, Dec. 2007.

[113] B. Yeganeh, C. M. Kull, M. S. Hull, and L. C. Marr, 'Characterization of Airborne Particles During Production of Carbonaceous Nanomaterials', *Environ. Sci. Technol.*, vol. 42, no. 12, pp. 4600–4606, Jun. 2008.

[114] T. A. J. Kuhlbusch and H. Fissan, 'Particle Characteristics in the Reactor and Pelletizing Areas of Carbon Black Production', *J. Occup. Environ. Hyg.*, vol. 3, no. 10, pp. 558–567, Oct. 2006.

[115] D. R. Johnson, M. M. Methner, A. J. Kennedy, and J. A. Steevens, 'Potential for Occupational Exposure to Engineered Carbon-Based Nanomaterials in Environmental Laboratory Studies', *Environ. Health Perspect.*, vol. 118, no. 1, pp. 49–54, Jan. 2010.

[116] A. D. Maynard, P. A. Baron, M. Foley, A. A. Shvedova, E. R. Kisin, and V. Castranova, 'Exposure to Carbon Nanotube Material: Aerosol Release During the Handling of Unrefined Single-Walled Carbon Nanotube Material', *J. Toxicol. Environ. Health A*, vol. 67, no. 1, pp. 87–107, 2004.

[117] D. Brouwer, B. van Duuren-Stuurman, M. Berges, E. Jankowska, D. Bard, and D. Mark, 'From Workplace Air Measurement Results toward Estimates of Exposure? Development of a Strategy to Assess Exposure to Manufactured Nano-Objects', *J. Nanoparticle Res.*, vol. 11, no. 8, pp. 1867–1881, Nov. 2009.

[118] Y.-F. Wang, P.-J. Tsai, C.-W. Chen, D.-R. Chen, and D.-J. Hsu, ‘Using a Modified Electrical Aerosol Detector To Predict Nanoparticle Exposures to Different Regions of the Respiratory Tract for Workers in a Carbon Black Manufacturing Industry’, *Environ. Sci. Technol.*, vol. 44, no. 17, pp. 6767–6774, Sep. 2010.

[119] J. Park, B. K. Kwak, E. Bae, J. Lee, Y. Kim, K. Choi, and J. Yi, ‘Characterization of Exposure to Silver Nanoparticles in a Manufacturing Facility’, *J. Nanoparticle Res.*, vol. 11, no. 7, pp. 1705–1712, Oct. 2009.

[120] S.-J. (Candace) Tsai, M. Hofmann, M. Hallock, E. Ada, J. Kong, and M. Ellenbecker, ‘Characterization and Evaluation of Nanoparticle Release during the Synthesis of Single-Walled and Multiwalled Carbon Nanotubes by Chemical Vapor Deposition’, *Environ. Sci. Technol.*, vol. 43, no. 15, pp. 6017–6023, Aug. 2009.

[121] D. E. Evans, B. K. Ku, M. E. Birch, and K. H. Dunn, ‘Aerosol Monitoring during Carbon Nanofiber Production: Mobile Direct-Reading Sampling’, *Ann. Occup. Hyg.*, vol. 54, no. 5, pp. 514–531, Jul. 2010.

[122] J. Wang, C. Asbach, H. J. Fissan, T. Hulser, T. A. J. Kuhlbusch, D. Thompson, and D. Y. H. Pui, ‘How can Nanobiotechnology Oversight Advance Science and Industry: Examples from Environmental, Health, and Safety Studies of Nanoparticles (nano-EHS)’, *J. Nanoparticle Res.*, vol. 13, no. 4, pp. 1373–1387, 2011.

[123] E. Demou, P. Peter, and S. Hellweg, ‘Exposure to Manufactured Nanostructured Particles in an Industrial Pilot Plant’, *Ann. Occup. Hyg.*, vol. 52, no. 8, pp. 695–706, Nov. 2008.

[124] E. Demou, W. J. Stark, and S. Hellweg, ‘Particle Emission and Exposure during Nanoparticle Synthesis in Research Laboratories’, *Ann. Occup. Hyg.*, vol. 53, no. 8, pp. 829–838, Nov. 2009.

[125] C. Möhlmann, J. Welter, M. Klenke, and J. Sander, 'Workplace Exposure at Nanomaterial Production Processes', *J. Phys. Conf. Ser.*, vol. 170, no. 1, p. 012004, May 2009.

[126] T. M. Peters, S. Elzey, R. Johnson, H. Park, V. H. Grassian, T. Maher, and P. O'Shaughnessy, 'Airborne Monitoring to Distinguish Engineered Nanomaterials from Incidental Particles for Environmental Health and Safety', *J. Occup. Environ. Hyg.*, vol. 6, no. 2, pp. 73–81, Feb. 2009.

[127] L. Manodori and A. Benedetti, 'Nanoparticles Monitoring in Workplaces devoted to Nanotechnologies', *J. Phys. Conf. Ser.*, vol. 170, no. 1, p. 012001, May 2009.

[128] C. Tsai and A. Ashter, 'Airborne Nanoparticle Release Associated with the Compounding of Nanocomposites Using Nanoalumina as Fillers', 2008.

[129] M. Methner, L. Hodson, A. Dames, and C. Geraci, 'Nanoparticle Emission Assessment Technique (NEAT) for the Identification and Measurement of Potential Inhalation Exposure to Engineered Nanomaterials—Part B: Results from 12 Field Studies', *J. Occup. Environ. Hyg.*, vol. 7, no. 3, pp. 163–176, 2009.

[130] J. H. Lee, M. Kwon, J. H. Ji, C. S. Kang, K. H. Ahn, J. H. Han, and I. J. Yu, 'Exposure Assessment of Workplaces Manufacturing Nanosized TiO2 and Silver', *Inhal. Toxicol.*, vol. 23, no. 4, pp. 226–236, Mar. 2011.

[131] B. Biscans and N. Ibaseta, 'Ultrafine Aerosol Emission from the Free Fall of TiO2 and SiO2 Nanopowders', *Kona Powder Part.*, no. n°25, Aug. 2007.

[132] T. Schneider and K. A. Jensen, 'Combined Single-Drop and Rotating Drum Dustiness Test of Fine to Nanosize Powders Using a Small Drum', *Ann. Occup. Hyg.*, vol. 52, no. 1, pp. 23–34, Jan. 2008.

[133] K. Jensen, I. Koponen, P. Clausen, and T. Schneider, ‘Dustiness Behaviour of Loose and Compacted Bentonite and Organoclay Powders: What is the Difference in Exposure Risk?’, *J. Nanoparticle Res.*, vol. 11, no. 1, pp. 133–146, 2009.

[134] I. Ogura, H. Sakurai, and M. Gamo, ‘Dustiness Testing of Engineered Nanomaterials’, *J. Phys. Conf. Ser.*, vol. 170, no. 1, p. 012003, May 2009.

[135] S.-B. Lee, J.-H. Lee, and G.-N. Bae, ‘Size Response of an SMPS–APS System to Commercial Multi-Walled Carbon Nanotubes’, *J. Nanoparticle Res.*, vol. 12, no. 2, pp. 501–512, Feb. 2010.

[136] B. Stahlmecke, S. Wagener, C. Asbach, H. Kaminski, H. Fissan, and T. A. J. Kuhlbusch, ‘Investigation of Airborne Nanopowder Agglomerate Stability in an Orifice under Various Differential Pressure Conditions’, *J. Nanoparticle Res.*, vol. 11, no. 7, pp. 1625–1635, Oct. 2009.

[137] S.-J. (Candace) Tsai, A. Ashter, E. Ada, J. L. Mead, C. F. Barry, and M. J. Ellenbecker, ‘Control of Airborne Nanoparticles Release during Compounding of Polymer Nanocomposites’, *Nano*, vol. 03, no. 04, pp. 301–309, Aug. 2008.

[138] L. K. Breggin and J. Pendergrass, ‘Where does the Nano Go? End-of-Life Regulation of Nanotechnologies’, Woodrow Wilson International Center for Scholars, 2007.

[139] BSI Standards, ‘PAS 138:2012 - Disposal of Manufacturing Process Waste Containing Manufactured Nano-Objects. Guide’. May-2012.

[140] US EPA, ‘Hazardous Waste Regulations’. [Online]. Available: https://www3.epa.gov/. [Accessed: 10-Jun-2014].

[141] D. Bello, B. L. Wardle, J. Zhang, N. Yamamoto, C. Santeufemio, M. Hallock, and M. A. Virji, ‘Characterization of Exposures to Nanoscale

Particles and Fibers during Solid Core Drilling of Hybrid CNT Advanced Composites', *Int. J. Occup. Environ. Health*, vol. 16, pp. 434–450, 2010.

[142] D. Bello, B. L. Wardle, N. Yamamoto, R. G. deVilloria, E. J. Garcia, A. J. Hart, K. Ahn, M. J. Ellenbecker, and M. Hallock, 'Exposure to Nanoscale Particles and Fibers during Machining of Hybrid Advanced Composites Containing Carbon Nanotubes', *J. Nanoparticle Res.*, vol. 11, pp. 231–249, 2009.

[143] W. Wohlleben, , S. Brill, M. W. Meier, M. Mertler, G. Cox, S. Hirth, B. von Vacano, V. Strauss, S. Treumann, K. Wiench, L. Ma-Hock, and R. Landsiedel, 'On the Lifecycle of Nanocomposites: Comparing Released Fragments and their In-Vivo Hazards from Three Release Mechanisms and Four Nanocomposites', *Small*, pp. 2384–2395, 2011.

[144] W. Wohlleben, M. W. Meier, S. Vogel, R. Landsiedel, G. Cox, S. Hirth, and Z. Tomovic, 'Elastic CNT–Polyurethane Nanocomposite: Synthesis, Performance and Assessment of Fragments Released during Use', *Nanoscale*, vol. 5, no. 1, p. 369, 2013.

[145] L. Schlagenhauf, B. T. T. Chu, J. Buha, F. Nueesch, and J. Wang, 'Release of Carbon Nanotubes from an Epoxy-Based Nanocomposite during an Abrasion Process', *Environ. Sci. Technol.*, vol. 46, no. 13, pp. 7366–7372, 2012.

[146] D. Fleury, B. R. Mili, and A. Janes, 'New Evidence Towards the Release of Airborne Carbon Nanotubes when Burning Nanocomposite Polymers', in *Nanotechnolog 2011: Advanced Materials, CNTs, Particles, Films and Composites*, vol. 1, 2011, p. 882.

[147] L. G. Cena and T. M. Peters, 'Characterization and Control of Airborne Particles Emitted During Production of Epoxy/Carbon Nanotube Nanocomposites', *J. Occup. Environ. Hyg.*, vol. 8, no. 2, pp. 86–92, 2011.

[148] P. C. Raynor, J. I. Cebula, J. S. Spangenberger, B. A. Olson, J. M. Dasch, and J. B. D'Arcy, 'Assessing Potential Nanoparticle Release During Nanocomposite Shredding Using Direct-Reading Instruments', *J. Occup. Environ. Hyg.*, vol. 9, no. 1, pp. 1–13, 2012.

[149] S. J. Froggett, S. F. Clancy, D. R. Boverhof, and R. A. Canady, 'A Review and Perspective of Existing Research on the Release of Nanomaterials from Solid Nanocomposites', *Part. Fibre Toxicol.*, vol. 11, p. 17, 2014.

[150] M. Vorbau, L. Hillemann, and M. Stintz, 'Method for the Characterization of the Abrasion Induced Nanoparticle Release into Air from Surface Coatings', *J. Aerosol Sci.*, vol. 40, pp. 209–217, 2009.

[151] M. Methner, C. Crawford, and C. Geraci, 'Evaluation of the Potential Airborne Release of Carbon Nanofibers during the Preparation, Grinding, and Cutting of Epoxy-Based Nanocomposite Material', *J. Occup. Environ. Hyg.*, vol. 9, no. 5, pp. 308–318, 2012.

[152] I. Ogura, M. Kotake, M. Shiegeta, M. Uejima, K. Saito, N. Hashimoto, and A. Kishimoto, 'Potential Release of Carbon Nanotubes from their Composites during Grinding', *J. Phys. Conf. Ser.*, vol. 429, p. 012049, Apr. 2013.

[153] S. Sachse, F. Silva, H. Zhu, A. Irfan, A. Leszczynska, K. Pielichowski, V. Ermini, M. Blazquez, O. Kuzmenko, and J. Njuguna, 'The Effect of Nanoclay on Dust Generation during Drilling of PA6 Nanocomposites', *J. Nanomater.*, vol. 2012, p. 8, 2012.

[154] S. Sachse, F. Silva, A. Irfan, H, Zhu, K. Pielichowski, A. Leszczynska, M. Blazquez, O. Kazmina, O. Kuzmenko, and J. Njuguna, 'Physical Characteristics of Nanoparticles Emitted during Drilling of Silica Based Polyamide 6 Nanocomposites', *IOP Conf. Ser. Mater. Sci. Eng.*, vol. 40, no. 1, p. 012012, 2012.

[155] A. Hellmann, K. Schmidt, and S. Ripperger, ‘Release of Ultrafine Dusts during the Machining of Nanocomposites’, *Gefahrstoffe Reinhalt. Luft*, vol. 72, no. 11–12, 2012.

[156] G. Huang, J. H. Park, L. G. Cena, B. L. Shelton, and T. M. Peters, ‘Evaluation of Airborne Particle Emissions from Commercial Products Containing Carbon Nanotubes’, *J. Nanoparticle Res.*, vol. 14, no. 11, pp. 1–13, Oct. 2012.

[157] A. Guiot, L. Golanski, and F. Tardif, ‘Measurement of Nanoparticle Removal by Abrasion’, *J. Phys. Conf. Ser.*, vol. 170, p. 012014, 2009.

[158] D. Gohler, M. Stintz, L. Hillemann, and M. Vorbau, ‘Characterization of Nanoparticle Release from Surface Coatings by the Simulation of a Sanding Process’, *Ann. Occup. Hyg.*, vol. 54, p. 615?624, 2010.

[159] L. Golanski, A. Gaborieau, A. Guiot, G. Uzu, J. Chatenet, and F. Tardif, ‘Characterization of Abrasion-Induced Nanoparticle Release from Paints into Liquids and Air’, *J. Phys. Conf. Ser.*, vol. 304, no. 1, p. 012062, 2011.

[160] L.-Y. Hsu and H.-M. Chein, ‘Evaluation of Nanoparticle Emission for TiO2 Nanopowder Coating Materials’, *J. Nanoparticle Res.*, vol. 9, no. 1, pp. 157–163, Nov. 2006.

[161] I. K. Koponen, K. A. Jensen, and T. Schneider, ‘Sanding Dust from Nanoparticle-Containing Paints: Physical Characterisation’, *J. Phys. Conf. Ser.*, vol. 151, no. 1, p. 012048, 2009.

[162] I. K. Koponen, K. A. Jensen, and T. Schneider, ‘Comparison of Dust Released from Sanding Conventional and Nanoparticle-Doped Wall and Wood Coatings’, *J. Expo. Sci. Environ. Epidemiol.*, vol. 21, no. 4, pp. 408–418, Jul. 2011.

[163] L. Golanski, A. Guiot, M. Pras, M. Malarde, and F. Tardif, ‘Release-Ability of Nano Fillers from Different Nanomaterials (toward the

Acceptability of Nanoproduct)', *J. Nanoparticle Res.*, vol. 14, no. 7, Jul. 2012.

[164] C.-J. Tsai, C-H. Wu, M-L. Leu, S-C. Chen, C-Y. Huang, P-J. Tsai, and F-H. Ko, 'Dustiness Test of Nanopowders Using a Standard Rotating Drum with a Modified Sampling Train', *J. Nanoparticle Res.*, vol. 11, no. 1, pp. 121–131, Jan. 2009.

[165] R. Kaegi, A. Ulrich, B. Sinnet, R. Vonbank, A. Wichser, S. Zuleeg, H. Simmler, S. Brunner, H. Vonmont, M. Burkhardt, and M. Boller, 'Synthetic TiO2 Nanoparticle Emission from Exterior Facades into the Aquatic Environment', *Environ. Pollut.*, vol. 156, no. 2, pp. 233–239, Nov. 2008.

[166] The Royal Society and the Royal Academy of Engineering, 'Nanoscience and Nanotechnologies: Opportunities and Uncertainties', 2004.

[167] S. Halliwell, 'End of Life Options for Composite Waste - Best Practice Guide'. National Composites Network, 2006.

[168] L. Schlagenhauf, F. Nüesch, and J. Wang, 'Release of Carbon Nanotubes from Polymer Nanocomposites', *Fibers*, vol. 2, no. 2, pp. 108–127, Mar. 2014.

[169] B. Schartel, P. Pötschke, U. Knoll, and M. Abdel-Goad, 'Fire Behaviour of Polyamide 6/Multiwall Carbon Nanotube Nanocomposites', *Eur. Polym. J.*, vol. 41, no. 5, pp. 1061–1070, May 2005.

[170] S. Fu, P. Song, H. Yang, Y. Jin, F. Lu, J. Ye, and Q. Wu, 'Effects of Carbon Nanotubes and its Functionalization on the Thermal and Flammability Properties of Polypropylene/Wood Flour Composites', *J. Mater. Sci.*, vol. 45, no. 13, pp. 3520–3528, Mar. 2010.

[171] J. X. Bouillard, B. R'Mili, D. Moranviller, A. Vignes, O. Le Bihan, A. Ustache, J. A. S. Bonfim, E. Frejafon, and D. Fleury, 'Nanosafety by

Design: Risks from Nanocomposite/Nanowaste Combustion', *J. Nanoparticle Res.*, vol. 15, no. 4, pp. 1–11, Mar. 2013.

[172] N. Uddin, M. Nyden, and R. Davis, 'Characterization of Nanoparticle Release from Polymer Nanocomposites Due to Fire', *Fire Mater.*, Jan. 2011.

[173] S. Sachse, 'Nano-sized Particles Emission during Drilling and Low Velocity Impact of Silica-based Thermoplastic Nanocomposites', PhD Thesis, Cranfield University, 2012.

[174] H. Kaminski, T. A. J. Kuhlbusch, S. Rath, U. Gotz, M. Sprenger, D. Wels, J. Polloczek, V. Bachmann, N. Dziurowitz, H-J. Kiesling, and A. Schwiegelshohn, 'Comparability of Mobility Particle Sizers and Diffusion Chargers', *J. Aerosol Sci.*, vol. 57, pp. 156–178, Mar. 2013.

[175] S. Sachse, A. Irfan, H. Zhu, and J. Njuguna, 'Morphology Studies of Nanodust Generated from Polyurethane/Nanoclay Nanofoams following Mechanical Fracture', *J. Nanostructured Polym. Nanocomposites*, vol. 7, pp. 5–9, 2011.

[176] J. Njuguna, S. Sachse, A. Irfan, S. Michalowski, K. Pielichowski, O. Kazmina, V. Ermini, H. Zhu, and M. Blazquez, 'Investigations into Nanoparticles Generated from Nanofiller Reinforced Polymer Nanocomposites during Structural Testing', presented at the Safety Issues of Nanomaterials along their life cycle, Barcelona, Spain, 2011, pp. 53–54.

[177] J. Wang, V. F. McNeill, D. R. Collins, and R. C. Flagan, 'Fast Mixing Condensation Nucleus Counter: Application to Rapid Scanning Differential Mobility Analyzer Measurement', *Aerosol Sci. Technol.*, vol. 36, pp. 678–689, 2002.

[178] The European Commission, 'Communication from the Commission to the European Parliament, the Council and the European Economic and

Social Committee - Second Regulatory Review on Nanomaterials'. 03-Oct-2012.

[179] The European commission, 'Procedure File: Regulatory Aspects of Nanomaterials - 2008/2208(INI)'.

[180] G. Gerritzen, L.-C. Huang, K. Killpack, M. Mircheva, and J. Conti, 'A Review of Current Practices in the Nanotechnology Industry - Phase Two Report: Survey of Current Practices in the Nanotechnology Workplace', 2006.

[181] 'Nanosafe - NANOSAFE 2012'. [Online]. Available: http://www.nanosafe.org/scripts/home/publigen/content/templates/show.asp?P=124&L=EN&ITEMID=54. [Accessed: 19-Nov-2013].

[182] B. Hansen, 'Workshop on the second regulatory review on nanomaterials', Brussels (Belgium), 30-Jan-2013.

[183] L. Reijnders, 'The Release of TiO2 and SiO2 Nanoparticles from Nanocomposites', *Polym. Degrad. Stab.*, vol. 94, pp. 873–876, 2009.

[184] BSI Standards, 'PD 6699-1:2007 Good Practice Guide for Specifying Manufactured Nanomaterials'.

[185] S. Kaluza, J. Kleine Balderhaar, B. Orthen, B. Honnert, E. Jankowska, P. Pietrowski, M. G. Rosell, C. Tanarro, J. Tejedor, and A. Zugasti, 'Literature Review -Workplace Exposure to Nanoparticles', EU-OSHA -European Agency for Safety and Health at Work, 2009.

[186] BSI Standards, 'BS EN 15051:2006 - Workplace Atmospheres. Measurement of the Dustiness of Bulk Materials. Requirements and Reference Test Methods'. 31-May-2006.

[187] ISO Standards, 'ISO 5470-1:1999 Rubber- or Plastics-Coated Fabrics - Determination of Abrasion Resistance - Part 1: Taber Abrader'. 30-Oct-2009.

[188] ASTM Standards, ‘ASTM C1353-07 - Standard Test Method Using the Taber Abraser for Abrasion Resistance of Dimension Stone Subjected to Foot Traffic’. 2007.

[189] Q. Chaudhry, C. George, and R. Watkins, ‘Nanotechnology Regulation: Developments in the United Kingdom’, in *New global frontiers in regulation: the age of nanotechnology*, 2009.

[190] G. A. Hodge, D. Bowman, and K. Ludlow, *New Global Frontiers in Regulation: The Age of Nanotechnology*. Edward Elgar Publishing, 2007.

[191] G. Oberdorster, E. Oberdorster, and J. Oberdorster, ‘Concepts of Nanoparticle Dose Metric and Response Metric’, *Environ. Health Perspect.*, vol. 115, no. 6, p. A290, Jun. 2007.

[192] ‘Nanomaterials - ECHA’. [Online]. Available: http://echa.europa.eu/regulations/nanomaterials. [Accessed: 24-Mar-2014].

[193] The European Parliament and The Council of the European Union, ‘Directive 2008/98/EC of the European Parliament and of the Council of 19 November 2008 on Waste’.

[194] The European Parliament and The Council of the European Union, ‘Directive 2001/95/EC of the European Parliament and of the Council of 3 December 2001 on General Product Safety’.

[195] The European Commission, ‘Council Directive 98/24/EC of 7 April 1998 on the Protection of the Health and Safety of Workers from the Risks Related to Chemical Agents at Work’.

[196] ‘EUR-Lex - 31989L0391 - EN’, *Official Journal L 183 , 29/06/1989 P. 0001 - 0008; Finnish special edition: Chapter 5 Volume 4 P. 0146; Swedish special edition: Chapter 5 Volume 4 P. 0146;* [Online]. Available: http://eur-

lex.europa.eu/LexUriServ/LexUriServ.do?uri=CELEX:31989L0391:EN:HTML. [Accessed: 05-Sep-2013].

[197] L.-J. Scherow, 'Engineered Nanoscale Materials and Derivative Products: Regulatory Challenges', RL34332, 2008.

[198] EPA, United States Environmental Protection Agency, 'Draft Nanomaterial Research Strategy (NRS)', Jan. 2008.

[199] The National Nanotechnology Initiative, 'Environmental, Health, and Safety Research Needs for Engineered Nanoscale Materials', 2006.

[200] NIOSH - Department of Health and Human Services, 'Approaches to Safe Nanotechnology - Managing the Health and Safety Concerns Associated with Engineered Nanomaterials', Mar. 2009.

[201] National Science and Technology Council Committe on Technology - Subcommitte on Nanoscale Science, Engineering, and Technology, 'Environmental Health, and Safety Research Strategy'. Oct-2011.

[202] Committee to Develop a Research Strategy for Environmental, Health, and Safety Aspects of Engineered Nanomaterials, *A Research Strategy for Environmental, Health, and Safety Aspects of Engineered Nanomaterials*. 2012.

[203] 'Regulation of Nanotechnology Materials'. [Online]. Available: http://www.understandingnano.com/nanotechnology-regulation.html. [Accessed: 24-Aug-2013].

[204] The European Commission, 'The Sixth Framework Programme in brief'. 2002.

[205] The European Commission, 'FP7 in Brief'. 2007.

[206] 'MARINA | Managing Risks of Nanomaterials'. [Online]. Available: http://www.marina-fp7.eu/. [Accessed: 29-May-2014].

[207] ‘NanoValid: Home’. [Online]. Available: http://www.nanovalid.eu/. [Accessed: 29-May-2014].

[208] ‘QualityNano Research Infrastructure - Welcome to QualityNano’. [Online]. Available: http://www.qualitynano.eu/. [Accessed: 29-May-2014].

[209] The European Commission, ‘Nanotechnologies, Advanced Materials, Advanced Manufacturing and Processing, and Biotechnology’, *Horizon 2020*. [Online]. Available: http://ec.europa.eu/programmes/horizon2020/en/h2020-section/nanotechnologies-advanced-materials-advanced-manufacturing-and-processing-and. [Accessed: 01-Jun-2014].

[210] GRIMM Aerosols, ‘Scanning Mobility Particle Sizer (SMPS+C)’, *Grimm Aerosol*, 15-Oct-2012. [Online]. Available: http://wiki.grimm-aerosol.de/images/6/6c/GrimmAerosolTechnik_Nano_SMPS_C.pdf. [Accessed: 11-Feb-2013].

[211] TSI Incorporated, ‘Fundamentals of CPC and SMPS Spectrometers’.

[212] W. Liu, J. Zhang, J. H. Hashim, J. Jalaludin, Z. Hashim, and B. D. Goldstein, ‘Mosquito Coil Emissions and Health Implications’, *Environ. Health Perspect.*, vol. 111, pp. 1454–1460, 2003.

[213] S. W. See, R. Balasubramanian, and U. M. Joshi, ‘Physical Characteristics of Nanoparticles Emitted from Incense Smoke’, *Sci. Technol. Adv. Mater.*, vol. 8, no. 1–2, p. 25, 2007.

[214] R. Khettabi, V. Songmene, and J. Masounave, ‘Effect of Tool Lead Angle and Chip Formation Mode on Dust Emission in Dry Cutting’, *J. Mater. Process. Technol.*, vol. 194, no. 1–3, pp. 100–109, 2007.

[215] W. Szymczak, N. Menzel, and L. Keck, ‘Emission of Ultrafine Copper Particles by Universal Motors Controlled by Phase Angle Modulation’, *J. Aerosol Sci.*, vol. 38, no. 5, pp. 520–531, mai 2007.

[216] K. Starost and J. Njuguna, ‘A Review on the Effect of Mechanical Drilling on Polymer Nanocomposites’, *IOP Conf. Ser. Mater. Sci. Eng.*, vol. 64, p. 012031, Aug. 2014.

[217] R. Zitoune, V. Krishnaraj, and F. Collombet, ‘Study of Drilling of Composite Material and Aluminium Stack’, *Compos. Struct.*, vol. 92, no. 5, pp. 1246–1255, Apr. 2010.

[218] A. Egizabal and C. Elizetxea, ‘Verification of the Improved Performance of Nano-Reinforced Materials vs Non Reinforced Ones’, presented at the SIRENA Project - Follow-up meeting, Cranfield University, Feb-2014.

[219] ‘Boedeker Plastics : Guide to Plastics Machining’. [Online]. Available: http://www.boedeker.com/fabtip.htm. [Accessed: 08-Feb-2016].

[220] M. J. Ellenbecker and C. S.-J. Tsai, ‘Exposure Characterization’, in *Exposure Assessment and Safety Considerations for Working with Engineered Nanoparticles*, John Wiley & Sons, Inc, 2015, pp. 112–165.

[221] V. Cecen, Y. Seki, M. Sarikanat, and I. H. Tavman, ‘FTIR and SEM Analysis of Polyester and Epoxy-Based Composites Manufactured by VARTM Process’, *J. Appl. Polym. Sci.*, vol. 108, no. 4, pp. 2163–2170, May 2008.

[222] L. A. S. A. Prado, M. Sriyai, M. Ghislandi, A. Barros-Timmons, and K. Schulte, ‘Surface Modification of Alumina Nanoparticles with Silane Coupling Agents’, *J. Braz. Chem. Soc.*, vol. 21, no. 12, pp. 2238–2245, Dec. 2010.

[223] I. F. Sáez del Bosque, S. Martínez-Ramírez, and M. T. Blanco-Varela, ‘FTIR Study of the Effect of Temperature and Nanosilica on the Nano Structure of C–S–H Gel Formed by Hydrating Tricalcium Silicate’, *Constr. Build. Mater.*, vol. 52, pp. 314–323, Feb. 2014.

[224] Sudirman, M. Anggaravidya, E. Budianto, and I. Gunawan, ‘Synthesis and Characterization of Polyester-Based Nanocomposite’, *Procedia Chem.*, vol. 4, pp. 107–113, 2012.

[225] N. Kouklin, M. Tzolov, D. Straus, A. Yin, and J. M. Xu, ‘Infrared Absorption Properties of Carbon Nanotubes Synthesized by Chemical Vapor Deposition’, *Appl. Phys. Lett.*, vol. 85, no. 19, p. 4463, 2004.

[226] S. N. Arshad, ‘High Strength Carbon Nanofibers derived from Electrospun Polyacrylonitrile’, Oct. 2011.

[227] M. Panapoy, A. Dankeaw, and B. Ksapabutr, ‘Electrical Conductivity of PAN-based Carbon Nanofibers Prepared by Electrospinning Method’, *Thammasat Int. J. Sci. Technol.*, vol. 13, Nov. 2008.

[228] Z. Navratilova, P. Wojtowicz, L. Vaculikova, and V. Sugarkova, ‘Sorption of Alkylammonium Cations on Montmorillonite’, *Acta Geodyn. Geomater.*, vol. 4, no. 3, pp. 59–65, Jan. 2007.

[229] L. Barbes, C. Radulescu, and C. Stihi, ‘ATR - FTIR Spectrometry Characterisation of Polymeric Materials’, *Romanian Rep. Phys.*, vol. 66, no. 3, Jun. 2014.

[230] B. J. Saikia and G. Parthasarathy, ‘Fourier Transform Infrared Spectroscopic Characterization of Kaolinite from Assam and Meghalaya, Northeastern India’, *J. Mod. Phys.*, vol. 01, no. 04, pp. 206–210, 2010.

[231] R. Puntharod, C. Sankram, N. Chantaramee, P. Pookmanee, and K. J. Haller, ‘Synthesis and Characterization of Wollastonite from Egg Shell and Diatomite by the Hydrothermal Method’, *J. Ceram. Process. Res.*, vol. 14, no. 2, pp. 198–201, Feb. 2013.

[232] S. Sachse , L. Gendre, F. Silva, H. Zhu, A. Lesczynska, K. Pielichowski, V. Ermini and J. Njuguna, ‘On Nanoparticles Release from Polymer Nanocomposites for Applications in Lightweight

Automotive Components', *J. Phys. Conf. Ser.*, vol. 429, p. 012046, Apr. 2013.

[233] F. Tardif, M. Malarde, L. Golanski, A. Guiot, and M. Pras, 'Nanotechnology 2011: Advanced Materials, CNTs, Particles, Films and Composites', Proceedings of the nanotech 2011 conference, Boston, 2011, pp. 495–498.

[234] 'Euro NCAP | General'. [Online]. Available: http://www.euroncap.com/en/for-engineers/protocols/general. [Accessed: 09-Feb-2016].

[235] R. Shalash, S. Khayat, and E. Sarah, 'Role of Fibre Reinforcement on the Impact Properties of Unsaturated Polyester Resin', Dec. 1989.

[236] M. T. Albdiry, H. Ku, and B. F. Yousif, 'Impact Fracture Behaviour of Silane-Treated Halloysite Nanotubes-Reinforced Unsaturated Polyester', *Eng. Fail. Anal.*, vol. 35, pp. 718–725, Dec. 2013.

[237] M. K. Akkapeddi, 'Glass Fiber Reinforced Polyamide-6 Nanocomposites', *Polym. Compos.*, vol. 21, no. 4, pp. 576–585, 2000.

[238] 'AEROSIL® R 974 - AEROSIL-R-974-EN.pdf'. [Online]. Available: https://www.aerosil.com/www2/uploads/productfinder/AEROSIL-R-974-EN.pdf. [Accessed: 23-May-2016].

[239] R. Kalpokaite-Dickuviene, I. Lukosiute, J. Cesniene, A. Baltusnikas, and K. Brinkiene, 'Influence of the Organically Modified Nanoclay on Properties of Cement Paste', 2011.

[240] V. Songmene, B. Balout, and J. Masounave, 'Clean Machining: Experimental Investigation on Dust Formation Part 1: Influence of machining parameters and chip formation', *Int. J. Environ. Conscious Des. Manuf.*, vol. 14, pp. 1–16, 2008.

[241] W.-C. Chen, ‘Some Experimental Investigations in the Drilling of Carbon Fiber-Reinforced Plastic (CFRP) Composite Laminates’, *Int. J. Mach. Tools Manuf.*, vol. 37, no. 8, pp. 1097–1108, 1997.

[242] J. P. B. de Souza and J. M. L. dos Reis, ‘Influence of Al2O3 and CuO nanoparticles on the thermal properties of polyester- and epoxy-based nanocomposites’, *J. Therm. Anal. Calorim.*, vol. 119, no. 3, pp. 1739–1746, Mar. 2015.

[243] F.-L. Jin, C.-J. Ma, and S.-J. Park, ‘Thermal and Mechanical Interfacial Properties of Epoxy Composites based on Functionalized Carbon Nanotubes’, *Mater. Sci. Eng. A*, vol. 528, no. 29–30, pp. 8517–8522, Nov. 2011.

[244] S. Bal and S. Saha, ‘Fabrication and Characterization of Carbon Nanofiber (CNF) Based Epoxy Composites’, *IOP Conf. Ser. Mater. Sci. Eng.*, vol. 75, no. 012018, 2015.

[245] S. Ponnuvel and T. V. Moorthy, ‘Investigation on the Influence of Multi Walled Carbon Nanotubes on Delamination in Drilling Epoxy/Glass Fabric Polymeric Nanocomposite’, *Procedia Eng.*, vol. 51, pp. 735–744, Jan. 2013.

[246] K. S. Umashankar, K. V. Gangadharan, V. Desai, and B. Shivamurthy, ‘Machining Characteristics of Nanocomposites’, *Adv. Mater. Lett.*, vol. 2, no. 3, pp. 222–226, 2011.

[247] R. A. da Paz, ‘Mechanical and Thermomechanical Properties of Polyamide 6/Brazilian Organoclay Nanocomposites’, 2016.

[248] Inkoa, Cranfield University, Tecnalia, and Robert Gordon University, ‘Best Practice Manual for the Simulation of the Release of Nanomaterials from Nanocomposite Products’. Dec-2015.

APPENDICES

Appendix A : Process Parameters for Twin Screw Extruder

Extrusion Conditions:

Compounder	Zone 1	Zone 2	Zone 3	Zone 4	Zone 5	Zone 6	Zone 7	Zone 8	Zone 9, 10, 11
Set value (°C)	x	240	250	250	250	260	260	260	270
Actual value (°C)	x	240	250	250	250	260	260	260	270
Compounder	hz12-01*	hz12-02*	hz12-03*	hz12-04*	hz12-05*	hz12-06*	hz12-07*		
Screw speed (rpm)	400	400	400	500	400	400	400		
Pressure (bar)	38	40	40	40	39	40	41		
Temperature (°C)	284	281	281	279	277	278	278		
Extruder efficiency (%)	66	65	67	45	66	68	70		
Degassing	yes	yes	yes	yes	yes	yes	yes		
GALA under water pelletizer	no	no	yes	yes	yes	yes	yes		
Die plate	x	x	300	300	300	300	300		
Diverter valve	x	x	280	280	280	280	280		
Cutter (rpm)	x	x	5000	5000	5000	5000	5000		
Strand pelletizer	yes	yes	no	no	no	no	no		
Take-off speed (m/min)	50	50	x	x	x	x	x		
Side-feeder (rpm)	400	400	400	400	400	400	400		
Output	50	50	50	25	30	25	25		
Feeder									
PA 6	main hopper								
Delitte	main hopper			x					
Aerosil	x			side feeder					

*hz12-01 = PA6-GF-OMMT-5%
*hz12-02 = PA6-GF-OMMT-7.5%
*hz12-03 = PA6-GF-OMMT-10%
*hz12-04 = PA6-GF-SiO2-1%
*hz12-05 = PA6-GF-SiO2-0.5%
*hz12-06 = PA6-GF-SiO2-1.5%
*hz12-07 = PA6-GF-SiO2-3%

Appendix B : Injection Moulding Parameters for the cones manufacturing

	Unit	Crash-Cone						
Material		hz12-01*	hz12-02*	hz12-03*	hz12-04*	hz12-05*	hz12-06*	hz12-07*
Pre-Drying		Yes, during 15 hours at 80 °C						
Injecion moulding machine		Ferromatik K110 with mould 'Crash-Cone'						
Clamping force	kN	1100	1100	1100	1100	1100	1100	1100
Temperature								
Feed zone	°C	45	45	45	45	45	45	45
Zone 4	°C	230	230	230	230	230	230	230
Zone 3	°C	240	240	240	240	240	240	240
Zone 2	°C	250	250	250	250	250	250	250
Zone 1	°C	260	260	260	260	260	260	260
Nozzle	°C	270	270	270	270	270	270	270
Mould temperature	°C	75	75	75	75	75	75	75
Mould (moving mould half)	°C		90	90	90			
Mould (stationary mould half)	°C		80	80	80			
Shot volume	cm^3	190	190	190	190	190	190	190
Metering stroke	mm	19.5	19.5	19.5	19.5	19.5	19.5	19.5
Srew speed	1/min	100	100	100	100	100	100	100
Peripheral velocity	mm/s							
Back pressure	bar	40	40	40	40	40	40	40
Setting time	s	35	35	35	35	35	35	35
Delayed feed	s	0,5	0,5	0,5	0,5	0,5	0,5	0,5
Injection pressure	bar	1400	1400	1400	1400	1400	1400	1400
Injection speed	cm^3/s	250	250	250	120	120	120	150
Mould filling time	s	0,81	0,81	0,81	1,61	1,61	1,62	1,3
Change-over point	cm^3	20	20	20	20	20	20	20
Follow-up pressure	bar	150	150	200	180	160	160	160
Holding pressure time	s	2	2	2	2	2	2	2
Holding pressure speed	cm^3/s	25	25	35	35	35	35	35
Melt cushion	cm^3	1.9	3	3	1.3	1.7	0.5	1.6

Appendix C : Injection Moulding Parameters for the tensile samples manufacturing

	Unit	Tensile + Flexural						
Material		hz12-01*	hz12-02*	hz12-03*	h12-04*	hz12-05*	hz12-06*	hz12-07*
Pre-Drying		Yes	Yes	Yes	Yes	Yes	Yes	Yes
Drying temperature	°C	80	80	80	80	80	80	80
Drying time	h	15	15	15	15	15	15	15
Injecion moulding machine		Engel ES200/60 HL ST						
Mould		Campus-Zug	Campus-Zug	Campus-Zug	Campus-Zug	Campus-Zug	Campus-Zug	Campus-Zug
Clamping force	kN	600	600	600	600	600	600	600
Temperature								
Feed zone	°C	35	35	35	35	35	35	35
Zone 3	°C	230	230	230	230	230	230	230
Zone 2	°C	250	250	250	250	250	250	250
Zone 1	°C	260	260	260	260	260	260	260
Nozzle	°C	270	270	270	270	270	270	270
Mould temperature	°C	85	85	85	85	85	85	85
Mould (moving mould half)	°C	83	83	84	84			
Mould (stationary mould half)	°C	83	83	84	84			
Screw retraction	cm^3	10	10	10	10	10	10	10
Metering stroke	mm	63	63	63	66	70	70	72
Srew speed	1/min	125	125	125	125	125	125	125
Back pressure	bar	6 hydr.	6 hydr.	5 hydr.	5 hydr.	5 hydr.	5 hydr.	5 hydr.
Setting time	s	20	20	20	20	20	20	20
Injection pressure	bar	200	200	200	200	200	200	200
Injection speed	mm/s	20	20	20	20	20	20	20
Mould filling time	s	1,42	1,38	1,38	3,5	3,56	3,54	
Change-over point	cm^3	10	10	10	9	11	11	13
Holding pressure time	s	6	6	6	6	6	6	6
Holding pressure speed	cm^3/s	20	20	20	20	20	20	20
Melt cushion	cm^3	7.5	7.6	1.1	7	10	6.4	2
Cycle time	s	33,2	33,12	33,12	41,5		41,6	

Appendix D : Injection Moulding Parameters for the plaques manufacturing

	Unit	Plaque 4mm (170x170)						
Material		hz12-01*	hz12-02*	hz12-03*	hz12-04*	hz12-05*	hz12-06*	hz12-07*
Pre-Drying		Yes, during 15 hours at 80 °C						
Injecion moulding machine		Ferromatik K110 with mould 'Fasum', clamping force of 1100 kN						
Temperature								
Feed zone	°C	45	45	45	45	45	45	45
Zone 4	°C	230	230	230	230	230	230	230
Zone 3	°C	240	240	240	240	240	240	240
Zone 2	°C	250	250	250	250	250	250	250
Zone 1	°C	260	260	260	260	260	260	260
Nozzle	°C	270	270	270	270	270	270	270
Mould temperature	°C	85	85	85	85	85	85	85
Mould (moving mould half)	°C	87	87	83	87	83	83	83
Mould (stationary mould half)	°C	84	84	83	84	83	83	80
Shot volume	cm^3	175	175	175	175	180	180	180
Metering stroke	mm	113	113	113	113	113	113	113
Screw speed	1/min	100	100	100	100	100	100	100
Peripheral velocity	mm/s	236	236	236	236	236	236	236
Back pressure	bar	35	35	35	35	35	35	35
Setting time	s	30	30	30	30	30	30	30
Delayed feed	s	0	0	0	0	0	0	0
Injection pressure	bar	1000	1000	1000	1000	1000	1000	1000
Injection speed	cm^3/s	200	200	200	60	60	60	60
Mould filling time	s	0,86	0,86	0,89	2,7	2,79	2,78	2,78
Change-over point	cm^3	30	30	35	30	30	30	30
Follow-up pressure	bar	400	400	400	400	450	460	480
Holding pressure time	s	3	3	3	3	3	3	3
Holding pressure speed	cm^3/s	50	50	50	50	50	50	50
Melt cushion	cm^3	10	18	22	12	3.2	5.4	0.5